Herpes simplex virus type 1 nuclear targeting is mediated by dynein and dynactin, but does not require the small capsid protein VP26

Von der Naturwissenschaftlichen Fakultät der Universität Hannover
zur Erlangung des Grades einer

Doktorin der Naturwissenschaften
Dr. rer. nat.

genehmigte Dissertation
von

Diplom-Biochemikerin Katinka Döhner

geboren am 21. Oktober 1974 in Leverkusen

2006

Referentin: HD PD Dr. Beate Sodeik
Korreferent: Prof. Dr. Ernst Ungewickell

Tag der Promotion: 17. Mai 2006

Table of Contents

List of Abbreviations

AAA	ATPase associated with various cellular activities
Ad	adenovirus
ADP	adenosine diphosphate
AMP-PNP	adenosine 5´-(β,γ-imido)triphosphate
Arp	actin-related protein
ATP	adenosine triphosphate
BAC	bacterial artificial chromosome
cGMP	cyclic guanosine monophosphate
CGN	*cis*-Golgi network
CLIP-170	cytoplasmic linker protein 170
DHC	dynein heavy chain
DIC	dynein intermediate chain
DLC	dynein light chain
DLIC	dynein light intermediate chain
DNA	deoxyribonucleic acid
EBV	Epstein-Barr virus
EHNA	erythro-9-3-[2-hydroxynonyl]adenine
ER	endoplasmic reticulum
GFP	green fluorescent protein
GST	glutathione-S-transferase
gX	glycoprotein X
HCMV	human cytomegalovirus
HHV	human herpesvirus
HIV	human immunodeficiency virus
HSV1	herpes simplex virus type 1
HSV2	herpes simplex virus type 2
HVEM	herpes virus entry mediator
ICP	infected cell protein
KAP	kinesin-associated protein
KHC	kinesin heavy chain
KLC	kinesin light chain
KSHV	Kaposi's sarcoma-associated herpesvirus
ND10	nuclear domain 10
NPC	nuclear pore complex
MOI	multiplicity of infection
mRFP	monomeric red fluorescent protein
mRNA	messenger ribonucleic acid
MT	microtubule
MTOC	microtubule organizing center
PAT1	protein interacting with amyloid precursor protein tail 1
PCR	polymerase chain reaction
PFU	plaque forming units
PRV	pseudorabies virus
RNA	ribonucleic acid
TGN	*trans*-Golgi network
UL	unique long
US	unique short
VP	virion protein
VV	vaccinia virus
VZV	varicella zoster virus
wt	wildtype

1 Abstract

Herpes simplex virus type 1 (HSV1) infects keratinocytes and epithelial cells of the oral and perioral region. Amplified virus enters neurons innervating that area and is transported retrogradely to the neuronal nuclei located in the cranial ganglia, where it can establish a latent infection. After reactivation, progeny virus is transported anterogradely to the synapse. After release from the synapse it can reinfect the epithelium and cause recurrent disease. Thus, during several stages of its life cycle, the neurotropic alphaherpesvirus HSV1 depends on intracellular long distance transport.

After fusion of the viral envelope and a cellular membrane, incoming capsids are transported along microtubules (MTs) to the MT-organizing center (MTOC) and further to the nucleus. At the nuclear pore they release their genome into the nucleoplasm, where viral replication, transcription and capsid assembly take place.

During my Ph.D. thesis I was involved in a project which confirmed with quantitative assays that MTs are required for efficient nuclear targeting of HSV1. Incoming HSV1 capsids colocalized with the minus-end directed MT motor cytoplasmic dynein and its cofactor dynactin. Interfering with dynein function by overexpressing the dynactin subunit dynamitin reduced nuclear targeting of HSV1, and as a consequence expression of immediate-early viral genes, while virus binding and virus internalization were not affected, and only slight alterations of the MT network were observed. Thus, dynein and its cofactor dynactin mediate nuclear targeting of HSV1. In some cells overexpressing dynamitin HSV1 particles accumulated in the cell periphery, and this peripheral accumulation required MTs, suggesting that it was mediated by a plus-end directed MT motor of the kinesin family.

The small capsid protein VP26 can interact with the 14 kDa dynein light chains Tctex-1 and rp3. Therefore, we analyzed the cell entry of HSV1-ΔVP26, which lacks VP26, and HSV1-GFPVP26, which contains GFPVP26 instead of VP26. Both required MTs and functional dynactin for efficient nuclear targeting in Vero and PtK_2 cells, and consequently for efficient expression of immediate-early viral genes. Since Vero cells are infected after fusion at the plasma membrane, we conclude that cytosolic capsids lacking the potential dynein receptor VP26 can use MTs, dynein and dynactin for efficient nuclear targeting. Moreover, capsids from HSV1-wildtype, HSV1-ΔVP26 and HSV1-GFPVP26 bound to dynein and dynactin *in vitro* with similar efficiency. Compared to nuclear capsids with almost no tegument and capsids with complete tegument, capsids which had partially lost their outer tegument bound to dynein and dynactin more efficiently and showed the strongest motility along MTs *in vitro*, suggesting that inner tegument proteins might engage with molecular motors.

In summary, cytosolic HSV1 capsids use MTs, cytoplasmic dynein and dynactin for efficient nuclear targeting. Our data suggest that besides VP26, HSV1 must encode at least one other receptor for dynein or dynactin and that inner tegument proteins are likely candidates.

Key words: herpes simplex virus, cytoplasmic dynein, dynactin

2 Zusammenfassung

Herpes-Simplex-Virus Typ 1 (HSV1) infiziert Keratinocyten und Epithelzellen im Mundbereich. Nach Vermehrung in diesen Zellen infiziert HSV1 Neuronen, die diesen Bereich innervieren, und wandert retrograd zu den neuronalen Zellkernen in den Kranialganglien. Dort kann es eine latente Infektion etablieren, nach deren Reaktivierung neu synthetisierte Viruspartikel anterograd zur Synapse transportiert werden. Dort freigesetzte HSV1-Viren infizieren erneut das Epithel mit ähnlichen Symptomen wie bei der Primärinfektion. Somit ist das neurotrope Alphaherpesvirus HSV1 zu unterschiedlichen Stadien seines Replikationszyklus auf einen intrazellulären Langstreckentransport angewiesen.

Nach Fusion der Virushülle mit einer zellulären Membran werden eintretende Kapside entlang von Mikrotubuli (MT) zum MT-organisierenden Zentrum (MTOC) und weiter zum Zellkern transportiert. An der Kernpore entlassen die Kapside ihr Genom in das Nukleoplasma, in dem virale Replikation, Transkription und Kapsidzusammenbau stattfinden.

Während meiner Doktorarbeit war ich daran beteiligt, mit quantitativen Messungen zu bestätigen, dass MT für den effizienten Transport von HSV1 zum Zellkern erforderlich sind (Mabit et al., 2002). Eintretende HSV1-Kapside kolokalisierten mit dem minus-gerichteten MT-Motor Dynein und dessen Kofaktor Dynactin. Eine Störung der Dynein-Funktion durch Überexpression der Dynactin-Untereinheit Dynamitin reduzierte den Transport von HSV1 zum Zellkern und infolgedessen die frühe virale Genexpression, wohingegen Virusbindung und -internalisierung nicht beeinträchtigt und nur geringe Veränderungen am MT-Netwerk zu beobachten waren. Dynein und sein Kofaktor Dynactin transportierten somit HSV1-Kapside zum Zellkern. In einigen Dynamitin überexprimierenden Zellen akkumulierten HSV1-Partikel in der Zellperipherie. Für diese periphere Akkumulierung waren MT erforderlich, was möglicherweise bedeutet, dass sie von einem plus-gerichteten MT-Motor aus der Kinesin-Familie vermittelt wurde.

Das kleine Kapsidprotein VP26 kann mit den 14 kDa leichten Ketten von Dynein, Tctex-1 und rp3, interagieren. Daher untersuchten wir den Zelleintritt von HSV1-ΔVP26 und HSV1-GFPVP26, in denen VP26 deletiert bzw. durch GFPVP26 ersetzt ist. Beide benötigten MT und funktionelles Dynactin für einen effizienten Transport zum Zellkern von Vero- und PtK_2-Zellen und infolgedessen für eine effiziente Expression früher viraler Gene. Da Vero-Zellen durch Fusion an der Plasmamembran infiziert werden, verwendeten vermutlich auch cytosolische Kapside, denen der potentielle Dynein-Rezeptor VP26 fehlte, MT, Dynein und Dynactin, um effizient zum Zellkern zu gelangen. Zudem banden Kapside von HSV1-Wildtyp, HSV1-ΔVP26 und HSV1-GFPVP26 Dynein und Dynactin *in vitro* mit ähnlicher Effizienz. Verglichen mit nukleären, beinahe tegumentfreien Kapsiden und Kapsiden mit innerem und äußerem Tegument, banden Kapside, deren äußere Tegumentschicht teilweise entfernt war, Dynein und Dynactin effizienter und zeigten *in vitro* mehr Bewegung entlang von MT. Daher vermuten wir, dass Proteine aus der inneren Tegumentschicht mit molekularen Motoren interagieren.

Insgesamt zeigen unsere Daten, dass HSV1 MT, Dynein und Dynactin benutzt, um effizient zum Zellkern zu gelangen. Neben VP26 hat HSV1 vermutlich mindestens einen weiteren Rezeptor für Dynein oder Dynactin, und innere Tegumentproteine stellen gute Kandidaten hierfür dar.

Schlagwörter: Herpes-Simplex-Virus, cytoplasmatisches Dynein, Dynactin

3 Introduction

3.1 Intracellular trafficking of viral particles

Incoming viral particles travel from the cell surface to sites of viral transcription and replication. In contrast, during assembly and egress, subviral particles move from these sites to sites of assembly, and virions are transported to the plasma membrane for egress. Although diffusion is efficient for translocation over short distances, it does not provide a means for directed long distance transport (Sodeik, 2000; Döhner and Sodeik, 2004). The presence of many organelles and the cytoskeleton, particularly the actin filaments, and molecular crowding caused by high protein concentrations restrict free diffusion of molecules larger than 500 kDa (Luby-Phelps, 2000; Verkman, 2002; Dauty and Verkman, 2005). Therefore, viruses and host organelles require active mechanisms for directed transport. Especially neurotropic viruses such as herpes simplex virus type 1 (HSV1) require efficient active axonal transport during pathogenesis. It has been calculated that an HSV1 capsid with a diameter of 125 nm would need 231 years for a diffusional translocation of one cm in axonal cytoplasm, and since diffusion depends on particle size, an enveloped HSV1 virion inside a transport vesicle is expected to be even less mobile (Sodeik, 2000; Döhner et al., 2005). Therefore, viruses exploit the host cell's transport machinery for intracellular transport. They use two alternative strategies, either cytoplasmic membrane traffic, namely endocytosis for cell entry and exocytosis for egress, or viral components interact directly with the cytoskeletal transport machinery.

3.2 The cytoskeleton and motor proteins

The cytoskeleton is a three-dimensional network of protein filaments that defines cell shape as well as internal cell organization. It consists of three principal types of filaments: microtubules (MTs), actin filaments, and intermediate filaments. These filaments are regulated by many kinases and phosphatases as well as tubulin- or actin-binding proteins. Moreover, these filaments operate together, and several proteins provide direct links between them (Rodriguez et al., 2003; Jefferson et al., 2004; Kodama et al., 2004). Three classes of motor proteins transport various cargoes along MTs and actin filaments. Myosins carry their cargoes along actin filaments, while dyneins and kinesins catalyze transport along MTs.

3.2.1 Intermediate filaments

Rope-like intermediate filaments span the entire cytosol and provide mechanical strength against shear forces (Strelkov et al., 2003; Coulombe and Wong, 2004; Styers et al., 2005). Intermediate filaments do not seem to play any role in intracellular transport, because they have no polarity, and no motor proteins have been identified that use them as tracks.

3.2.2 Actin filaments

Actin filaments, also known as microfilaments or F-actin, are flexible structures with a diameter of 7-9 nm. They are built by head-to-tail assembly of globular actin monomers (G-actin). Actin filaments have an intrinsic polarity with fast growing barbed or plus-ends and slow growing pointed or minus-ends (Welch and Mullins, 2002). Actin filaments are organized into a variety of linear bundles, two-dimensional networks or three-dimensional gels. Besides actin filaments dispersed throughout the entire cell, all cells contain a cortical network of actin filaments underneath the plasma membrane, and possibly also around intracellular membrane compartments (Medalia et al., 2002).

In addition to its structural role, actin is a key player in various cell motility processes which are either based on actin polymerization or on the action of ATP-dependent motors of the myosin family (Welch and Mullins, 2002; Kieke and Titus, 2003; Krendel and Mooseker, 2005). Actin filaments play a role during the life cycles of several viruses (Cudmore et al., 1997; Sodeik, 2000; Ploubidou and Way, 2001; Smith and Enquist, 2002; Döhner and Sodeik, 2004; Smith et al., 2004). The best understood example is vaccinia virus that utilizes actin polymerization for efficient cell-to-cell spread (Smith et al., 2003).

Besides its various functions within the cytoplasm, actin was identified in several nuclear complexes implicating it in diverse nuclear activities including transcription, splicing, mRNA export and chromatin remodelling (Bettinger et al., 2004; Pederson and Aebi, 2005). Additionally, nuclear actin might have a structural function as part of a nucleoskeleton and the nuclear lamina. Several actin-binding proteins including myosin I are present in the nucleus, and nuclear myosin I is involved in transcription. Moreover, studies on energy-dependent movement of ND10 domains (nuclear domain 10) suggest that nuclear actin-myosin complexes mediate the dynamics of nuclear processes (Muratani et al., 2002).

3.2.3 Myosins catalyze transport along actin filaments

Myosins are composed of one or two heavy chains, and one to six light chains (Kieke and Titus, 2003; Krendel and Mooseker, 2005). The heavy chain consists of a relatively conserved N-terminal motor domain which binds actin filaments and hydrolyzes ATP, a converter domain which generates the force required for movement, a neck domain which binds the light chains, and a divergent C-terminal globular tail implicated in cargo binding. Based on sequence homology, 20 myosin classes have been designated.

Myosin II is called conventional myosin, all other types of myosin are referred to as unconventional. Myosins move unidirectionally along actin filaments, either towards the plus-end or the minus-end. The arrangement of actin filaments in the cell periphery is generally with the plus-ends towards the plasma membrane. Therefore, plus-end directed myosins, like myosin I or V, are expected to carry their cargo to the cell periphery. In contrast, minus-end directed myosins, such as myosin VI

and possibly myosin IXb, may have complementary roles (Kieke and Titus, 2003; Krendel and Mooseker, 2005).

3.2.4 Microtubules are the highways for long distance transport

MTs are long hollow cylindrical filaments with a diameter of 25 nm. They are built of equally oriented heterodimers of α-and β-tubulin and MT-associated proteins (Nogales, 2000). This head-to-tail assembly gives MTs an intrinsic polarity. The MT minus end depolymerizes if not stabilized by other proteins, and its polymerization rate is three times lower than at the plus-end. Thus, MTs grow primarily at the plus-end, but they can also depolymerize from the plus-end. This dynamic instability leads to alternating phases of growth and shrinkage and enables temporal and spatial flexibility in MT organization (Mitchison and Kirschner, 1984). Typically, the minus-ends are attached to a MT-organizing center (MTOC) which nucleates MT assembly. MTs can detach from an MTOC, and the resulting noncentrosomal MTs either depolymerize, or are stabilized by minus-end binding proteins (Dammermann et al., 2003). Plus-end binding proteins stabilize the plus-ends, and enable interactions with the actin cortex, organelles or kinetochores. Different cell types contain different MT arrays (Fig. 1).

MTs are the highways for long distance transport. Their ATP hydrolyzing motor proteins are dyneins and kinesins. Because a particular motor moves only in one direction, the cell specific MT organization determines the destination a specific motor can reach. MTs mediate the intracellular transport of many viral structures, either within vesicles or by a direct interaction of MT motors and viral proteins. Many viruses replicating in the nucleus including HSV1 (Sodeik et al., 1997), human cytomegalovirus (HCMV; Ogawa-Goto et al., 2003), human immunodeficiency virus (HIV; McDonald et al., 2002), adenovirus (Ad; Suomalainen et al., 1999; Leopold et al., 2000), parvoviruses (Seisenberger et al., 2001; Suikkanen et al., 2003), simian virus 40 (Pelkmans et al., 2001), influenza virus (Lakadamyali et al., 2003) and hepatitis B virus (Funk et al., 2004) use MTs for efficient nuclear targeting during cell entry. Even incoming cores of vaccinia virus (VV), which replicates in cytoplasmic viral factories, are transported along MTs (Carter et al., 2003). During assembly and egress, viruses also need MTs for trafficking inside exocytic vesicles or for cytosolic transport of subviral particles to the budding compartment. HIV, VV and African Swine Fever Virus are examples of viruses which use MTs during assembly and egress (Ploubidou et al., 2000; Sanderson et al., 2000; Geada et al., 2001; Heath et al., 2001; Hollinshead et al., 2001; Mouland et al., 2001; Rietdorf et al., 2001; Ward and Moss, 2001a; Ward and Moss, 2001b; Jouvenet et al., 2004; Ward, 2005). The neurotropic alphaherpesviruses HSV1 and the porcine pseudorabies virus (PRV) absolutely require MTs for anterograde axonal transport during egress (Miranda-Saksena et al., 2000; Tomishima et al., 2001).

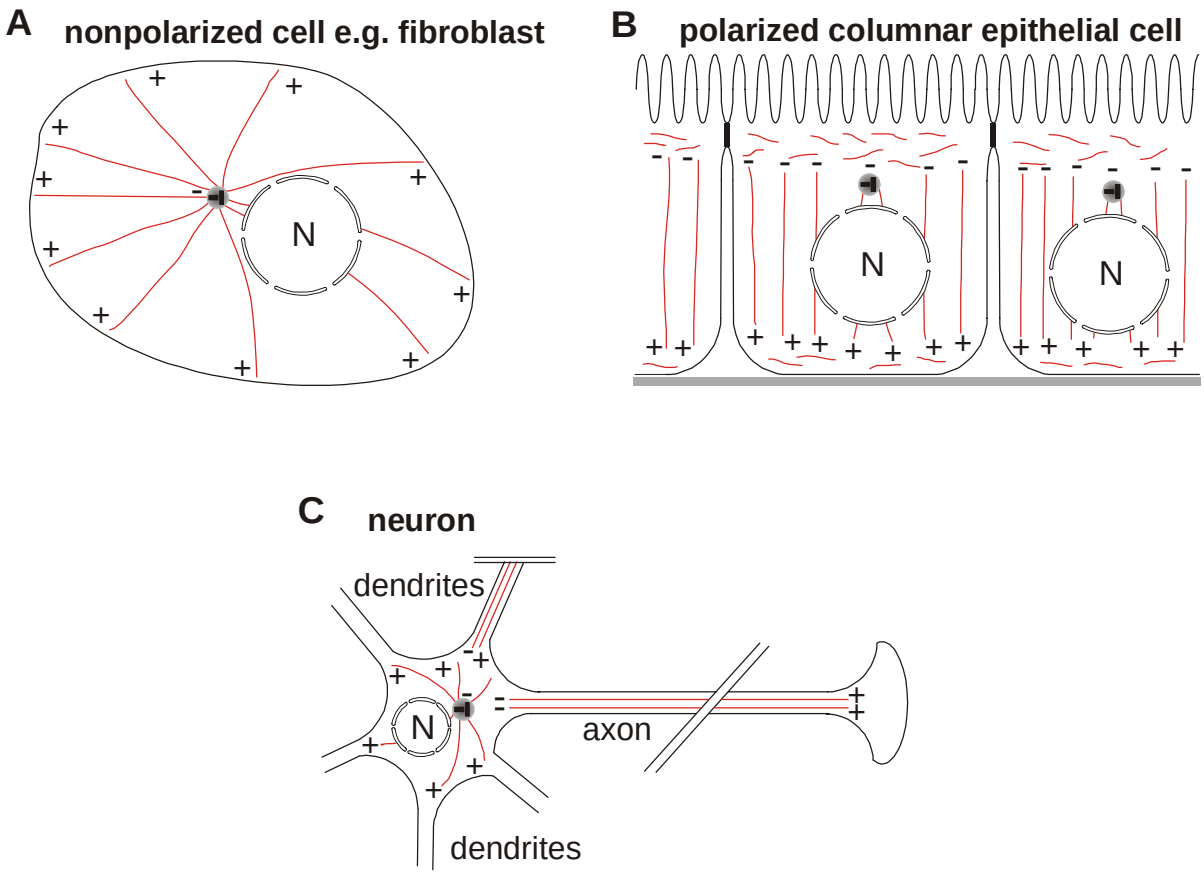

Figure 1: Organization of microtubules (MTs) in different cell types. (a) MTs (red) of unpolarized fibroblasts or epithelial cells radiate from the MT-organizing center (MTOC) to the cell periphery, where their plus-ends (+) are located. The MTOC nucleates MT minus-ends (-) and is often close to the nucleus (N) (Dammermann et al., 2003). (b) In polarized columnar epithelial cells, MTs form an apico-basal array with their plus-ends near the basal surface and the minus-ends pointing to the apical membrane. Moreover, there is an apical and a basal MT web composed of short filaments. Only few MTs are associated with the MTOC under the cell apex (Dammermann et al., 2003; Müsch, 2004). (c) In the soma of neurons, MTs are radially arranged with their minus-ends attached to the MTOC. Axons and dendrites contain noncentrosomal MTs. Axons have MTs of uniform polarity, with their plus-ends pointing towards the synapse. In the proximal region of dendrites, the polarity of MTs is mixed, whereas at the distal end, the polarity is the same as in the axon (Baas et al., 1988; Hirokawa and Takemura, 2005). This figure was taken from Döhner et al., 2005 and has been modified.

3.2.5 Cytoplasmic dynein and its cofactor dynactin

Most minus-end directed MT transport is powered by cytoplasmic dynein (Fig. 2), a 20 S protein complex consisting of two dynein heavy chains (DHCs; 520 kDa), two dynein intermediate chains (DICs; 74 kDa), several dynein light intermediate chains (DLICs; 53-57 kDa) and a series of dynein light chains (DLCs) of the LC8, Tctex/rp3 and LC7/roadblock families (Vale, 2003; Vallee et al., 2004). The C-terminus of DHC comprises both the globular head that hydrolyzes ATP and a 10-15 nm stalk that terminates in a MT-binding domain. The N-terminus mediates DHC dimerization and binding to DLIC and to DIC, which in turn also binds to DLCs. DIC, DLIC and DLC are implicated in cargo binding and regulation of motor activity. There are two DHC, two DIC, two DLIC, two LC7 and

three LC8 genes, and further diversity is generated by different isoforms of DIC and DLC. Dynein holoenzymes with different subunit compositions can recognize diverse cargos (Susalka et al., 2000; Tynan et al., 2000; Tai et al., 2001; King et al., 2002).

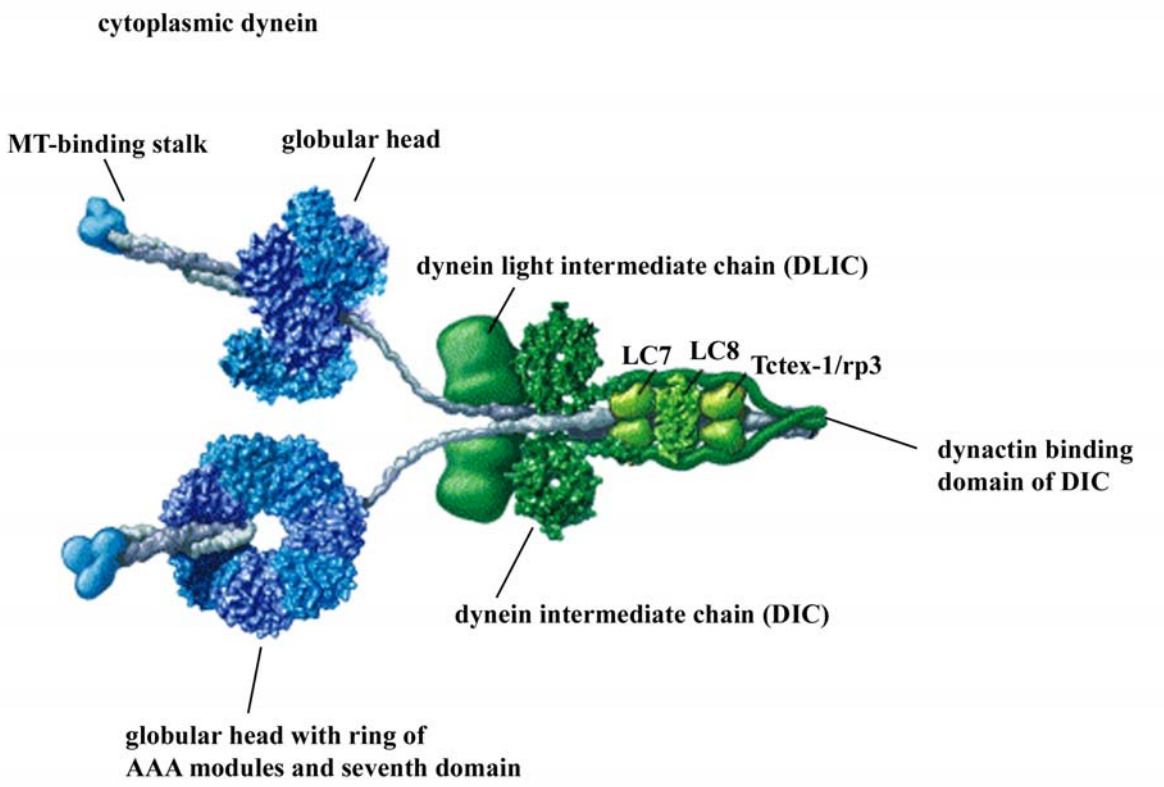

Figure 2: The minus-end directed MT motor cytoplasmic dynein is a 20 S multiprotein complex. The dynein globular head is shown in mixed purple, blue shading to illustrate the distinct domains that comprise the motor head. The stalks extending from the rings bind to MTs with their globular tips. Tightly associated motor subunits (light intermediate, intermediate and light chains) are shown in green. Domains described in the text are labeled. Surface features are rendered based upon atomic resolution structures when available and appear as smooth images for domains of unknown structure. This picture was taken from Vale, 2003.

DHC belongs to the AAA family of ATPases, where AAA stands for ATPase associated with various cellular activities (Oiwa and Sakakibara, 2005). Electron microscopy revealed that DHC has a complex morphology, in which six sequentially linked AAA modules together with a seventh domain are arranged in a ring. A principal site of ATP hydrolysis has been mapped to the first AAA module, while three additional AAA modules possibly act in a regulatory manner by binding either ADP or ATP (Oiwa and Sakakibara, 2005). Single molecule measurements have shown that cytoplasmic dynein makes steps of 8-32 nm length depending on the load (Mallik et al., 2004).

Cytoplasmic dynein is assisted by dynactin (Fig. 3), another large protein complex of 20 S (Schroer, 2004). Dynactin enhances the processivity of dynein catalyzed transport, and is involved in cargo binding (Roghi and Allan, 1999; King and Schroer, 2000). It consists of a filament of the actin-related protein 1 (Arp1) and a flexible sidearm projecting from this filament. The Arp1 filament is

capped at its plus-end by the actin capping protein CapZ, and at its minus-end by a heterotetrameric complex of Arp11, p62, p25 and p27. The projecting sidearm consists of two molecules of $p150^{Glued}$, four copies of dynamitin and the homodimer p24/p22. The latter two form a shoulder-like structure that connects the $p150^{Glued}$ sidearm to the Arp1 filament (Schroer, 2004). If dynamitin is present in large excess, the 20 S dynactin complex separates in two non-functional subcomplexes (Echeverri et al., 1996; Eckley et al., 1999). This inhibits most if not all transport mediated by cytoplasmic dynein (Echeverri et al., 1996; Burkhardt et al., 1997; Valetti et al., 1999).

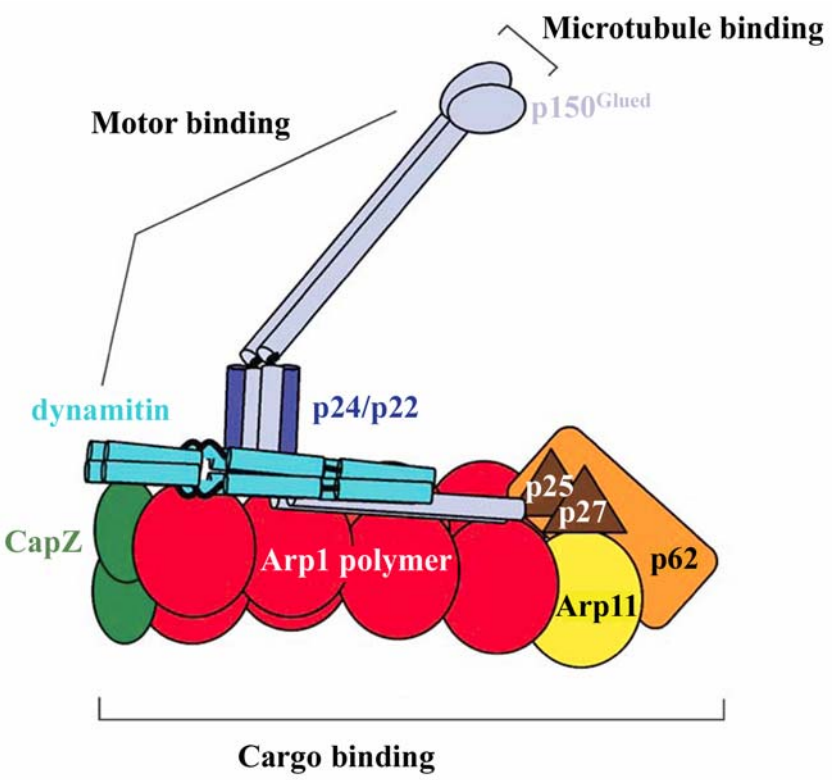

Figure 3: Schematic illustrating the location and approximate structural features of dynactin. The overall structure of dynactin was inferred from electron microscopy (Schafer et al., 1994; Hodgkinson et al., 2005). Dynactin consists of a 10 nm × 40 nm rod made mainly of Arp1 (in red) which is capped at its plus-end by the actin capping protein CapZ (in green) and at its minus-end by the pointed-end complex consisting of Arp11 (in yellow), p25, p27 (both in brown) and p62 (in orange). A flexible sidearm of $p150^{Glued}$ (light blue) with a length of 25-50 nm projects from this Arp1 filament (Schroer, 2004). Dynein and other motors are thought to bind to dynactin along or near the base of this $p150^{Glued}$ sidearm. Each globular head of $p150^{Glued}$ has a MT-binding site, whereas the Arp1 filament has been implicated in cargo binding. The flexible sidearm and the Arp1 filament are linked by p24/22 (dark blue) and dynamitin (turquoise). This picture was taken from Schroer, 2004.

Cytoplasmic dynein and dynactin drive a variety of fundamental cellular processes, including nuclear envelope breakdown, mitotic spindle organization, chromosome separation during mitosis, the positioning of many intracellular organelles, and fast retrograde axonal transport (Vallee et al., 2004). Furthermore, several viruses including Ad, HSV1, Kaposi's sarcoma-associated herpesvirus, VV, African swine fever virus, influenza virus, canine parvovirus and several retroviruses use dynein mediated transport during several stages of their life cycle (Sodeik et al., 1997; Suomalainen et al., 1999; Leopold et al., 2000; Ploubidou et al., 2000; Sanderson et al., 2000; Alonso et al., 2001; Heath et al., 2001; Döhner et al., 2002; McDonald et al., 2002; Lakadamyali et al., 2003; Petit et al., 2003; Sfakianos and Hunter, 2003; Sfakianos et al., 2003; Suikkanen et al., 2003; Naranatt et al., 2005).

3.2.6 The kinesin superfamily

Kinesins are members of a superfamily containing 45 human proteins. They contain a MT-binding motor domain of 320 amino acids that is folded similarly to myosins and G proteins. The kinesins have been classified into three major groups according to the position of the motor domain at the N-terminus, in the middle, or at the C-terminus, hence the names N-kinesins, M-kinesins and C-kinesins, respectively (Hirokawa and Takemura, 2005). There are 39 N-kinesins, three M-kinesins and three C-kinesins. Based on sequence homology, kinesins are further subdivided into 14 families (Lawrence et al., 2004). N-kinesins move their cargo towards the MT plus-ends, whereas C-kinesins catalyze transport towards the minus-ends. M-kinesins most likely do not work as motors but depolymerize MTs (Ovechkina and Wordeman, 2003).

Conventional kinesin (Fig. 4) has two heavy chains (KHCs, kinesin-1, 120 kDa) and two light chains (KLCs; 64 kDa). Each KHC consists of an N-terminal motor head, a neck linker, a long coiled coil dimerization region and a globular tail domain. The N-terminus of KLC interacts with the C-terminus of KHC, and a tetratricopeptide motif in the C-terminus of KLC and the KHC tail mediate cargo binding. Three KHC and three KLC genes may give rise to differently assembled motors. Kinesin-1 can interact with cytoplasmic dynein via KLC and DIC (Ligon et al., 2004). It makes 8 nm steps and walks by moving its two heads in a hand-over-hand mechanism (Yildiz and Selvin, 2005). Kinesin-1 carries axonal vesicles, mitochondria, lysosomes, endocytic vesicles, tubulin oligomers, intermediate filament proteins and mRNA complexes, and participates in the subcellular localization of the ER and the Golgi apparatus (Hirokawa and Takemura, 2005). It is also be involved in cytosolic viral transport (Rietdorf et al., 2001; Jouvenet et al., 2004; Ward and Moss, 2004).

Heterotrimeric kinesin-2 (Fig. 4) comprises two motor subunits, KIF3A and either KIF3B or KIF3C (85-95 kDa), and a non-motor subunit called kinesin-associated protein (KAP; 115 kDa). Kinesin-2 participates in a variety of transport processes, including intraciliary, intraflagellar and axonal transport (Hirokawa and Takemura, 2005), membrane transport between the ER and the Golgi complex (Le Bot et al., 1998), and outward movement of melanosomes (Tuma et al., 1998).

Furthermore, kinesin-2 contributes to the proper localization of late endosomes and lysosomes (Bananis et al., 2004; Brown et al., 2005). KAP interacts with the dynactin subunit $p150^{Glued}$, and excess dynamitin reduces kinesin-2 mediated transport of melanosomes to the cell periphery (Deacon et al., 2003).

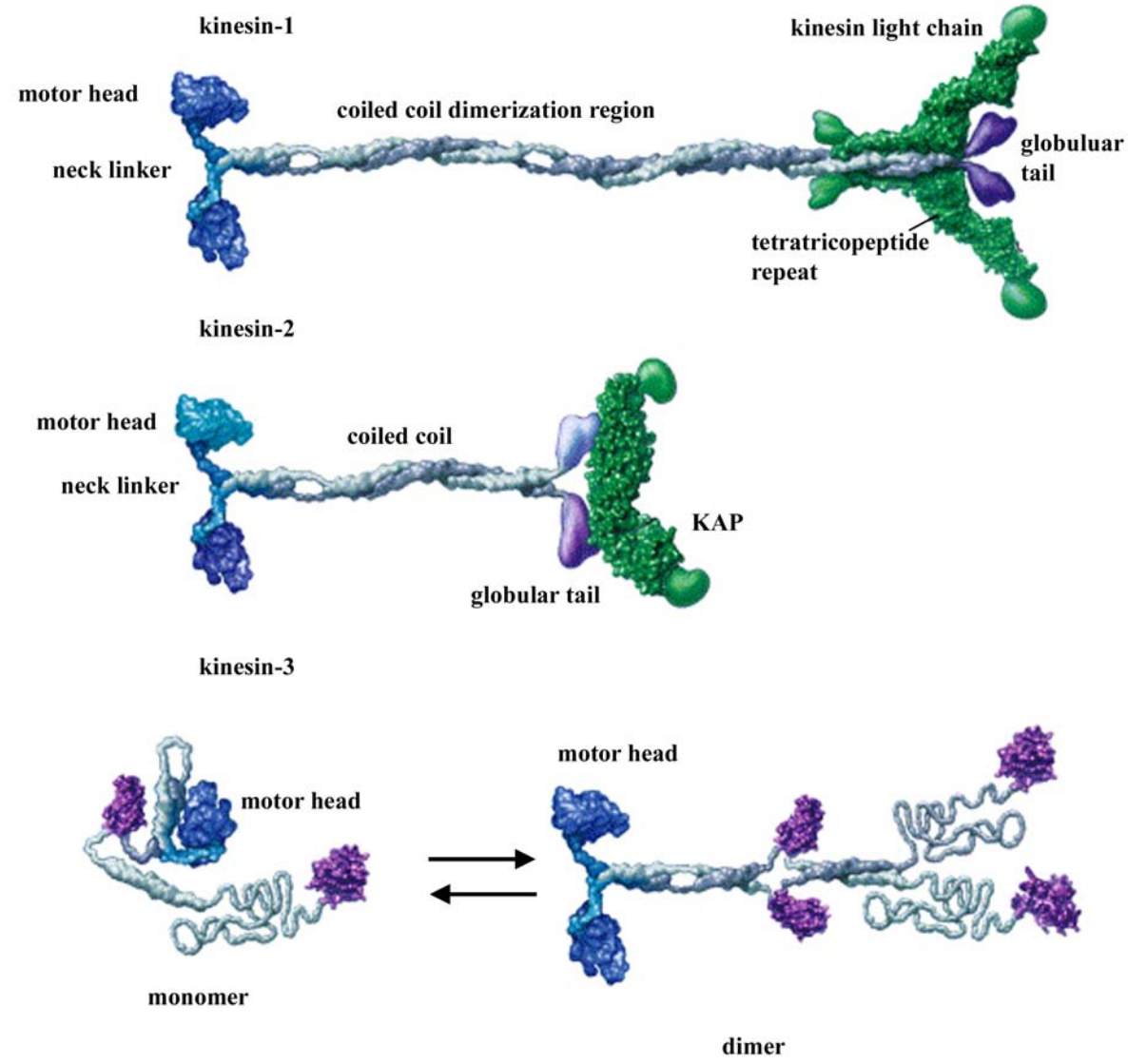

Figure 4: A selection of plus-end directed N-type kinesins: kinesin-1, kinesin-2 and kinesin-3. The catalytic motor domains are displayed in blue, mechanical amplifiers in light blue, and tail domains implicated in cargo attachment are shown in purple. Kinesin-2 contains two distinct motor subunits, which is reflected in the two different colour shadings. Tightly associated motor subunits (light chains, KAP) are shown in green. Domains described in the text are labeled. Kinesin-3 can exist as a monomer and dimer, as indicated by the equilibrium. Surface features are rendered based upon atomic resolution structures when available and appear as smooth images for domains of unknown structure. This picture was taken from Vale, 2003.

Members of the kinesin-3 family are monomeric in solution, but dimerize on membranes, and thereby become processive (Tomishige et al., 2002; Al-Bassam et al., 2003). Via a pleckstrin-homology domain, they attach to membranes (Klopfenstein et al., 2002; Klopfenstein and Vale, 2004). They transport mitochondria and convey transport vesicles to the nerve terminals of motor neurons (Nangaku et al., 1994; Okada et al., 1995).

Kinesin-14 proteins carry their motor domain at the C-terminus, and catalyze minus-end directed transport. They have been implicated in the organization of bipolar spindles, retrograde transport in neurons, Golgi apparatus positioning and motility of early endosomes (Nielsen et al., 1999; Bananis et al., 2003; Ovechkina and Wordeman, 2003). Other kinesins, not further discussed here, are involved in membrane traffic, mitosis and cytokinesis (Hirokawa and Takemura, 2005; Zhu et al., 2005).

3.3 Herpesviridae

The herpesviridae are a large family of enveloped double-stranded DNA viruses (Roizman and Pellet, 2001; Cleator and Klapper, 2004). Members of this family encode a large array of enzymes involved in nucleic acid metabolism and DNA synthesis. Viral replication and capsid assembly occur in the nucleus and the production of infectious progeny virus is invariably accompanied by the lysis of the infected cells. Following infection of their natural host, herpesviruses establish a lifelong latent infection (Roizman and Pellet, 2001; Cleator and Klapper, 2004).

Members of the herpesviridae have been identified in a wide range of vertebrates, and interestingly one invertebrate, the Pacific oyster (Minson et al., 2000). The vertebrate herpesviruses fall into two major phylogenetic groups. Those in the first group have mammalian or avian hosts, and are classified into the subfamilies alpha-, beta- and gammaherpesvirinae, and each subfamily is in turn divided into a series of genera (McGeoch et al., 2000). Reptilian herpesviruses probably also belong to the alphaherpesvirinae. Viruses in the second group infect amphibians and bony fish (Davison et al., 1999).

There are presently nine members of the Herpesviridae known to infect man (Table 1). The official names, human herpesviruses (HHV) 1-8, are rarely used, with the exception of human herpesviruses 6A, 6B, 7 and 8. The other herpesviruses are generally described using their common names. Herpes simplex virus type 1 (HSV1) is officially named human herpesvirus 1 and belongs to the genus simplexvirus of the subfamily alphaherpesvirinae. The members of the subfamily alphaherpesvirinae show a variable host range, short reproductive cycle, rapid spread in culture, efficient lysis of infected cells, and capacity to establish latent infections, primarily but not exclusively, in sensory ganglia (Roizman and Knipe, 2001; Cleator and Klapper, 2004).

Official name and abbreviation	Subfamily	Genus	Common name and abbreviation
Human herpesvirus 1 (HHV-1)	Alphaherpesvirinae	Simplexvirus	Herpes simplex virus type 1 (HSV1)
Human herpesvirus 2 (HHV-2)	Alphaherpesvirinae	Simplexvirus	Herpes simplex virus type 2 (HSV2)
Human herpesvirus 3 (HHV-3)	Alphaherpesvirinae	Varicellovirus	Varicella zoster virus (VZV)
Human herpesvirus 4 (HHV-4)	Gammaherpesvirinae	Lymphocryptovirus	Epstein-Barr virus (EBV)
Human herpesvirus 5 (HHV-5)	Betaherpesvirinae	Cytomegalovirus	Human cytomegalovirus (HCMV)
Human herpesvirus 6A (HHV-6A)	Betaherpesvirinae	Roseolovirus	HHV-6A
Human herpesvirus 6B (HHV-6B)	Betaherpesvirinae	Roseolovirus	HHV-6B
Human herpesvirus 7 (HHV-7)	Betaherpesvirinae	not determined	HHV-7
Human herpesvirus 8 (HHV-8)	Gammaherpesvirinae	Rhadinovirus	Kaposi's sarcoma-associated herpesvirus (KSHV)

Table 1. Classification of the human herpesviruses. This table was taken from Cleator and Klapper, 2004.

3.4 Herpes simplex virus type 1

In most immunocompetent humans, a primary infection with HSV1 is unremarkable. HSV1 mainly infects keratinocytes and epithelial cells of the oral and perioral region (Fig. 5). Amplified virus then enters sensory or autonomic neurons innervating that area, and is transported retrogradely to the neuronal nuclei located in the cranial ganglia (Enquist et al., 1998; Vrabec and Alford, 2004). In neurons, HSV1 either initiates an acute infection resulting in the production of progeny virions, or the viral DNA circularizes and establishes a latent infection. During latency, the episomal viral genome is largely inactive, and viral replication appears to be repressed by the host's immune system (Bloom, 2004; Khanna et al., 2004). Upon stress, latent viral genomes can be reactivated, a lytic infection begins, and progeny virus is anterogradely transported via the axon to the nerve terminal. After release at the presynapse, HSV1 reinfects the epithelium resulting in secretion of infectious virus and, in some cases, lesion formation (Jerome and Ashley, 2003). This generally mild course of infection is in sharp contrast to HSV1 associated diseases like disseminated infection or life-threatening HSV1 encephalitis in neonates and immunocompromised patients, and ocular HSV1 infections that can lead to scarring, opacification of the cornea and ultimately blindness.

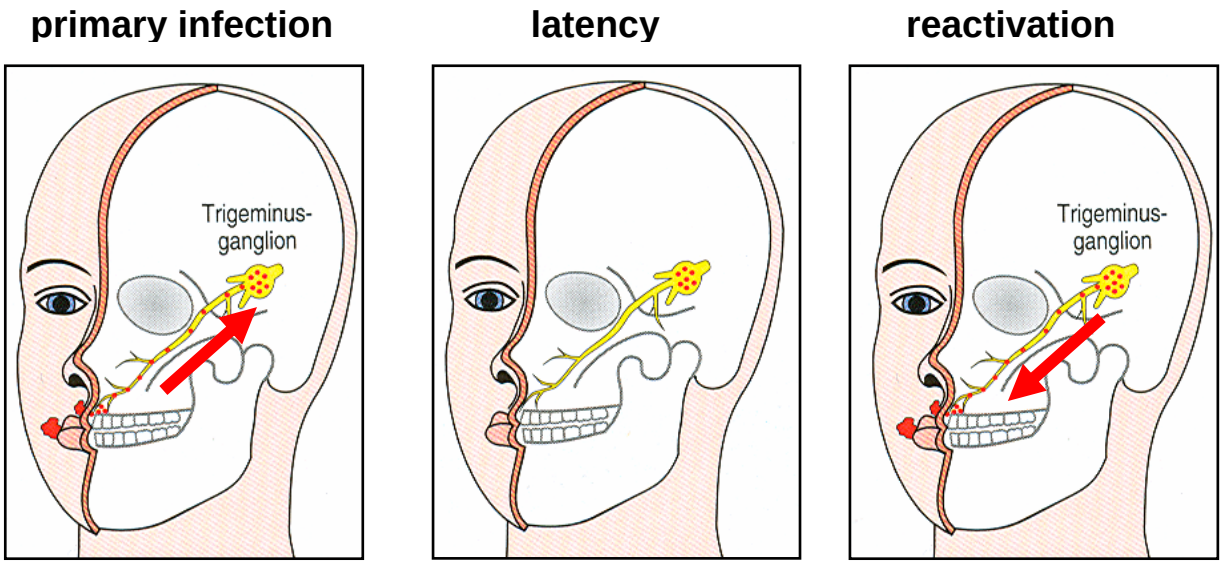

Figure 5: HSV1 latency and reactivation: HSV1 initially infects keratinocytes and epithelial cells of the oral and perioral area (left). Amplified virus then enters neurons innervating that region and is transported retrogradely to cranial ganglia, for example the trigeminal ganglion (left), where a latent infection is established (middle). Upon stress, the latent virus becomes reactivated and progeny virus is transported anterogradely from the trigeminal ganglion to the synapse (right). After release from the synapse it reinfects the epithelium eventually causing cold sores and blisters (right). This figure was taken from Janeway et al., 2001 and has been modified.

The infectious HSV1 virion consists of four structural components: (1) the viral DNA, (2) an icosahedral capsid, (3) the tegument, and (4) the envelope (Roizman and Knipe, 2001). The double-stranded DNA of 152 kbp encodes about 80 proteins (Rajcani et al., 2004), half of which are structural proteins. HSV1 proteins are named according to their genes that are either located on the unique long (UL1, UL2 etc.) or the unique short (US1, US2 etc.) genome region, in descending order by apparent molecular weight (VP1-3, VP5 etc.) or by their function (e.g. vhs – virus host shut off protein).

The icosahedral capsid has a diameter of 125 nm and is organized into 12 pentagonal vertices and 20 triangular faces. It consists of 162 capsomers that are linked by 320 triplexes composed of two copies of VP23 and one copy of VP19C (Zhou et al., 2000). Each capsomer has a chimney-like protrusion and is traversed by an axial channel (Zhou et al., 1999). There are three types of capsomers: hexons that form the capsid faces and edges, pentons that are located at 11 of the 12 vertices, and the portal found at one of the 12 vertices (Newcomb et al., 2001; Trus et al., 2004). The major capsid protein VP5 forms hexamers or pentamers which form the 150 hexons and the 11 pentons, respectively. The tips of the hexons, but not the pentons, are decorated with six copies of the 12 kDa capsid protein VP26 (Wingfield et al., 1997). The portal is a dodecamer of the portal protein UL6. It

has approximately the same size as a penton and is cylindrical, with an axial channel through which the DNA passes as it is packaged (Newcomb et al., 2001; Trus et al., 2004). After DNA packaging UL25 is believed to seal the portal (Ogasawara et al., 2001; Sheaffer et al., 2001).

The tegument, the hallmark of all herpesviruses, is a protein layer between the capsid and the viral envelope. The HSV1 envelope contains about twelve viral membrane proteins that are involved in binding to and entry into host cells, envelopment during virus assembly, cell-to-cell spread and modulation of the host immune response (Roizman and Knipe, 2001; Mettenleiter, 2002; Mettenleiter, 2003; Mettenleiter, 2004; Spear, 2004).

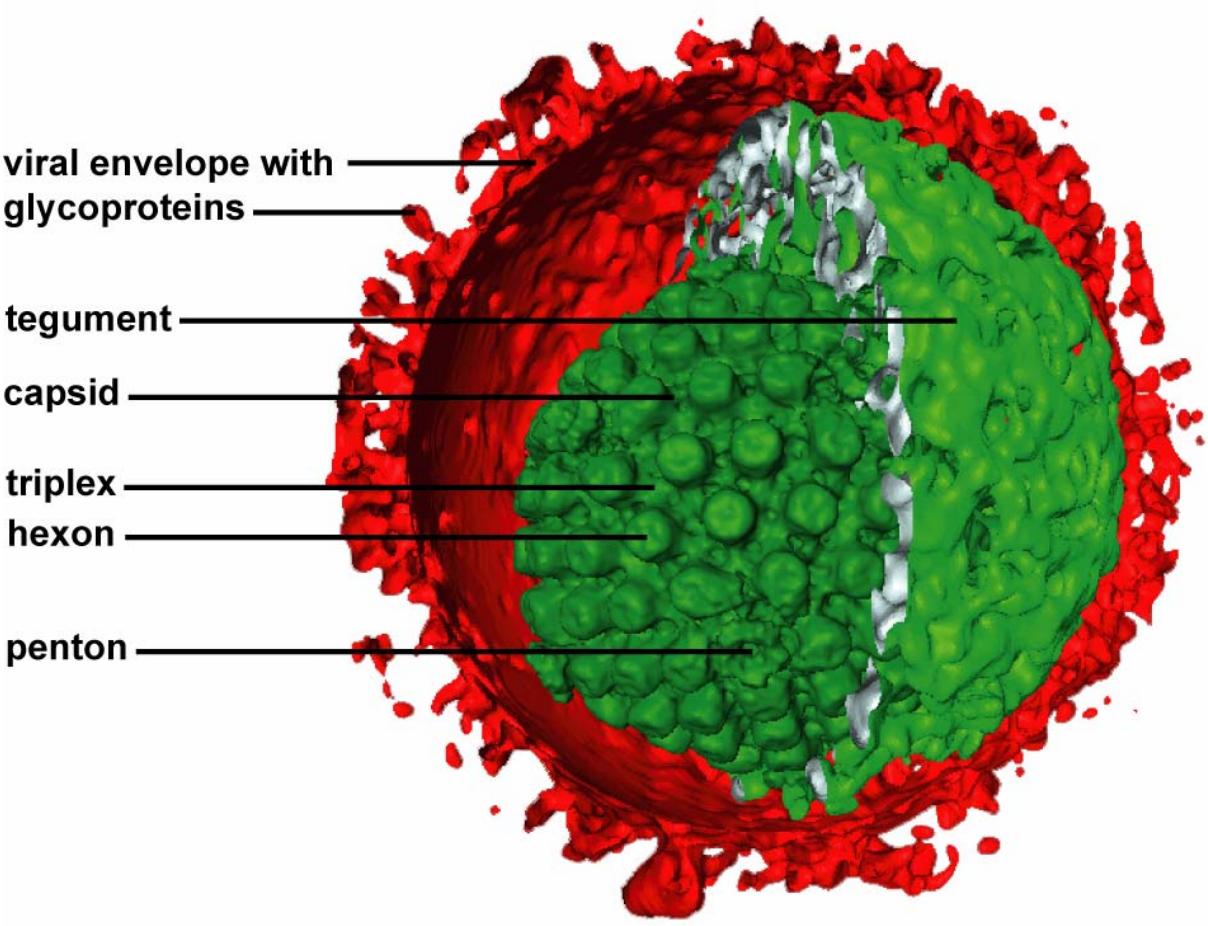

Fig. 6: Cryoelectronmicroscopy tomogram of an HSV1 virion. The host derived envelope with the viral membrane proteins (red), the tegument (light green), and the icosahedral capsid (dark green) are illustrated. The capsid is built by 162 capsomers: 150 VP5 hexons at the edges and surfaces and 11 VP5 pentons at 11 of the 12 vertices. At one vertex, the VP5 penton is supposed to be replaced by the UL6 portal complex. The capsomers are connected at the bottom by triplexes of VP19C and VP23. The tegument has an asymmetric distribution: at the bottom of the depicted virion, the capsid closely approaches the envelope, whereas at the top it is separated by about 35 nm of tegument. In HSV1, the tegument contains about 20 different proteins. This image was kindly provided by Dr. Kay Grünewald, Max-Planck Institute of Biochemistry, Martinsried, Germany (Grünewald et al., 2003).

Cryoelectronmicroscopy and image reconstruction revealed the three-dimensional structure of the HSV1 virion in a near-native state (Zhou et al., 1999; Zhou et al., 2000; Grünewald et al., 2003; Fig. 6). The diameter of the approximately 5 nm thick envelope ranges from 170-200 nm, averaging 186 nm. An array of spikes with a length of 10 to 25 nm protrudes from each virion, making the full diameter, on average, ~ 225 nm. Inside the envelope, the capsid occupies an eccentric position. On the proximal pole it is close to the envelope, whereas on the distal pole, capsid and envelope are separated by 30 to 35 nm of tegument (Grünewald et al., 2003). Most of the tegument is not icosahedrally ordered, but a small portion appears as filamentous structures around the pentons. The interaction between the capsid and the tegument seems to be confined to the pentons and the directly neighbouring hexons (Zhou et al., 1999; Grünewald et al., 2003).

3.4.1 HSV1 entry into cells

Any viral life cycle can be roughly divided into the following phases: (1) adsorption to the cell, (2) penetration of the plasma or endosomal membrane, (3) genome uncoating and release from a viral nucleoprotein complex or capsid, (4) early viral protein synthesis, (5) genome replication, (6) late viral protein synthesis, (7) virus assembly/maturation, and finally (8) viral release or egress. I define here phases (1)–(3), up to the stage at which the viral genome has been uncoated for transcription and replication, collectively as “viral cell entry” (Whittaker et al., 2000; Döhner and Sodeik, 2004; Smith and Helenius, 2004).

To enter cells HSV1 binds via the viral glycoproteins gB and gC to its primary receptors heparan sulfate or other glycosaminoglycan chains of cell surface proteoglycans (Fig. 7; Spear et al., 2000; Roizman and Knipe, 2001; Spear and Longnecker, 2003; Spear, 2004). The interaction between gB and/or gC with glycosaminoglycans significantly enhances the efficiency of HSV1 infection, but is neither absolutely required, nor sufficient for viral entry. For successful entry into cells, the viral glycoprotein gD has to interact with one of several secondary receptors. This interaction triggers fusion of the viral envelope with a cellular membrane, either the plasma membrane or an endosomal membrane, and results in release of the viral nucleocapsid and tegument into the cytoplasm. Fusion of the viral envelope with a cellular membrane requires the viral glycoproteins gB and the heterodimer of gH and gL in addition to gD and the gD receptor.

The so far known secondary receptors fall into three classes. They include HVEM (herpes virus entry mediator), a member of the tumor necrosis factor receptor family, nectin-1, a member of the immunoglobulin superfamily, and specific sites in heparan sulfate generated by certain 3-O-sulfotransferases (Spear, 2004). Moreover, expression of the type II cell surface membrane protein B5 that is broadly expressed in human tissues, renders replication competent but entry deficient porcine cells susceptible for HSV1 infection (Perez et al., 2005; Perez-Romero and Fuller, 2005). Recently, the RGD motif in the gH ectodomain was shown to bind to αvβ3 integrins (Parry et al., 2005). Although blocking this interaction does not abrogate HSV1 infection, it might be involved in signaling

during virus entry (Qie et al., 1999; Zachos et al., 1999; Cheshenko et al., 2003; Cheshenko et al., 2005).

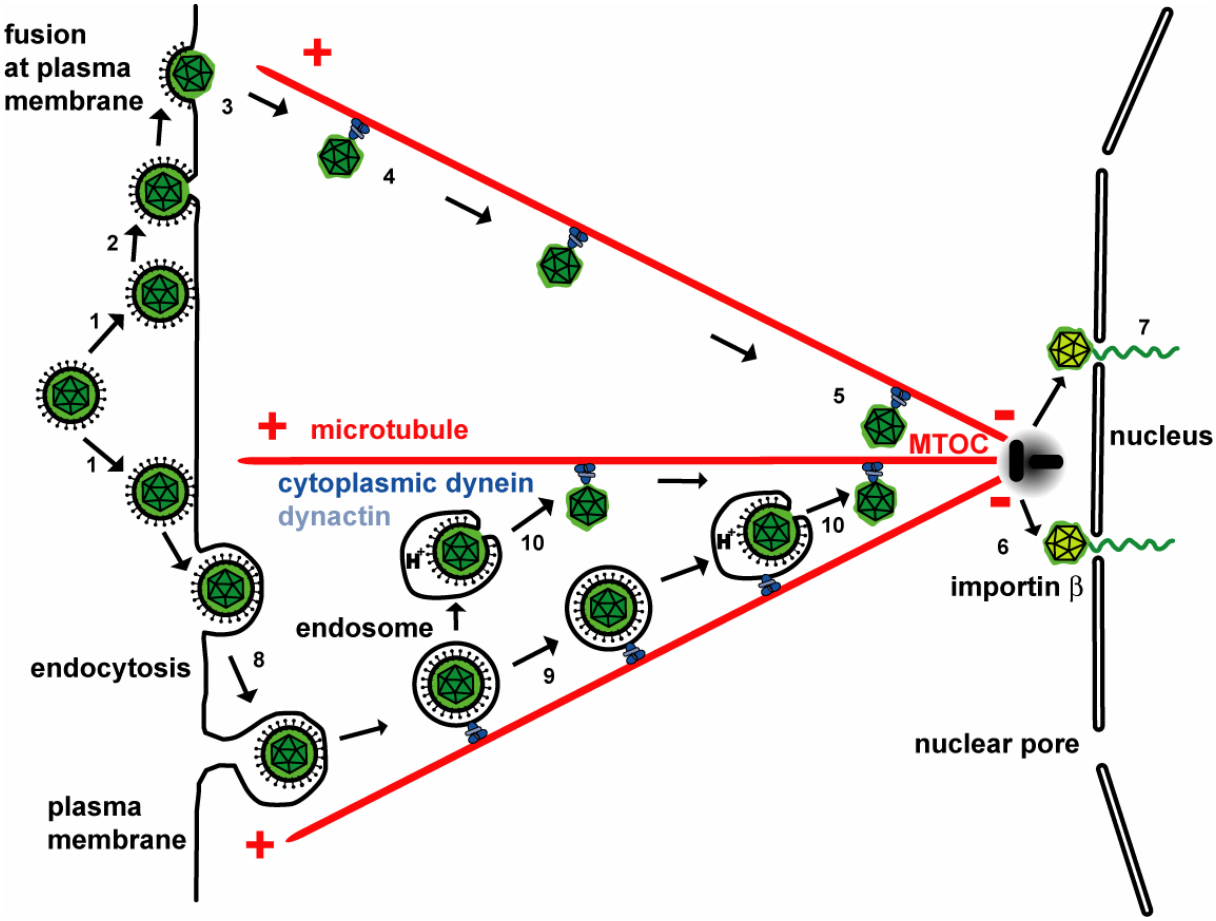

Figure 7: MT mediated transport during HSV1 cell entry. Herpes simplex virus type 1 (HSV1) binds via viral glycoproteins to the plasma membrane of host cells (1). It enters many cells by fusion of its envelope with the plasma membrane (2), thereby releasing the capsid (dark green) and tegument (green) into the cytosol (3). The capsid with some tegument is transported along microtubules (MTs, red, 4) to the MT-organizing center (MTOC; 5) that is close to the nucleus in many cell types. This transport is catalyzed by the minus-end directed MT motor cytoplasmic dynein (dark blue) and its cofactor dynactin (light blue). From the MTOC the capsid moves further to the nuclear envelope (6). Importin β is required for capsid binding to the nuclear pore. At the nuclear pore, the viral genome is released into the nucleoplasm (7) where viral replication and transcription take place. Some cell types are productively infected by endocytosis (8). Endosomes containing HSV1 are presumably also transported along MT (9). Release from endosomes (10) might already take place in the cell periphery or in the perinuclear area. To initiate an infection, capsids released from endosomes also inject their genome into the nucleoplasm (7).

HSV1 enters many cell types by fusion of the viral envelope with the plasma membrane (Fig. 7). Examples are Vero, BHK, Hep2, COS and 143tk- cells, several neuroblastoma cell lines like SK-N-SH, IMR32 and SH-SY5Y, human CNS progenitor cells and human dorsal root ganglion neurons (Koyama and Uchida, 1987; Lycke et al., 1988; Wittels and Spear, 1991; Sodeik et al., 1997; Nicola et al., 2003; Gianni et al., 2004; Nicola and Straus, 2004; Nicola et al., 2005). However, some cell types

are productively infected after entry by endocytosis. Examples for this entry mechanism are CHO-nectin1, CHO-HVEM, and HeLa cells, or keratinocytes such as HaCaT, SCC13, and NHEK cells (Nicola et al., 2003; Gianni et al., 2004; Nicola and Straus, 2004; Nicola et al., 2005). Evidence for entry by endocytosis is based on electron microscopy or pharmacological inhibitors of the endocytic pathway (Nicola et al., 2003; Nicola and Straus, 2004), or on drugs interfering with endosomal acidification (Gianni et al., 2004; Nicola et al., 2005). Since the HSV1 envelope can fuse with the plasma membrane at neutral pH, a lack of sensitivity to changes in the endosomal pH does not exclude an infection via endocytic organelles (Milne et al., 2005).

An interesting question is how the choice is made between entry by fusion of the viral envelope with the plasma membrane and entry by endocytosis. In principle, this might be host or virally determined. It has been suggested that a dense cortical cytoskeleton might prevent productive infection after fusion of the viral envelope and the plasma membrane (Marsh and Bron, 1997). In contrast, virions inside endosomes might circumvent this cortical actin barrier, and after release from the endosome into the cytosol the viral particle can initiate a productive infection (Marsh and Bron, 1997; Sodeik, 2000; Döhner and Sodeik, 2004; Smith and Helenius, 2004; Milne et al., 2005).

3.4.2 HSV1 cytosolic transport during entry

After fusion of the viral envelope with the plasma membrane, the capsid and the tegument are released into the cytosol. Part of the tegument remains at the plasma membrane (Sodeik et al., 1997). After traversing the actin cortex beneath the plasma membrane, the capsid with residual tegument is transported along MTs to the MTOC that is close to the nucleus in many cell types (Fig. 7; Kristensson et al., 1986; Lycke et al., 1988; Topp et al., 1994; Hammonds et al., 1996; Topp et al., 1996; Sodeik et al., 1997; Mabit et al., 2002; Marozin et al., 2004). This transport is catalyzed be the minus-end directed MT-motor cytoplasmic dynein and its cofactor dynactin (Kristensson et al., 1986; Sodeik et al., 1997; Döhner et al., 2002). It is currently unknown how capsids are further translocated from the MTOC to the nuclear envelope (Sodeik, 2002; Döhner et al., 2005). While capsids initially accumulate at the nuclear site facing the MTOC, they later spread over the entire nuclear envelope indicating additional transport mechanisms (Sodeik et al., 1997; Döhner et al., 2002; Everett et al., 2004). In injured axons, minus-end directed transport is coupled to nuclear import (Hanz et al., 2003). Cytoplasmic dynein can interact with the nuclear import receptor importin α and recruit a nuclear import cargo that is bound to importin β. A similar mechanism might be involved in transport of HSV1 capsids from the MTOC to the nuclear envelope. Alternatively, viral particles might utilize plus-end directed MT motors to proceed (Döhner et al., 2002; Sodeik, 2002).

After arrival at the nucleus, capsids are oriented with a penton toward the nuclear pore, and they are often attached to the cytoplasmic fibrils of the nuclear pore complex (NPC; Granzow et al., 1997; Sodeik et al., 1997; Ojala et al., 2000). Importin β is required for capsid binding to the nuclear pores.

The interaction with the nuclear pore destabilizes the capsid and triggers viral genome uncoating (Batterson and Roizman, 1983; Ojala et al., 2000). The viral DNA is released into the nucleoplasm, where viral replication and transcription take place. VP16 of the incoming tegument together with host transcription factors transactivates the expression of five immediate-early HSV1 genes (Roizman and Knipe, 2001; Wysocka and Herr, 2003). The immediate-early gene products cooperate with host transcription factors to regulate the expression of HSV1 early genes. The HSV1 early gene products are involved in nucleotide metabolism and DNA replication. More than 35 HSV1 gene products expressed with late kinetics form structural components of the virion (Roizman and Knipe, 2001).

3.4.3 Potential role of microtubules during assembly and egress of HSV1

Potential functions of MTs during HSV1 assembly and egress are less well understood. If MTs are depolymerized during assemby, virus yields are reduced, but HSV1 infection is not completely blocked in cultured epithelial cells (Avitabile et al., 1995; Kotsakis et al., 2001). In contrast, MTs are essential for axonal transport of viral particles and virus release at the axon terminal in cultured neurons (Miranda-Saksena et al., 2000; Tomishima et al., 2001).

HSV1 replication and capsid assembly take place within the nucleus. Therefore, capsid proteins and proteins required for DNA packaging have to be imported into the nucleus. The viral genome is then packaged into preassembled procapsids via the UL6 portal (Newcomb et al., 2001; White et al., 2003; Trus et al., 2004). After DNA packaging, the UL6 portal is supposed to be sealed by UL25 (Ogasawara et al., 2001; Sheaffer et al., 2001).

Within infected nuclei, HSV1 capsids are actively transported away from sites of capsid assembly. This movement is sensitive to the unspecific myosin inhibitor 2,3-butanedione monoxime and to actin depolymerization with latrunculin A, but insensitive to actin depolymerization with cytochalasin D (Forest et al., 2005). Insensitivity to cytochalasin D is consistent with the idea that nuclear actin is structurally distinct from cytoplasmic F-actin (Bettinger et al., 2004). The authors speculate that this intranuclear movement might either be catalyzed by a viral protein e.g. the capsid-associated DNA-packaging motor or by a cellular intranuclear transport system, such as that proposed to transport some ND10 domains (Muratani et al., 2002).

By budding at the inner nuclear membrane the DNA-containing capsids acquire the protein kinase US3, the primary tegument protein UL31 and the primary viral membrane protein UL34, and reach the periplasmic space, the lumen between the inner and outer nuclear membrane that is continuous with the ER lumen (Fig. 8). The primary envelope of these periplasmic virions then fuses with the outer nuclear membrane or the ER membrane, and the resulting capsids reach the cytosol (Enquist et al., 1998; Mettenleiter, 2002; Mettenleiter, 2004). These cytosolic capsids are then transported to the site of secondary envelopment, which is most likely related to the *trans*-Golgi network (TGN) or possibly to endosomes (Brunetti et al., 1998; Alconada et al., 1999; Granzow et al., 2001; Harley et al., 2001;

McMillan and Johnson, 2001; Wisner and Johnson, 2004; Turcotte et al., 2005). Infectious virions are then released from infected cells either by cell lysis, or more likely by fusion of virion containing membrane vesicles with the plasma membrane (Roizman and Knipe, 2001; Mettenleiter, 2002; Mettenleiter, 2004).

Late during HSV1 infection, the radial MT organization is lost, at least in some epithelial cell types (Avitabile et al., 1995). Instead, the MTs are fragmented, particularly in the cell periphery, form bundles which surround the nucleus, and an apparent MTOC is lost, but may regenerate later (Avitabile et al., 1995; Elliott and O'Hare, 1998; Ward et al., 1998; Kotsakis et al., 2001). This reorganization of the MT network late in infection has hampered the analyzis of the contribution of MTs and MT motors during assembly and egress. The predicted functions of MTs, dynein and kinesin, which are hypothesized below, would only facilitate assembly and egress, if they occurred prior to the reorganization of the MT network.

MTs could mediate transport of cytosolic capsids to the secondary budding compartment, and secretory vesicles containing virions might be carried along MTs to the plasma membrane. If budding occurred at the TGN or at endosomes, which are often concentrated around the MTOC, capsids might recruit dynein and its cofactor dynactin or a minus-end directed kinesin for this transport. In contrast, plus-end directed kinesins might carry virion-containing vesicles to the plasma membrane.

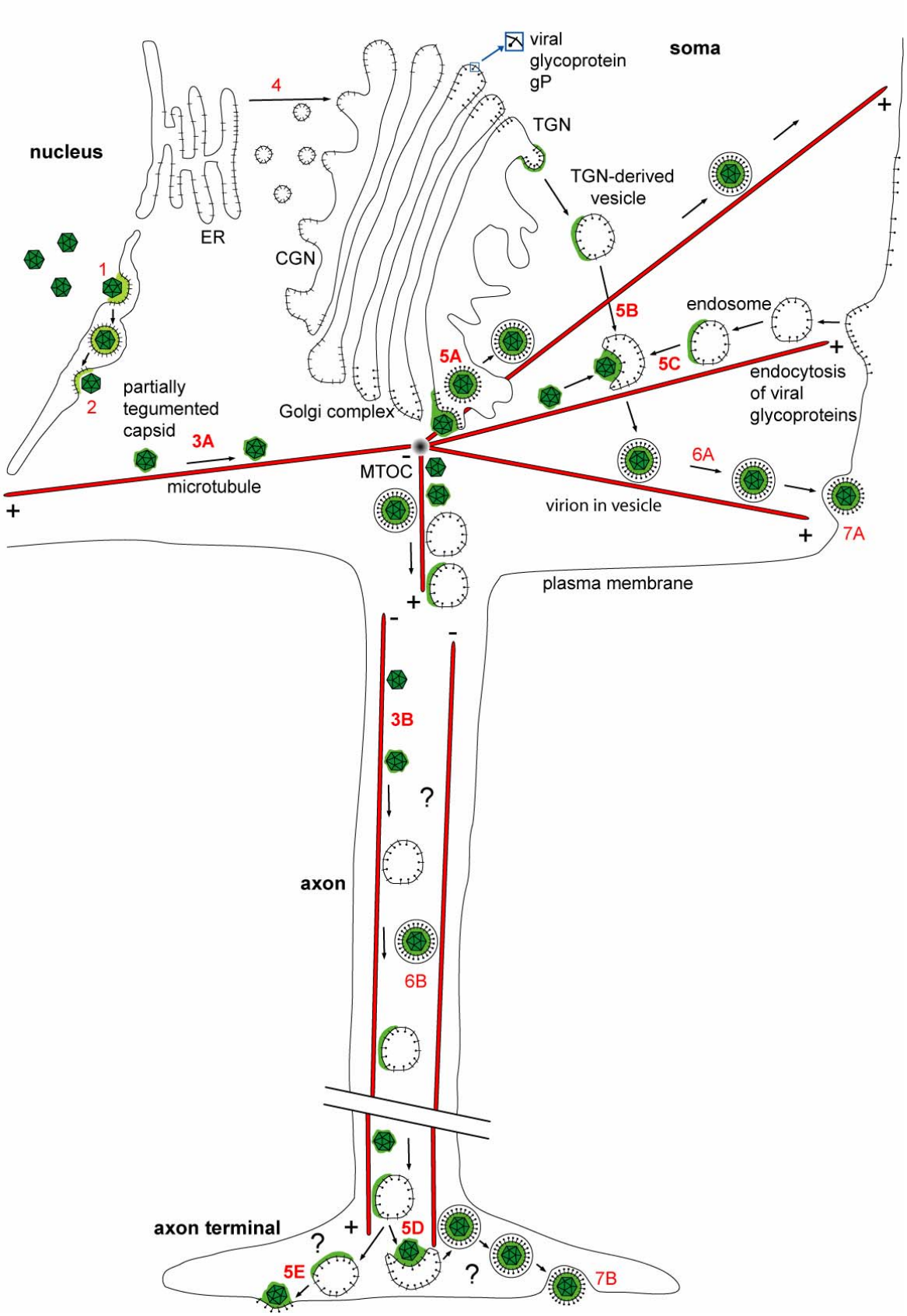

Figure 8: Potential functions of microtubules during neuronal HSV1 assembly and egress. After nuclear DNA-packaging, capsids (dark green) acquire a primary tegument (light green) and a primary envelope by budding at the inner nuclear membrane (1) leading to the formation of periplasmic virions. Such periplasmic virions fuse with the outer nuclear membrane to release capsids into the cytosol (2). Cytosolic capsids are

transported, presumably along MTs (MT, red), to another membrane compartment for secondary envelopment (3A) or by axonal transport to the synapse (3B). Cytosolic capsids may already bind some tegument (green). Viral glycoproteins (gP) are transported from the endoplasmic reticulum (ER) to the *cis*-Golgi network (CGN; 4), and further through the Golgi apparatus to the *trans*-Golgi network (TGN), or even to the plasma membrane. Some gPs contain endocytosis signals in their cytosolic tail and may be targeted to endocytic organelles. The cytosolic tails of some viral gPs interact with some tegument proteins (green).

Secondary envelopment may occur at the TGN (5A), at TGN-derived vesicles (5B), at endosomes localized in the soma (5C), or in the axon terminal (5D). TGN and endosomes are often clustered around the MT-organizing center (MTOC). After secondary envelopment, secretory vesicles containing virions can be transported, presumably along MTs, to the plasma membrane of the soma (6A) where the viral membrane fuses with the plasma membrane (7A), and releases mature virions into the medium. Most likely, viral assembly intermediates are also transported along axonal MTs: capsids with or without tegument (3B), vesicles with viral gPs and tegument proteins on the outside, or vesicles with virions (6B). Virions may be released by exocytosis (7B), or final budding might occur at the synapse resulting in virus secretion (7B). Vesicles may also fuse with the plasma membrane (5E), and insert gPs and attached tegument into the presynaptic plasma membrane. Partially tegumented capsids might then bud there resulting in virion release into the medium.

In neurons, cytosolic capsids might bud at compartments related either to the TGN or to endosomes in the soma as described above, and might then be transported inside secretory vesicles to the plasma membrane of the soma (Miranda-Saksena et al., 2002) or to the presynapse. Alternatively, cytosolic capsids might enter axons and might move along MTs to the nerve terminals. Several studies found that capsids and envelope proteins were conveyed separately in the axon, suggesting that final virion assembly takes place in the presynapse (Penfold et al., 1994; Holland et al., 1999; Miranda-Saksena et al., 2000; Tomishima and Enquist, 2001; Diefenbach et al., 2002). In axons of retinal ganglion cells, HSV1 antigens and DNA were found in unenveloped particles of 110 nm diameter consistent with transport of unenveloped capsids (LaVail et al., 2005). Additionally, membrane-bound particles of 150-180 nm diameter containing HSV1 antigens were reported.

However, recent experiments in PRV, the porcine alphaherpesvirus, revealed that the viral glycoprotein gE is required for axonal entry of capsids, as well as at least one tegument protein (Ch'ng and Enquist, 2005a). Moreover, brefeldin A treatment blocked entry of capsid, tegument and viral membrane proteins into axons, whereas in untreated cells capsids enclosed within vesicles entered axons (Ch'ng and Enquist, 2005b; del Rio et al., 2005). These studies indicate that viral capsids may be transported in association with tegument and possibly viral membrane proteins within vesicles rather than as unenveloped capsids.

3.4.4 Potential receptors for dynein, dynactin and kinesins on the HSV1 virion

In contrast to many cellular structures transported along MTs, the protein composition of HSV1 is known and can be specifically altered by directed mutagenesis. Therefore, the potential significance of interactions of HSV1 proteins with molecular motors identified *in vitro* by yeast two-hybrid assays,

glutathione-S-transferase(GST)-pulldowns, coimmunoprecipitation, pepscan techniques or other assays can be validated by analyzing viral strains deleted for potential interaction partners.

Moreover, HSV1 particles are conveyed predominantly to the MT minus-ends during entry, while during egress, at least in neurons, they preferentially move to the MT plus-ends. The viral cargo might be structurally similar during both stages of the viral life cycle, and the change in transport direction might be achieved by some regulatory mechanisms. Upon entry, HSV1 induces signaling events (Qie et al., 1999; Zachos et al., 1999; Cheshenko et al., 2003; Cheshenko et al., 2005), and it is possible that this signaling plays a role in regulating the direction of transport as has been shown for Ad (Suomalainen et al., 2001). The viral protein kinases UL13 and US3, which are components of the tegument, may also modify viral or cellular proteins, and thereby influence the transport direction.

Alternatively, the viral structure transported during entry – possibly a capsid surrounded only by inner tegument proteins – might differ from the viral cargo during egress – for example a viral capsid surrounded by more tegument proteins or even a capsid enclosed in a membrane (Ch'ng and Enquist, 2005b; del Rio et al., 2005; Granzow et al., 2005; Luxton et al., 2005).

In principle, all tegument and those capsid and capsid-associated proteins located on the capsid surface could be involved in cytosolic MT transport. Moreover, viral membrane proteins or nonstructural viral proteins might also interact with the host cytoskeleton, and mediate MT transport of virion containing vesicles, or of capsids associated with the cytosolic surface of a vesicle.

3.4.4.1 Potential motor receptors among the viral membrane proteins

Cytosolic domains of viral membrane proteins might recruit MT motors to secretory vesicles either enclosing complete virions, or containing viral membrane proteins embedded in the vesicle's membrane, and thus contribute to the viral life cycle. The cytosolic tail of the HSV1 integral membrane protein **UL34** can interact with the DIC subunit of cytoplasmic dynein in GST-pulldown assays (Ye et al., 2000). UL34 is targeted to the inner nuclear membrane, and during budding at the inner nuclear membrane it is incorporated into the primary envelope of periplasmic virions (Fig. 9; Klupp et al., 2000; Reynolds et al., 2002). Cytoplasmic membranes, cytoplasmic virions and extracellular virions do not contain UL34. Thus, UL34 is less likely to function in cytoplasmic MT transport of HSV1 particles.

The HSV protein **UL56** is a C-terminal-anchored, type II membrane protein. In yeast-two hybrid and GST-pulldown assays HSV2-UL56 interacts with KIF1A, a member of the kinesin-3 family. While the precise role of UL56 during virus infection remains to be elucidated, UL56 might function in plus-end directed MT transport of secretory vesicles containing viral membrane proteins or even complete virions (Koshizuka et al., 2005). However, PRV which also undergoes anterograde transport during egress does not code for a UL56 homolog (Smith et al., 2001; Klupp et al., 2004).

3.4.4.2 Potential motor receptors among the tegument proteins

Viral tegument proteins are exposed to the cytosol and may recruit MT motors for capsid transport either after fusion of the viral envelope with a cellular membrane during entry or prior to secondary budding during egress,. Moreover, tegument proteins may bind simultaneously to MT motors and to the cytosolic domains of viral membrane proteins, and thereby mediate MT transport of vesicles containing viral components.

Based on studies of PRV and HSV1, the **major tegument proteins VP11/12 [UL46], VP13/14 [UL47], and VP22 [UL49]** were recently classified as outer tegument proteins (Mettenleiter, 2004; Vittone et al., 2005; Wolfstein et al., 2006). **VP16 [UL48]** can interact with VP11/12, VP13/14, VP22 and the inner tegument protein VP1-3 [UL36] suggesting that VP16 may provide a **connecting link between outer and inner tegument** (Elliott et al., 1995; Hafezi et al., 2005; Mouzakitis et al., 2005; Vittone et al., 2005). HSV1-VP22 colocalizes with MT when expressed in the absence of other HSV1 proteins and induces MT stabilization and hyperacetylation (Elliott and O'Hare, 1997; Elliott and O'Hare, 1998; Martin et al., 2002). Moreover, VP22 can interact with the heavy chain of nonmuscle myosin II (van Leeuwen et al., 2002). After penetration, VP13/14, VP16, VP22, and the myristoylated protein UL11 are lost from incoming PRV capsids (Granzow et al., 2005; Luxton et al., 2005), whereas during egress in neurons VP13/14, VP16 and VP22 are either transported in association with or independent of capsids (Luxton et al., 2005). Thus, VP13/14, VP16, VP22 and UL11 are less likely to mediate the interaction between incoming capsids and MT motors.

VP1-3 [UL36], UL37, and **US3** are postulated to constitute the **inner tegument shell** (Mettenleiter, 2004; Vittone et al., 2005; Wolfstein et al., 2006). Coimmunoprecipitation and yeast two-hybrid assays revealed that VP1-3 can bind to the major capsid protein VP5, to UL37 and to VP16 that might connect the inner and the outer tegument shell (McNabb and Courtney, 1992a; Vittone et al., 2005). Although they are probably exposed on the surface of incoming capsids (Granzow et al., 2005; Luxton et al., 2005), none of these proteins have so far been reported to interact with MTs or MT motors. However, in blot overlay assays the HCMV VP1-3 homolog UL48 interacts with ES130/p180 which contains a region homologous to kinectin which was originally identified as a candidate receptor for kinesin-1 on the ER (Ogawa-Goto et al., 2002). During assembly in the absence of VP1-3 or UL37, unenveloped capsids accumulate in the cytosol indicating that VP1-3 or UL37 either mediate transport to the compartment of secondary envelopment, or are required for the attachment of further tegument proteins which are needed for transport or secondary envelopment (Desai, 2000; Desai et al., 2001). Moreover, a temperature-sensitive mutation mapped to VP1-3 results in accumulation of incoming DNA-containing capsids at the nuclear pore implicating VP1-3 in DNA release at the nuclear pore (Batterson et al., 1983; Ojala et al., 2000). The N-terminal 500 residues of VP1-3 function as deubiquitinating enzyme after cleavage from full-length VP1-3 (Kattenhorn et al., 2005).

Tegument proteins with established enzymatic activities are the protein kinases **UL13** and **US3**, the ribonucleotide reductase subunits **UL39** and **UL40,** and the RNase **UL41**, involved in shutt off of host protein synthesis (Smiley, 2004). Further tegument proteins are **US10**, **US11**, **UL14** and **UL11**, the latter being membrane-associated after posttranslational myristoylation. In contrast to the others, the tegument proteins US10 and US11 are not conserved across the neurotropic alphaherpesvirsuses (Davison and McGeoch, 1986; Klupp et al., 2004). Of these proteins, only the product of the late gene US11 was reported to interact with MT motors.

US11 binds to kinesin-1, the heavy chain of conventional kinesin, in affinity chromatography and GST-pull down assays (Diefenbach et al., 2002). During egress, axonal HSV1 capsids colocalize with kinesin-1, and the predicted cargo-binding domain of kinesin-1 binds the major capsid protein VP5, and the tegument proteins VP16, VP22 and US11 from an infected cell lysate (Diefenbach et al., 2002). With VP16 and VP22 also binding to US11, the latter is perceived as the direct binding partner of kinesin-1. US11 also interacts with PAT1 (protein interacting with amyloid precursor protein tail 1) in a region with sequence similarity to the cargo binding domain of kinesin light chains (Benboudjema et al., 2003). PAT1 is a nucleocytoplasmic host protein that binds to the cytosolic tail of amyloid precursor protein and to MTs in a nucleotide dependent manner, but it is unclear whether it can really function as an accessory subunit of a kinesin motor (Zheng et al., 1998). US11 genes are only found in the highly related alphaherpesviruses HSV1, HSV2, and simian B virus, but not in PRV or varicella zoster virus, which are also transported anterogradely during their life cycles (Davison and McGeoch, 1986; Smith et al., 2001; Ohsawa et al., 2002; Klupp et al., 2004). This raises the question which proteins of the latter viruses interact with kinesins in the absence of US11. During virus infection, protein kinase R can phosphorylate the eukaryotic initiation factor 2α, thereby blocking translation. US11 cooperates with the early viral gene product $\gamma_1$34.5 to overcome this antiviral response of the host and to ensure that viral protein synthesis continues (Mohr, 2004).

3.4.4.3 Potential motor receptors among the capsid and capsid-associated proteins

Of the bona fide **capsid proteins**, VP5, VP19C, VP23, VP24 and V26, **VP5** and **VP26** are located on the capsid surface, and therefore potentially accessible for direct or indirect interactions with MTs and/or MT motors. Other minor **capsid-associated proteins** involved in DNA cleavage and packaging are the portal protein **UL6** as well as **UL15, UL16, UL17** and the proposed capsid plug **UL25**. Of those, there is experimental data suggesting MT interactions for VP26 and for UL25.

VP26 is a basic, multiply phosphorylated protein with a molecular weight of 12 kDa (McNabb and Courtney, 1992b). It is located on the tips of the VP5 hexons, but not on the pentons (Booy et al., 1994; Trus et al., 1995; Zhou et al., 1995; Wingfield et al., 1997). VP26 is not essential for virus replication, but its deletion decreases virus yields twofold in cultured cells, as well as in a mouse infection model (Desai et al., 1998). HSV1-VP26 interacts with the 14 kDa dynein light chains

Tctex-1 and rp3 in yeast two-hybrid and GST-pulldown assays (Douglas et al., 2004). Moreover, after microinjection into cells, *in vitro* assembled capsids lacking VP26 show reduced nuclear targeting when compared to capsids containing VP26. However, after corneal infection of mice, HSV1-ΔVP26 is transported to the trigeminal ganglia, indicating that even in the absence of VP26, HSV1 is able to undergo retrograde transport (Desai et al., 1998).

UL25 is an essential capsid-associated protein supposed to seal the capsid after DNA packaging in the nucleus (Ogasawara et al., 2001; Sheaffer et al., 2001). The UL25 protein of PRV was reported to colocalize with MTs after transient transfection (Kaelin et al., 2000). Based on this observation a potential function in MT-mediated transport was proposed.

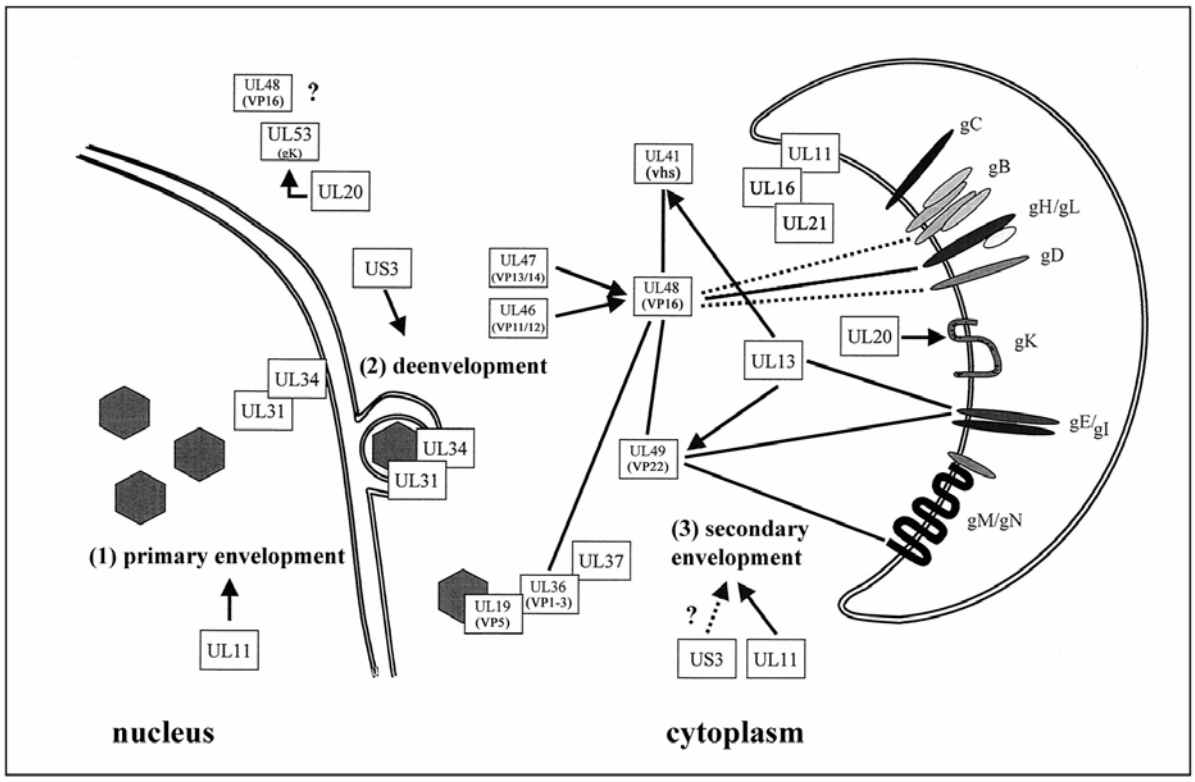

Figure 9: Interactions between HSV1 or PRV gene products during virus assembly. Solid lines or direct contacts between the rectangles representing the designated gene products indicate physical interactions. Arrows point to functional interactions. Dotted lines and question marks denote suggested, but not firmly established interactions or involvements of proteins. Between glycoproteins only direct contacts resulting in complex formation are depicted (Roizman and Knipe, 2001; Mettenleiter, 2002; Mettenleiter, 2003; Mettenleiter, 2004; Spear, 2004). The picture was taken from Mettenleiter, 2002 and modified by A. Wolfstein, Institute of Virology.

3.5 Life cell imaging of alphaherpesvirinae

Light and electron microscopy of fixed cells has provided elementary information on the function of MTs and MT motors during the life cycle of many viruses. However, with recombinant fluorescent

proteins and sensitive digital cameras it is now possible to analyze the dynamics of motile virus particles in living cells.

Nuclear targeting has been demonstrated *in vivo* with green fluorescent protein (GFP)-VP26-tagged PRV in neurons (Smith et al., 2004), GFP-Vpr-tagged HIV (McDonald et al., 2002), GFP-UL32-tagged HCMV (Sampaio et al., 2005), fluorescent dyes directly coupled to Ad, simian virus 40 or adeno-associated virus (Suomalainen et al., 1999; Leopold et al., 2000; Seisenberger et al., 2001) or intercalated in the membrane of influenza virus (Lakadamyali et al., 2003). Transport during egress has been shown *in vivo* using GFPVP26-tagged PRV in neurons (Smith et al., 2001), and VV containing GFP fused to the membrane proteins F13L or B5R (Geada et al., 2001; Hollinshead et al., 2001; Rietdorf et al., 2001; Ward and Moss, 2001a; Ward and Moss, 2001b).

To analyze the transport of HSV1 virions and subviral particles, fluorescent proteins have been attached to several structural proteins: VP22 (Elliott and O'Hare, 1999), VP16 (Bearer et al., 2000; La Boissiere et al., 2004), VP13/14 (Donnelly and Elliott, 2001), and VP11/12 (Willard, 2002). Moreover, the small capsid protein VP26 was tagged with GFP or monomeric red fluorescent protein (mRFP) and reintroduced into HSV1 (Desai and Person, 1998; Nagel, Fathollahy, Strive, Borst, Messerle, and Sodeik; manuscript in preparation), PRV (Smith et al., 2001; del Rio et al., 2005) and bovine herpesvirus (Wild et al., 2005). HSV1-GFPVP26 is very well suited for *in vivo* experiments, since VP26 is not essential for virus replication in cultured cells (Desai et al., 1998) and the incorporation of GFPVP26 does not significantly disturb virus assembly (Desai and Person, 1998). Furthermore, VP26 stays on the capsid until it reaches the nucleus (our unpublished observations), while several tegument proteins are lost from incoming capsids (Sodeik et al., 1997; Morrison et al., 1998; Granzow et al., 2005; Luxton et al., 2005).

After injection into squid axons VP16GFP containing detergent stripped HSV1 particles moved exclusively in the retrograde direction with a mean velocity of 2.2 µm/s (Bearer et al., 2000). In contrast, during entry into axons PRV particles underwent bidirectional and saltatory movement to the cell body (Smith et al., 2004). Retrograde and anterograde runs during entry had average velocities of 1.2 µm/s and 0.6 µm/s, respectively. Bidirectional transport was also observed during egress of PRV, but in this situation transport to the axon terminals predominated (Smith et al., 2001). During egress, retrograde and anterograde runs had average velocities of 1.3 µm/s and 2 µm/s, respectively. These data indicate that the net transport to the cell body during entry and to the axon terminal during exit is probably regulated by modulation of the plus-end directed motor (Smith et al., 2004).

3.6 Aim of the study

During entry, HSV1 capsids are transported along MTs to the MTOC which lies close to the nucleus in many cell types (Kristensson et al., 1986; Lycke et al., 1988; Hammonds et al., 1996; Topp et al., 1996; Sodeik et al., 1997; Mabit et al., 2002; Marozin et al., 2004). Electron microscopy studies revealed that incoming capsids colocalize with cytoplasmic dynein implicating dynein in minus-end directed transport of HSV1 capsids (Sodeik et al., 1997).

Moreover, during my diploma thesis I showed that nuclear targeting of HSV1 capsids and viral immediate-early gene expression were reduced in transfected cells expressing high levels of dynamitin, a subunit of the dynein cofactor dynactin. One task during this Ph.D. thesis was to confirm and more importantly to quantify the effect of dynamitin overexpression on nuclear targeting and viral immediate early gene expression. Furthermore, it was investigated whether reduced nuclear targeting was due to an effect of excess dynamitin on virus binding, on virus internalization, on the MT cytoskeleton, or on cytosolic capsid transport. Since dynamitin overexpression affects the endocytic and the secretory pathway (Burkhardt et al., 1997; Presley et al., 1997; Valetti et al., 1999), it may alter cell surface expression of HSV1 receptors, and consequently virus binding and/or internalization. Dynactin is involved in MT anchoring at the MTOC, and excess dynamitin affects the MT organization in several cell types to different extent (Burkhardt et al., 1997; Quintyne et al., 1999; Quintyne and Schroer, 2002). Therefore, I compared the MT organization of untransfected PtK_2 cells and PtK_2 cells overexpressing dynamitin. Another idea was to further analyze the colocalization of incoming capsids with antibodies to several dynein and dynactin subunits.

In addition to the cellular requirements for HSV1 transport, our group wants to identify viral factors required for efficient nuclear targeting. Therefore, we characterized the nuclear targeting of several viral mutants lacking potential viral motor receptors. To compare different viral strains in their entry behavior, the particle composition of different viral inocula had to be characterized quantitatively. Therefore, another aim of this Ph.D. thesis was to optimize the preparation of purified virus to be used for entry experiments, to compare several methods for quantification of virus preparations, and to develop rational criteria for evaluating the quality of virus preparations.

To analyze the intracellular transport of HSV1 in living cells and in *in vitro* motility assays, we wanted to use digital time lapse microscopy and HSV1-GFPVP26, in which the small capsid protein VP26 was replaced by GFPVP26 (Desai and Person, 1998). A potential dynein receptor among the HSV1 proteins is VP26 that interacts with the 14 kDa dynein light chains Tctex-1 and rp3 in yeast two hybrid and GST-pulldown assays (Douglas et al., 2004). Therefore, I characterized the cell entry of HSV1-GFPVP26 (Desai and Person, 1998) and HSV1-ΔVP26 (Desai et al., 1998), which is deleted for the putative dynein receptor VP26. I analyzed viral immediate-early gene expression and capsid transport of HSV1-GFPVP26 and HSV1-ΔVP26 in the presence and absence of MTs, and the capsid transport after overexpression of dynamitin-GFP.

4 Discussion

4.1 MTs are required for efficient nuclear targeting of Ad and HSV1

HSV1 enters many cell types by fusion at the plasma membrane, thereby releasing the capsid and the tegument into the cytosol (Koyama and Uchida, 1987; Lycke et al., 1988; Wittels and Spear, 1991; Sodeik et al., 1997; Nicola et al., 2003; Gianni et al., 2004; Nicola and Straus, 2004; Nicola et al., 2005). Part of the HSV1 and PRV tegument remains at the cytosolic side of the plasma membrane (Sodeik et al., 1997; Granzow et al., 2005; Luxton et al., 2005), while the capsid with residual tegument is transported along MTs to the MTOC (Sodeik et al., 1997). During entry, incoming HSV1 capsids colocalize with MTs (Lycke et al., 1988; Sodeik et al., 1997), and MT-depolymerizing drugs reduce nuclear targeting, viral gene expression and virus yields (Kristensson et al., 1986; Topp et al., 1994; Hammonds et al., 1996; Topp et al., 1996; Sodeik et al., 1997).

Spedies C Ad2 and 5 are taken up by clathrin-mediated endocytosis (Meier et al., 2002). After release from early endosomes, nuclear targeting of species C Ad also requires MTs, cytoplasmic dynein and dynactin (Greber et al., 1993; Suomalainen et al., 1999; Leopold et al., 2000). Ad2 moves in both directions, towards and away from the nucleus, but transport towards the nucleus predominates (Suomalainen et al., 1999). After depolymerization of MTs, motility of Ad2 and Ad5 is severely reduced (Suomalainen et al., 1999; Leopold et al., 2000).

In contrast to these observations, Glotzer and colleagues reported that depolymerization of MTs neither affected adenoviral gene expression, nor motility of adenoviruses, which were labeled with a GFP-tetracycline repressor fusion protein bound to operator sequences introduced into their genome (Glotzer et al., 2001). Furthermore, the authors claimed that depolymerization of MTs during infection prevented adenoviral accumulation around the MTOC, but did not abolish perinuclear localization of adenoviral particles. Since this study challenged the role of MTs during virus entry, the group of Prof. Urs Greber (University of Zürich, Switzerland) and our group reassessed the function of MTs during adenovirus and HSV1 infection (Mabit et al., 2002). In these studies HSV1 served as a positive control, since it had been well established that agents interfering with MT function reduce HSV1 gene expression.

The colleagues from Zürich analyzed Ad5 mediated transgene expression quantitatively with Ad5 expressing β-galactosidase or luciferase under the control of a CMV-promoter, which is constitutively active in eukaryotic cells (Mabit et al., 2002; Fig. 1). Efficient adenoviral gene expression after infection at 10 to 10,000 particles per cell required MTs, and the assays were linear in this range. The effect of the MT-depolymerizing drug nocodazole was reversible, it did not reduce cell viability, and when added at 3 h p.i., a time point when most Ad5 particles had already reached the nuclear envelope, nocodazole only marginally inihibited Ad-mediated transgene expression. Additionally, quantitative confocal fluorescence microscopy (Nakano and Greber, 2000) confirmed that MTs were required for efficient nuclear targeting of Texas-Red labeled Ad2 (Mabit et al., 2002; Fig. 2).

We analyzed HSV1-mediated transgene expression quantitatively using an HSV1 strain expressing β-galactosidase under the control of the HSV1 immediate-early promoter ICP4 (Warner et al., 1998). The amount of β-galactosidase expressed after HSV1 infection depended on the multiplicity of infection, and increased from 3 to 7 h of infection (Mabit et al., 2002; Fig. 3). Nocodazole reduced HSV1-mediated transgene expression in a concentration dependent manner, reaching maximal inhibition of about 90% at 25 μM in cells infected for 4 h with 10 plaque forming units per cell. Quantitative confocal fluorescence microscopy (Nakano and Greber, 2000) revealed that depolymerization of MTs strongly reduced nuclear targeting of HSV1 at 2 and 3 h of infection (Mabit et al., 2002; Fig. 4). Consistent with earlier studies (Kristensson et al., 1986; Sodeik et al., 1997), the MT-stabilizing drug taxol had no significant effect on nuclear accumulation of HSV1 suggesting that dynamic MTs and MT treadmilling were not required for efficient transport of HSV1. Nuclear targeting of Ad is even enhanced when MTs are stabilized (Giannakakou et al., 2002).

However, the inhibition of nuclear targeting and virus mediated gene expression was not complete in epithelial cells. Viral particles which enter from the plasma membrane proximal to the nuclear envelope are separated from the nucleus by only a few micrometers, and may cover this distance in the absence of an intact MT network (discussed in Sodeik et al., 1997). Ad particles are able to travel a few μm in the absence of MTs (Suomalainen et al., 1999; Glotzer et al., 2001). Thus, particles entering from the apical plasma membrane proximal to or above the nucleus will most likely not require MTs to reach the nucleus. In addition, actin-based transport or transport along short, randomly oriented MT filaments resistant to nocodazole might have accounted for the residual nuclear targeting activity and virus mediated gene expression in the absence of an intact MT network (discussed in Mabit et al., 2002).

Our results clearly demonstrated that MTs were required for efficient nuclear targeting of both, Ad and HSV1, and consequently for efficient Ad and HSV1 mediated transgene expression (Mabit et al., 2002). In this respect our findings contradict the results obtained by Glotzer and colleagues (2001), but confirm earlier studies on Ad (Suomalainen et al., 1999; Leopold et al., 2000) and HSV1 (Kristensson et al., 1986; Topp et al., 1994; Hammonds et al., 1996; Topp et al., 1996; Sodeik et al., 1997) showing a role for MT-mediated transport during cell entry. While we measured within the linear range of the β-galactosidase and luciferase assays (Mabit et al., 2002), Glotzer et al. (2001) did not report any studies on analyzing the linearity of their read-out.

In living cells, Ad2 and Ad5 motility over longer distances requires MTs (Suomalainen et al., 1999; Leopold et al., 2000; Suomalainen et al., 2001). MTs are also required for long range transport of HSV1 in living cells (Willard, 2002; Döhner, Büttner, Wolfstein, Prank, Ewers, and Sodeik; manuscript in preparation). In contrast to these results, Glotzer and coworkers (2001) did not observe fast minus-end directed transport of Ad particles. Instead they reported that Ad particles moved along similar paths and with similar velocities in the presense and absence of MTs. These conflicting results may be explained by different experimental set-ups. Compared to other studies (Suomalainen et al.,

1999; Leopold et al., 2000; Suomalainen et al., 2001; Döhner, Büttner, Wolfstein, Prank, Ewers, and Sodeik; manuscript in preparation), Glotzer et al. (2001) measured *in vivo* motility at room temperature, maintained the cells in phosphate buffered saline without nutrients during the experiments, recorded at lower temporal resolution, used a shorter wavelength of higher energy for excitation and longer exposure times, recorded from the middle of the cells, and analyzed a smaller data set (discussed in Mabit et al., 2002). At room temperature, the activity of molecular motors may be reduced compared to 37°C, and in the absence of nutrients the cells may be depleted of ATP. At low temporal resolution, fast movements are not detected, because unambiguous tracking is no longer possible. Furthermore, the shorter wavelength and extended exposure times may have lead to higher phototoxic damage resulting in lower motility. Tracking in the middle of the cells, where cells are elevated compared to the flat cell periphery, may have resulted in an apparent disappearance of moving particles due to translocation out of the focus plane.

In summary, the quantitative assays used in our study (Mabit et al., 2002), confirmed that MTs were required for efficient nuclear targeting of Ad and HSV1, and as a consequence for efficient expression of viral genes or virus mediated expression of transgenes.

4.2 Function of dynein and dynactin in HSV1 capsid transport

In epithelial cells and neurons, incoming HSV1 is transported along MTs to the MTOC (Kristensson et al., 1986; Lycke et al., 1988; Topp et al., 1994; Hammonds et al., 1996; Topp et al., 1996; Sodeik et al., 1997). This minus-end directed transport could be catalyzed by cytoplasmic dynein or by minus-end directed C-type kinesins. Although most C-type kinesins function during mitosis (Ovechkina and Wordeman, 2003), some are involved in cytoplasmic transport during interphase (Hanlon et al., 1997; Saito et al., 1997; Nielsen et al., 1999; Bananis et al., 2000; Noda et al., 2001; Xu et al., 2002; Bananis et al., 2003; Bananis et al., 2004; Brown et al., 2005).

EHNA (erythro-9-3-[2-hydroxynonyl]adenine), an inhibitor of axonemal and cytoplasmic dynein, blocks HSV1 infection in neuronal cells, suggesting a role for cytoplasmic dynein during retrograde axonal transport of HSV1 capsids (Kristensson et al., 1986). However, EHNA also affects adenosine deaminase, cGMP stimulated phosphodiesterase, and the actin cytoskeleton (Penningroth, 1986; Mery et al., 1995). In some cases, electron-dense material attached to the vertices of incoming HSV1 capsids has the dimensions and the shape of cytoplasmic dynein (Sodeik et al., 1997). Moreover, quantitative immunelectron microscopy with antibodies to the DHC revealed that incoming cytosolic HSV1 capsids colocalize with cytoplasmic dynein (Sodeik et al., 1997).

During this Ph.D. thesis, I analyzed the colocalization of incoming capsids with further dynein and dynactin subunits using immunofluorescence microscopy (Döhner et al., 2002; Fig. 1). Approximately 15 to 20% of incoming capsids were labeled with antibodies to dynein (15% for DIC) or dynactin (20% for $p150^{Glued}$). This incomplete colocalization might have been due to steric hindrance, and thus limited epitope access in a putative ternary complex of capsid, dynein, and dynactin. Moreover, it is

possible that only a subset of viral capsids bound to dynein and/or dynactin at any given time point. Consistently, in a time interval of about 5 min, only a fraction of about 10% of HSV1 particles underwent substantial movement in living cells (Döhner, Büttner, Wolfstein, Prank, Ewers, and Sodeik; manuscript in preparation). Because most dynein and dynactin subunits only exist in 20 S complexes and not as soluble proteins, these data showed that both protein complexes, namely dynein and dynactin, were at least transiently present on incoming capsids.

To test whether functional dynein and dynactin were required during HSV1 entry, I transfected cells with dynamitin. Overexpression of dynamitin disrupts the dynactin complex and inhibits dynein and kinesin-2 mediated transport (Echeverri et al., 1996; Burkhardt et al., 1997; Eckley et al., 1999; Valetti et al., 1999; Deacon et al., 2003). Overexpression of dynamitin-GFP reduced transgene expression after infection with HSV1 expressing β-galactosidase (Warner et al., 1998; Mabit et al., 2002) by 25% compared to overexpression of GFP alone (Döhner et al., 2002; Fig. 2). Single cell analysis by immunofluorescence microscopy confirmed that expression of the immediate-early HSV1 gene ICP4 was significantly reduced in cells overexpressing dynamitin (Döhner et al., 2002; Fig. 3).

Dynactin is involved in anchoring MTs at the MTOC (Quintyne et al., 1999; Quintyne and Schroer, 2002), and overexpression of dynamitin affects the organization of the MT-network in fibroblastic cells (Burkhardt et al., 1997; Quintyne et al., 1999). After overexpression of dynamitin in PtK_2 cells, MTs still emanated from the perinuclear region, but compared to control cells, there were less cells with a single, well-defined MTOC (Döhner et al., 2002; Fig. 4). Cells in which MTs emanated from a broad zone in the perinuclear area were also observed among untransfected cells, and nuclear targeting in these cells was as efficient as in cells with a well-defined MTOC. The organization of the actin cytoskeleton was not affected by dynamitin overexpression (not shown; Burkhardt et al., 1997). Therefore, the reduced immediate-early viral gene expression after overexpression of dynamitin was most likely not due to alterations in the cytoskeleton.

Since dynamitin overexpression affects the secretory and the endocytic pathway (Burkhardt et al., 1997; Presley et al., 1997; Valetti et al., 1999; Schroer, 2004) reduced immediate-early viral gene expression could have been due to impaired virus binding or internalization caused by altered expression of viral receptors on the cell surface. However, immunfluorescence microscopy (Döhner et al., 2002; Fig. 5), radioactive virus binding and virus internalization assays (Döhner et al., 2002; Fig. 6) showed that HSV1 binding and internalization were not reduced after overexpression of dynamitin. Thus, reduced immediate-early gene expression after dynamitin overexpression was not due to less efficient virus internalization. While virus internalization was not impaired, dynamitin overexpression reduced nuclear targeting of HSV1 by about 50%, and in cells expressing high levels of dynamitin even by 85% (Döhner et al., 2002; Fig. 7 and 8).

In summary, these data show that overexpressing dynamitin reduced nuclear targeting of HSV1, and as a consequence immediate-early viral gene expression. Reduced nuclear targeting and immediate-early viral gene expression by high amounts of dynamitin were not due to impaired virus

binding, virus internalization, or changes in the MT network, but rather caused by decreased cytosolic HSV1 capsid transport along MTs. The other target of dynamitin overexpression, kinesin-2, is a plus-end directed MT motor, and is therefore most likely not responsible for minus-end directed MT transport of HSV1. Therefore, our data suggest that incoming HSV1 capsids were propelled along MTs by dynein, and that dynein and dynactin were required for efficient HSV1 capsid transport to the nucleus.

4.3 Bidirectional HSV1 transport along MTs

While incoming capsids are distributed randomly over the entire cytoplasm at early time points (Sodeik et al., 1997), capsids in dynamitin overexpressing cells were often concentrated in peripheral parts of the cells at 3 h post infection (Döhner et al., 2002; Fig. 7 and 9). This peripheral accumulation depended on MTs, suggesting that a plus-end directed MT motor of the kinesin family might transport capsids to the cell periphery when dynein function was inhibited.

Peripheral accumulation of dynein cargo after overexpression of dynamitin or microinjection of function-blocking dynein antibodies is also observed with endosomes (Burkhardt et al., 1997; Valetti et al., 1999), adenoviral capsids (Suomalainen et al., 1999) and HIV reverse transcription complexes (McDonald et al., 2002). Thus, these structures can be transported by minus- and plus-end directed motors, and after inhibition of dynein, kinesins may take over and catalyze transport to the MT plus-ends.

Consistently, GFP-tagged PRV is transported bidirectionally during entry and egress in neurons (Smith et al., 2001; Smith et al., 2004) with a bias towards the cell body during entry. In contrast, transport to the synapse predominates during egress. Bidirectional transport of HSV1-GFPVP11/12 containing particles along MTs was also observed during assembly in Vero cells (Willard, 2002). Early during infection of PtK_2 cells, GFP-tagged HSV1 particles also moved towards and away from the nucleus (Döhner, Büttner, Wolfstein, Prank, Ewers and Sodeik; manuscript in preparation). Transport to the nucleus was more frequent, faster and proceeded over longer distances, finally resulting in accumulation of viral particles at the nuclear envelope. In contrast, detergent-extracted VP16-GFP tagged HSV1 particles moved exclusively in the retrograde direction after microinjection into squid axoplasm (Bearer et al., 2000). These conflicting results might reflect a different composition of mammalian versus invertebrate cytoplasm. Alternatively, detergent-treated HSV1 particles might differ in their composition from HSV1 particles which are present in cells after entry or after assembly.

As has been suggested for other cargo, plus-end directed HSV1 motility during entry could prevent being trapped in “traffic jams” on MTs. Alternatively plus-end directed motors could catalyze the translocation from the MTOC further to the nucleus. HSV1 capsids initially accumulate at the site of the nuclear envelope facing the MTOC (Döhner et al., 2002; Fig. 4; Everett et al., 2004) and later distribute over the entire nuclear envelope (Sodeik et al., 1997; Döhner et al., 2002). Similar

observations were reported for human foamy virus, a retrovirus, and Ad2 (Petit et al., 2003; Strunze et al., 2005). Kinesins could then mediate the transport from the MTOC further to the nuclear envelope. Interestingly, dynein and kinesin-1 can interact with members of the importin family (Mavlyutov et al., 2002; Hanz et al., 2003), and kinesin-1 interacts with RanBP2 which is located on cytoplasmic NPC fibrils (Cai et al., 2001). Importins transport cargo with nuclear localization signals through the NPC into the nucleus, whereas exportins convey cargo with nuclear export signals into the cytoplasm. The transport direction is regulated by the small GTPase Ran, and RanBP2 helps to dissassemble transport complexes after passage through the NPC (Pemberton and Paschal, 2005). Several cytosolic proteins bearing nuclear localization signals bind dynein and importin β, and are transported towards the nucleus along MTs (Mesika et al., 2005; Salman et al., 2005). These interactions might couple cytoplasmic transport and nucleocytoplasmic shuttling.

Kinesin-1 can interact with HSV1-US11, and axonal HSV1 capsids colocalize with kinesin-1 during egress (Diefenbach et al., 2002). Therefore, Jessica Janus and Simone Schmidt from our lab (Institute of Virology, Hannover Medical School) analyzed the subcellular localization of HSV1-ΔUS11 which is deleted for the potential kinesin-1 receptor US11 (Schmidt, 2003; Janus, 2005; Janus, Döhner, Schmidt, Nagel, Roller, and Sodeik; manuscript in preparation). HSV1-ΔUS11 required MTs and functional dynactin for efficient nuclear targeting. Like HSV1-wt, HSV1-ΔUS11 often accumulated in the periphery of dynamitin overexpressing cells, and this peripheral accumulation also required MTs. This shows that during cell entry, US11 was required neither for MT-dependent nuclear targeting in untransfected cells, nor for peripheral HSV1 accumulation after dynamitin overexpression. The interaction between US11 and kinesin-1 might rather be involved during assembly and egress (Diefenbach et al., 2002). However, only the highly related alphaherpesviruses HSV1, HSV2, and simian B virus, but not PRV or varicella zoster virus have genes coding for US11, nevertheless all these alphaherpesviruses are transported anterogradely during their life cycle (Davison and McGeoch, 1986; Smith et al., 2001; Ohsawa et al., 2002; Klupp et al., 2004). Therefore, other viral proteins besides US11 must provide receptors for plus-end directed kinesins.

Different motors could catalyze plus-end directed transport during different stages of the viral life cycle. Other cellular cargoes also switch between different MT motors: early endosomes use kinesin-1 for plus- and C-type kinesins for minus-end directed transport, while late endosomes use kinesin-2 for plus- and dynein for minus-end directed transport (Burkhardt et al., 1997; Nielsen et al., 1999; Valetti et al., 1999; Bananis et al., 2000; Bananis et al., 2003; Bananis et al., 2004; Brown et al., 2005).

Jessica Janus showed that incoming viral particles colocalized with kinesin-2, but not with kinesin-1 (Janus, 2005; Janus, Döhner, Schmidt, Nagel, Roller, and Sodeik; manuscript in preparation) suggesting that kinesin-2 might be involved in plus-end directed HSV1 transport during cell entry. In addition to dynein mediated transport, dynamitin overexpression inhibits kinesin-2 mediated transport of melanosomes (Deacon et al., 2003) and possibly other cargoes. Therefore, kinesin-2 is a less likely candidate to mediate the peripheral accumulation of HSV1 in dynamitin overexpressing cells.

To analyze transport after dynamitin overexpression in more detail, Jessica Janus infected living cells overexpressing dynamitin-mRFP with GFP-tagged HSV1. Preliminary experiments showed that after overexpression of dynamitin, no long range transport to the cell center or the cell periphery was observed (Janus, 2005; Janus, Döhner, Schmidt, Nagel, Roller, and Sodeik; manuscript in preparation). No HSV1 movement after dynamitin overexpression was consistent with dynein mediating minus-end, and kinesin-2 catalyzing plus-end directed transport during cell entry. However, it does not explain the peripheral accumulation of HSV1 often observed after dynamitin overexpression (Döhner et al., 2002; Schmidt, 2003; Janus, 2005). Similarly, endosomes accumulate in the cell periphery after dynamitin overexpression, but long distance transport of endosomes is also reduced, and bidirectional motility of lipid droplets is almost completely abolished under these conditions (Valetti et al., 1999). Valetti and colleagues speculated that the immediate effect of dynamitin overexpression might have been to initially inhibit dynein-based movement selectively, resulting in the dominance of plus end-directed movement for a short time (Burkhardt et al., 1997; Valetti et al., 1999). However, since they observed no plus-end directed particle movements in dynamitin overexpressing cells, they suggested that, at steady state, kinesin based motility is also inhibited. MT-dependent peripheral accumulation or retention of late endosomes and lysosomes might be explained by a latent MT plus-end binding activity (e.g., CLIP-170; Burkhardt et al., 1997; Valetti et al., 1999). A similar hypothesis might reconcile the apparently conflicting results that we obtained with HSV1. Further experiments are needed to test these hypotheses, to identify the motor(s) for plus-end directed motility during entry, and to characterize the composition of the peripheral HSV1 particles, and whether they represent cytosolic capsids, endocytosed virions, or cytosolic capsids taken up into autophagosomes (c.f. Outlook).

4.4 High quality virus preparations are required to analyze cell entry of HSV1

The small capsid protein VP26 can interact with the 14 kDa dynein light chains Tctex-1 and rp3 (Douglas et al., 2004). Microinjected recombinant viral capsids containing VP26 were reported to "congregate near the nuclear rim, while capsids lacking VP26 did not" (Douglas et al., 2004). Therefore, we analyzed the nuclear targeting of incoming HSV1-ΔVP26 capsids, which are deleted for VP26, and of HSV1-GFPVP26 capsids, which express GFPVP26 instead of VP26 (Desai et al., 1998; Desai and Person, 1998).

To be able to compare the entry of HSV1-wt (wildtype) with mutants, which may differ in the efficiency of virus assembly, and in the particle to plaque forming units (PFU) ratio, we analyzed several of our wildtype and mutant virus preparations by plaque assays, polymerase chain reaction (PCR), Coomassie stained polyacrylamid gels, immunoblots, electron and immunofluorescence microscopy. Different preparations of the same strain varied significantly with regard to their particle to PFU ratio (Döhner, Schmidt, Radtke, and Sodeik; manuscript in preparation, Table 1, c.f. Appendix). Virus preparations with a higher viral genome to PFU ratio also contained more viral

protein per PFU and showed a higher number of viral particles in electron microscopy. Since such preparations were also targeted to the nucleus less efficiently, they were considered to be of lower quality than preparations with a lower DNA, lower protein, and lower particle to PFU ratio (Döhner, Schmidt, Radtke, and Sodeik; manuscript in preparation, Table 1, Fig. 2 and 3). Based on these criteria, my best HSV1-ΔVP26 preparations were of lower quality than my best wildtype preparations. This was most likely due to the less efficient virus assembly of the mutants (Desai et al., 1998; Desai and Person, 1998; Desai et al., 2003). Nevertheless, HSV1-ΔVP26 of good preparations was efficiently transported to the nucleus (Döhner, Schmidt, Radtke, and Sodeik; manuscript in preparation, Fig. 3e). If I had compared a high quality preparation of HSV1-wt (Fig. 3a and c) with an HSV1-ΔVP26 preparation of lower quality (Fig. 3f), I might have concluded, that VP26 was required for efficient nuclear targeting. However, as discussed below, HSV1-ΔVP26 used MTs as HSV1-wt during cell entry. Therefore, it was crucial to use high quality virus preparation and to carefully characterize the inocula, especially when the entry of HSV1 mutants was to be analyzed.

4.5 The formation of hexon-specific VP5 epitopes requires VP26

VP26 is localized on VP5 hexons, but not on pentons, even if present in 8-fold molar excess (Booy et al., 1994; Zhou et al., 1994; Trus et al., 1995; Zhou et al., 1995; Wingfield et al., 1997). In contrast to HSV1-wt strains F and KOS, viral particles of HSV1-ΔVP26 and HSV1-GFPVP26 did not display VP5 epitopes 5C10 and 8F5, which are specific to mature hexons, while they were efficiently recognized by other anti-VP5 and anti-capsid antibodies (Döhner, Schmidt, Radtke, and Sodeik; manuscript in preparation, Fig. 4). This suggests that the formation of the mature hexon-specific 5C10 and 8F5 epitopes required VP26 during virus assembly, and it neither occured in the absence of VP26, nor in the presence of GFPVP26. Alternatively, HSV1-ΔVP26 and HSV1-GFPVP26 might contain mutations in VP5.

The formation of mature hexon-specific epitopes requires ATP (Dasgupta and Wilson, 1999), as does the assembly of VP26 onto the hexons of angularized capsids (Chi and Wilson, 2000). Nevertheless, it was unclear whether VP26 binding caused or was a consequence of mature hexon-specific epitope formation. My data now suggest that VP26 binding caused mature hexon-specific epitope formation, possibly by inducing conformational changes in VP5.

4.6 HSV1-ΔVP26 and HSV1-GFPVP26 require dynein/dynactin for efficient nuclear targeting

VP26 has been shown to interact with the 14 kDa DLCs Tctex-1 and rp3 in yeast two-hybrid and GST-pulldown assays (Douglas et al., 2004). Some Tctex-1 binding partners like DIC, parathyroid hormone receptor and CD155α contain a bipartite Tctex-1 binding motif, consisting of a proximal (K/R)(K/R)XX(K/R) and a distal VS(K/H)(T/S)X(V/T)(T/S)(N/Q)V motif (Sugai et al., 2003). However, in the latter motif, gaps of varying length need to be inserted and parts are missing in some Tctex-1 binding proteins. In contrast, some binding partners contain either only the proximal binding

motif (for example Doc2α and Doc2β and CD5; Mok et al., 2001), or the distal motif (rhodopsin; Tai et al., 1999).

The binding motifs for the VP26-rp3 and VP26-Tctex-1 interactions have so far not been mapped. However, VP26 contains neither the proximal, nor the distal Tctex-1 binding motif, and thus must bind via a motif to Tctex-1 which differs from the Tctex-1 binding motif of DIC. Therefore, Tctex-1 might simultaneously bind to HSV1 via VP26 and to the dynein complex via DIC, and the interaction between VP26 and Tctex-1 could contribute to dynein mediated MT transport of incoming HSV1 capsids. Thus, we tested the roles of MTs and dynein during entry of HSV1-ΔVP26 and HSV1-GFPVP26.

After infection with HSV1-ΔVP26 or HSV1-GFPVP26 efficient expression of the immediate-early HSV1 gene ICP0 required MTs (Döhner, Schmidt, Radtke, and Sodeik; manuscript in preparation, Fig. 5). Moreover, HSV1-ΔVP26 and HSV1-GFPVP26 capsids accumulated at the nuclear envelope of PtK_2 and Vero cells in a MT-dependent manner (Döhner, Schmidt, Radtke, and Sodeik; manuscript in preparation, Fig. 6 and 7). Compared to infection with HSV1-wt, the nuclear targeting of HSV1-ΔVP26 was slightly less efficient. This was most likely due to a higher proportion of defective particles in the virus preparations of the mutants.

To distinguish between cytosolic capsids and virions inside endosomes, I performed double-labeling experiments with anti-capsid antibodies and antibodies to the viral membrane protein gD. I assumed that virions inside endosomes will contain capsid as well as viral membrane antigens, while cytosolic capsids should not be labeled with gD-antibodies. After infection of PtK_2 cells with HSV1-wt, most of the capsid signal had already separated from the gD signal as early as 30 min post infection (Döhner, Schmidt, Radtke, and Sodeik; manuscript in preparation; Fig. 6d). At this time point, most capsids were still distributed over the entire cytoplasm, suggesting that in PtK_2 cells HSV1-wt traveled most of its way to the nucleus as a cytosolic capsid and not within endosomes.

However, at later time points, the gD signal was strongly diminished (Fig. 6e), and it was therefore no longer possible to determine whether capsid signals that did not colocalize with gD represented free cytosolic capsids or virions inside endosomes whose gD had been denatured or degraded by endosomal or lysosomal enzymes. After 30 min of infection with HSV1-ΔVP26, many capsid signals had also separated from the gD signal, but the fraction of particles containing both epitopes was higher if compared to wildtype infection (compare Fig. 6d and 6j). This might be due to more defective particles in the virus preparations which either bound, but did not enter cells, or were taken up by endocytosis.

While the entry mechanism into PtK_2 cells has not been elucidated, Vero cells are known to be productively infected after fusion at the plasma membrane (Sodeik et al., 1997; Nicola et al., 2003; Nicola and Straus, 2004). Since HSV1-ΔVP26 and HSV1-GFPVP26 required MTs for efficient nuclear targeting also in Vero cells (Fig. 7, g-l), most likely free cytosolic HSV1-ΔVP26 and HSV1-GFPVP26 capsids interacted with MTs via MT motor proteins. Even after endocytic uptake, capsids

are released from endosomes as early as 30 min p.i. (Nicola and Straus, 2004). At this early time point, the capsid signal was still distributed over the entire cytoplasm (Fig. 6 and 7), suggesting that even if the mutants had entered these cells by endocytosis, cytosolic capsids released from endosomes rather than virions inside endosomes were transported along MTs to the nucleus.

Moreover, HSV1-GFPVP26 capsids isolated from extracellular virions after detergent lysis moved along MTs in an *in vitro* motility assay which also contained Cy3 labeled MTs and membrane-free Xenopus cytosol (Wolfstein et al., 2006; movies S1-S5, Fig. 1 and 3, and Supplementary Fig. S2). *In vitro* motility of HSV1-GFPVP26 capsids required ATP and cytosolic factors (Wolfstein et al., 2006; Fig. 2 and Supplementary table S1), further supporting the hypothesis that HSV1-GFPVP26 capsids can interact directly with the cytosolic transport machinery in the absence of any membranes.

Taken together these data suggest that cytosolic capsids of HSV1-ΔVP26 and HSV1-GFPVP26 can be transported along MTs to the MTOC.

Dynein in cooperation with dynactin catalyzes most minus-end directed transport. However, some C-type kinesins can also convey cargo to the MT minus-ends during interphase (Hanlon et al., 1997; Saito et al., 1997; Nielsen et al., 1999; Bananis et al., 2000; Noda et al., 2001; Xu et al., 2002; Bananis et al., 2003; Bananis et al., 2004), and could therefore theoretically transport HSV1 to the nucleus in the absence of the potential dynein receptor VP26. To this end, I analyzed the subcellular localization of HSV1-ΔVP26 and HSV1-GFPVP26 in PtK_2 and Vero cells overexpressing dynamitin. In both cell lines, nuclear targeting was reduced by dynamitin overexpression (Döhner, Schmidt, Radtke, and Sodeik; manuscript in preparation; Fig. 8). Consistently, addition of recombinant dynamitin reduced the number of motile HSV1-GFPVP26 capsids in the *in vitro* motility assay (Wolfstein et al., 2006; Fig. 2 and Supplementary Table S1). Since kinesin-2, the other target of dynamitin overexpression, is a plus-end directed MT motor, it cannot convey HSV1 capsids to the MTOC in Vero and PtK_2 cells. To my knowledge, effects of dynamitin overexpression on minus-end directed kinesins were not reported. Function-blocking anti-dynamitin antibodies do not reduce binding of early endosomes to MTs, which is mediated by kinesin-1 and the minus-end directed kinesin KIFC2. However, they do reduce binding of late endosomes to MTs which is mediated by dynein and kinesin-2 (Bananis et al., 2004; Brown et al., 2005). This suggests that interfering with dynactin function does not disturb the interaction of at least KIFC2 with its cargo and MTs.

Although I cannot completely exclude that minus-end directed kinesins contributed to nuclear targeting of HSV1, I think that it is more likely that dynein in cooperation with its cofactor dynactin catalyzed the transport of HSV1-ΔVP26 and HSV1-GFPVP26 to the nucleus. My data are in line with results from Desai and coworkers (1998) who showed that in the mouse ocular model, transport to the trigeminal ganglia is not reduced in the absence of VP26. This is consistent with my finding that VP26 has no important function in minus-end directed MT transport during cell entry. Instead, the potential interaction between VP26 and the dynein light chains might play a role during HSV1 assembly, when cytosolic capsids are transported to the site of secondary budding (Mettenleiter, 2002; Mettenleiter,

2004). However, in an *in vitro* binding assay, capsids from HSV1-ΔVP26 and HSV1-GFPVP26 bound dynein and dynactin from Xenopus cytosol as efficiently as capsids from HSV1-wt (Wolfstein et al., 2006; Fig. 4). In summary, our data indicate that HSV1-ΔVP26 and HSV1-GFPVP26 cytosolic capsids use cytoplasmic dynein and dynactin for MT transport to the nucleus as HSV1-wt does. Therefore, HSV1-GFPVP26 is an excellent model to study MT-mediated transport in living cells (Döhner, Büttner, Wolfstein, Prank, Ewers, and Sodeik; manuscript in preparation) and *in vitro* (Wolfstein et al., 2006).

Furthermore, compared to nuclear capsids which contained VP26 but little tegument, and to low salt extracted capsids with inner and outer tegument, high salt extracted capsids that had partially lost their outer tegument showed the strongest motility along MTs and the best binding of dynein and dynactin (Wolfstein et al., 2006; Fig. 3 and 4 and Supplementary Figure S3). High salt extracted viral capsids still contained the inner tegument proteins VP1-3 and UL37 as well as VP16 which might connect inner and outer tegument. This suggests that inner tegument proteins like VP1-3, UL37 or US3 or the potential linker VP16 might mediate motor binding and motility along MTs (Wolfstein et al., 2006). Altogether our data argue that besides VP26, HSV1 must encode at least one additional receptor for dynein or dynactin, and that HSV1 inner tegument proteins are likely candidates.

5 Conclusions

After entry at the presynapse, the neurotropic alphaherpesvirus herpes simplex virus (HSV1) moves retrogradely to the neuronal nucleus, where it eventually establishes a latent infection. After reactivation from latency, progeny virus travels anterogradely to the synapse (Enquist et al., 1998). Thus, HSV1 is conveyed over long distances and requires efficient active transport during pathogenesis. We developed tools to analyze MT transport quantitatively and to identify MT motors recruited by HSV1.

In summary, we confirmed with quantitative assays that MTs are required for efficient nuclear targeting and immediate early gene expression of Ad and HSV1 in nonpolarized epithelial cells (Mabit et al., 2002). This is consistent with earlier studies in epithelial and neuronal cells (Kristensson et al., 1986; Lycke et al., 1988; Topp et al., 1994; Hammonds et al., 1996; Topp et al., 1996; Sodeik et al., 1997; Suomalainen et al., 1999; Leopold et al., 2000).

Incoming HSV1 capsids colocalized with the minus-end directed MT motor dynein and its cofactor dynactin (Sodeik et al., 1997; Döhner et al., 2002). Overexpression of the dynactin cofactor dynamitin, which inhibits dynein and kinesin-2 catalyzed transport, reduced nuclear targeting of HSV1 capsids, and consequently immediate-early viral gene expression. The reduced nuclear targeting in dynamitin overexpressing cells was not due to impaired virus binding, virus internalization, or the slight changes in the MT network. Since kinesin-2 is a plus-end directed motor, reduced minus-end directed transport after dynamitin overexpression was most likely due to interference with dynein function. Therefore, dynein and its cofactor dynactin mediate efficient nuclear targeting of wildtype HSV1 (Döhner et al., 2002).

After overexpression of dynamitin, viral particles accumulated in the cell periphery in some cells (Döhner et al., 2002). This peripheral accumulation required MTs suggesting that it was mediated by a plus-end directed motor of the kinesin family. Minus- and plus-end directed motility was also observed early in infection in living cells (Döhner, Büttner, Wolfstein, Prank, Ewers, and Sodeik, manuscript in preparation), further supporting the idea that already early in infection HSV1 can engage with minus- and plus-end directed motors.

Characterization of several virus preparations of HSV1-wildtype and mutants showed that high quality virus preparations with a low particle to PFU ratio were required for a meaningful evaluation and interpretation of cell entry experiments (Döhner, Schmidt, Radtke, and Sodeik; manuscript in preparation).

VP26 can interact with the 14 kDa dynein light chains Tctex-1 and rp3 (Douglas et al., 2004), and this interaction might contribute to MT-mediated transport of HSV1. Therefore, I analyzed nuclear targeting of HSV1-ΔVP26 and HSV1-GFPVP26 (Desai et al., 1998; Desai and Person, 1998). Both viral strains required MTs for efficient nuclear targeting and efficient expression of immediate-early viral genes (Döhner, Schmidt, Radtke, and Sodeik; manuscript in preparation). Nuclear targeting was reduced by overexpression of dynamitin, suggesting that it was mediated by cytoplasmic dynein and

its cofactor dynactin. Moreover, capsids of HSV1-ΔVP26 and HSV1-GFPVP26 bound dynein and dynactin as efficiently as wildtype capsids (Wolfstein et al., 2006). In summary, these data suggest that besides VP26, HSV1 encodes at least one other receptor for dynein or dynactin.

Our *in vitro* motility assay showed that envelope-free capsids of HSV1-GFPVP26 moved along Cy3-labeled MTs (Wolfstein et al., 2006). This motility required ATP and cytosolic factors including functional dynactin, but neither actin filaments nor membranes. Capsids which have partially lost their outer tegument bound more dynein and dynactin and moved more frequently along MTs *in vitro* than capsids with no tegument and capsids with inner and outer tegument (Wolfstein et al., 2006). This suggests that inner tegument proteins like VP1-3, UL37, and US3 as well as VP16, which might link inner and outer tegument, are likely candidates for motor receptors of HSV1.

In summary, our data show that MTs, cytoplasmic dynein and dynactin mediate nuclear targeting of HSV1-wt, HSV1-ΔVP26 and HSV1-GFPVP26. Our data suggest, that besides the potential dynein receptor VP26, HSV1 must encode at least one additional receptor for dynein or dynactin, and that HSV1 inner tegument proteins are likely candidates for this function.

6 Outlook

We already started to use HSV1-GFPVP26 to analyze the early phases of HSV1 infection in living cells (Döhner, Büttner, Wolfstein, Prank, Ewers, and Sodeik; manuscript in preparation). To be able to distinguish between diffusion and restricted diffusion from directed movement, the data can be further analyzed by calculating the mean square displacement, and the slope of the moment scaling spectrum as described by Ewers et al. (2005). Furthermore, drugs which depolymerize MTs or actin filaments will help to discriminate between passive diffusion and active motility along MTs or actin filaments, and to determine whether the cytoskeleton confines diffusion. In the future, we will perform *in vivo* motility assays in the presence of dynamitin, dominant-negative kinesin constructs, after knockdown of molecular motors by small interfering RNAs, or after injection of function-blocking antibodies against motor proteins, adaptors like dynactin or against nucleocytoplasmic shuttling factors. This will hopefully allow us to determine if and how these factors contribute to HSV1 nuclear targeting. Transport from the MTOC further to the nucleus has to be analyzed in living cells rather than in fixed samples. For these experiments, we plan to engineer an HSV1 tagged with a photoactivable GFP (Patterson and Lippincott-Schwartz, 2002) which would allow selective visualization of particles on their way from the MTOC to the nucleus.

In vivo and *in vitro* motility assays with GFP- or mRFP-tagged HSV1 deleted for or mutated in candidate viral genes will help us to define the viral requirements for intracellular transport. Defined viral mutants will be constructed using the bacterial artificial chromosome (BAC) containing the entire HSV1 genome that was recently generated in our lab (Nagel, Fathollahy, Strive, Borst, Messerle, and Sodeik; manuscript in preparation).

To be able to interprete the *in vivo* motility and the cell infection experiments correctly, it is imperative to determine whether cytosolic capsids, capsids attached to the cytosolic surface of endosomes, or virions inside endosomes are tracked. While HSV1 infects many cell types by fusion of the viral envelope and the plasma membrane (Koyama and Uchida, 1987; Lycke et al., 1988; Wittels and Spear, 1991; Sodeik et al., 1997; Nicola et al., 2003; Gianni et al., 2004; Nicola and Straus, 2004; Nicola et al., 2005), other cells are productively infected after entry by endocytosis (Nicola et al., 2003; Gianni et al., 2004; Nicola and Straus, 2004; Milne et al., 2005; Nicola et al., 2005). Since the entry mechanism into PtK_2 cells that we used for *in vivo* and many other microscopic experiments has not been elucidated, it is so far unclear whether the moving GFP particles that I analyzed in living cells are cytosolic capsids, capsids attached to the cytosolic surface of membrane-bound organelles or virions inside endosomes (Döhner, Büttner, Wolfstein, Prank, Ewers, and Sodeik; manuscript in preparation). Similarly, it is not formerly proven, although highly likely that the viral particles that I studied in fixed PtK_2 cells were free cytosolic capsids, and not virions inside endosomes (c.f. 2.6). Therefore, many of my conclusions rely on similar observations made in Vero cells, which are productively infected after fusion at the plasma membrane (Sodeik et al., 1997; Nicola et al., 2003; Nicola and Straus, 2004).

To further analyze the entry mechanism into PtK_2 cells, I performed double-labeling experiments using endocytic markers like clathrin, early endosomal antigen 1, lysophosphatidic acid, cation-independent mannose-6-phosphate receptor and caveolin. Although some incoming HSV1 particles colocalized with each of these markers, the majority did not, suggesting that HSV1-wt, HSV1-ΔVP26 and HSV1-GFPVP26 were not taken up by clathrin or caveolin mediated endocytosis. Since these experiments were not performed with high quality virus preparations, they have to be repeated before further conclusions can be drawn.

In first electron microscopy experiments with PtK_2 cells, I found cytosolic HSV1-wt capsids as well as virions inside vesicles after 1 h of infection. Vesicles often contained several viral particles. Fusion intermediates with the plasma membrane were not observed. These experiments have to be extended to earlier time points like 5 and 15 min p.i. using Vero and PtK_2 cells, and comparing HSV1-wt with HSV1-ΔVP26 and HSV1-GFPVP26 infection. It is possible that some HSV1 particles are taken up by endocytosis, but that this is rather a dead-end than an infectious pathway as described for Vero cells (Sodeik et al., 1997).

Furthermore, I used several inhibitors of endosomal acidification (ammonium chloride and bafilomycin A) and endosomal trafficking (phosphatidylinositol 3-kinase inhibitor wortmannin) in PtK_2, HeLa and Vero cells. Since Vero cells are entered by fusion at the plasma membrane, and HeLa cells are productively infected after endocytosis (Sodeik et al., 1997; Nicola et al., 2003; Gianni et al., 2004; Nicola and Straus, 2004), these two cell types served as controls. So far, I was unable to reproduce the effects of the drugs as described in the literature (Nicola et al., 2003; Gianni et al., 2004; Nicola and Straus, 2004). The reasons for this are unclear, but may simply reflect a different HeLa cell clone or some other differences in the experimental set-up. Therefore, I will further optimize these assays. However, wortmannin did not reduce nuclear targeting and immediate early gene expression of HSV1 in Vero and PtK_2 cells, suggesting that PtK_2 cells were also productively infected with HSV1 by fusion at the plasma membrane.

Interestingly, the macropinocytosis inhibitor amiloride reduced immediate-early HSV1 gene expression, and its effect was highest in HeLa cells and lowest in Vero cells, wheras PtK_2 cells showed an intermediate sensitivity to amiloride. However, amiloride causes the cytoplasm to become more alkaline, and this might affect other cellular structures and functions besides membrane ruffling and macropinocytosis. In addition, macropinocytosis should also have been inhibited by wortmannin (Sieczkarski and Whittaker, 2002), but wortmannin did not affect nuclear targeting of HSV1 in my experiments. Therefore, further experiments are required to elucidate the HSV1 entry mechanism into PtK_2 cells.

Endocytosis can be more specifically inhibited by dominant-negative constructs or function-blocking antibodies. Dominant-negative dynamin constructs inhibit clathrin as well as caveolin mediated endocytosis. Clathrin mediated endocytosis can be specifically blocked by function-blocking anti-clathrin antibodies or by overexpressing dominant-negative Eps15 mutants, clathrin hub domain

or AP-2 μ2 subunit (Sieczkarski and Whittaker, 2002). Caveolae mediated endocytosis can be specifically inhibited by overexpressing dominant-negative caveolin (Pelkmans et al., 2001). Overexpression of Rab GTPase mutants affects endosome motility more specifically than wortmannin (Sieczkarski and Whittaker, 2002). In the future, I will use such constructs to further analyze the entry into PtK_2 and HeLa cells.

To address the question whether cytosolic capsids or virions inside endosomes are transported along MTs in PtK_2 cells, living cells could be incubated with rhodamine-labeled dextran and HSV1-GFPVP26. Dextran labels macropinosomes with highest efficiency because of their high volume, but should also stain other endocytic organelles (Renate Fuchs, Center for Physiology and Pathophysiology, Medical University of Vienna; personal communication). Alternating recording of GFP and rhodamine signals with a high temporal resolution should reveal, whether moving GFP particles colocalize with rhodamine-dextran. If GFP particles not colocalizing with rhodamine-dextrane required MTs for long distance transport, this would demonstrate that cytosolic capsids rather than virions inside endosomes moved along MTs in PtK_2 cells. Since dynamitin overexpressing cells can be identified by an altered localization of endosomes (Burkhardt et al., 1997; Valetti et al., 1999), this experiment could also be performed to characterize, whether viral particles in the periphery of dynamitin overexpressing cells are cytosolic capsids or virions inside endosomes.

Additionally, HSV1 labeled with different dyes in its membrane and at its capsid would also allow us to differentiate between cytosolic capsids and endosomal virions in living cells. Triple-labeled virions with fluorescent tags on viral DNA, capsid and viral membrane would eventually even allow us to follow viral DNA release into the nucleus in living cells. Falk Büttner started to prepare such a virus during his diploma thesis using a similar approach as described by McDonald et al. (2002) and Lakadamyali et al. (2003). He used HSV1-GFPVP26 and the fluorescent dye DiD (1,1´-dioctadecyl-3,3,3´,3´-tetramethylindodicarbocyanine), and could show that such an approach is feasible. Moreover, he was able to stain herpesviral DNA with Hoechst 33258 (Büttner, 2004). Further optimization of the labeling conditions should enable us to achieve efficient double and triple labelings while preserving viral infectivity at the same time. In addition, the envelope of HSV1-GFPVP26 could be labeled with quantum dots (Lidke et al., 2004) or fluorochromes (Suomalainen et al., 1999; Leopold et al., 2000; Pelkmans et al., 2001; Seisenberger et al., 2001).

Another idea is to construct a virus with a GFP-tagged VP26 and an mRFP-tagged viral membrane protein or vice versa. Recently, the successful construction of infectious HSV1 tagged with GFP on the viral glycoprotein gB or gD was reported (Potel et al., 2002; Milne et al., 2005).

The *in vitro* motility assay consisting of envelope-free capsids derived from HSV1-GFPVP26, Cy3-labeled MTs and membrane-free Xenopus cytosol (Wolfstein et al., 2006) avoids the difficulties in discriminating between cytosolic capsids and virions inside endosomes. This *in vitro* assay can be further developed by the use of polarity-marked MTs, which would allow a distinction between plus- and minus-end directed motility. Then, several inhibitors of dynein and kinesin, such as EHNA,

vanadate (dynein), AMP-PNP (adenosine 5´-(β,γ-imido)triphosphate) or adociasulfate (kinesin) could be applied. More specifically, function-blocking antibodies against dynein, dynactin or several kinesins or immunodepletion of cytosolic components could be used to further dissect the cytosolic requirements for HSV1 capsid transport. Addition of excess dynamitin will also be more instructive in an *in vitro* assay with MTs of known polarity. In the future, it should also be possible to reconstitute *in vitro* motility using purified cytosolic factors instead of cytosol which is a complex mixture of many components.

The molecular requirements on the viral side can be analyzed by using capsids derived from HSV1 mutants with deletions in putative motor receptors generated by mutagenesis of a bacterial artificial chromosome containing the HSV1 genome (Nagel, Fathollahy, Strive, Borst, Messerle, and Sodeik; manuscript in preparation). Moreover, capsids isolated from synaptosomes which resemble the presynapse and thus the typical entry site during natural infection could be used for the *in vitro* motility assay (Borsutzky, 2000; Nagel, 2002; Nagel, Borsutzky, Wolfstein, Bauerfeind, and Sodeik; manuscript in preparation). With immunofluorescence and live cell imaging experiments, the *in vitro* motility and binding assays, and the possibility to generate specific HSV1 mutants we have now the platform to identify the viral proteins required for transport along MTs and their cellular interaction partners. Live cell imaging will reveal the dynamics of intracellular HSV1 transport, and since HSV1 moves to the MT minus- or plus-ends depending on the stage of the viral life cycle, it is the ideal cargo to study how the direction of MT transport is regulated.

7 Acknowledgements

First of all, I would like to thank HD PD Dr. Beate Sodeik for giving me the opportunity to work on this fascinating project, for the scientific education I obtained in her lab, for her encouragement especially in difficult times, and for many scientific and personal discussions. During the years in Beate's lab I became more and more excited by the cell biology of virus infection.

I wish to thank Prof. Dr. Ernst Ungewickell and HD PD Dr. Beate Sodeik for being referees for my thesis, and Prof. Dr. Ernst Ungewickell, Prof. Dr. Rita Gerardy-Schahn, HD PD Dr. Beate Sodeik and PD Dr. Bernd Hitzmann for being examiners for my disputation.

I am greatly indepted to Prof. Dr. Thomas F. Schulz and Dr. Rudi Bauerfeind for many helpful discussions and critical readings of our manuscripts. Furthermore, I thank Rudi for his advice on deconvolution and electron microscopy, and on the use of drugs affecting the endocytic pathway.

I am thankful to Kristina Theusner, Kerstin Radtke, Jessica Janus, Claus-Henning Nagel, Kathrin Rode, André Wolfstein, and Julia Schipke for proof-reading my thesis. Thank you very much, it was a great help!

Furthermore, I would like to express my gratitude to Claus-Henning Nagel for performing the plaque-assays, Sabine Hübner for carrying out the real-time detection PCR, and Ute Prank, Jessica Janus and Kathrin Rode for assisting me with immunofluorescence experiments. Doris Meder (now at the University of Zürich, Switzerland) and Ute Prank set up the quantitative beta-galactosidase assay in our lab. Thank you very much! I thank Kathrin Rode for planning our first electron microscopic experiment, Prof. Dr. Ernst Ungewickell for giving me the opportunity to use the electron microscope in his department, Elke Mallon and Christiane Lemke for cutting my specimens, and Gerd Preiss for his help with the electron microscope and for developing my pictures. I am thankful to André Wolfstein for explaining the secrets of digital time lapse microscopy and image editing with Metamorph, for many discussions about the interpretation of motility experiments and for writing programs for the analysis of motility data. Falk Büttner is acknowledged for performing and analyzing *in vivo* experiments, Simone Schmidt for investigating the viral immediate-early gene expression of HSV1 mutants and Kerstin Radtke for characterizing several virus preparations by electron microscopy. Many thanks to Kathrin Rode und Claus-Henning Nagel for their help with analyzing the VP26 sequence regarding potential Tctex-1 binding motifs.

Furthermore, I would like to thank P. Desai (Johns Hopkins University School of Medicine, Baltimore, Maryland, USA) for HSV1-ΔVP26 and HSV1-GFPVP26, P.G. Spear (Feinberg School of Medicine of Northwestern University, Chicago, USA) for HSV1-wt strain KOS and the mutant strain HSV[KOS]tk12, and Bernard Roizman (University of Chicago, Chicago, USA) for the mutant strain R7202 deleted for the HSV1-Fc-receptor.

Denis Dujardin, Christophe Echeverri and Richard Vallee (Columbia University, New York, USA) are acknowledged for many helpful discussions and for providing dynamitin expression constructs and dynein antibodies. Melissa Gee (Applied Biosystems, California, USA), Kevin Vaughan (University

of Notre Dame, Notre Dame, USA), Bernhard Hoflack (Bioinnovation Centre - Proteomics, Technical University of Dresden, Dresden, Germany), Roselyn Eisenberg, Gary Cohen (both at the University of Pennsylvania, Philadelphia, USA), Bill Newcomb, Jay Brown (both at the University of Virginia, Charlottesville, USA), Roger Everett (MRC Virology Unit, Glasgow, Scotland), A.C. Minson (University of Cambridge, Cambridge, United Kingdom), Ari Helenius (Institute of Biochemistry, Swiss Federal Institute of Technology, Zürich, Switzerland) and the late Thomas Kreis (University of Geneva, Switzerland) all graciously provided antibodies. Jürgen Wehland (Gesellschaft für Biotechnologische Forschung, Braunschweig, Germany) generously provided the PtK_2 cells and Patrick Keller the YFP-tubulin-PtK_2 cells (Max Planck Institute of Molecular Cell Biology and Genetics, Dresden, Germany).

I thank all members of the Sodeik lab for the great working atmosphere and many enjoyable parties and Laborstammtische.

My parents Gabriele and Manfred Döhner, my mother-in-law Gabriele Rosemeyer and my husband's aunt Gudrun Blaack cared for our children during my husband's and my working hours. Thank you very much! Without your help, I would have never finished this thesis!

Finally, I thank my husband Michael Rosemeyer, my parents Gabriele and Manfred Döhner and my sister Natascha Langner for their love and support.

8 References

Al-Bassam, J., Cui, Y., Klopfenstein, D., Carragher, B.O., Vale, R.D. and Milligan, R.A. (2003) Distinct conformations of the kinesin Unc104 neck regulate a monomer to dimer motor transition. *J Cell Biol*, 163, 743-753.

Alconada, A., Bauer, U., Sodeik, B. and Hoflack, B. (1999) Intracellular traffic of herpes simplex virus glycoprotein gE: characterization of the sorting signals required for its trans-Golgi network localization. *J Virol*, 73, 377-387.

Alonso, C., Miskin, J., Hernaez, B., Fernandez-Zapatero, P., Soto, L., Canto, C., Rodriguez-Crespo, I., Dixon, L. and Escribano, J.M. (2001) African swine fever virus protein p54 interacts with the microtubular motor complex through direct binding to light-chain dynein. *J Virol*, 75, 9819-9827.

Avitabile, E., Di Gaeta, S., Torrisi, M.R., Ward, P.L., Roizman, B. and Campadelli-Fiume, G. (1995) Redistribution of microtubules and Golgi apparatus in herpes simplex virus-infected cells and their role in viral exocytosis. *J Virol*, 69, 7472-7482.

Baas, P.W., Deitch, J.S., Black, M.M. and Banker, G.A. (1988) Polarity orientation of microtubules in hippocampal neurons: uniformity in the axon and nonuniformity in the dendrite. *Proc Natl Acad Sci U S A*, 85, 8335-8339.

Bananis, E., Murray, J.W., Stockert, R.J., Satir, P. and Wolkoff, A.W. (2000) Microtubule and motor-dependent endocytic vesicle sorting in vitro. *J Cell Biol*, 151, 179-186.

Bananis, E., Murray, J.W., Stockert, R.J., Satir, P. and Wolkoff, A.W. (2003) Regulation of early endocytic vesicle motility and fission in a reconstituted system. *J Cell Sci*, 116, 2749-2761.

Bananis, E., Nath, S., Gordon, K., Satir, P., Stockert, R.J., Murray, J.W. and Wolkoff, A.W. (2004) Microtubule-dependent movement of late endocytic vesicles in vitro: requirements for Dynein and Kinesin. *Mol Biol Cell*, 15, 3688-3697.

Batterson, W., Furlong, D. and Roizman, B. (1983) Molecular genetics of herpes simplex virus. VIII. further characterization of a temperature-sensitive mutant defective in release of viral DNA and in other stages of the viral reproductive cycle. *J Virol*, 45, 397-407.

Batterson, W. and Roizman, B. (1983) Characterization of the herpes simplex virion-associated factor responsible for the induction of alpha genes. *J Virol*, 46, 371-377.

Bearer, E.L., Breakefield, X.O., Schuback, D., Reese, T.S. and LaVail, J.H. (2000) Retrograde axonal transport of herpes simplex virus: evidence for a single mechanism and a role for tegument. *Proc Natl Acad Sci U S A*, 97, 8146-8150.

Benboudjema, L., Mulvey, M., Gao, Y., Pimplikar, S.W. and Mohr, I. (2003) Association of the herpes simplex virus type 1 Us11 gene product with the cellular kinesin light-chain-related protein PAT1 results in the redistribution of both polypeptides. *J Virol*, 77, 9192-9203.

Bettinger, B.T., Gilbert, D.M. and Amberg, D.C. (2004) Actin up in the nucleus. *Nat Rev Mol Cell Biol*, 5, 410-415.

Bloom, D.C. (2004) HSV LAT and neuronal survival. *Int Rev Immunol*, 23, 187-198.

Booy, F.P., Trus, B.L., Newcomb, W.W., Brown, J.C., Conway, J.F. and Steven, A.C. (1994) Finding a needle in a haystack: detection of a small protein (the 12-kDa VP26) in a large complex (the 200-MDa capsid of herpes simplex virus). *Proc Natl Acad Sci U S A*, 91, 5652-5656.

Borsutzky, S. (2000) Synaptosomen als Modell für den Zelleintritt des Herpes-Simplex-Virus Typ 1. Diploma thesis. Institute of Biochemistry. Hannover Medical School.

Brown, C.L., Maier, K.C., Stauber, T., Ginkel, L.M., Wordeman, L., Vernos, I. and Schroer, T.A. (2005) Kinesin-2 is a Motor for Late Endosomes and Lysosomes. *Traffic*, 6, 1114-1124.

Brunetti, C.R., Dingwell, K.S., Wale, C., Graham, F.L. and Johnson, D.C. (1998) Herpes simplex virus gD and virions accumulate in endosomes by mannose 6-phosphate-dependent and -independent mechanisms. *J Virol*, 72, 3330-3339.

Burkhardt, J.K., Echeverri, C.J., Nilsson, T. and Vallee, R.B. (1997) Overexpression of the dynamitin (p50) subunit of the dynactin complex disrupts dynein-dependent maintenance of membrane organelle distribution. *J Cell Biol*, 139, 469-484.

Büttner, F. (2004) Entwicklung neuer Verfahren zur Fluorochromierung des Herpes-Simplex-Virus Typ 1. Diploma thesis. Institute of Virology. Hannover Medical School.

Cai, Y., Singh, B.B., Aslanukov, A., Zhao, H. and Ferreira, P.A. (2001) The docking of kinesins, KIF5B and KIF5C, to Ran-binding protein 2 (RanBP2) is mediated via a novel RanBP2 domain. *J Biol Chem*, 276, 41594-41602.

Carter, G.C., Rodger, G., Murphy, B.J., Law, M., Krauss, O., Hollinshead, M. and Smith, G.L. (2003) Vaccinia virus cores are transported on microtubules. *J Gen Virol*, 84, 2443-2458.

Cheshenko, N., Del Rosario, B., Woda, C., Marcellino, D., Satlin, L.M. and Herold, B.C. (2003) Herpes simplex virus triggers activation of calcium-signaling pathways. *J Cell Biol*, 163, 283-293.

Cheshenko, N., Liu, W., Satlin, L.M. and Herold, B.C. (2005) Focal adhesion kinase plays a pivotal role in herpes simplex virus entry. *J Biol Chem*, 280, 31116-31125.

Chi, J.H. and Wilson, D.W. (2000) ATP-Dependent localization of the herpes simplex virus capsid protein VP26 to sites of procapsid maturation. *J Virol*, 74, 1468-1476.

Ch'ng, T.H. and Enquist, L.W. (2005a) Efficient axonal localization of alphaherpesvirus structural proteins in cultured sympathetic neurons requires viral glycoprotein E. *J Virol*, 79, 8835-8846.

Ch'ng, T.H. and Enquist, L.W. (2005b) Neuron-to-cell spread of pseudorabies virus in a compartmented neuronal culture system. *J Virol*, 79, 10875-10889.

Cleator, G.M. and Klapper, P.E. (2004) The herpesviridae. In Zuckerman, A.J., Banatvala, J.E., Pattison, J.R., Griffiths, P.D. and Schoub, B.D. (eds.), *Principles and Practice of Clinical Virology*. John Wiley & Sons, pp. 23-198.

Coulombe, P.A. and Wong, P. (2004) Cytoplasmic intermediate filaments revealed as dynamic and multipurpose scaffolds. *Nat Cell Biol*, 6, 699-706.

Cudmore, S., Reckmann, I. and Way, M. (1997) Viral manipulations of the actin cytoskeleton. *Trends Microbiol*, 5, 142-148.

Dammermann, A., Desai, A. and Oegema, K. (2003) The minus end in sight. *Curr Biol*, 13, R614-624.

Dasgupta, A. and Wilson, D.W. (1999) ATP depletion blocks herpes simplex virus DNA packaging and capsid maturation. *J Virol*, 73, 2006-2015.

Dauty, E. and Verkman, A.S. (2005) Actin cytoskeleton as the principal determinant of size-dependent DNA mobility in cytoplasm: a new barrier for non-viral gene delivery. *J Biol Chem*, 280, 7823-7828.

Davison, A.J. and McGeoch, D.J. (1986) Evolutionary comparisons of the S segments in the genomes of herpes simplex virus type 1 and varicella-zoster virus. *J Gen Virol*, 67 (Pt 4), 597-611.

Davison, A.J., Sauerbier, W., Dolan, A., Addison, C. and McKinnell, R.G. (1999) Genomic studies of the Lucke tumor herpesvirus (RaHV-1). *J Cancer Res Clin Oncol*, 125, 232-238.

Deacon, S.W., Serpinskaya, A.S., Vaughan, P.S., Lopez Fanarraga, M., Vernos, I., Vaughan, K.T. and Gelfand, V.I. (2003) Dynactin is required for bidirectional organelle transport. *J Cell Biol*, 160, 297-301.

del Rio, T., Ch'ng, T.H., Flood, E.A., Gross, S.P. and Enquist, L.W. (2005) Heterogeneity of a fluorescent tegument component in single pseudorabies virus virions and enveloped axonal assemblies. *J Virol*, 79, 3903-3919.

Desai, P., Akpa, J.C. and Person, S. (2003) Residues of VP26 of herpes simplex virus type 1 that are required for its interaction with capsids. *J Virol*, 77, 391-404.

Desai, P., DeLuca, N.A. and Person, S. (1998) Herpes simplex virus type 1 VP26 is not essential for replication in cell culture but influences production of infectious virus in the nervous system of infected mice. *Virology*, 247, 115-124.

Desai, P. and Person, S. (1998) Incorporation of the green fluorescent protein into the herpes simplex virus type 1 capsid. *J Virol*, 72, 7563-7568.

Desai, P., Sexton, G.L., McCaffery, J.M. and Person, S. (2001) A null mutation in the gene encoding the herpes simplex virus type 1 UL37 polypeptide abrogates virus maturation. *J Virol*, 75, 10259-10271.

Desai, P.J. (2000) A null mutation in the UL36 gene of herpes simplex virus type 1 results in accumulation of unenveloped DNA-filled capsids in the cytoplasm of infected cells. *J Virol*, 74, 11608-11618.

Diefenbach, R.J., Miranda-Saksena, M., Diefenbach, E., Holland, D.J., Boadle, R.A., Armati, P.J. and Cunningham, A.L. (2002) Herpes simplex virus tegument protein US11 interacts with conventional kinesin heavy chain. *J Virol*, 76, 3282-3291.

Döhner, K., Nagel, C.H. and Sodeik, B. (2005) Viral stop-and-go along microtubules: taking a ride with dynein and kinesins. *Trends Microbiol*, 13, 320-327.

Döhner, K. and Sodeik, B. (2004) The role of the cytoskeleton during viral infection. *Curr Top Microbiol Immunol*, 285, 67-108.

Döhner, K., Wolfstein, A., Prank, U., Echeverri, C., Dujardin, D., Vallee, R. and Sodeik, B. (2002) Function of dynein and dynactin in herpes simplex virus capsid transport. *Mol Biol Cell*, 13, 2795-2809.

Donnelly, M. and Elliott, G. (2001) Fluorescent tagging of herpes simplex virus tegument protein VP13/14 in virus infection. *J Virol*, 75, 2575-2583.

Douglas, M.W., Diefenbach, R.J., Homa, F.L., Miranda-Saksena, M., Rixon, F.J., Vittone, V., Byth, K. and Cunningham, A.L. (2004) Herpes simplex virus type 1 capsid protein VP26 interacts with dynein light chains RP3 and Tctex1 and plays a role in retrograde cellular transport. *J Biol Chem*, 279, 28522-28530.

Echeverri, C.J., Paschal, B.M., Vaughan, K.T. and Vallee, R.B. (1996) Molecular characterization of the 50-kD subunit of dynactin reveals function for the complex in chromosome alignment and spindle organization during mitosis. *J Cell Biol*, 132, 617-633.

Eckley, D.M., Gill, S.R., Melkonian, K.A., Bingham, J.B., Goodson, H.V., Heuser, J.E. and Schroer, T.A. (1999) Analysis of dynactin subcomplexes reveals a novel actin-related protein associated with the arp1 minifilament pointed end. *J Cell Biol*, 147, 307-320.

Elliott, G., Mouzakitis, G. and O'Hare, P. (1995) VP16 interacts via its activation domain with VP22, a tegument protein of herpes simplex virus, and is relocated to a novel macromolecular assembly in coexpressing cells. *J Virol*, 69, 7932-7941.

Elliott, G. and O'Hare, P. (1997) Intercellular trafficking and protein delivery by a herpesvirus structural protein. *Cell*, 88, 223-233.

Elliott, G. and O'Hare, P. (1998) Herpes simplex virus type 1 tegument protein VP22 induces the stabilization and hyperacetylation of microtubules. *J Virol*, 72, 6448-6455.

Elliott, G. and O'Hare, P. (1999) Live-cell analysis of a green fluorescent protein-tagged herpes simplex virus infection. *J Virol*, 73, 4110-4119.

Enquist, L.W., Husak, P.J., Banfield, B.W. and Smith, G.A. (1998) Infection and spread of alphaherpesviruses in the nervous system. *Adv Virus Res*, 51, 237-347.

Everett, R.D., Sourvinos, G., Leiper, C., Clements, J.B. and Orr, A. (2004) Formation of nuclear foci of the herpes simplex virus type 1 regulatory protein ICP4 at early times of infection: localization, dynamics, recruitment of ICP27, and evidence for the de novo induction of ND10-like complexes. *J Virol*, 78, 1903-1917.

Ewers, H., Smith, A.E., Sbalzarini, I.F., Lilie, H., Koumoutsakos, P. and Helenius, A. (2005) Single-particle tracking of murine polyoma virus-like particles on live cells and artificial membranes. *Proc Natl Acad Sci U S A*, 102, 15110-15115.

Forest, T., Barnard, S. and Baines, J.D. (2005) Active intranuclear movement of herpesvirus capsids. *Nat Cell Biol*, 7, 429-431.

Funk, A., Mhamdi, M., Lin, L., Will, H. and Sirma, H. (2004) Itinerary of hepatitis B viruses: delineation of restriction points critical for infectious entry. *J Virol*, 78, 8289-8300.

Geada, M.M., Galindo, I., Lorenzo, M.M., Perdiguero, B. and Blasco, R. (2001) Movements of vaccinia virus intracellular enveloped virions with GFP tagged to the F13L envelope protein. *J Gen Virol*, 82, 2747-2760.

Giannakakou, P., Nakano, M., Nicolaou, K.C., O'Brate, A., Yu, J., Blagosklonny, M.V., Greber, U.F. and Fojo, T. (2002) Enhanced microtubule-dependent trafficking and p53 nuclear accumulation by suppression of microtubule dynamics. *Proc Natl Acad Sci U S A*, 99, 10855-10860.

Gianni, T., Campadelli-Fiume, G. and Menotti, L. (2004) Entry of herpes simplex virus mediated by chimeric forms of nectin1 retargeted to endosomes or to lipid rafts occurs through acidic endosomes. *J Virol*, 78, 12268-12276.

Glotzer, J.B., Michou, A.I., Baker, A., Saltik, M. and Cotten, M. (2001) Microtubule-independent motility and nuclear targeting of adenoviruses with fluorescently labeled genomes. *J Virol*, 75, 2421-2434.

Granzow, H., Klupp, B.G., Fuchs, W., Veits, J., Osterrieder, N. and Mettenleiter, T.C. (2001) Egress of alphaherpesviruses: comparative ultrastructural study. *J Virol*, 75, 3675-3684.

Granzow, H., Klupp, B.G. and Mettenleiter, T.C. (2005) Entry of pseudorabies virus: an immunogold-labeling study. *J Virol*, 79, 3200-3205.

Granzow, H., Weiland, F., Jons, A., Klupp, B.G., Karger, A. and Mettenleiter, T.C. (1997) Ultrastructural analysis of the replication cycle of pseudorabies virus in cell culture: a reassessment. *J Virol*, 71, 2072-2082.

Greber, U.F., Willetts, M., Webster, P. and Helenius, A. (1993) Stepwise dismantling of adenovirus 2 during entry into cells. *Cell*, 75, 477-486.

Grünewald, K., Desai, P., Winkler, D.C., Heymann, J.B., Belnap, D.M., Baumeister, W. and Steven, A.C. (2003) Three-dimensional structure of herpes simplex virus from cryo-electron tomography. *Science*, 302, 1396-1398.

Hafezi, W., Bernard, E., Cook, R. and Elliott, G. (2005) Herpes Simplex Virus Tegument Protein VP22 Contains an Internal VP16 Interaction Domain and a C-Terminal Domain That Are Both Required for VP22 Assembly into the Virus Particle. *J Virol*, 79, 13082-13093.

Hammonds, T.R., Denyer, S.P., Jackson, D.E. and Irving, W.L. (1996) Studies to show that with podophyllotoxin the early replicative stages of herpes simplex virus type 1 depend upon functional cytoplasmic microtubules. *J Med Microbiol*, 45, 167-172.

Hanlon, D.W., Yang, Z. and Goldstein, L.S. (1997) Characterization of KIFC2, a neuronal kinesin superfamily member in mouse. *Neuron*, 18, 439-451.

Hanz, S., Perlson, E., Willis, D., Zheng, J.Q., Massarwa, R., Huerta, J.J., Koltzenburg, M., Kohler, M., van-Minnen, J., Twiss, J.L. and Fainzilber, M. (2003) Axoplasmic importins enable retrograde injury signaling in lesioned nerve. *Neuron*, 40, 1095-1104.

Harley, C.A., Dasgupta, A. and Wilson, D.W. (2001) Characterization of herpes simplex virus-containing organelles by subcellular fractionation: role for organelle acidification in assembly of infectious particles. *J Virol*, 75, 1236-1251.

Heath, C.M., Windsor, M. and Wileman, T. (2001) Aggresomes resemble sites specialized for virus assembly. *J Cell Biol*, 153, 449-455.

Hirokawa, N. and Takemura, R. (2005) Molecular motors and mechanisms of directional transport in neurons. *Nat Rev Neurosci*, 6, 201-214.

Hodgkinson, J.L., Peters, C., Kuznetsov, S.A. and Steffen, W. (2005) Three-dimensional reconstruction of the dynactin complex by single-particle image analysis. *Proc Natl Acad Sci U S A*, 102, 3667-3672.

Holland, D.J., Miranda-Saksena, M., Boadle, R.A., Armati, P. and Cunningham, A.L. (1999) Anterograde transport of herpes simplex virus proteins in axons of peripheral human fetal neurons: an immunoelectron microscopy study. *J Virol*, 73, 8503-8511.

Hollinshead, M., Rodger, G., Van Eijl, H., Law, M., Hollinshead, R., Vaux, D.J. and Smith, G.L. (2001) Vaccinia virus utilizes microtubules for movement to the cell surface. *J Cell Biol*, 154, 389-402.

Janus, J. (2005) Bidirektionaler Mikrotubuli-Transport während des Zelleintritts von Herpes-Simplex-Virus Typ 1: Die Rolle von US11 und Kinesinen. Diploma thesis. Institute of Virology. Hannover Medical School.

Jefferson, J.J., Leung, C.L. and Liem, R.K. (2004) Plakins: goliaths that link cell junctions and the cytoskeleton. *Nat Rev Mol Cell Biol*, 5, 542-553.

Jerome, K.R. and Ashley, R.L. (2003) Herpes simplex viruses and herpes B virus. In Murray, P.R., Baron, E.J., Jorgensen, J.H., Pfaller, M.A. and Yolken, R.H. (eds.), *Manual of clinical microbiology*. ASM press, Washington.

Jouvenet, N., Monaghan, P., Way, M. and Wileman, T. (2004) Transport of African swine fever virus from assembly sites to the plasma membrane is dependent on microtubules and conventional kinesin. *J Virol*, 78, 7990-8001.

Kaelin, K., Dezelee, S., Masse, M.J., Bras, F. and Flamand, A. (2000) The UL25 protein of pseudorabies virus associates with capsids and localizes to the nucleus and to microtubules. *J Virol*, 74, 474-482.

Kattenhorn, L.M., Korbel, G.A., Kessler, B.M., Spooner, E. and Ploegh, H.L. (2005) A deubiquitinating enzyme encoded by HSV-1 belongs to a family of cysteine proteases that is conserved across the family Herpesviridae. *Mol Cell*, 19, 547-557.

Khanna, K.M., Lepisto, A.J., Decman, V. and Hendricks, R.L. (2004) Immune control of herpes simplex virus during latency. *Curr Opin Immunol*, 16, 463-469.

Kieke, M.C. and Titus, M.A. (2003) The Myosin Superfamily: An Overview. In Schliwa, M. (ed.), *Molecular Motors*. Wiley-VCH Verlag GmbH & Co. KGaA, Weinheim, pp. 3-44.

King, S.J., Bonilla, M., Rodgers, M.E. and Schroer, T.A. (2002) Subunit organization in cytoplasmic dynein subcomplexes. *Protein Sci*, 11, 1239-1250.

King, S.J. and Schroer, T.A. (2000) Dynactin increases the processivity of the cytoplasmic dynein motor. *Nat Cell Biol*, 2, 20-24.

Klopfenstein, D.R., Tomishige, M., Stuurman, N. and Vale, R.D. (2002) Role of phosphatidylinositol(4,5)bisphosphate organization in membrane transport by the Unc104 kinesin motor. *Cell*, 109, 347-358.

Klopfenstein, D.R. and Vale, R.D. (2004) The lipid binding pleckstrin homology domain in UNC-104 kinesin is necessary for synaptic vesicle transport in Caenorhabditis elegans. *Mol Biol Cell*, 15, 3729-3739.

Klupp, B.G., Granzow, H. and Mettenleiter, T.C. (2000) Primary envelopment of pseudorabies virus at the nuclear membrane requires the UL34 gene product. *J Virol*, 74, 10063-10073.

Klupp, B.G., Hengartner, C.J., Mettenleiter, T.C. and Enquist, L.W. (2004) Complete, annotated sequence of the pseudorabies virus genome. *J Virol*, 78, 424-440.

Kodama, A., Lechler, T. and Fuchs, E. (2004) Coordinating cytoskeletal tracks to polarize cellular movements. *J Cell Biol*, 167, 203-207.

Koshizuka, T., Kawaguchi, Y. and Nishiyama, Y. (2005) Herpes simplex virus type 2 membrane protein UL56 associates with the kinesin motor protein KIF1A. *J Gen Virol*, 86, 527-533.

Kotsakis, A., Pomeranz, L.E., Blouin, A. and Blaho, J.A. (2001) Microtubule reorganization during herpes simplex virus type 1 infection facilitates the nuclear localization of VP22, a major virion tegument protein. *J Virol*, 75, 8697-8711.

Koyama, A.H. and Uchida, T. (1987) The mode of entry of herpes simplex virus type 1 into Vero cells. *Microbiol Immunol*, 31, 123-130.

Krendel, M. and Mooseker, M.S. (2005) Myosins: tails (and heads) of functional diversity. *Physiology (Bethesda)*, 20, 239-251.

Kristensson, K., Lycke, E., Roytta, M., Svennerholm, B. and Vahlne, A. (1986) Neuritic transport of herpes simplex virus in rat sensory neurons in vitro. Effects of substances interacting with microtubular function and axonal flow [nocodazole, taxol and erythro-9-3-(2-hydroxynonyl)adenine]. *J Gen Virol*, 67 (Pt 9), 2023-2028.

La Boissiere, S., Izeta, A., Malcomber, S. and O'Hare, P. (2004) Compartmentalization of VP16 in cells infected with recombinant herpes simplex virus expressing VP16-green fluorescent protein fusion proteins. *J Virol*, 78, 8002-8014.

Lakadamyali, M., Rust, M.J., Babcock, H.P. and Zhuang, X. (2003) Visualizing infection of individual influenza viruses. *Proc Natl Acad Sci U S A*, 100, 9280-9285.

LaVail, J.H., Tauscher, A.N., Hicks, J.W., Harrabi, O., Melroe, G.T. and Knipe, D.M. (2005) Genetic and molecular in vivo analysis of herpes simplex virus assembly in murine visual system neurons. *J Virol*, 79, 11142-11150.

Lawrence, C.J., Dawe, R.K., Christie, K.R., Cleveland, D.W., Dawson, S.C., Endow, S.A., Goldstein, L.S., Goodson, H.V., Hirokawa, N., Howard, J., Malmberg, R.L., McIntosh, J.R., Miki, H., Mitchison, T.J., Okada, Y., Reddy, A.S., Saxton, W.M., Schliwa, M., Scholey, J.M., Vale, R.D., Walczak, C.E. and Wordeman, L. (2004) A standardized kinesin nomenclature. *J Cell Biol*, 167, 19-22.

Le Bot, N., Antony, C., White, J., Karsenti, E. and Vernos, I. (1998) Role of xklp3, a subunit of the Xenopus kinesin II heterotrimeric complex, in membrane transport between the endoplasmic reticulum and the Golgi apparatus. *J Cell Biol*, 143, 1559-1573.

Leopold, P.L., Kreitzer, G., Miyazawa, N., Rempel, S., Pfister, K.K., Rodriguez-Boulan, E. and Crystal, R.G. (2000) Dynein- and microtubule-mediated translocation of adenovirus serotype 5 occurs after endosomal lysis. *Hum Gene Ther*, 11, 151-165.

Lidke, D.S., Nagy, P., Heintzmann, R., Arndt-Jovin, D.J., Post, J.N., Grecco, H.E., Jares-Erijman, E.A. and Jovin, T.M. (2004) Quantum dot ligands provide new insights into erbB/HER receptor-mediated signal transduction. *Nat Biotechnol*, 22, 198-203.

Ligon, L.A., Tokito, M., Finklestein, J.M., Grossman, F.E. and Holzbaur, E.L. (2004) A direct interaction between cytoplasmic dynein and kinesin I may coordinate motor activity. *J Biol Chem*, 279, 19201-19208.

Luby-Phelps, K. (2000) Cytoarchitecture and physical properties of cytoplasm: volume, viscosity, diffusion, intracellular surface area. *Int Rev Cytol*, 192, 189-221.

Luxton, G.W., Haverlock, S., Coller, K.E., Antinone, S.E., Pincetic, A. and Smith, G.A. (2005) Targeting of herpesvirus capsid transport in axons is coupled to association with specific sets of tegument proteins. *Proc Natl Acad Sci U S A*, 102, 5832-5837.

Lycke, E., Hamark, B., Johansson, M., Krotochwil, A., Lycke, J. and Svennerholm, B. (1988) Herpes simplex virus infection of the human sensory neuron. An electron microscopy study. *Arch Virol*, 101, 87-104.

Mabit, H., Nakano, M.Y., Prank, U., Saam, B., Döhner, K., Sodeik, B. and Greber, U.F. (2002) Intact microtubules support adenovirus and herpes simplex virus infections. *J Virol*, 76, 9962-9971.

Mallik, R., Carter, B.C., Lex, S.A., King, S.J. and Gross, S.P. (2004) Cytoplasmic dynein functions as a gear in response to load. *Nature*, 427, 649-652.

Marozin, S., Prank, U. and Sodeik, B. (2004) Herpes simplex virus type 1 infection of polarized epithelial cells requires microtubules and access to receptors present at cell-cell contact sites. *J Gen Virol*, 85, 775-786.

Marsh, M. and Bron, R. (1997) SFV infection in CHO cells: cell-type specific restrictions to productive virus entry at the cell surface. *J Cell Sci*, 110 (Pt 1), 95-103.

Martin, A., O'Hare, P., McLauchlan, J. and Elliott, G. (2002) Herpes simplex virus tegument protein VP22 contains overlapping domains for cytoplasmic localization, microtubule interaction, and chromatin binding. *J Virol*, 76, 4961-4970.

Mavlyutov, T.A., Cai, Y. and Ferreira, P.A. (2002) Identification of RanBP2- and kinesin-mediated transport pathways with restricted neuronal and subcellular localization. *Traffic*, 3, 630-640.

McDonald, D., Vodicka, M.A., Lucero, G., Svitkina, T.M., Borisy, G.G., Emerman, M. and Hope, T.J. (2002) Visualization of the intracellular behavior of HIV in living cells. *J Cell Biol*, 159, 441-452.

McGeoch, D.J., Dolan, A. and Ralph, A.C. (2000) Toward a comprehensive phylogeny for mammalian and avian herpesviruses. *J Virol*, 74, 10401-10406.

McMillan, T.N. and Johnson, D.C. (2001) Cytoplasmic domain of herpes simplex virus gE causes accumulation in the trans-Golgi network, a site of virus envelopment and sorting of virions to cell junctions. *J Virol*, 75, 1928-1940.

McNabb, D.S. and Courtney, R.J. (1992a) Characterization of the large tegument protein (ICP1/2) of herpes simplex virus type 1. *Virology*, 190, 221-232.

McNabb, D.S. and Courtney, R.J. (1992b) Posttranslational modification and subcellular localization of the p12 capsid protein of herpes simplex virus type 1. *J Virol*, 66, 4839-4847.

Medalia, O., Weber, I., Frangakis, A.S., Nicastro, D., Gerisch, G. and Baumeister, W. (2002) Macromolecular architecture in eukaryotic cells visualized by cryoelectron tomography. *Science*, 298, 1209-1213.

Meier, O., Boucke, K., Hammer, S.V., Keller, S., Stidwill, R.P., Hemmi, S. and Greber, U.F. (2002) Adenovirus triggers macropinocytosis and endosomal leakage together with its clathrin-mediated uptake. *J Cell Biol*, 158, 1119-1131.

Mery, P.F., Pavoine, C., Pecker, F. and Fischmeister, R. (1995) Erythro-9-(2-hydroxy-3-nonyl)adenine inhibits cyclic GMP-stimulated phosphodiesterase in isolated cardiac myocytes. *Mol Pharmacol*, 48, 121-130.

Mesika, A., Kiss, V., Brumfeld, V., Ghosh, G. and Reich, Z. (2005) Enhanced intracellular mobility and nuclear accumulation of DNA plasmids associated with a karyophilic protein. *Hum Gene Ther*, 16, 200-208.

Mettenleiter, T.C. (2002) Herpesvirus assembly and egress. *J Virol*, 76, 1537-1547.

Mettenleiter, T.C. (2003) Pathogenesis of neurotropic herpesviruses: role of viral glycoproteins in neuroinvasion and transneuronal spread. *Virus Res*, 92, 197-206.

Mettenleiter, T.C. (2004) Budding events in herpesvirus morphogenesis. *Virus Res*, 106, 167-180.

Milne, R.S., Nicola, A.V., Whitbeck, J.C., Eisenberg, R.J. and Cohen, G.H. (2005) Glycoprotein D receptor-dependent, low-pH-independent endocytic entry of herpes simplex virus type 1. *J Virol*, 79, 6655-6663.

Minson, A.C., Davison, A., Eberle, R., Desrosiers, R.C., Fleckenstein, B., McGeoch, D.J., Pellet, P.E., Roizman, B. and Studdert, M.J. (2000) Family Herpesviridae. In *Virus Taxonomy. Seventh report of the international commitee on taxonomy of viruses*. van Regenmortel, M.H.V.,

Fauquet, C.M., Bishop, D.H.L., Carstens, E.B., Estes, M.K., Lemon, S.M., Maniloff, J., Mayo, M.A., McGeoch, D.J., Pringle, C.R. and Wickner, R.B. Academic Press. San Diego.

Miranda-Saksena, M., Armati, P., Boadle, R.A., Holland, D.J. and Cunningham, A.L. (2000) Anterograde transport of herpes simplex virus type 1 in cultured, dissociated human and rat dorsal root ganglion neurons. *J Virol*, 74, 1827-1839.

Miranda-Saksena, M., Boadle, R.A., Armati, P. and Cunningham, A.L. (2002) In rat dorsal root ganglion neurons, herpes simplex virus type 1 tegument forms in the cytoplasm of the cell body. *J Virol*, 76, 9934-9951.

Mitchison, T. and Kirschner, M. (1984) Dynamic instability of microtubule growth. *Nature*, 312, 237-242.

Mohr, I. (2004) Neutralizing innate host defenses to control viral translation in HSV-1 infected cells. *Int Rev Immunol*, 23, 199-220.

Mok, Y.K., Lo, K.W. and Zhang, M. (2001) Structure of Tctex-1 and its interaction with cytoplasmic dynein intermediate chain. *J Biol Chem*, 276, 14067-14074.

Morrison, E.E., Stevenson, A.J., Wang, Y.F. and Meredith, D.M. (1998) Differences in the intracellular localization and fate of herpes simplex virus tegument proteins early in the infection of Vero cells. *J Gen Virol*, 79 (Pt 10), 2517-2528.

Mouland, A.J., Xu, H., Cui, H., Krueger, W., Munro, T.P., Prasol, M., Mercier, J., Rekosh, D., Smith, R., Barbarese, E., Cohen, E.A. and Carson, J.H. (2001) RNA trafficking signals in human immunodeficiency virus type 1. *Mol Cell Biol*, 21, 2133-2143.

Mouzakitis, G., McLauchlan, J., Barreca, C., Kueltzo, L. and O'Hare, P. (2005) Characterization of VP22 in herpes simplex virus-infected cells. *J Virol*, 79, 12185-12198.

Muratani, M., Gerlich, D., Janicki, S.M., Gebhard, M., Eils, R. and Spector, D.L. (2002) Metabolic-energy-dependent movement of PML bodies within the mammalian cell nucleus. *Nat Cell Biol*, 4, 106-110.

Müsch, A. (2004) Microtubule organization and function in epithelial cells. *Traffic*, 5, 1-9.

Nagel, C.H. (2002) Der Zelleintritt von Herpes-Simplex-Virus Typ I in isolierte Synaptosomen - die Zusammensetzung des cytosolischen Kapsids. Diploma thesis. Institute of Biochemistry. Hannover Medical School.

Nakano, M.Y. and Greber, U.F. (2000) Quantitative microscopy of fluorescent adenovirus entry. *J Struct Biol*, 129, 57-68.

Nangaku, M., Sato-Yoshitake, R., Okada, Y., Noda, Y., Takemura, R., Yamazaki, H. and Hirokawa, N. (1994) KIF1B, a novel microtubule plus end-directed monomeric motor protein for transport of mitochondria. *Cell*, 79, 1209-1220.

Naranatt, P.P., Krishnan, H.H., Smith, M.S. and Chandran, B. (2005) Kaposi's sarcoma-associated herpesvirus modulates microtubule dynamics via RhoA-GTP-diaphanous 2 signaling and utilizes the dynein motors to deliver its DNA to the nucleus. *J Virol*, 79, 1191-1206.

Newcomb, W.W., Juhas, R.M., Thomsen, D.R., Homa, F.L., Burch, A.D., Weller, S.K. and Brown, J.C. (2001) The UL6 gene product forms the portal for entry of DNA into the herpes simplex virus capsid. *J Virol*, 75, 10923-10932.

Nicola, A.V., Hou, J., Major, E.O. and Straus, S.E. (2005) Herpes simplex virus type 1 enters human epidermal keratinocytes, but not neurons, via a pH-dependent endocytic pathway. *J Virol*, 79, 7609-7616.

Nicola, A.V., McEvoy, A.M. and Straus, S.E. (2003) Roles for endocytosis and low pH in herpes simplex virus entry into HeLa and Chinese hamster ovary cells. *J Virol*, 77, 5324-5332.

Nicola, A.V. and Straus, S.E. (2004) Cellular and viral requirements for rapid endocytic entry of herpes simplex virus. *J Virol*, 78, 7508-7517.

Nielsen, E., Severin, F., Backer, J.M., Hyman, A.A. and Zerial, M. (1999) Rab5 regulates motility of early endosomes on microtubules. *Nat Cell Biol*, 1, 376-382.

Noda, Y., Okada, Y., Saito, N., Setou, M., Xu, Y., Zhang, Z. and Hirokawa, N. (2001) KIFC3, a microtubule minus end-directed motor for the apical transport of annexin XIIIb-associated Triton-insoluble membranes. *J Cell Biol*, 155, 77-88.

Nogales, E. (2000) Structural insights into microtubule function. *Annu Rev Biochem*, 69, 277-302.

Ogasawara, M., Suzutani, T., Yoshida, I. and Azuma, M. (2001) Role of the UL25 gene product in packaging DNA into the herpes simplex virus capsid: location of UL25 product in the capsid and demonstration that it binds DNA. *J Virol*, 75, 1427-1436.

Ogawa-Goto, K., Irie, S., Omori, A., Miura, Y., Katano, H., Hasegawa, H., Kurata, T., Sata, T. and Arao, Y. (2002) An endoplasmic reticulum protein, p180, is highly expressed in human cytomegalovirus-permissive cells and interacts with the tegument protein encoded by UL48. *J Virol*, 76, 2350-2362.

Ogawa-Goto, K., Tanaka, K., Gibson, W., Moriishi, E., Miura, Y., Kurata, T., Irie, S. and Sata, T. (2003) Microtubule network facilitates nuclear targeting of human cytomegalovirus capsid. *J Virol*, 77, 8541-8547.

Ohsawa, K., Black, D.H., Sato, H. and Eberle, R. (2002) Sequence and genetic arrangement of the U(S) region of the monkey B virus (cercopithecine herpesvirus 1) genome and comparison with the U(S) regions of other primate herpesviruses. *J Virol*, 76, 1516-1520.

Oiwa, K. and Sakakibara, H. (2005) Recent progress in dynein structure and mechanism. *Curr Opin Cell Biol*, 17, 98-103.

Ojala, P.M., Sodeik, B., Ebersold, M.W., Kutay, U. and Helenius, A. (2000) Herpes simplex virus type 1 entry into host cells: reconstitution of capsid binding and uncoating at the nuclear pore complex in vitro. *Mol Cell Biol*, 20, 4922-4931.

Okada, Y., Yamazaki, H., Sekine-Aizawa, Y. and Hirokawa, N. (1995) The neuron-specific kinesin superfamily protein KIF1A is a unique monomeric motor for anterograde axonal transport of synaptic vesicle precursors. *Cell*, 81, 769-780.

Ovechkina, Y. and Wordeman, L. (2003) Unconventional motoring: an overview of the Kin C and Kin I kinesins. *Traffic*, 4, 367-375.

Parry, C., Bell, S., Minson, T. and Browne, H. (2005) Herpes simplex virus type 1 glycoprotein H binds to alphavbeta3 integrins. *J Gen Virol*, 86, 7-10.

Patterson, G.H. and Lippincott-Schwartz, J. (2002) A photoactivatable GFP for selective photolabeling of proteins and cells. *Science*, 297, 1873-1877.

Pederson, T. and Aebi, U. (2005) Nuclear actin extends, with no contraction in sight. *Mol Biol Cell*, 16, 5055-5060.

Pelkmans, L., Kartenbeck, J. and Helenius, A. (2001) Caveolar endocytosis of simian virus 40 reveals a new two-step vesicular-transport pathway to the ER. *Nat Cell Biol*, 3, 473-483.

Pemberton, L.F. and Paschal, B.M. (2005) Mechanisms of receptor-mediated nuclear import and nuclear export. *Traffic*, 6, 187-198.

Penfold, M.E., Armati, P. and Cunningham, A.L. (1994) Axonal transport of herpes simplex virions to epidermal cells: evidence for a specialized mode of virus transport and assembly. *Proc Natl Acad Sci U S A*, 91, 6529-6533.

Penningroth, S.M. (1986) Erythro-9-[3-(2-hydroxynonyl)]adenine and vanadate as probes for microtubule-based cytoskeletal mechanochemistry. *Methods Enzymol*, 134, 477-487.

Perez, A., Li, Q.X., Perez-Romero, P., Delassus, G., Lopez, S.R., Sutter, S., McLaren, N. and Fuller, A.O. (2005) A new class of receptor for herpes simplex virus has heptad repeat motifs that are common to membrane fusion proteins. *J Virol*, 79, 7419-7430.

Perez-Romero, P. and Fuller, A.O. (2005) The C terminus of the B5 receptor for herpes simplex virus contains a functional region important for infection. *J Virol*, 79, 7431-7437.

Petit, C., Giron, M.L., Tobaly-Tapiero, J., Bittoun, P., Real, E., Jacob, Y., Tordo, N., De The, H. and Saib, A. (2003) Targeting of incoming retroviral Gag to the centrosome involves a direct interaction with the dynein light chain 8. *J Cell Sci*, 116, 3433-3442.

Ploubidou, A., Moreau, V., Ashman, K., Reckmann, I., Gonzalez, C. and Way, M. (2000) Vaccinia virus infection disrupts microtubule organization and centrosome function. *Embo J*, 19, 3932-3944.

Ploubidou, A. and Way, M. (2001) Viral transport and the cytoskeleton. *Curr Opin Cell Biol*, 13, 97-105.

Potel, C., Kaelin, K., Gautier, I., Lebon, P., Coppey, J. and Rozenberg, F. (2002) Incorporation of green fluorescent protein into the essential envelope glycoprotein B of herpes simplex virus type 1. *J Virol Methods*, 105, 13-23.

Presley, J.F., Cole, N.B., Schroer, T.A., Hirschberg, K., Zaal, K.J. and Lippincott-Schwartz, J. (1997) ER-to-Golgi transport visualized in living cells. *Nature*, 389, 81-85.

Qie, L., Marcellino, D. and Herold, B.C. (1999) Herpes simplex virus entry is associated with tyrosine phosphorylation of cellular proteins. *Virology*, 256, 220-227.

Quintyne, N.J., Gill, S.R., Eckley, D.M., Crego, C.L., Compton, D.A. and Schroer, T.A. (1999) Dynactin is required for microtubule anchoring at centrosomes. *J Cell Biol*, 147, 321-334.

Quintyne, N.J. and Schroer, T.A. (2002) Distinct cell cycle-dependent roles for dynactin and dynein at centrosomes. *J Cell Biol*, 159, 245-254.

Rajcani, J., Andrea, V. and Ingeborg, R. (2004) Peculiarities of herpes simplex virus (HSV) transcription: an overview. *Virus Genes*, 28, 293-310.

Reynolds, A.E., Wills, E.G., Roller, R.J., Ryckman, B.J. and Baines, J.D. (2002) Ultrastructural localization of the herpes simplex virus type 1 UL31, UL34, and US3 proteins suggests specific roles in primary envelopment and egress of nucleocapsids. *J Virol*, 76, 8939-8952.

Rietdorf, J., Ploubidou, A., Reckmann, I., Holmstrom, A., Frischknecht, F., Zettl, M., Zimmermann, T. and Way, M. (2001) Kinesin-dependent movement on microtubules precedes actin-based motility of vaccinia virus. *Nat Cell Biol*, 3, 992-1000.

Rodriguez, O.C., Schaefer, A.W., Mandato, C.A., Forscher, P., Bement, W.M. and Waterman-Storer, C.M. (2003) Conserved microtubule-actin interactions in cell movement and morphogenesis. *Nat Cell Biol*, 5, 599-609.

Roghi, C. and Allan, V.J. (1999) Dynamic association of cytoplasmic dynein heavy chain 1a with the Golgi apparatus and intermediate compartment. *J Cell Sci*, 112 (Pt 24), 4673-4685.

Roizman, B. and Knipe, D.M. (2001) Herpes simplex viruses and their replication. In Fields, B.N., Knipe, D.M., Howley, P.M. and al., e. (eds.), *Fundamental Virology, 4th edition*. Lippincott-Raven Publishers, Philadelphia, pp. 2399-2459.

Roizman, B. and Pellet, P.E. (2001) The familiy herpesviridae: a brief introduction. In Knipe, D.M. and Howley, P.M. (eds.), *Virology*. Lippincott Williams & Wilkins, Philadelphia, Vol. 1, pp. 2381-2397.

Saito, N., Okada, Y., Noda, Y., Kinoshita, Y., Kondo, S. and Hirokawa, N. (1997) KIFC2 is a novel neuron-specific C-terminal type kinesin superfamily motor for dendritic transport of multivesicular body-like organelles. *Neuron*, 18, 425-438.

Salman, H., Abu-Arish, A., Oliel, S., Loyter, A., Klafter, J., Granek, R. and Elbaum, M. (2005) Nuclear localization signal peptides induce molecular delivery along microtubules. *Biophys J*, 89, 2134-2145.

Sampaio, K.L., Cavignac, Y., Stierhof, Y.D. and Sinzger, C. (2005) Human cytomegalovirus labeled with green fluorescent protein for live analysis of intracellular particle movements. *J Virol*, 79, 2754-2767.

Sanderson, C.M., Hollinshead, M. and Smith, G.L. (2000) The vaccinia virus A27L protein is needed for the microtubule-dependent transport of intracellular mature virus particles. *J Gen Virol*, 81, 47-58.

Schafer, D.A., Gill, S.R., Cooper, J.A., Heuser, J.E. and Schroer, T.A. (1994) Ultrastructural analysis of the dynactin complex: an actin-related protein is a component of a filament that resembles F-actin. *J Cell Biol*, 126, 403-412.

Schmidt, S. (2003) Der Mikrotubuli-abhängige Transport verschiedener Tegumentprotein-Mutanten des Herpes-Simplex-Virus-Typ 1 von der Plasmamembran zum Zellkern. Ph.D. thesis. Institute of Biochemistry. Hannover Medical School.

Schroer, T.A. (2004) Dynactin. *Annu Rev Cell Dev Biol*, 20, 759-779.

Seisenberger, G., Ried, M.U., Endress, T., Buning, H., Hallek, M. and Brauchle, C. (2001) Real-time single-molecule imaging of the infection pathway of an adeno-associated virus. *Science*, 294, 1929-1932.

Sfakianos, J.N. and Hunter, E. (2003) M-PMV capsid transport is mediated by Env/Gag interactions at the pericentriolar recycling endosome. *Traffic*, 4, 671-680.

Sfakianos, J.N., LaCasse, R.A. and Hunter, E. (2003) The M-PMV cytoplasmic targeting-retention signal directs nascent Gag polypeptides to a pericentriolar region of the cell. *Traffic*, 4, 660-670.

Sheaffer, A.K., Newcomb, W.W., Gao, M., Yu, D., Weller, S.K., Brown, J.C. and Tenney, D.J. (2001) Herpes simplex virus DNA cleavage and packaging proteins associate with the procapsid prior to its maturation. *J Virol*, 75, 687-698.

Sieczkarski, S.B. and Whittaker, G.R. (2002) Dissecting virus entry via endocytosis. *J Gen Virol*, 83, 1535-1545.

Smiley, J.R. (2004) Herpes simplex virus virion host shutoff protein: immune evasion mediated by a viral RNase? *J Virol*, 78, 1063-1068.
Smith, A.E. and Helenius, A. (2004) How viruses enter animal cells. *Science*, 304, 237-242.
Smith, G.A. and Enquist, L.W. (2002) Break ins and break outs: viral interactions with the cytoskeleton of Mammalian cells. *Annu Rev Cell Dev Biol*, 18, 135-161.
Smith, G.A., Gross, S.P. and Enquist, L.W. (2001) Herpesviruses use bidirectional fast-axonal transport to spread in sensory neurons. *Proc Natl Acad Sci U S A*, 98, 3466-3470.
Smith, G.A., Pomeranz, L., Gross, S.P. and Enquist, L.W. (2004) Local modulation of plus-end transport targets herpesvirus entry and egress in sensory axons. *Proc Natl Acad Sci U S A*, 101, 16034-16039.
Smith, G.L., Murphy, B.J. and Law, M. (2003) Vaccinia virus motility. *Annu Rev Microbiol*, 57, 323-342.
Sodeik, B. (2000) Mechanisms of viral transport in the cytoplasm. *Trends Microbiol*, 8, 465-472.
Sodeik, B. (2002) Unchain my heart, baby let me go--the entry and intracellular transport of HIV. *J Cell Biol*, 159, 393-395.
Sodeik, B., Ebersold, M.W. and Helenius, A. (1997) Microtubule-mediated transport of incoming herpes simplex virus 1 capsids to the nucleus. *J Cell Biol*, 136, 1007-1021.
Spear, P.G. (2004) Herpes simplex virus: receptors and ligands for cell entry. *Cell Microbiol*, 6, 401-410.
Spear, P.G., Eisenberg, R.J. and Cohen, G.H. (2000) Three classes of cell surface receptors for alphaherpesvirus entry. *Virology*, 275, 1-8.
Spear, P.G. and Longnecker, R. (2003) Herpesvirus entry: an update. *J Virol*, 77, 10179-10185.
Strelkov, S.V., Herrmann, H. and Aebi, U. (2003) Molecular architecture of intermediate filaments. *Bioessays*, 25, 243-251.
Strunze, S., Trotman, L.C., Boucke, K. and Greber, U.F. (2005) Nuclear targeting of adenovirus type 2 requires CRM1-mediated nuclear export. *Mol Biol Cell*, 16, 2999-3009.
Styers, M.L., Kowalczyk, A.P. and Faundez, V. (2005) Intermediate filaments and vesicular membrane traffic: the odd couple's first dance? *Traffic*, 6, 359-365.
Sugai, M., Saito, M., Sukegawa, I., Katsushima, Y., Kinouchi, Y., Nakahata, N., Shimosegawa, T., Yanagisawa, T. and Sukegawa, J. (2003) PTH/PTH-related protein receptor interacts directly with Tctex-1 through its COOH terminus. *Biochem Biophys Res Commun*, 311, 24-31.
Suikkanen, S., Antila, M., Jaatinen, A., Vihinen-Ranta, M. and Vuento, M. (2003) Release of canine parvovirus from endocytic vesicles. *Virology*, 316, 267-280.
Suomalainen, M., Nakano, M.Y., Boucke, K., Keller, S. and Greber, U.F. (2001) Adenovirus-activated PKA and p38/MAPK pathways boost microtubule-mediated nuclear targeting of virus. *Embo J*, 20, 1310-1319.
Suomalainen, M., Nakano, M.Y., Keller, S., Boucke, K., Stidwill, R.P. and Greber, U.F. (1999) Microtubule-dependent plus- and minus end-directed motilities are competing processes for nuclear targeting of adenovirus. *J Cell Biol*, 144, 657-672.
Susalka, S.J., Hancock, W.O. and Pfister, K.K. (2000) Distinct cytoplasmic dynein complexes are transported by different mechanisms in axons. *Biochim Biophys Acta*, 1496, 76-88.
Tai, A.W., Chuang, J.Z., Bode, C., Wolfrum, U. and Sung, C.H. (1999) Rhodopsin's carboxy-terminal cytoplasmic tail acts as a membrane receptor for cytoplasmic dynein by binding to the dynein light chain Tctex-1. *Cell*, 97, 877-887.
Tai, A.W., Chuang, J.Z. and Sung, C.H. (2001) Cytoplasmic dynein regulation by subunit heterogeneity and its role in apical transport. *J Cell Biol*, 153, 1499-1509.
Tomishige, M., Klopfenstein, D.R. and Vale, R.D. (2002) Conversion of Unc104/KIF1A kinesin into a processive motor after dimerization. *Science*, 297, 2263-2267.
Tomishima, M.J. and Enquist, L.W. (2001) A conserved alpha-herpesvirus protein necessary for axonal localization of viral membrane proteins. *J Cell Biol*, 154, 741-752.
Tomishima, M.J., Smith, G.A. and Enquist, L.W. (2001) Sorting and transport of alpha herpesviruses in axons. *Traffic*, 2, 429-436.
Topp, K.S., Bisla, K., Saks, N.D. and Lavail, J.H. (1996) Centripetal transport of herpes simplex virus in human retinal pigment epithelial cells in vitro. *Neuroscience*, 71, 1133-1144.

Topp, K.S., Meade, L.B. and LaVail, J.H. (1994) Microtubule polarity in the peripheral processes of trigeminal ganglion cells: relevance for the retrograde transport of herpes simplex virus. *J Neurosci*, 14, 318-325.

Trus, B.L., Cheng, N., Newcomb, W.W., Homa, F.L., Brown, J.C. and Steven, A.C. (2004) Structure and polymorphism of the UL6 portal protein of herpes simplex virus type 1. *J Virol*, 78, 12668-12671.

Trus, B.L., Homa, F.L., Booy, F.P., Newcomb, W.W., Thomsen, D.R., Cheng, N., Brown, J.C. and Steven, A.C. (1995) Herpes simplex virus capsids assembled in insect cells infected with recombinant baculoviruses: structural authenticity and localization of VP26. *J Virol*, 69, 7362-7366.

Tuma, M.C., Zill, A., Le Bot, N., Vernos, I. and Gelfand, V. (1998) Heterotrimeric kinesin II is the microtubule motor protein responsible for pigment dispersion in Xenopus melanophores. *J Cell Biol*, 143, 1547-1558.

Turcotte, S., Letellier, J. and Lippe, R. (2005) Herpes simplex virus type 1 capsids transit by the trans-Golgi network, where viral glycoproteins accumulate independently of capsid egress. *J Virol*, 79, 8847-8860.

Tynan, S.H., Purohit, A., Doxsey, S.J. and Vallee, R.B. (2000) Light intermediate chain 1 defines a functional subfraction of cytoplasmic dynein which binds to pericentrin. *J Biol Chem*, 275, 32763-32768.

Vale, R.D. (2003) The molecular motor toolbox for intracellular transport. *Cell*, 112, 467-480.

Valetti, C., Wetzel, D.M., Schrader, M., Hasbani, M.J., Gill, S.R., Kreis, T.E. and Schroer, T.A. (1999) Role of dynactin in endocytic traffic: effects of dynamitin overexpression and colocalization with CLIP-170. *Mol Biol Cell*, 10, 4107-4120.

Vallee, R.B., Williams, J.C., Varma, D. and Barnhart, L.E. (2004) Dynein: An ancient motor protein involved in multiple modes of transport. *J Neurobiol*, 58, 189-200.

van Leeuwen, H., Elliott, G. and O'Hare, P. (2002) Evidence of a role for nonmuscle myosin II in herpes simplex virus type 1 egress. *J Virol*, 76, 3471-3481.

Verkman, A.S. (2002) Solute and macromolecule diffusion in cellular aqueous compartments. *Trends Biochem Sci*, 27, 27-33.

Vittone, V., Diefenbach, E., Triffett, D., Douglas, M.W., Cunningham, A.L. and Diefenbach, R.J. (2005) Determination of interactions between tegument proteins of herpes simplex virus type 1. *J Virol*, 79, 9566-9571.

Vrabec, J.T. and Alford, R.L. (2004) Quantitative analysis of herpes simplex virus in cranial nerve ganglia. *J Neurovirol*, 10, 216-222.

Ward, B.M. (2005) Visualization and characterization of the intracellular movement of vaccinia virus intracellular mature virions. *J Virol*, 79, 4755-4763.

Ward, B.M. and Moss, B. (2001a) Vaccinia virus intracellular movement is associated with microtubules and independent of actin tails. *J Virol*, 75, 11651-11663.

Ward, B.M. and Moss, B. (2001b) Visualization of intracellular movement of vaccinia virus virions containing a green fluorescent protein-B5R membrane protein chimera. *J Virol*, 75, 4802-4813.

Ward, B.M. and Moss, B. (2004) Vaccinia virus A36R membrane protein provides a direct link between intracellular enveloped virions and the microtubule motor kinesin. *J Virol*, 78, 2486-2493.

Ward, P.L., Avitabile, E., Campadelli-Fiume, G. and Roizman, B. (1998) Conservation of the architecture of the Golgi apparatus related to a differential organization of microtubules in polykaryocytes induced by syn- mutants of herpes simplex virus 1. *Virology*, 241, 189-199.

Warner, M.S., Geraghty, R.J., Martinez, W.M., Montgomery, R.I., Whitbeck, J.C., Xu, R., Eisenberg, R.J., Cohen, G.H. and Spear, P.G. (1998) A cell surface protein with herpesvirus entry activity (HveB) confers susceptibility to infection by mutants of herpes simplex virus type 1, herpes simplex virus type 2, and pseudorabies virus. *Virology*, 246, 179-189.

Welch, M.D. and Mullins, R.D. (2002) Cellular control of actin nucleation. *Annu Rev Cell Dev Biol*, 18, 247-288.

White, C.A., Stow, N.D., Patel, A.H., Hughes, M. and Preston, V.G. (2003) Herpes simplex virus type 1 portal protein UL6 interacts with the putative terminase subunits UL15 and UL28. *J Virol*, 77, 6351-6358.

Whittaker, G.R., Kann, M. and Helenius, A. (2000) Viral entry into the nucleus. *Annu Rev Cell Dev Biol*, 16, 627-651.

Wild, P., Engels, M., Senn, C., Tobler, K., Ziegler, U., Schraner, E.M., Loepfe, E., Ackermann, M., Mueller, M. and Walther, P. (2005) Impairment of nuclear pores in bovine herpesvirus 1-infected MDBK cells. *J Virol*, 79, 1071-1083.

Willard, M. (2002) Rapid directional translocations in virus replication. *J Virol*, 76, 5220-5232.

Wingfield, P.T., Stahl, S.J., Thomsen, D.R., Homa, F.L., Booy, F.P., Trus, B.L. and Steven, A.C. (1997) Hexon-only binding of VP26 reflects differences between the hexon and penton conformations of VP5, the major capsid protein of herpes simplex virus. *J Virol*, 71, 8955-8961.

Wisner, T.W. and Johnson, D.C. (2004) Redistribution of cellular and herpes simplex virus proteins from the trans-golgi network to cell junctions without enveloped capsids. *J Virol*, 78, 11519-11535.

Wittels, M. and Spear, P.G. (1991) Penetration of cells by herpes simplex virus does not require a low pH-dependent endocytic pathway. *Virus Res*, 18, 271-290.

Wolfstein, A., Nagel, C.H., Radtke, K., Döhner, K., Allan, V.J. and Sodeik, B. (2006) The inner tegument promotes herpes simplex virus capsid motility along microtubules in vitro. *Traffic*, 7, 227-237

Wysocka, J. and Herr, W. (2003) The herpes simplex virus VP16-induced complex: the makings of a regulatory switch. *Trends Biochem Sci*, 28, 294-304.

Xu, Y., Takeda, S., Nakata, T., Noda, Y., Tanaka, Y. and Hirokawa, N. (2002) Role of KIFC3 motor protein in Golgi positioning and integration. *J Cell Biol*, 158, 293-303.

Ye, G.J., Vaughan, K.T., Vallee, R.B. and Roizman, B. (2000) The herpes simplex virus 1 U(L)34 protein interacts with a cytoplasmic dynein intermediate chain and targets nuclear membrane. *J Virol*, 74, 1355-1363.

Yildiz, A. and Selvin, P.R. (2005) Kinesin: walking, crawling or sliding along? *Trends Cell Biol*, 15, 112-120.

Zachos, G., Clements, B. and Conner, J. (1999) Herpes simplex virus type 1 infection stimulates p38/c-Jun N-terminal mitogen-activated protein kinase pathways and activates transcription factor AP-1. *J Biol Chem*, 274, 5097-5103.

Zheng, P., Eastman, J., Vande Pol, S. and Pimplikar, S.W. (1998) PAT1, a microtubule-interacting protein, recognizes the basolateral sorting signal of amyloid precursor protein. *Proc Natl Acad Sci U S A*, 95, 14745-14750.

Zhou, Z.H., Chen, D.H., Jakana, J., Rixon, F.J. and Chiu, W. (1999) Visualization of tegument-capsid interactions and DNA in intact herpes simplex virus type 1 virions. *J Virol*, 73, 3210-3218.

Zhou, Z.H., Dougherty, M., Jakana, J., He, J., Rixon, F.J. and Chiu, W. (2000) Seeing the herpesvirus capsid at 8.5 A. *Science*, 288, 877-880.

Zhou, Z.H., He, J., Jakana, J., Tatman, J.D., Rixon, F.J. and Chiu, W. (1995) Assembly of VP26 in herpes simplex virus-1 inferred from structures of wild-type and recombinant capsids. *Nat Struct Biol*, 2, 1026-1030.

Zhou, Z.H., Prasad, B.V., Jakana, J., Rixon, F.J. and Chiu, W. (1994) Protein subunit structures in the herpes simplex virus A-capsid determined from 400 kV spot-scan electron cryomicroscopy. *J Mol Biol*, 242, 456-469.

Zhu, C., Zhao, J., Bibikova, M., Leverson, J.D., Bossy-Wetzel, E., Fan, J.B., Abraham, R.T. and Jiang, W. (2005) Functional analysis of human microtubule-based motor proteins, the kinesins and dyneins, in mitosis/cytokinesis using RNA interference. *Mol Biol Cell*, 16, 3187-3199.

9 Appendix

9.1 Curriculum vitae

Name:	Katinka Döhner
Position:	Ph.D student at the Department of Virology Center of Laboratory Medicine, Hannover Medical School
Date and place of Birth:	21 October 1974, in Leverkusen, Germany
Nationality:	German
Address:	Institute of Virology, OE 5230 Zentrum für Laboratoriumsmedizin Medizinische Hochschule Hannover (MHH) Carl-Neuberg-Str. 1 D-30625 Hannover, Germany
Phone:	+49 - (0) 511 532 4313
FAX:	+49 - (0) 511 532 8736
E-Mail:	Katinka.doehner@stud.uni-hannover.de
Family status	married to Michael Rosemeyer two children: Niklas (6 April 2002) and Friederike Rosemeyer (13 July 2003)

Education

since Sept. 1999 :	Ph.D student in the group of Dr. Beate Sodeik, Institute of Virology, Hannover Medical School: “Herpes simplex virus type 1 nuclear targeting is mediated by dynein and dynactin, but does not require the capsid protein VP26”
August 1999:	Diploma in Biochemistry
Febr.-Aug. 1999:	Diploma thesis in the group of assistant professor Dr. Beate Sodeik, Department of Physiological Chemistry, Hannover Medical School: “The function of microtubule-associated proteins during the transport of incoming capsids of the herpes simplex virus type 1 (HSV1) from the cell periphery to the nucleus”
Sept. 1996:	Prediploma in Biochemistry
1994-1999:	Student of Biochemistry at the University of Hannover
July 1994:	University entrance qualification (“Abitur”), Bischöfliches Gymnasium Josephinum, Hildesheim, Germany)

Publications.

Peer reviewed original papers:

K Döhner, A Wolfstein, U Prank, C Echeverri, D Dujardin, R Valle & B Sodeik (2002).
Function of dynein and dynactin in Herpes simplex virus capsid transport
Molecular Biology of the Cell 13: 2795-2809

H Mabit, MY Nakano, U Prank, B Saam, **K Döhner**, B Sodeik & UF Greber (2002).
Intact microtubules support adenovirus and herpes simplex virus infection
Journal of Virology 76: 9962-9971

A Wolfstein, CH Nagel, K Radtke, **K Döhner**, V Allan & B Sodeik (2006).
The inner tegument promotes herpes simplex virus capsid motility along microtubules *in vitro*
Traffic 7: 227-237

Reviews:

K Döhner & B Sodeik (2004).
The role of the host cytoskeleton for viral replication
Current Topics in Microbiology and Immunology 285, 67-108

K Döhner, CH Nagel & B Sodeik (2005).
Viral stop-and-go along microtubules – Taking a ride with dynein and kinesin
Trends in Microbiology 13: 320-327

K Radtke, **K Döhner** & B Sodeik (2006).
Viral interactions with the cytoskeleton: a hitchhiker's guide to the cell
Cellular Microbiology 8: 387-400

Ongoing projects and manuscripts in preparation:

K Döhner, S Schmidt, K Radtke & B Sodeik.
The eclipse phase of herpes simplex virus type 1 infection: efficient dynein-mediated nuclear targeting in the absence of the small capsid protein VP26

K Döhner, F Büttner, A Wolfstein, U Prank, H Ewers & B Sodeik.
Plus- and minus-end directed microtubule transport during the cell entry of herpes simplex virus type 1

J Janus, **K Döhner**, S Schmidt, CH Nagel, R Roller & B Sodeik.
US11 is not required for plus- or minus-end directed microtubule-mediated capsid transport during herpes simplex virus cell entry

K Rode, **K Döhner**, T Strive, R. Bauerfeind and B Sodeik.
Transiently expressed HSV1-UL25 blocks early viral gene expression

Presentations (presenting author underlined)

Gordon Conference 2001

A Wolfstein, **K Döhner**, U Prank, C Echeverri, P Desai, R Vallee & B Sodeik
Dynein-mediated transport of HSV1 capsids to the nucleus

Annual Meeting of the German Society of Virology, 2001, Dresden

K Döhner, A Wolfstein, U Prank, C Echeverri, P Desai, R Vallee & B Sodeik
Dynein-mediated transport of HSV1 capsids to the nucleus

26th International Herpesvirus Workshop, 2001, Regensburg

K Döhner, A Wolfstein, U Prank, C Echeverri, D Dujardin, R Vallee & B Sodeik
Dynein-mediated transport of HSV1 capsids to the nucleus

A Wolfstein, **K Döhner**, P Keller, VJ Allan & B Sodeik
In vivo and *in vitro* HSV1 capsid motility along microtubules

EMBO-Workshop: *The Cell Biology of Virus Infection*, 2001, EMBL, Heidelberg

K Döhner, A Wolfstein, U Prank, C Echeverri, D Dujardin, R Vallee & B Sodeik
Dynein-mediated transport of HSV1 capsids to the nucleus

A Wolfstein, **K Döhner**, P Keller, VJ Allan & B Sodeik
In vivo and *in vitro* HSV1 capsid motility along microtubules

1st Workshop of the Study Group in the Society of Virology on the Cell Biology of Viral Infections, October 2002, Zeilitzheim

K Döhner, A Wolfstein, U Prank, C Echeverri, D Dujardin, R Vallee & B Sodeik
Function of dynein and dynactin in Herpes Simplex Virus Capsid Transport

A Wolfstein, **K Döhner**, VJ Allan & B Sodeik
In vivo and *in vitro* HSV1 capsid motility along microtubules

S Schmidt, **K Döhner**, T Strive, U Prank & B Sodeik
The role of the tegument protein US11 during cell entry of HSV1

2nd Workshop of the Study Group in the Society of Virology on the Cell Biology of Viral Infections, September 2003, Zeilitzheim

A Wolfstein, **K Döhner**, CH Nagel, S Schmidt, VJ Allan & B Sodeik
Plus- and minus-end directed microtubule transport of Herpes Simplex Virus capsids *in vivo* and *in vitro*

K Rode, **K Döhner**, T Strive & B Sodeik
Overexpression of HSV1-UL25 reduces early HSV1 gene expression

EMBO-Workshop: The CellBiology of Virus Infection, 2004, EMBL, Heidelberg

K Döhner, F Büttner, A Wolfstein, S Schmidt & B Sodeik
Plus- and minus-end directed microtubule-mediated transport of HSV1-GFPVP26 during early phases of infection

A Wolfstein, CH Nagel, **K Döhner**, VJ Allan & B Sodeik
The inner tegument of Herpes Simplex Virus promotes capsid transport along microtubules *in vitro*

3rd Workshop of the Study Group in the Society of Virology on the Cell Biology of Viral Infections, September 2004, Zeilitzheim

K Rode, **K Döhner**, T Strive & B Sodeik
Overexpression of HSV1-UL25 reduces early HSV1 gene expression

A Wolfstein, CH Nagel, **K Döhner**, VJ Allan & B Sodeik
The inner tegument of Herpes Simplex Virus promotes capsid transport along microtubules *in vitro*

Annual Meeting of the German Society of Virology, March 2005, Hannover

K Döhner, F Büttner, A Wolfstein, S Schmidt & B Sodeik
Plus- and minus-end directed microtubule transport of herpes simplex virus type 1 early in infection

K Rode, **K Döhner**, T Strive, R Bauerfeind & B Sodeik
Transiently expressed HSV1-UL25 blocks early viral gene expression

30th International Herpesvirus Workshop, 2005, Turku

K Döhner, F Büttner, A Wolfstein, S Schmidt & B Sodeik
Plus- and minus-end directed microtubule-transport of herpes simplex virus type 1 early in infection

K Rode, **K Döhner**, T Strive, R Bauerfeind & B Sodeik
Transiently expressed herpes simplex virus 1 UL25 blocks early viral gene expression

A Wolfstein, K Radtke, CH Nagel, **K Döhner**, VJ Allan and B Sodeik
The inner tegument promotes HSV1 capsid motility along microtubules *in vitro*

9.2 Publications

Peer reviewed original research papers

1) **K Döhner**, A Wolfstein, U Prank, C Echeverri, D Dujardin, R Vallee, B Sodeik.
Function of dynein and dynactin in herpes simplex virus capsid transport
Molecular Biology of the Cell, 2002, 13: 2795-2809

2) H Mabit, MY Nakano, U Prank, B Saam, **K Döhner**, B Sodeik, UF Greber.
Intact microtubules support adenovirus and herpes simplex virus infections
Journal of Virology, 2002, 76: 9962-9971

3) A Wolfstein, CH Nagel, K Radtke, **K Döhner**, VJ Allan, B Sodeik.
The inner tegument promotes herpes simplex virus capsid motility along microtubules *in vitro*
Traffic, 2006, 7: 227-237

4) **K Döhner**, S Schmidt, K Radtke, B Sodeik.
The eclipse phase of herpes simplex virus type 1infection: efficient dynein-mediated nuclear targeting in the absence of the small capsid protein VP26
manuscript in preparation

Reviews

1) **K Döhner**, B Sodeik.
The role of the cytoskeleton during viral infection.
Current Topics in Microbiology and Immunology, 2004, 285: 67-108

2) **K Döhner**, CH Nagel, B Sodeik.
Viral stop-and-go along microtubules: taking a ride with dynein and kinesins.
Trends in Microbiology, 2005, 13: 320-327

3) K Radtke, **K Döhner**, B Sodeik.
Viral interactions with the cytoskeleton: a hitchhiker's guide to the cell.
Cellular Microbiology, 2006, 8: 387-400

Döhner K., Wolfstein A., Prank U., Echeverri C., Dujardin D., Vallee R., Sodeik B.
Function of dynein and dynactin in herpes simplex virus capsid transport.
Molecular Biology of the Cell, 2002, 13: 2795-2809

I performed the experiments for figures 1, 2, 3B, 6, 7, 8 and 9 during my Ph.D. work, the experiments for figures 3A, 4, 5 and preliminary experiments for figures 6 and 7 were part of my diploma thesis (K. Döhner: Die Rolle Mikrotubuli-assoziierter Proteine beim Transport eintretender Kapside des Herpes-Simplex-Virus Typ 1 von der Peripherie zum Zellkern, 1999). During my diploma, I obtained initial data suggesting that dynamitin overexpression may reduce immediate early viral gene expression and capsid transport. In my Ph.D. time, I validated and quantified these effects, and I established assays to quantify virus binding, virus internalization and immediate early viral gene expression biochemically in transiently transfected cells. André Wolfstein introduced me into digital microscopy and the Metamorph software, which was used for quantification of microscopy data. Ute Prank technically assisted me with experiments for figure 1. Chris Echeverri, Denis Dujardin, and R. Vallee (Columbia Universität, New York, USA) provided antibodies and plasmids. Beate Sodeik and I wrote the manuscript.

Molecular Biology of the Cell
Vol. 13, 2795–2809, August 2002

Function of Dynein and Dynactin in Herpes Simplex Virus Capsid Transport

Katinka Döhner,* André Wolfstein,* Ute Prank,* Christophe Echeverri,† Denis Dujardin,† Richard Vallee,† and Beate Sodeik*‡

*Institute of Biochemistry, Hannover Medical School, Hannover D-30623, Germany; and †Department of Pathology, Columbia University, New York, NY 10032-3702

Submitted July 13, 2001; Revised May 21, 2002; Accepted June 5, 2002
Monitoring Editor: Lawrence S. Goldstein

After fusion of the viral envelope with the plasma membrane, herpes simplex virus type 1 (HSV1) capsids are transported along microtubules (MTs) from the cell periphery to the nucleus. The motor ATPase cytoplasmic dynein and its multisubunit cofactor dynactin mediate most transport processes directed toward the minus-ends of MTs. Immunofluorescence microscopy experiments demonstrated that HSV1 capsids colocalized with cytoplasmic dynein and dynactin. We blocked the function of dynein by overexpressing the dynactin subunit dynamitin, which leads to the disruption of the dynactin complex. We then infected such cells with HSV1 and measured the efficiency of particle binding, virus entry, capsid transport to the nucleus, and the expression of immediate-early viral genes. High concentrations of dynamitin and dynamitin-GFP reduced the number of viral capsids transported to the nucleus. Moreover, viral protein synthesis was inhibited, whereas virus binding to the plasma membrane, its internalization, and the organization of the MT network were not affected. We concluded that incoming HSV1 capsids are propelled along MTs by dynein and that dynein and dynactin are required for efficient viral capsid transport to the nucleus.

INTRODUCTION

To initiate a successful infection, animal viruses bind to the cell surface, penetrate into the cytosol, and target their genome to the sites of viral transcription and replication. For many viruses this is the host nucleus (Whittaker *et al.*, 2000). Particular neurotropic viruses that enter at the presynaptic plasma membrane, such as herpes simplex viruses, are transported over long distances because the site of entry is far away from the nucleus. Herpes simplex virus type 1 (HSV1) is a human pathogen that initially replicates in epithelial cells of the oral cavity. Amplified virus enters neurons and is transported to the neuronal nuclei located in the trigeminal ganglion (reviewed in Enquist *et al.*, 1998). After lytic infection of some neurons, a latent infection is established (Wagner and Bloom, 1997).

Article published online ahead of print. Mol. Biol. Cell 10.1091/mbc.01–07–0348. Article and publication date are at www.molbiolcell.org/cgi/doi/10.1091/mbc.01–07–0348.

‡ Corresponding author. E-mail address: Sodeik.Beate@MH-Hannover.de.

Abbreviations used: DHC, dynein heavy chain; DIC, dynein intermediate chain; HSV1, herpes simplex virus type 1; gX, viral glycoprotein X; GFP, green fluorescent protein; mAb, monoclonal antibody; MOI, multiplicity of infection; MT, microtubule; MTOC, MT organizing center; pAb, polyclonal antibody; PFU, plaque-forming units.

We have calculated that it would take 231 years for a herpes virus capsid to diffuse by 10 mm in the axonal cytoplasm (Sodeik, 2000). High concentrations of protein, the cytoskeleton, and organelles cause molecular crowding in the cytoplasm, which effectively restricts free diffusion of molecules larger than 500 kDa (Luby-Phelps, 2000). Thus, virions and subviral particles are transported by active processes. Besides hijacking vesicular transport during endocytosis and secretion, viruses also exploit the host's cytoskeleton directly for their itinerary (Sodeik, 2000; Ploubidou and Way, 2001).

HSV1 virions consist of four structural components: DNA, capsid, tegument, and envelope (Steven and Spear, 1997; Zhou *et al.*, 2000). The icosahedral capsid with a diameter of 125 nm surrounds the double-stranded viral DNA of 152 kb. The tegument, the hallmark of all herpes viruses, is an amorphous layer of ~20 proteins. It is localized between the capsid and the viral envelope that contains ~12 membrane proteins.

For cell entry the envelope of HSV1 fuses with the plasma membrane. Different molecules such as heparan sulfate proteoglycans, members of the tumor necrosis receptor family (HVEM), and the immunoglobulin family (nectins) serve as receptors for the HSV1 viral glycoproteins gB, gC, and most importantly gD (reviewed in Spear *et al.*, 2000). The fusion of the viral envelope with the plasma membrane is mediated by the viral glycoproteins gB, gD, gH, and gL (Spear *et al.*, 2000).

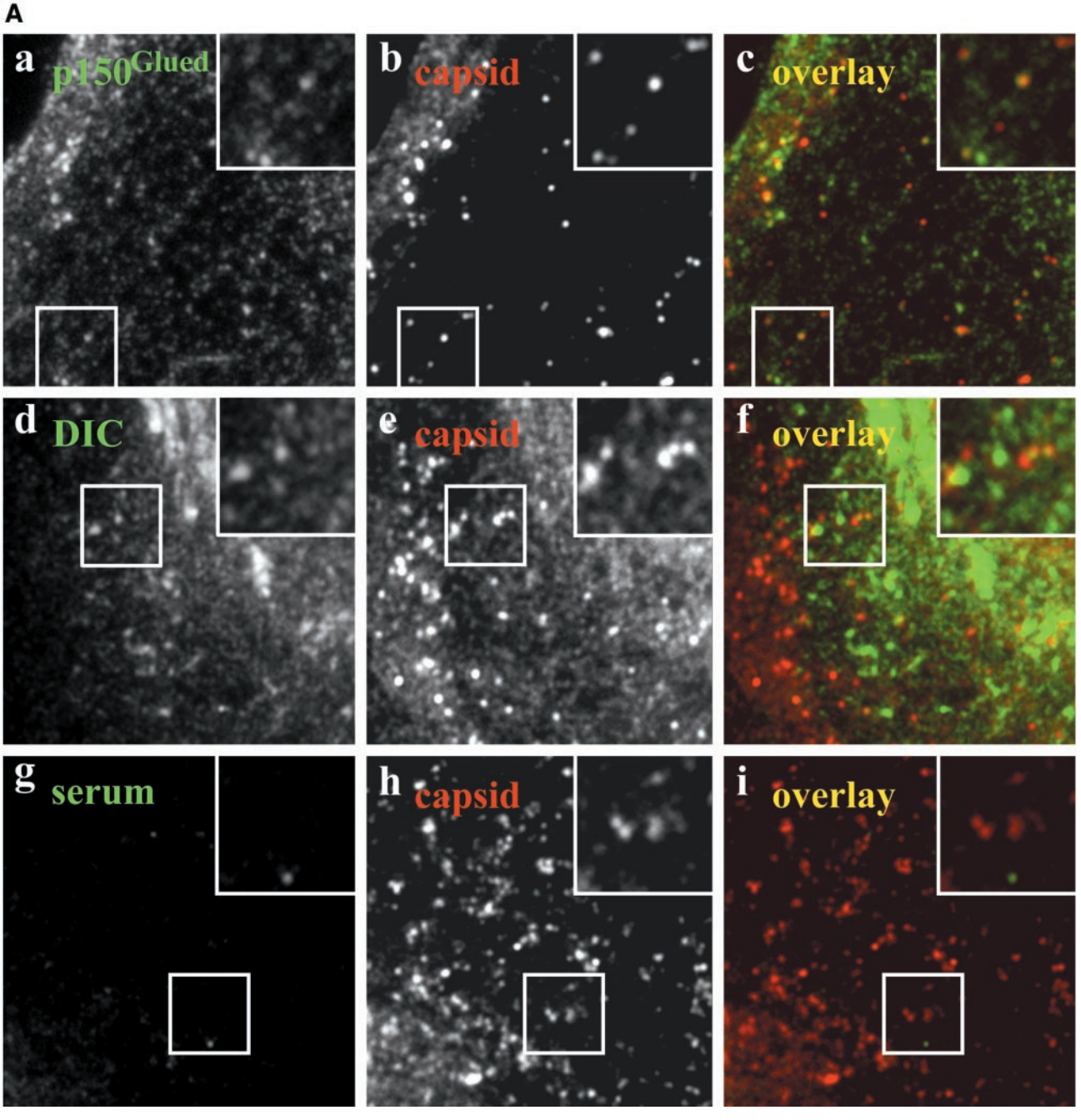

Figure 1. (A) Incoming wild-type HSV1 capsids colocalize with p150^{Glued} and DIC. A significant fraction of incoming HSV1 capsids colocalizes with p150^{Glued} and DIC (yellow dots in the overlays, c and f). This apparent colocalization is not due to binding of rabbit IgG to the herpes virus Fc receptor on the surface of infected cells because there is no signal from a nonimmune rabbit serum (i). Moreover, immunoblots confirmed that there is no unspecific cross-reactivity of the anti-dynactin or anti-dynein antibodies to structural viral proteins (our unpublished results). Immunofluorescence microscopy of PtK_2 cells infected with wild-type HSV1 for 1 h in the presence of 0.5 mM cycloheximide. Cells were fixed with PHEMO-fix at room temperature, blocked with 0.2 mg/ml pooled human IgG and 5 mg/ml BSA and double-labeled with anti-p150^{Glued} (pAb Portos; a), anti-DIC (pAb L5, d) or a nonimmune rabbit serum (serum, g) and anti-VP5 (mAb 5C10; b, e, and h). Note, that the anti-VP5 antibodies cross-reacted in PtK_2 cells weakly with the cortical actin and stress fibers. (B) Incoming HSV1 capsids of a gE deletion mutant colocalize with p150^{Glued} and DIC. Incoming HSV1 capsids of the mutant strain R7202 that does not express a viral Fc receptor colocalize with p150^{Glued} and DIC (yellow dots in the overlays, c and f). Moreover, there is no colocalization (i) after double labeling with a nonimmune rabbit serum (g) and capsid antibodies (h). Immunofluorescence microscopy of PtK_2 cells infected with HSV1 deleted for gE (R7202) for 1 h in the presence of 0.5 mM cycloheximide. Cells were fixed with PHEMO-fix at room temperature, blocked with 0.2 mg/ml pooled human IgG and 5 mg/ml BSA and double-labeled with anti-p150^{Glued} (pAb Portos; a), anti-DIC (pAb L5, d), or a nonimmune rabbit serum (g) and anti-VP5 (mAb 5C10; b, e, and h).

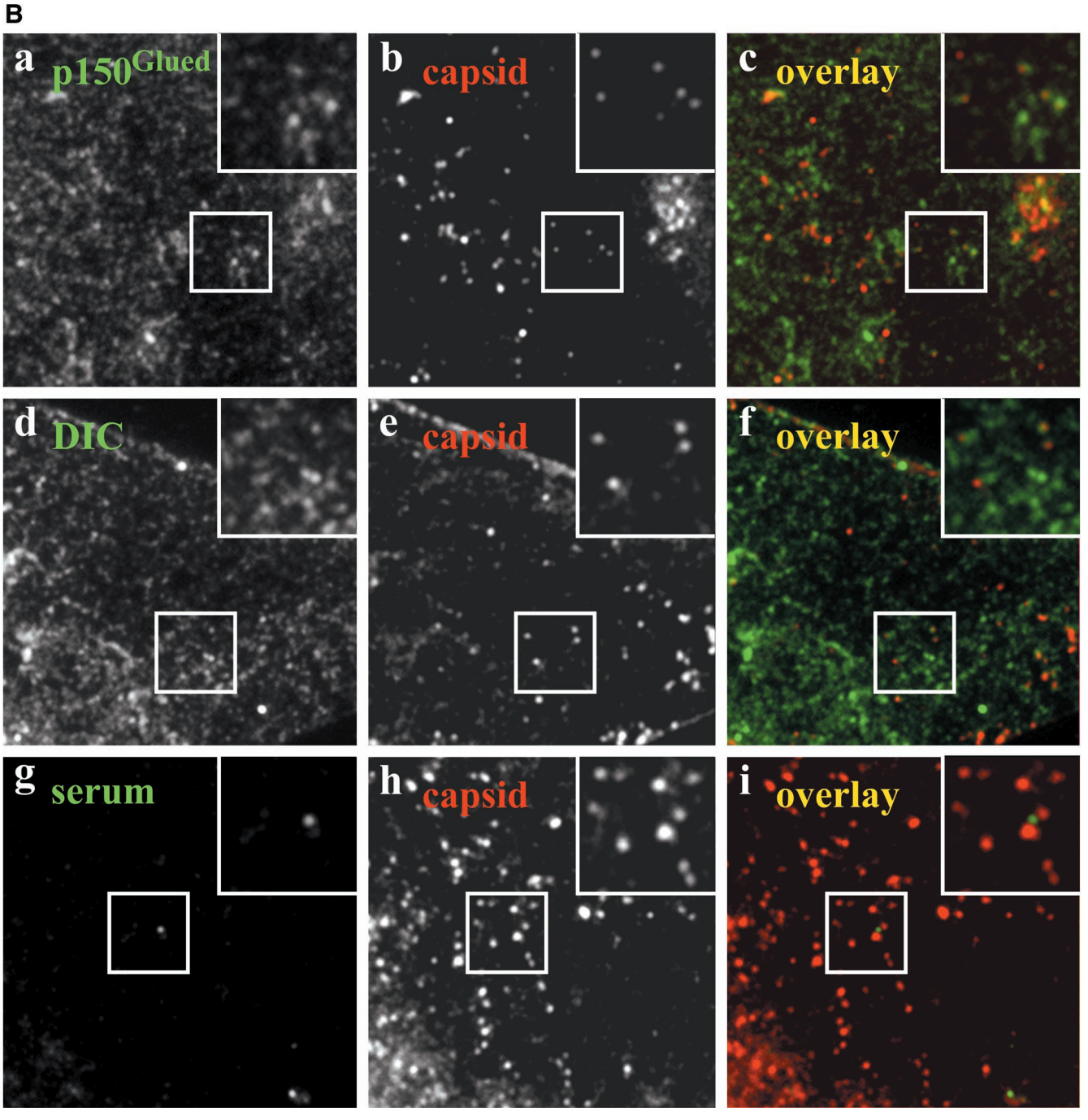

Figure 1 (legend on facing page).

All tegument proteins and the capsid with the DNA are released into the cytosol. In epithelial cells and in axons of cultured neuronal cells, incoming cytosolic capsids are transported along microtubules (MTs) to the nucleus (Kristensson *et al.*, 1986; Topp *et al.*, 1994; Topp *et al.*, 1996; Sodeik *et al.*, 1997). Electron microscopy and careful quantification demonstrated that ~70% of cytosolic capsids bind to nuclear pores and that concomitantly these capsids have lost their electron-dense core (Sodeik *et al.*, 1997). Using an in vitro uncoating assay, Ojala *et al.* (2000) demonstrated that capsid binding to the nucleus requires importin-β and that the release of the viral DNA is triggered by the interaction with the nuclear pore. Transcription, viral replication, and capsid assembly take place in

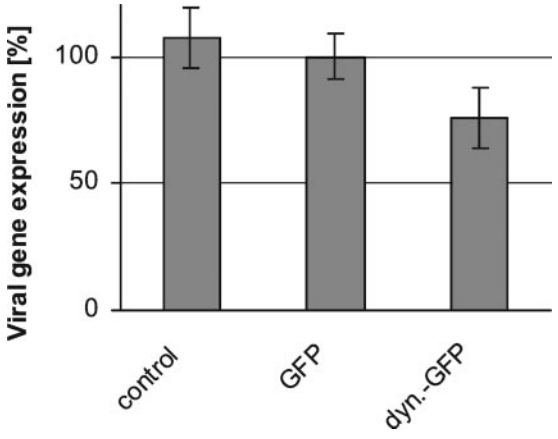

Figure 2. Quantification of immediate-early viral gene expression in transfected cells. β-Galactosidase activity per cell was reduced in dynamitin-GFP–overexpressing cells compared with untransfected or GFP-transfected cells. Two-sided Student's *t* test confirmed that viral protein synthesis is significantly lower in dynamitin-GFP–transfected cells compared with either GFP-transfected cells ($p = 1.13 \times 10^{-4}$) or to untransfected control cells ($p = 2.1 \times 10^{-5}$). There was no significant difference in β-galactosidase expression between control and GFP-transfected cells ($p = 1.58 \times 10^{-1}$). The mean values for five independent experiments each performed in duplicates are shown.

the nucleus (for reviews see Steven and Spear, 1997; Roizman and Knipe, 2001).

MTs are polar hollow protein cylinders of tubulin with a fast-growing and -shrinking plus end usually located toward the cell periphery and a minus-end mostly stabilized by attachment to the centrosome, the major microtubule organizing center (MTOC; Nogales, 2000). Most if not all minus-end–directed MT transport is mediated during interphase by dynein motors, whereas kinesins transport cargo toward the opposite direction (Vallee and Sheetz, 1996; Hirokawa, 1998). Cytoplasmic dynein is a 20 S MT-activated ATPase consisting of two dynein heavy chains (DHC), two intermediate chains (DIC), four light intermediate chains (DLIC) and four different classes of light chains (DLC; Karki and Holzbaur, 1999; King, 2000). Dynein is responsible for the perinuclear localization of several organelles around the MTOC and retrograde organelle transport in axons and is active during mitosis (Vallee and Sheetz, 1996; Hirokawa, 1998).

In many cases dynein is assisted by a second 20 S protein complex, called dynactin (Vallee and Sheetz, 1996; Karki and Holzbaur, 1999). It consists of 2 copies of $p150^{Glued}$, 4 molecules of dynamitin, p62, ~10 copies of Arp1 (actin-related-protein 1), possibly 1 conventional actin, Arp11, and actin capping protein (p37 and p32), p27, p25, and p24 (Holleran *et al.*, 1998; Eckley *et al.*, 1999). $p150^{Glued}$ can bind directly to DIC and thus link dynein to dynactin (Karki and Holzbaur, 1995; Vaughan and Vallee, 1995). Dynamitin, at high concentrations after transient transfection, dissociates the dynactin complex (Echeverri *et al.*, 1996; Eckley *et al.*, 1999). Excess dynamitin affects all tested dynein-mediated transports in vivo and in vitro: e.g., spindle organization, chromosome transport, and the subcellular localization of several membrane organelles (Echeverri *et al.*, 1996; Burkhardt *et al.*, 1997; Presley *et al.*, 1997; Valetti *et al.*, 1999; Sharp *et al.*, 2000).

Quantitative immunoelectron microscopy showed that DHC colocalizes with incoming herpes virus capsids (Sodeik *et al.*, 1997). Here, we demonstrate that incoming HSV1 capsids also colocalized with DIC and the $p150^{Glued}$ subunit of dynactin. To test whether HSV1 capsids use cytoplasmic dynein for their transport to the nucleus, we transiently transfected cells with dynamitin, subsequently challenged them with HSV1, and measured virus binding, internalization, capsid transport to the nucleus, and immediate-early viral gene expression. High concentrations of dynamitin and dynamitin-GFP clearly reduced the number of viral capsids transported to the nucleus compared with untransfected cells. Because fewer capsids reached the nucleus, presumably fewer viral genomes were delivered to the nucleoplasm, and the amount of viral protein synthesis was reduced. Overexpression of dynamitin did not downregulate virus receptors at the plasma membrane, because both virus binding and internalization were not reduced. We propose that incoming HSV1 capsids are propelled by dynein along MTs and that functional dynactin is required for their efficient transport.

MATERIALS AND METHODS

Cells and Antibodies

PtK_2 cells (ATCC CCL-56) were grown in 10%, Vero cells (ATCC CCL-81) in 7.5%, and BHK-21 cells (ATCC CCL-10) in 15% fetal calf serum. The media contained MEM, 2 mM glutamine, nonessential amino acids, and with the exception of the PtK_2 medium 100 U/ml penicillin and 100 μg/ml streptomycin.

Dynamitin expression was analyzed using mAb 50.1 (Paschal *et al.*, 1993) or a rabbit anti-myc antibody (Gee *et al.*, 1997), DHC was detected with affinity-purified rabbit pAb (Vaisberg *et al.*, 1993), DIC with a rabbit pAb L5 (Vaughan and Vallee, 1995), $p150^{Glued}$ with rabbit pAbs D'Artagnon, Aramis, or Portos (Vaughan and Vallee, 1995), and the cation-independent mannose-6-phosphate receptor with a rabbit pAb (Griffiths *et al.*, 1988). MTs were visualized using mouse mAb 1A2 (Kreis, 1987) and actin filaments with TRITC-Phalloidin (Sigma-Aldrich, Schnelldorf, Germany). We used preadsorbed rabbit pAbs raised against DNA-containing capsids (anti-HC) and empty capsids (anti-LC; Cohen *et al.*, 1980) and a mouse mAb 5C10 against VP5 (Newcomb *et al.*, 1996) to detect incoming viral capsids by immunofluorescence microscopy (Sodeik *et al.*, 1997). Immediate-early viral gene expression was measured with a mouse mAb against ICP4 (Showalter *et al.*, 1981). Viral glycoproteins were labeled with mouse mAb DL6 against gD and rabbit pAb R68 against gB (Eisenberg *et al.*, 1985, 1987). Secondary antibodies were purchased from Dianova (Hamburg, Germany).

Virological Techniques

Preparation of Stock Virus Cold and radioactively labeled virus stocks of HSV1 were prepared as described (Sodeik *et al.*, 1997). We used wild-type strain F (ATCC VR-733) and two HSV1 mutants: strain [KOS]tk12, which expresses the LacZ gene controlled by the immediate-early ICP4 promoter (Warner *et al.*, 1998) and strain R7202, which lacks the majority of the glycoprotein E codons including the start codon and therefore does not exhibit viral Fc receptor activity (Baines and Roizman, 1993).

Plaque Assay Virus was diluted in 10-fold steps in RPMI with 0.2% wt/vol BSA, 20 mM HEPES, pH 7.0 (RPMI/BSA) and incubated in six-well dishes with just-confluent Vero cells for 1 h at room tem-

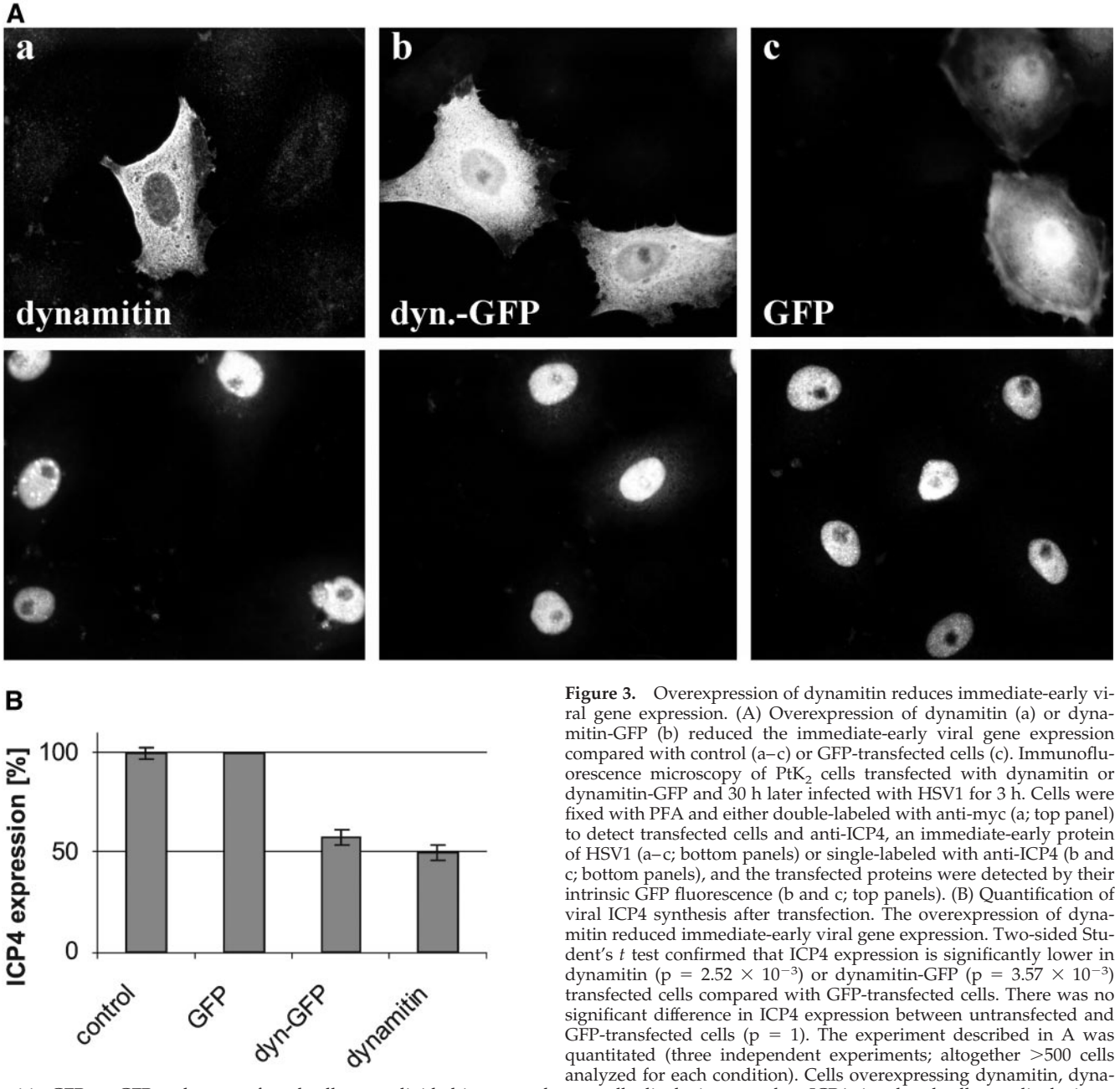

Figure 3. Overexpression of dynamitin reduces immediate-early viral gene expression. (A) Overexpression of dynamitin (a) or dynamitin-GFP (b) reduced the immediate-early viral gene expression compared with control (a–c) or GFP-transfected cells (c). Immunofluorescence microscopy of PtK_2 cells transfected with dynamitin or dynamitin-GFP and 30 h later infected with HSV1 for 3 h. Cells were fixed with PFA and either double-labeled with anti-myc (a; top panel) to detect transfected cells and anti-ICP4, an immediate-early protein of HSV1 (a–c; bottom panels) or single-labeled with anti-ICP4 (b and c; bottom panels), and the transfected proteins were detected by their intrinsic GFP fluorescence (b and c; top panels). (B) Quantification of viral ICP4 synthesis after transfection. The overexpression of dynamitin reduced immediate-early viral gene expression. Two-sided Student's *t* test confirmed that ICP4 expression is significantly lower in dynamitin ($p = 2.52 \times 10^{-3}$) or dynamitin-GFP ($p = 3.57 \times 10^{-3}$) transfected cells compared with GFP-transfected cells. There was no significant difference in ICP4 expression between untransfected and GFP-transfected cells ($p = 1$). The experiment described in A was quantitated (three independent experiments; altogether >500 cells analyzed for each condition). Cells overexpressing dynamitin, dynamitin-GFP, or GFP and untransfected cells were divided into two classes: cells displaying a nuclear ICP4 signal and cells not displaying a nuclear ICP4 signal.

perature on a rocking platform. The inoculum was removed, and 2 ml/well normal growth medium containing 10 μg/ml pooled human IgG (Sigma-Aldrich) was added. The cells were further cultured for 2 d at 37°C, 5% CO_2 and fixed in absolute methanol. After incubation with a mAb to gD (DL6) and a secondary anti-mouse antibody conjugated to alkaline phosphatase, the cells were washed with TSM (100 mM Tris-HCl, pH 9.5, 100 mM NaCl, 5 mM $MgCl_2$) and treated with 0.2 mM nitroblue tetrazolium chloride and 0.8 mM 5-bromo-4-chloro-3-indolyl phosphate until dark plaques became visible. We routinely obtained titers around 10^{10} PFU/ml for cold wild-type and HSV1[KOS]tk12 virus and 10^7 PFU/ml for ^{3}H-thymidine labeled virus.

Virus Infection Control and transfected Vero, BHK, or PtK_2 cells were inoculated with virus in RPMI/BSA for 2 h on ice to allow virus binding. After three washes with ice-cold RPMI/BSA, they were shifted to growth medium at 37°C and 5% CO_2. In those experiments analyzing the subcellular localization of incoming

viral particles, 0.5 mM cycloheximide was added to prevent synthesis of new viral proteins (Sodeik *et al.*, 1997). When nocodazole (50 μM) was used to depolymerize MTs, cells were pretreated for 1 h at 37°C, and the drug was present during all further incubation steps. For immunofluorescence microscopy in 24-well plates we used 8×10^6 PFU/well HSV1 for entry experiments, 1×10^7 PFU/well for virus binding experiments, and 4×10^5 PFU/well for ICP4 experiments.

Light Microscopy

Cells grown on coverslips were fixed with 3% (wt/vol) paraformaldehyde (PFA in PBS) for 20 min followed by 50 mM NH_4Cl/PBS for 10 min and 0.1% Triton X-100/PBS for 5 min. For colocalization studies and visualization of MTs, cells were fixed with PHEMO-fix (3.7% [wt/vol] PFA, 0.05% [wt/vol] glutaraldehyde, 0.5% Triton X-100 in PHEMO buffer) either at room temperature or at 37°C for 10 min, and washed with PHEMO buffer (68 mM PIPES, 25 mM HEPES, pH 6.9, 15 mM EGTA, 3 mM $MgCl_2$, 10% [vol/vol] DMSO) followed by 50 mM NH_4Cl/PBS for 10 min.

In most experiments we used 10% (vol/vol) goat serum with 5 mg/ml BSA as blocking reagent and performed the immunolabeling essentially as described (Sodeik *et al.*, 1997). For the experiments described in Figure 1 we used 0.2 mg/ml human immunoglobulins (IgGs, I4506; Sigma, Taufkirchen, Germany) with 5 mg/ml BSA to block nonspecific protein binding.

HSV1 carries in its envelope a Fc-receptor with strong affinity for human IgGs, decreasing affinity for rabbit, sheep, and goat and no affinity for murine IgGs (reviewed in Dubin *et al.*, 1992). The degree of the Fc-receptor–specific signal in the absence of human IgGs depended strongly on the protocol used: it was most prominent under the conditions we found optimal for the colocalization studies, namely after PHEMO fixation at room temperature, but surprisingly only weak after PHEMO fixation at 37°C or after PFA fixation followed by TX-100 (our unpublished results). Initial double-labeling experiments for dynein or dynactin with HSV1 capsids demonstrated that in the presence of human IgGs, primary rabbit and secondary goat antibodies bound only with their antigen-binding domain but not with their Fc-domain to infected cells. Without human IgGs, the membrane of incoming virions was also detected by preimmune and immune rabbit sera but not by unspecific mouse antibodies (our unpublished results).

The cells were examined with a fluorescence microscope (DM IRB/E; Leica, Wetzlar, Germany), and micrographs were taken on Kodak TMAX-400 (Eastman Kodak, Rochester, NY) or Ilford HP5 400 films (Ilford, Cheshire, United Kingdom). All digitized images (using a Nikon LS-1000 35-mm film scanner; Tokyo, Japan) were image processed using Adobe Photoshop version 5.5 (San Jose, CA). Colocalization and expression levels were analyzed using a digital interline charge coupled device camera (MicroMax-5MHz-782Y; Princeton Instruments Inc., Princeton, NJ) and the Metamorph software version 4.01 (Universal Imaging Corporation, West Chester, PA). Dynamitin-GFP and GFP-expressing cells were scored as high expressors (see Figure 8B) when their average gray values in the cytoplasm were above 400 (exposure time: 0.2 s) using the function "show region statistics" of the Metamorph software. Cells overexpressing dynamitin (mAb 50.1) were scored as high expressors when their average gray values in the cytoplasm were above 600 (exposure time: 0.5 s).

Transient Transfection

Plasmids For transient transfections we used the plasmids pEGFP-N1 (Clontech Laboratories Inc., Palo Alto, CA) expressing enhanced green fluorescent protein (GFP) and p50 expressing myc-tagged dynamitin (Echeverri *et al.*, 1996). For the dynamitin-GFP–expressing construct (p50-GFP), the full dynamitin cDNA sequence was inserted upstream of GFP into the pEGFP-N1 vector between the *Eco*RI and the *Bam*HI sites. The proper restriction sites were created by PCR, and subsequent products were sequenced to ensure that no mutation was created. All constructs are under the control of the cytomegalovirus immediate-early promotor (Clontech).

Experiments Measuring Virus Binding, Internalization, and Protein Synthesis PtK_2 cells were seeded in 10-cm diameter culture dishes at a density of 5×10^5. Twenty-four hours later the cells were transfected with 30 μg DNA per dish using calcium phosphate (Sambrook *et al.*, 1989). After 24 h, the cells were washed once with PBS, and 10 ml/dish normal growth medium was added for 19–22 h.

Experiments Analyzed by Immunofluorescence Microscopy Transfections were made with calcium phosphate or lipofectamine reagent (Life Technologies, Karlsruhe, Germany). For the latter, cells were seeded onto coverslips (12-mm diameter) in a 24-well cell culture dish at a density of 4×10^4 (Vero) or 3×10^4 (PtK_2) cells per well. After 16–18 h, the cells were washed twice with serum-free, antibiotic-free MEM and incubated with 300 μl/well serum-free, antibiotic-free MEM containing 1.5 μl/well lipofectamine and 150 ng DNA for 5 h. The transfection mixture was removed, and 1 ml/well normal growth medium was added for 24–28 h. For transfections with calcium phosphate, PtK_2 cells were seeded onto coverslips (12-mm diameter) in a 24-well cell culture dish at a density of 2×10^4 cells per well. After 24 h cells were transfected with 1.1 μg DNA per well. Twenty-four hours later 1 ml/well normal growth medium was added for 19–22 h.

Immediate-early Viral Gene Expression

Immediate-early viral gene expression was analyzed using the mutant HSV1(KOS)tk12, which expresses the bacterial LacZ gene coding for the enzyme β-galactosidase under the control of the immediate-early ICP4 promotor of HSV1 (Warner *et al.*, 1998). PtK_2 cells transfected for 44 h with dynamitin-GFP or GFP were inoculated with 2 ml per 10-cm dish RPMI/BSA containing $4–8 \times 10^6$ PFU of HSV1(KOS)tk12 for 2 h on ice and then shifted to 37°C for 3–4 h. The cells were harvested by trypsinization, and trypsin was immediately inhibited by adding trypsin inhibitor, and further protein synthesis by cycloheximide. Transfection efficiencies were determined by flow cytometry (FACSCalibur; Becton Dickinson, Heidelberg, Germany), cell densities by BCA assay (Pierce, Rockford, IL) after lysis in 1% SDS/PBS, and β-galactosidase activities after lysis in 0.5% TX-100/PBS with 1 mg/ml BSA and protease inhibitors using *O*-nitrophenyl-β-D-galactopyranoside as substrate. β-Galactosidase activity per cell was normalized to GFP-transfected cells.

Quantification of Virus Binding and Internalization

We assayed for virus binding and internalization essentially as described using a protease protection assay (Sodeik *et al.*, 1997). PtK_2 cells transfected for 44 h with dynamitin-GFP or GFP were inoculated with 2 ml per 10-cm dish RPMI/BSA containing ^{3}H-thymidine labeled HSV1 (5–10 kBq and 8×10^6 to 1.6×10^7 PFU). Cell-associated radioactivity—representing the amount of bound virions—was determined by scintillation counting. Virus binding was expressed as radioactivity per cell and normalized to GFP-transfected cells. To assay for virus internalization, ^{3}H-thymidine-labeled virus was bound to transfected cells at 4°C for 2 h. The cells were washed to remove unbound virus, shifted to 37°C for 30 min, transferred back to ice, and washed with ice-cold RPMI. Cell associated radioactivity after proteinase K treatment was determined by scintillation counting (Sodeik *et al.*, 1997). In these virus binding and internalization experiments, the transfection efficiencies were measured by flow cytometry and cell densities using a hemocytometer.

RESULTS

Colocalization of Incoming HSV1 Capsids with Cytoplasmic Dynein and Dynactin

We have shown previously by quantitative immune electron microscopy that in Vero cells incoming cytosolic HSV1 capsids colocalize with DHC (Sodeik *et al.*, 1997). Here, we used PtK_2 cells that are extremely flat in the periphery to analyze the subcellular distribution of HSV1 relative to dynein and dynactin. In uninfected cells, anti-DHC, anti-DIC, and anti $p150^{Glued}$ revealed a weak diffuse labeling throughout the cytoplasm that was strongest around the nucleus; moreover, centrosomes and numerous tubules and vesicles concentrated around the nucleus were labeled (our unpublished results). These structures might represent host organelles that use dynein for transport along MTs (Burkhardt *et al.*, 1997; Sodeik *et al.*, 1997; Harada *et al.*, 1998; Valetti *et al.*, 1999; Habermann *et al.*, 2001).

After 1 h of infection, a mouse mAb to the capsid protein VP5 labeled numerous small fluorescent spots that represented individual capsids distributed over the entire cytoplasm (Figure 1, A and B, b, e, and h). After 2 h and more so after 3 h, the majority of capsids had accumulated at the nucleus (see Figure 7). Numerous small dots of dynactin (Figure 1Ac), DHC (our unpublished results), and DIC (Figure 1Af) colocalized with viral capsids, whereas there was no colocalization after double labeling with the mouse anti-VP5 and a preimmune rabbit serum (Figure 1Ai).

HSV1 carries in its envelope the viral protein complex gE/gI that has a strong Fc-receptor binding activity for human IgGs, decreasing affinity for rabbit, sheep, and goat, but does not bind to murine IgGs (reviewed in Dubin *et al.*, 1992). However, none of eight mouse monoclonal antibodies generated against different subunits of dynein (DHC, DIC, DLC) or dynactin ($p150^{Glued}$, dynamitin) showed any colocalization with viral capsids despite testing several fixation and permeabilization protocols. In the presence of rabbit or goat sera, we therefore blocked the Fc-receptor with human IgGs (cf. MATERIALS AND METHODS). Moreover, we used the HSV1 mutant R7202, which is deleted for gE and does not contain a Fc-binding activity (Baines and Roizman, 1993). After 1 h of infection with R7202, numerous viral capsids were also labeled for dynactin and dynein, in the presence (Figure 1B) and also absence (our unpublished results) of human IgGs.

Approximately 15–20% of incoming capsids from wild-type HSV1 and the mutant R7202 were labeled with antibodies to dynactin (20% for $p150^{Glued}$; $n = 130$) and dynein (15% for DIC; $n = 100$). The lacking reactivity of monoclonal antibodies and the incomplete colocalization using polyclonal rabbit sera directed against dynein or dynactin subunits might suggest that there was steric hindrance and thus only limited epitope access in a putative ternary complex of capsids, dynein, and dynactin. Alternatively, it is possible that only a subset of viral capsids binds to dynein and/or dynactin at a given time point. Because most subunits of dynein and dynactin only exist in 20 S complexes and not as soluble proteins, these data showed that both protein complexes, dynein and dynactin, were at least transiently present on incoming viral capsids.

Immediate-early Viral Gene Expression after Overexpression of Dynamitin

To test whether functional dynein and dynactin were required during HSV1 entry, we transfected PtK_2 cells with dynamitin, which inhibits many dynein-mediated transport processes (Echeverri *et al.*, 1996; Burkhardt *et al.*, 1997; Presley *et al.*, 1997; Valetti *et al.*, 1999). In cells overexpressing dynamitin or dynamitin-GFP, mannose-6-phosphate receptor containing organelles were scattered over the entire cytoplasm rather than concentrated in the perinuclear region (our unpublished results), indicating that the function of dynein was disrupted (Burkhardt *et al.*, 1997; Valetti *et al.*, 1999). We routinely obtained transfection efficiencies of 65–75% for dynamitin-GFP and 70–85% for GFP as measured by flow cytometry (our unpublished results).

We next infected transfected PtK_2 cells with a HSV1 mutant expressing β-galactosidase under the control of an immediate-early HSV1 promoter (HSV1[KOS]tk12; Warner *et al.*, 1998), and the enzyme activity was quantified as an indicator for immediate-early viral gene expression. β-galactosidase activity was highest in untransfected cells and lowest in cells transfected with dynamitin-GFP (Figure 2). Overexpressing dynamitin-GFP reduced the amount of β-galactosidase by 25% compared with overexpression of GFP alone.

To analyze single cells, we infected PtK_2 cells with wild-type HSV1 and double-labeled them with antibodies to the transiently expressed proteins and ICP4, an immediate-early, nuclear herpes virus protein (Everett, 2000). After overexpression of dynamitin and dynamitin-GFP there were about half as many cells labeled for ICP4 compared with GFP expressing or untransfected cells (Figure 3, A and B). Thus, the expression of ICP4 and β-galactosidase, both under the control of the ICP4 promotor, were reduced after overexpressing dynamitin or dynamitin-GFP compared with controls. Inhibition of immediate-early viral gene expression might be due to changes in 1) the MT-network, 2) virus binding to the cell surface, 3) virus internalization, or 4) a reduced cytosolic transport of incoming capsids to the nucleus.

The Cytoskeleton after Transient Transfection

Dynactin contains conventional actin, Arp1 and Arp11 (Schafer *et al.*, 1994; Eckley *et al.*, 1999). We therefore tested whether dynamitin overexpression affected the actin cytoskeleton in PtK_2 cells but detected no changes in filamentous actin upon transfection (our unpublished results; Burkhardt *et al.*, 1997). The overexpression of dynamitin can affect the organization of MTs in fibroblastic cells (Burkhardt *et al.*, 1997; Quintyne *et al.*, 1999). Because nuclear targeting of capsids is MT dependent (Sodeik *et al.*, 1997), we analyzed the MT-network in PtK_2 cells by immunofluorescence microscopy. In many cells, the MTs emanated to the peripheral cytoplasm from one location in the perinuclear region that most likely represents the position of the MTOC or centrosome (arrows in Figure 4). However, there were also cells in which there were several MT organizing zones around the nucleus rather than a single, well-defined MTOC or in which MTs emanated more broadly from the nuclear surface (asterisks in Figure 4). The number of cells without an apparent MTOC increased after overexpression of dynamitin (a) or

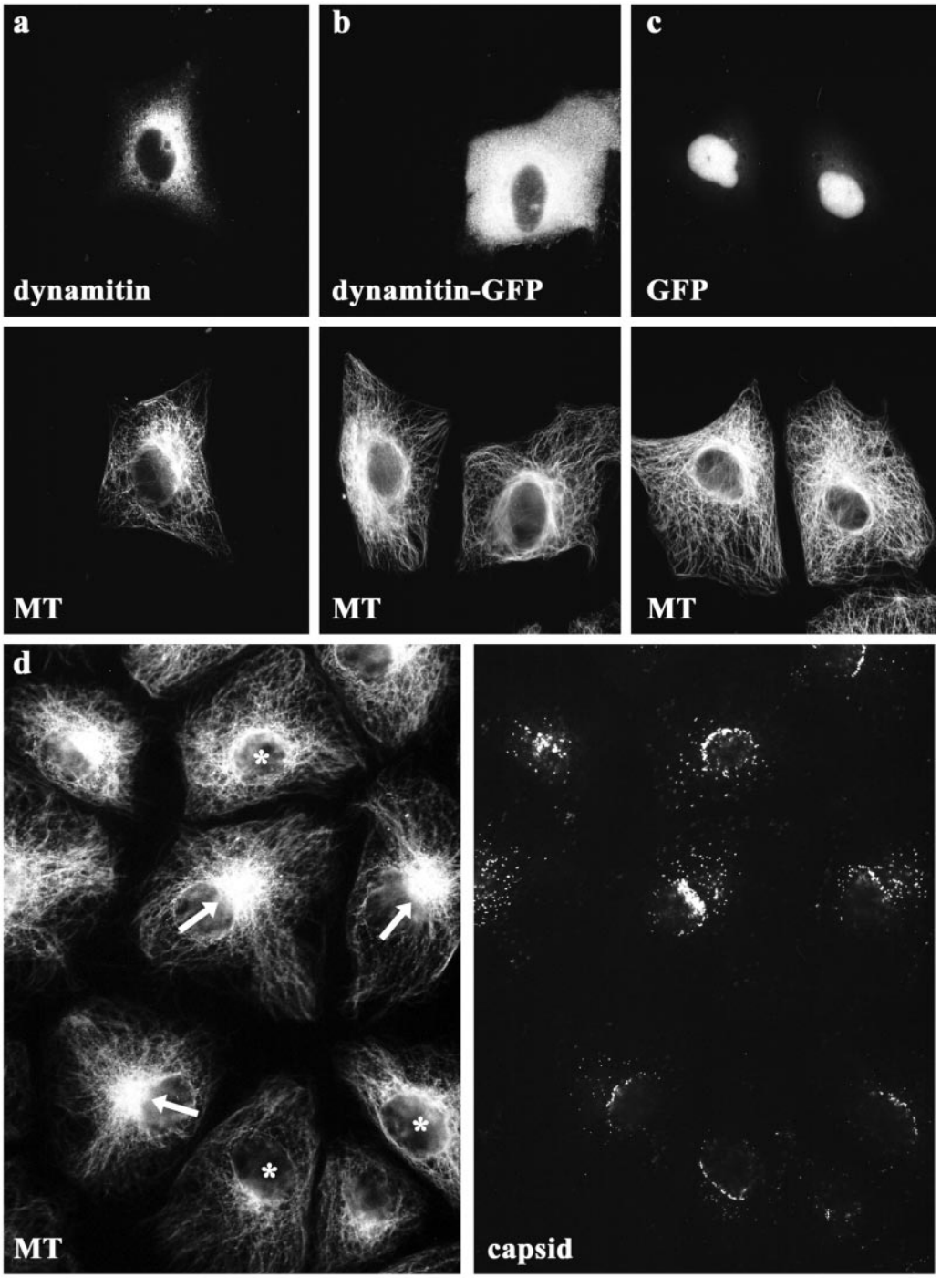

Figure 4. Organization of the microtubule network in transfected PtK_2 cells. Immunofluorescence microscopy showing the MT network of PtK_2 cells after overexpression of dynamitin or dynamitin-GFP. In almost all cells the MTs emanated from the perinuclear region of the cell. After overexpression of dynamitin (a) or dynamitin-GFP (b), there seemed to be fewer cells with a well-defined MTOC. In untransfected cells (b and d) and in cells overexpressing GFP (c), the MTs were focused at the MTOC in many cells. In untransfected cells with an apparent MTOC (arrows in d) and in cells with unfocussed MTs (asterisks in d) numerous capsids reached the nucleus (d, capsids). Twenty-eight hours after transfection, cells were fixed with PHEMO-fix and double-labeled with anti-myc (pAb, a; top panel) and anti-tubulin (mAb 1A2, a; bottom panel). Cells transfected with GFP proteins were only labeled with anti-tubulin (mAb 1A2, b and c; bottom panels). Note that because of the PHEMO-fixation, GFP was relocalized to the nucleus. In unfixed cells, most of the transiently expressed GFP was localized to the cytoplasm. In d, untransfected PtK_2 cells were infected with HSV1 for 3 h and fixed with PHEMO-fix at 37°C. Capsids were labeled with anti-LC (d; right panel) and MTs with 1A2 (d; left panel).

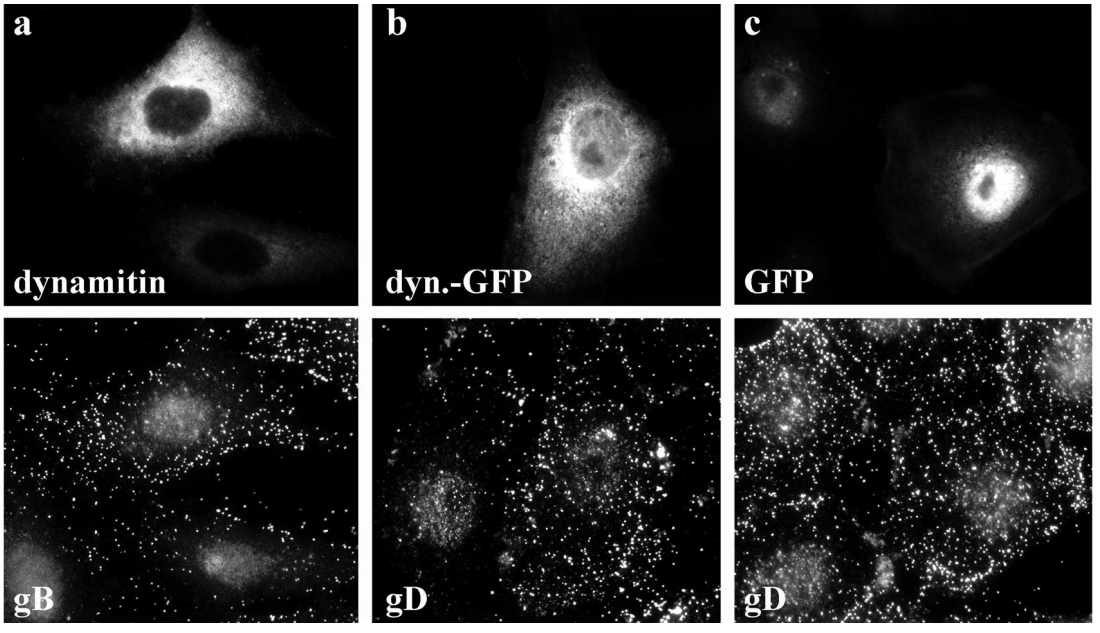

Figure 5. HSV1 binding and internalization in transfected cells. In cells overexpressing dynamitin (a) or dynamitin-GFP (b) virus binding was not reduced compared with untransfected cells or cells overexpressing GFP (c). Immunofluorescence microscopy of PtK_2 cells transfected with dynamitin or dynamitin-GFP and 20 h later inoculated with HSV1 for 2 h at 4°C. After 2 h at 4°C cells were washed and shifted to 37°C for 15 min to reduce unspecific binding, fixed in PFA and permeabilized with TX-100. They were double-labeled with anti-dynamitin (a; top panel) and anti-gB (a; bottom panel), and cells transfected with GFP proteins were only labeled with anti-gD (mAb DL6, b and c; bottom panels).

dynamitin-GFP (b), whereas GFP (c) did not have such an effect. However, also in untransfected cells without an obvious MTOC and unfocussed MTs many capsids reached the nucleus (Figure 4d, asterisks), suggesting that MTs but not focused MTs are required for nuclear targeting of HSV1 capsids.

Virus Binding and Internalization after Transfection

Overexpression of dynamitin affects both, secretory and endocytic membrane traffic (Burkhardt *et al.*, 1997; Presley *et al.*, 1997; Valetti *et al.*, 1999), and the concentration of HSV1 cell surface receptors present at the plasma membrane might therefore have been changed by the transfected proteins. Because several different molecules can serve as HSV receptors (Spear *et al.*, 2000), we decided to measure virus binding and internalization directly rather than trying to determine the subcellular localization of all potential viral surface receptors. To this end, cells overexpressing dynamitin, dynamitin-GFP, or GFP were infected with HSV1 for 15 min, fixed, and then labeled for the overexpressed proteins and viral glycoproteins. Compared with untransfected cells and with cells overexpressing GFP, glycoprotein labeling was unchanged by overexpression of dynamitin or dynamitin-GFP (Figure 5). Thus, the sum of surface-bound and internalized virus was similar under all conditions tested. Next we determined virus binding by measuring the amount of cell-bound virus and internalization using a protease protection assay (Sodeik *et al.*, 1997). After 2 h binding on ice ~50% of ^{3}H-thymidine–labeled HSV1 resist washing with buffer, and 95% of the bound virus can be detached from cells by proteinase treatment. If, however, the cells are warmed up, 70% of the bound HSV1 enters the cells with a half time of ~8 min (Sodeik *et al.*, 1997; our unpublished results).

Using these assays we determined that compared with untransfected or GFP-transfected PtK_2 cells, neither binding (Figure 6A) nor internalization (Figure 6B) of ^{3}H-thymidine–labeled HSV1 were reduced after overexpression of dynamitin-GFP. There seemed to be a slight increase of virus internalization in dynamitin-GFP– and GFP-transfected cells compared with control cells (Figure 6B). The reasons for that are unclear. However, the reduced viral protein synthesis after overexpression of dynamitin or dynamitin-GFP could neither result from reduced virus binding nor from reduced internalization.

Dynamitin Reduces Cytosolic Viral Capsid Transport to the Nucleus

The reduced amount of viral protein synthesis after overexpression of dynamitin could be due to impaired cytosolic transport of incoming capsids from the periphery to the nucleus. We therefore transiently transfected PtK_2 cells with dynamitin or dynamitin-GFP and infected them with HSV1 in the presence of cycloheximide.

Most capsids had reached the nucleus in untransfected cells as well as in cells overexpressing GFP 3 h after infection (Figure 7). In cells overexpressing dynamitin or dynamitin-GFP, fewer capsids were present at the nucleus. Interestingly, in many cells overexpressing dynamitin or dynamitin-

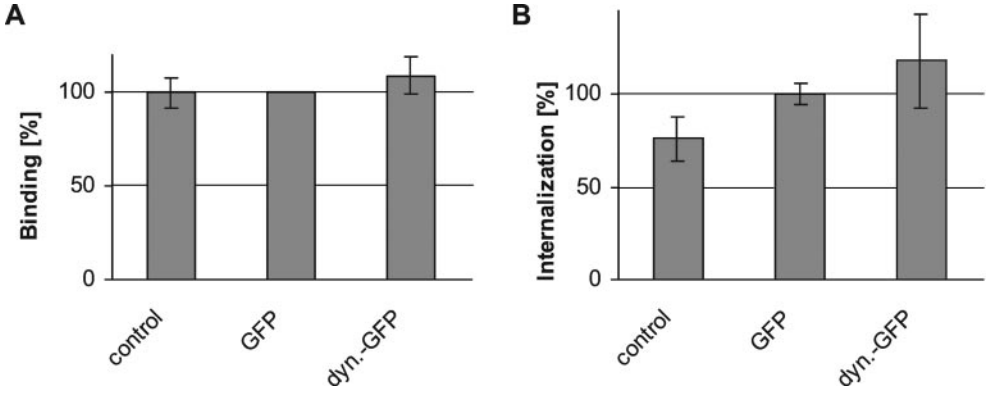

Figure 6. Quantification of HSV1 virus binding and internalization in transfected cells. (A) Virus binding after overexpression of dynamitin-GFP or GFP was identical to virus binding to mock-transfected cells (n = 2). Two-sided Student's *t* test confirmed that viral binding was not significantly different in dynamitin-GFP–transfected cells compared with either GFP-transfected cells ($p = 4.21 \times 10^{-1}$) or to untransfected control cells ($p = 4.03 \times 10^{-1}$). There was also no significant difference in viral binding between control and GFP-transfected cells ($p = 9.42 \times 10^{-1}$). Virus binding was calculated as radioactivity per cell and expressed as percent of radioactivity per cell compared with GFP-transfected cells. (B) Virus internalization after overexpression of dynamitin-GFP was not reduced compared with GFP-transfected cells (n = 6). Two-sided Student's *t* test confirmed that viral internalization was not significantly different in dynamitin-GFP–transfected cells compared with GFP-transfected cells ($p = 1.45 \times 10^{-1}$). However, compared with untransfected cells, virus internalization was higher in cells transfected with GFP ($p = 2.46 \times 10^{-3}$) or dynamitin-GFP ($p = 7.11 \times 10^{-3}$). Virus internalization was calculated as radioactivity per cell and expressed as percent of radioactivity per cell compared with GFP-transfected cells.

GFP the capsids were not randomly distributed over the entire cytoplasm as they are early in the infection (Sodeik *et al.*, 1997), but rather the capsids had accumulated in the cell margins (arrows in Figure 7, a and b). Similar results were obtained using BHK and Vero cells. However, BHK and Vero cells sometimes showed dramatic changes in cell morphology, whereas the morphology of PtK_2 cells was largely not affected by overexpressed dynamitin.

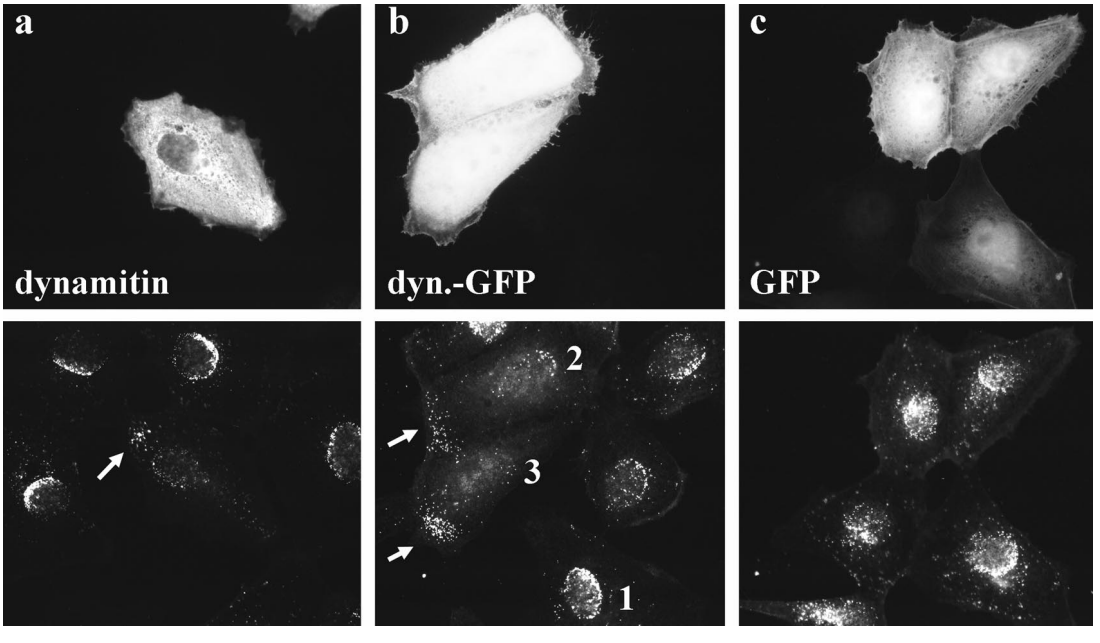

Figure 7. Overexpression of dynamitin reduces HSV1 capsid transport to the nucleus. Three hours after infection most capsids were bound to the nucleus in untransfected cells (a–c) and in cells overexpressing GFP (c). In cells overexpressing dynamitin (a) or dynamitin-GFP (b), only a few capsids reached the nucleus, and several capsids were seen in the periphery of the cells (arrows in a and b, bottom panels). Immunofluorescence microscopy of PtK_2 cells transfected with dynamitin or dynamitin-GFP and 46 h later infected with HSV1 for 3 h in the presence of cycloheximide. Cells were fixed with PFA, permeabilized with TX-100, and double-labeled with anti-dynamitin (mAb p50; a, top panel) and anti-HC (pAb; a, bottom panel). Cells transfected with GFP proteins were labeled with anti-HC (pAb; b and c, bottom panels).

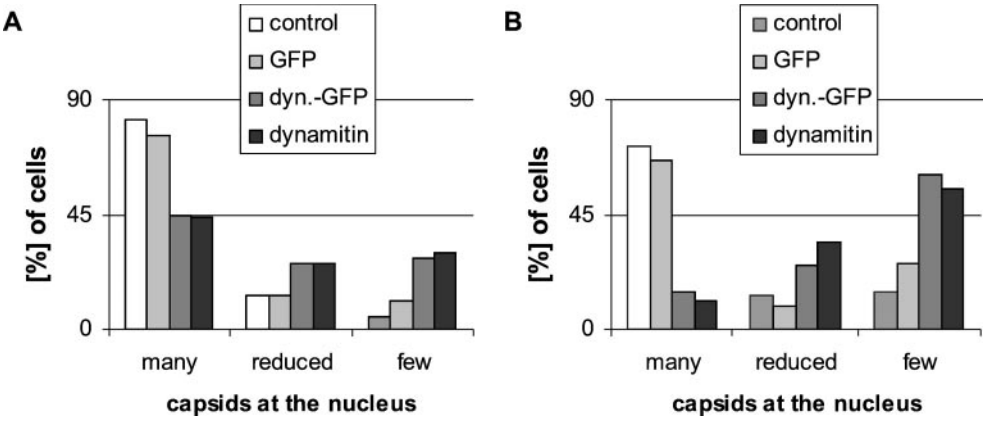

Figure 8. Quantification of viral capsid transport in transfected cells. For quantification, untransfected and transfected cells were randomly selected and classified into three different groups: cells with many capsids at the nucleus, typically forming a nuclear rim (Figure 7b, 1), cells with a reduced amount of capsids at the nucleus (Figure 7b, 2), and cells with <10 capsids at the nucleus (Figure 7b, 3). Either all (A) or only high expressing (B) cells were analyzed. Expression levels in the cytoplasm were determined using a digital camera. One can directly compare the expression levels for GFP with dynamitin-GFP (cf. MATERIALS AND METHODS). Dynamitin and dynamitin-GFP strongly inhibited HSV1 entry, whereas GFP had no effect on viral infection. Forty-five or 46 h after transfection with dynamitin, dynamitin-GFP, or GFP, PtK_2 cells were infected with HSV1 for 3 or 2 h (A and B, respectively), in the presence of cycloheximide. Cells were fixed with PFA, permeabilized with TX-100, and double-labeled with anti-capsid (anti-HC or anti-LC) and anti-dynamitin (cf. Figure 8). Cells with aggregated protein or abnormal morphology were excluded from analysis.

Occasionally, there seemed to be fewer capsids visible in cells overexpressing dynamitin or dynamitin-GFP than in control cells. This was due to the fact that in control cells most capsids were concentrated at the nuclear envelope and were thus visualized in one focus plane. In contrast in cells overexpressing dynamitin or dynamitin-GFP, capsids were distributed throughout the entire cytoplasm and therefore were not visualized in one focus plane. For quantification, PtK_2 cells were randomly selected and grouped into three different classes (cf. Figure 7b): 1) cells with many capsids at the nuclear envelope typically forming a nuclear crescent, 2) cells with a reduced amount of nuclear capsids, and 3) cells with very few capsids at the nucleus. The overexpression of dynamitin or dynamitin-GFP clearly reduced the number of cells that showed many capsids at the nucleus by ~50% compared with control or GFP-transfected cells (Figure 8A). Similar results were obtained using Vero cells overexpressing dynamitin (our unpublished results). As in other systems (Burkhardt *et al.*, 1997; Suomalainen *et al.*, 1999), we noticed that the degree of inhibition on capsid transport was dependent on the dose of the transfected protein. We therefore estimated expression levels using a digital camera and specifically analyzed cells expressing high amounts of the transfected proteins (Figure 8B). In these cells, dynamitin-GFP and dynamitin inhibited viral capsid transport by 85% compared with GFP-transfected or control cells.

At early time points, incoming capsids are distributed randomly over the entire cytoplasm (Sodeik *et al.*, 1997). However, in the cells in which the function of dynein was inhibited by the overexpression of dynamitin, the capsids were often concentrated in peripheral parts of the cells (Figure 9a). If dynamitin-transfected cells were infected in the presence of nocodazole, which disrupts the MT network, the capsids were also distributed randomly over the entire cytoplasm (Figure 9b). This experiment suggested that without the minus-end–directed MT motor dynein, the capsids might be transported by a plus-end–directed MT motor to the cell periphery.

In summary our data show that overexpressing dynamitin reduced the number of cytosolic viral capsids transported to the nucleus. Because under this condition fewer viral genomes reached the nucleoplasm, immediate-early viral gene expression was also reduced. The inhibition of virus entry by high amounts of dynamitin was not due to impaired virus binding, virus internalization, or the slight changes in the MT network but to a block of dynein function in cytosolic HSV1 capsid transport along MTs.

DISCUSSION

Incoming cytosolic HSV1 capsids are efficiently targeted along MTs from the plasma membrane to the nucleus (Hammonds *et al.*, 1996; Sodeik *et al.*, 1997; Mabit, Nakano, Prank, Saam, Döhner, Sodeik, Greber, unpublished data). The typical organization and polarity of MTs in cultured cells and axons require the use of a minus-end–directed MT motor for transport to the nucleus (Kristensson *et al.*, 1986; Topp *et al.*, 1994; Sodeik *et al.*, 1997; Bearer *et al.*, 2000). Cytoplasmic dynein is responsible for most minus-end–directed MT transport during interphase and thus a prime candidate for viral trafficking (Sodeik, 2000; Ploubidou and Way, 2001).

The dynein subunits DHC, DIC, and $p150^{Glued}$, a subunit of the dynein cofactor dynactin, colocalized with incoming HSV1 (Sodeik *et al.*, 1997; Figure 1). Moreover, EHNA (erythro-9–3-[2-hydroxynonyl]adenine), an inhibitor of axonemal and cytoplasmic dynein, blocks HSV1 infection in neuronal cells (Kristensson *et al.*, 1986). However, EHNA also affects adenosine deaminase, cGMP-stimulated phosphodiesterase, and the actin cytoskeleton (Penningroth, 1986; Mery *et al.*, 1995), and it is unclear which phase of the viral life cycle was inhibited. We therefore asked whether incoming HSV1 capsids use the host factor dynein for riding along MTs to the nucleus.

Inhibition of Dynein and Dynactin Does not Affect HSV1 Internalization

The function of dynactin and dynein can be inhibited by transiently overexpressing one dynactin subunit, the 50-kDa

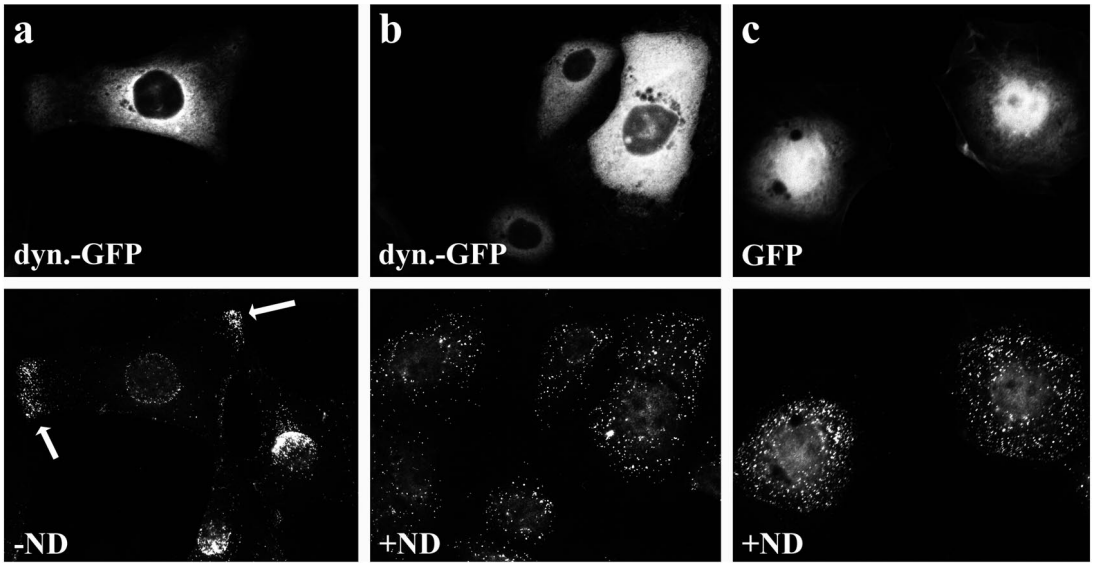

Figure 9. The peripheral accumulation in dynamitin expressing cells requires an intact MT network. In cells overexpressing dynamitin-GFP (a) or dynamitin, few incoming capsids reach the nucleus, and many accumulate in the peripheral cytoplasm 3 h after infection. If such cells are infected in the absence of MTs, incoming capsids are distributed randomly over the entire cytoplasm, and there is no peripheral accumulation (b). Immunofluorescence microscopy of PtK_2 cells transfected with dynamitin-GFP or GFP and 46 h later infected with HSV1 for 3 h in the presence of cycloheximide and in the absence (a) or presence (b and c) of nocodazole (ND). Cells were fixed with PFA, permeabilized with TX-100, and labeled with anti-VP5 (mAb 5C10; bottom panels).

protein dynamitin (Echeverri *et al.*, 1996). Because endocytic and exocytic membrane traffic involve dynein-mediated vesicular transport steps (Burkhardt *et al.*, 1997; Presley *et al.*, 1997; Valetti *et al.*, 1999), the subcellular localization of viral receptors might have been changed upon such treatment. However, none of the transfected proteins we tested reduced the efficiency of HSV1 binding or particle uptake. Thus, any influence on virus infection was not simply due to reduced surface expression of viral receptors and less efficient fusion of virions with the cells.

Inhibition of Dynein and Dynactin Blocks Cytosolic HSV1 Capsid Transport along MTs

Although virus entered transfected cells normally, overexpressed dynamitin inhibited the transport of cytosolic HSV1 capsids from the cell periphery to the nucleus by ~50% and in cells expressing high levels of dynamitin even by 85%. As a consequence viral immediate-early gene expression was reduced, too.

Two factors may have prevented a complete inhibition of virus infection in our set up. First, about a third of all cells were not transfected, and immunofluorescence microscopy confirmed that those were infected normally. Second, single cell analysis strongly suggested that the degree of capsid transport inhibition correlated with the level of dynamitin expression (Figure 8). This is consistent with biochemical experiments, which show that excess dynamitin blasts dynactin into two subcomplexes of 9 and 18 S, presumably by saturating dynamitin binding sites on them, thus destroying the architecture of dynactin (Echeverri *et al.*, 1996; Eckley *et al.*, 1999). Because this is likely to be a dose-dependent effect, it was expected that dynactin-dependent transport and virus infection were only completely inhibited in cells expressing high levels of dynamitin.

As in the absence of MTs (Sodeik *et al.*, 1997; Mabit, Nakano, Prank, Saam, Döhner, Sodeik, Greber, unpublished data), we detected a few capsids at the nuclear membrane in cells with high concentrations of dynamitin. This was no surprise, because virions can bind to the "apical" plasma membrane just on top of the nucleus. Capsids derived from these virions most likely reach the nuclear pores without MTs or dynein and dynactin. Dynein and dynactin–mediated MT transport is therefore not essential for infecting nonpolarized cells in culture. However, it is likely to be required during pathogenesis when HSV1 infects highly polarized epithelial and elongated neuronal cells (Enquist *et al.*, 1998), but also in less polarized cells, as described here, dynactin and the molecular motor dynein transport HSV1 capsids efficiently along MTs.

Functions of Dynein and Dynactin during HSV1 Capsid Transport?

ATP hydrolysis induces conformational changes in the DHC head domain, which produce a power stroke toward the MT minus end, whereas the smaller subunits DIC, DLIC, and DLC are attached to the stem domain (Habura *et al.*, 1999; Tynan *et al.*, 2000a), which is involved in cargo binding (Vaughan and Vallee, 1995; King, 2000; Tynan *et al.*, 2000b). Dynactin is needed for dynein-mediated vesicle transport (Gill *et al.*, 1991; Schroer and Sheetz, 1991) and transport of nonmembranous cargo such as NuMA aggregates, aggresomes, adenovirus capsids, neurofilaments, chromosomes, and pericentrin particles (Merdes and Cleveland, 1997; Gar-

cia-Mata *et al.*, 1999; Suomalainen *et al.*, 1999; Shah *et al.*, 2000; Sharp *et al.*, 2000; Young *et al.*, 2000).

Earlier electron microscopy data suggested that dynein binds with its stem domain to HSV1 capsids (Sodeik *et al.*, 1997). Our immunofluorescence microscopy data are consistent with either an indirect interaction via dynactin or a direct binding of HSV1 capsids to dynein. Dynactin might serve as an initial or permanent anchor for dynein on the capsid (Echeverri *et al.*, 1996) or tether between MT and capsid while dynein is detaching from the MT to make its next step (King and Schroer, 2000). The ATPase activity of dynein has also been reported to be regulated by dynactin-dependent phosphorylation (Kumar *et al.*, 2000).

Bidirectional HSV1 Capsid Transport along Microtubules?

Many subcellular structures and progeny GFP-tagged alphaherpes viruses (Smith *et al.*, 2001; Willard, 2002) can move bidirectionally along MTs. Interestingly, overexpression of dynamitin did not lead to a random capsid distribution but to their MT-mediated accumulation in the cell margins (Figures 7 and 9). This suggested that besides dynein, HSV1 capsids might also use a plus-end–directed MT motor. Plus-end–directed capsid motility could be involved in further transport from the MTOC to the nucleus, as would be required in cells where the MTOC is not directly neighboring the nucleus. MT-mediated, plus-end–directed capsid transport could also be involved in apical entry of polarized epithelial cells (Topp *et al.*, 1996). Moreover, during HSV1 egress from neurons, capsids are transported anterogradely to the presynapse (Miranda-Saksena *et al.*, 2000; Ohara *et al.*, 2000). Because of the uniform polarity of MTs in axons, this transport has to be catalyzed by a plus-end–directed motor.

If capsids were indeed able to travel along MTs in both directions, to the minus and plus ends, specific signals must regulate which motor the capsid is supposed to use during the different steps of the viral life cycle. Thus, the direction of capsid motility must be tightly controlled. The main transport direction during virus entry must be to MT minus-ends to ensure net movement to the cell center and the nucleus. However, if minus-end–directed, dynein-mediated transport was inhibited by overexpressing dynamitin, these putative plus-end–directed motors might have taken over and transported capsids to the cell margins.

Dynein or Kinesin Receptors Encoded by HSV1

In contrast to other cargo transported along MTs, the protein composition of HSV1 is known. There are ~20 tegument and capsid proteins that could function in motor or dynactin binding. The HSV1 gene product of UL34 interacts with DIC in GST pull down assays (Ye *et al.*, 2000). However, because UL34 has properties of a type-II membrane protein and in pseudorabies virus is not present in purified virions (Klupp *et al.*, 2000; Reynolds *et al.*, 2001), it remains to be seen how its interaction with DIC subunit could participate in viral capsid transport. The HSV1 tegument protein US11 was shown recently to interact with the heavy chain of conventional kinesin (Diefenbach *et al.*, 2002). Additional candidates for motor receptors include VP22 (UL49) and UL25, that both, upon transient transfection, seem to localize to MTs (Elliott and O'Hare, 1998; Kaelin *et al.*, 2000). In contrast to VP22 that dissociates from the capsid upon virus entry, UL25 and also VP1–3 (UL36) remain on the capsid until it reaches the nucleus (Morrison *et al.*, 1998; Kaelin *et al.*, 2000; Sodeik, Szmak and Prank, unpublished results).

Reconstitution of MT capsid motility in vitro (Wolfstein, Döhner, Allan and Sodeik, unpublished results) and HSV1 mutants can now be used to identify structural viral proteins required for capsid targeting to the nucleus.

ACKNOWLEDGMENTS

We thank Rudi Bauerfeind and Thomas F. Schulz (Hannover Medical School) for many helpful discussions and critical readings of the manuscript. We thank Bernard Roizman (University of Chicago, Chicago, IL) for providing the mutant strain R7202 and Patricia Spear (Northwestern University Medical School, Chicago, IL) for the mutant strain HSV[KOS]tk12. Doris Meder (Hannover Medical School) was instrumental in setting up the quantitative β-galactosidase assay in our laboratory. Melissa Gee, Kevin Vaughan (University of Massachusetts, Worcester, MA), Bernhard Hoflack (University of Lille, France), Roselyn Eisenberg, Gary Cohen (both at the University of Pennsylvania, Philadelphia, PA), Bill Newcomb, Jay Brown (both at the University of Virginia, Charlottesville, VA), Roger Everett (MRC Virology Unit, Glasgow, Scotland), and the late Thomas Kreis (University of Geneva, Switzerland) all graciously provided antibodies, and Jürgen Wehland (Gesellschaft für Biotechnologische Forschung, Braunschweig, Germany) the PtK_2 cells. K.D, A.W., U.P., and B.S. were supported by a grant from the Deutsche Forschungsgemeinschaft (So403/1), D.D by a fellowship from the Human Frontiers Science Program, and C.E., D.D. and R.V. by a National Institutes of Health (NIH) grant (GM 47434). Initial experiments for this study were performed at Yale University (New Haven, CT) and funded by an NIH grant to A.H. (AI 18599; now at the ETH, Zürich, Switzerland).

REFERENCES

Baines, J.D., and Roizman, B. (1993). The UL10 gene of herpes simplex virus 1 encodes a novel viral glycoprotein, gM, which is present in the virion and in the plasma membrane of infected cells. J. Virol. *67*, 1441–1452.

Bearer, E.L., Breakefield, X.O., Schuback, D., Reese, T.S., and LaVail, J.H. (2000). Retrograde axonal transport of herpes simplex virus: evidence for a single mechanism and a role for tegument. Proc. Natl. Acad. Sci. USA *97*, 8146–8150.

Burkhardt, J.K., Echeverri, C.J., Nilsson, T., and Vallee, R.B. (1997). Overexpression of the dynamitin (p50) subunit of the dynactin complex disrupts dynein-dependent maintenance of membrane organelle distribution. J. Cell Biol. *139*, 469–484.

Cohen, G.H., Ponce de Leon, M., Diggelmann, H., Lawrence, W.C., Vernon, S.K., and Eisenberg, R.J. (1980). Structural analysis of the capsid polypeptides of herpes simplex virus types 1 and 2. J. Virol. *34*, 521–531.

Diefenbach, R.J., Miranda-Saksena, M., Diefenbach, E., Holland, D.J., Boadle, R.A., Armati, P.J., and Cunningham, A.L. (2002). Herpes simplex virus tegument Protein US11 interacts with conventional kinesin heavy chain. J. Virol. *76*, 3282–3291.

Dubin, G., Fishman, N.O., Eisenberg, R.J., Cohen, G.H., and Friedman, H.M. (1992). The role of herpes simplex virus glycoproteins in immune evasion. Curr. Top. Microbiol. Immunol. *179*, 111–120.

Echeverri, C.J., Paschal, B.M., Vaughan, K.T., and Vallee, R.B. (1996). Molecular characterization of the 50-kD subunit of dynactin reveals function for the complex in chromosome alignment and spindle organization during mitosis. J. Cell Biol. *132*, 617–633.

Eckley, D.M., Gill, S.R., Melkonian, K.A., Bingham, J.B., Goodson, H.V., Heuser, J.E., and Schroer, T.A. (1999). Analysis of dynactin subcomplexes reveals a novel actin-related protein associated with the arp1 minifilament pointed end. J. Cell Biol. *147*, 307–320.

Eisenberg, R.J., *et al.* (1985). Localization of epitopes of herpes simplex virus type 1 glycoprotein D. J. Virol. *53*, 634–644.

Eisenberg, R.J., Ponce de Leon, M., Friedman, H.M., Fries, L.F., Frank, M.M., Hastings, J.C., and Cohen, G.H. (1987). Complement component C3b binds directly to purified glycoprotein C of herpes simplex virus types 1 and 2. Microb. Pathog. *3*, 423–435.

Elliott, G., and O'Hare, P. (1998). Herpes simplex virus type 1 tegument protein VP22 induces the stabilization and hyperacetylation of microtubules. J. Virol. *72*, 6448–6455.

Enquist, L.W., Husak, P.J., Banfield, B.W., and Smith, G.A. (1998). Infection and spread of alphaherpesviruses in the nervous system. Adv. Virus Res. *51*, 237–347.

Everett, R.D. (2000). ICP0, a regulator of herpes simplex virus during lytic and latent infection. Bioessays *22*, 761–770.

Garcia-Mata, R., Bebok, Z., Sorscher, E.J., and Sztul, E.S. (1999). Characterization and dynamics of aggresome formation by a cytosolic GFP-chimera. J. Cell Biol. *146*, 1239–1254.

Gee, M.A., Heuser, J.E., and Vallee, R.B. (1997). An extended microtubule-binding structure within the dynein motor domain. Nature *390*, 636–639.

Gill, S.R., Schroer, T.A., Szilak, I., Steuer, E.R., Sheetz, M.P., and Cleveland, D.W. (1991). Dynactin, a conserved, ubiquitously expressed component of an activator of vesicle motility mediated by cytoplasmic dynein. J. Cell Biol. *115*, 1639–1650.

Griffiths, G., Hoflack, B., Simons, K., Mellman, I., and Kornfeld, S. (1988). The mannose 6-phosphate receptor and the biogenesis of lysosomes. Cell *52*, 329–341.

Habermann, A., Schroer, T.A., Griffiths, G., and Burkhardt, J.K. (2001). Immunolocalization of cytoplasmic dynein and dynactin subunits in cultured macrophages: enrichment on early endocytic organelles. J. Cell Sci. *114*, 229–240.

Habura, A., Tikhonenko, I., Chisholm, R.L., and Koonce, M.P. (1999). Interaction mapping of a dynein heavy chain. Identification of dimerization and intermediate-chain binding domains. J. Biol. Chem. *274*, 15447–15453.

Hammonds, T.R., Denyer, S.P., Jackson, D.E., and Irving, W.L. (1996). Studies to show that with podophyllotoxin the early replicative stages of herpes simplex virus type 1 depend upon functional cytoplasmic microtubules. J. Med. Microbiol. *45*, 167–172.

Harada, A., Takei, Y., Kanai, Y., Tanaka, Y., Nonaka, S., and Hirokawa, N. (1998). Golgi vesiculation and lysosome dispersion in cells lacking cytoplasmic dynein. J. Cell Biol. *141*, 51–59.

Hirokawa, N. (1998). Kinesin and dynein superfamily proteins and the mechanism of organelle transport. Science *279*, 519–526.

Holleran, E.A., Karki, S., and Holzbaur, E.L. (1998). The role of the dynactin complex in intracellular motility. Int. Rev. Cytol. *182*, 69–109.

Kaelin, K., Dezelee, S., Masse, M.J., Bras, F., and Flamand, A. (2000). The UL25 protein of pseudorabies virus associates with capsids and localizes to the nucleus and to microtubules. J. Virol. *74*, 474–482.

Karki, S., and Holzbaur, E.L. (1995). Affinity chromatography demonstrates a direct binding between cytoplasmic dynein and the dynactin complex. J. Biol. Chem. *270*, 28806–28811.

Karki, S., and Holzbaur, E.L. (1999). Cytoplasmic dynein and dynactin in cell division and intracellular transport. Curr. Opin. Cell Biol. *11*, 45–53.

King, S.J., and Schroer, T.A. (2000). Dynactin increases the processivity of the cytoplasmic dynein motor. Nat. Cell Biol. *2*, 20–24.

King, S.M. (2000). The dynein microtubule motor. Biochim. Biophys. Acta *1496*, 60–75.

Klupp, B.G., Granzow, H., and Mettenleiter, T.C. (2000). Primary envelopment of pseudorabies virus at the nuclear membrane requires the UL34 gene product. J. Virol. *74*, 10063–10073.

Kreis, T.E. (1987). Microtubules containing detyrosinated tubulin are less dynamic. EMBO J. *6*, 2597–2606.

Kristensson, K., Lycke, E., Roytta, M., Svennerholm, B., and Vahlne, A. (1986). Neuritic transport of herpes simplex virus in rat sensory neurons in vitro. Effects of substances interacting with microtubular function and axonal flow [nocodazole, taxol and erythro-9–3-(2-hydroxynonyl)adenine]. J. Gen. Virol. *67*, 2023–2028.

Kumar, S., Lee, I.H., and Plamann, M. (2000). Cytoplasmic dynein ATPase activity is regulated by dynactin-dependent phosphorylation. J. Biol. Chem. *275*, 31798–31804.

Luby-Phelps, K. (2000). Cytoarchitecture and physical properties of cytoplasm: volume, viscosity, diffusion, intracellular surface area. Int. Rev. Cytol. *192*, 189–221.

Merdes, A., and Cleveland, D.W. (1997). Pathways of spindle pole formation: different mechanisms; conserved components. J. Cell Biol. *138*, 953–956.

Mery, P.F., Pavoine, C., Pecker, F., and Fischmeister, R. (1995). Erythro-9-(2-hydroxy-3-nonyl)adenine inhibits cyclic GMP-stimulated phosphodiesterase in isolated cardiac myocytes. Mol. Pharmacol. *48*, 121–130.

Miranda-Saksena, M., Armati, P., Boadle, R.A., Holland, D.J., and Cunningham, A.L. (2000). Anterograde transport of herpes simplex virus type 1 in cultured, dissociated human and rat dorsal root ganglion neurons. J. Virol. *74*, 1827–1839.

Morrison, E.E., Stevenson, A.J., Wang, Y.F., and Meredith, D.M. (1998). Differences in the intracellular localization and fate of herpes simplex virus tegument proteins early in the infection of Vero cells. J. Gen. Virol. *79*, 2517–2528.

Newcomb, W.W., Homa, F.L., Thomsen, D.R., Booy, F.P., Trus, B.L., Steven, A.C., Spencer, J.V., and Brown, J.C. (1996). Assembly of the herpes simplex virus capsid: characterization of intermediates observed during cell-free capsid formation. J. Mol. Biol. *263*, 432–446.

Nogales, E. (2000). Structural insights into microtubule function. Annu. Rev. Biochem. *69*, 277–302.

Ohara, P.T., Chin, M.S., and LaVail, J.H. (2000). The spread of herpes simplex virus type 1 from trigeminal neurons to the murine cornea: an immunoelectron microscopy study. J. Virol. *74*, 4776–4786.

Ojala, P.M., Sodeik, B., Ebersold, M.W., Kutay, U., and Helenius, A. (2000). Herpes simplex virus type 1 entry into host cells: reconstitution of capsid binding and uncoating at the nuclear pore complex in vitro. Mol. Cell. Biol. *20*, 4922–4931.

Paschal, B.M., Holzbaur, E.L., Pfister, K.K., Clark, S., Meyer, D.I., and Vallee, R.B. (1993). Characterization of a 50-kDa polypeptide in cytoplasmic dynein preparations reveals a complex with $p150^{Glued}$ and a novel actin. J. Biol. Chem. *268*, 15318–15323.

Penningroth, S.M. (1986). Erythro-9-[3-(2-hydroxynonyl)]adenine and vanadate as probes for microtubule-based cytoskeletal mechanochemistry. Methods Enzymol. *134*, 477–487.

Ploubidou, A., and Way, M. (2001). Viral transport and the cytoskeleton. Curr. Opin. Cell Biol. *13*, 97–105.

Presley, J.F., Cole, N.B., Schroer, T.A., Hirschberg, K., Zaal, K.J., and Lippincott-Schwartz, J. (1997). ER-to-Golgi transport visualized in living cells. Nature *389*, 81–85.

Quintyne, N.J., Gill, S.R., Eckley, D.M., Crego, C.L., Compton, D.A., and Schroer, T.A. (1999). Dynactin is required for microtubule anchoring at centrosomes. J. Cell Biol. *147*, 321–334.

Reynolds, A.E., Ryckman, B.J., Baines, J.D., Zhou, Y., Liang, L., and Roller, R.J. (2001). U(L)31 and U(L)34 proteins of herpes simplex virus type 1 form a complex that accumulates at the nuclear rim and is required for envelopment of nucleocapsids. J. Virol. *75*, 8803–8817.

Roizman, B., and Knipe, D.M. (2001). Herpes simplex viruses and their replication. In: Fundamental Virology, 4th ed., ed. B.N. Fields, D.M. Knipe, and P.M. Howley, *et al.,* Philadelphia: Lippincott-Raven Publishers, 2399–2459.

Sambrook, J., Fritsch, E.F., and Maniatis, T. (1989). Expression of cloned genes in cultured mammalian cells. In: Molecular Cloning: A Laboratory Manual, vol. 3, ed. C. Nolan, Cold Spring Harbor, NY: Cold Spring Harbor Laboratory Press.

Schafer, D.A., Gill, S.R., Cooper, J.A., Heuser, J.E., and Schroer, T.A. (1994). Ultrastructural analysis of the dynactin complex: an actin-related protein is a component of a filament that resembles F-actin. J. Cell Biol. *126*, 403–412.

Schroer, T.A., and Sheetz, M.P. (1991). Two activators of microtubule-based vesicle transport. J. Cell Biol. *115*, 1309–1318.

Shah, J.V., Flanagan, L.A., Janmey, P.A., and Leterrier, J.F. (2000). Bidirectional translocation of neurofilaments along microtubules mediated in part by dynein/dynactin. Mol. Biol. Cell *11*, 3495–3508.

Sharp, D.J., Rogers, G.C., and Scholey, J.M. (2000). Cytoplasmic dynein is required for poleward chromosome movement during mitosis in Drosophila embryos. Nat. Cell Biol. *2*, 922–930.

Showalter, S.D., Zweig, M., and Hampar, B. (1981). Monoclonal antibodies to herpes simplex virus type 1 proteins, including the immediate-early protein ICP 4. Infect. Immun. *34*, 684–692.

Smith, G.A., Gross, S.P., and Enquist, L.W. (2001). Herpesviruses use bidirectional fast-axonal transport to spread in sensory neurons. Proc. Natl. Acad. Sci. USA *98*, 3466–3470.

Sodeik, B. (2000). Mechanisms of viral transport in the cytoplasm. Trends Microbiol. *8*, 465–472.

Sodeik, B., Ebersold, M.W., and Helenius, A. (1997). Microtubule-mediated transport of incoming herpes simplex virus 1 capsids to the nucleus. J. Cell Biol. *136*, 1007–1021.

Spear, P.G., Eisenberg, R.J., and Cohen, G.H. (2000). Three classes of cell surface receptors for alphaherpesvirus entry. Virology *275*, 1–8.

Steven, A.C., and Spear, P.G. (1997). Herpesvirus capsid assembly and envelopment. In: Structural Biology of Viruses, ed. W. Chiu, R. Burnett, and R. Garcea, New York: Oxford University Press, 312–351.

Suomalainen, M., Nakano, M.Y., Keller, S., Boucke, K., Stidwill, R.P., and Greber, U.F. (1999). Microtubule-dependent plus- and minus end-directed motilities are competing processes for nuclear targeting of adenovirus. J. Cell Biol. *144*, 657–672.

Topp, K.S., Bisla, K., Saks, N.D., and Lavail, J.H. (1996). Centripetal transport of herpes simplex virus in human retinal pigment epithelial cells in vitro. Neuroscience *71*, 1133–1144.

Topp, K.S., Meade, L.B., and LaVail, J.H. (1994). Microtubule polarity in the peripheral processes of trigeminal ganglion cells: relevance for the retrograde transport of herpes simplex virus. J. Neurosci. *14*, 318–325.

Tynan, S.H., Gee, M.A., and Vallee, R.B. (2000a). Distinct but overlapping sites within the cytoplasmic dynein heavy chain for dimerization and for intermediate chain and light intermediate chain binding. J. Biol. Chem. *275*, 32769–32774.

Tynan, S.H., Purohit, A., Doxsey, S.J., and Vallee, R.B. (2000b). Light intermediate chain 1 defines a functional subfraction of cytoplasmic dynein which binds to pericentrin. J. Biol. Chem. *275*, 32763–32768.

Vaisberg, E.A., Koonce, M.P., and McIntosh, J.R. (1993). Cytoplasmic dynein plays a role in mammalian mitotic spindle formation. J. Cell Biol. *123*, 849–858.

Valetti, C., Wetzel, D.M., Schrader, M., Hasbani, M.J., Gill, S.R., Kreis, T.E., and Schroer, T.A. (1999). Role of dynactin in endocytic traffic: effects of dynamitin overexpression and colocalization with CLIP-170. Mol. Biol. Cell *10*, 4107–4120.

Vallee, R.B., and Sheetz, M.P. (1996). Targeting of motor proteins. Science *271*, 1539–1544.

Vaughan, K.T., and Vallee, R.B. (1995). Cytoplasmic dynein binds dynactin through a direct interaction between the intermediate chains and $p150^{Glued}$. J. Cell Biol. *131*, 1507–1516.

Wagner, E.K., and Bloom, D.C. (1997). Experimental investigation of herpes simplex virus latency. Clin. Microbiol. Rev. *10*, 419–443.

Warner, M.S., Geraghty, R.J., Martinez, W.M., Montgomery, R.I., Whitbeck, J.C., Xu, R., Eisenberg, R.J., Cohen, G.H., and Spear, P.G. (1998). A cell surface protein with herpesvirus entry activity (HveB) confers susceptibility to infection by mutants of herpes simplex virus type 1, herpes simplex virus type 2, and pseudorabies virus. Virology *246*, 179–189.

Whittaker, G.R., Kann, M., and Helenius, A. (2000). Viral entry into the nucleus. Annu. Rev. Cell Dev. Biol. *16*, 627–651.

Willard, M. (2002). Rapid directional translocations in virus replication. J. Virol. *76*, 5220–5232.

Ye, G.J., Vaughan, K.T., Vallee, R.B., and Roizman, B. (2000). The herpes simplex virus 1 U(L)34 protein interacts with a cytoplasmic dynein intermediate chain and targets nuclear membrane. J. Virol. *74*, 1355–1363.

Young, A., Dictenberg, J.B., Purohit, A., Tuft, R., and Doxsey, S.J. (2000). Cytoplasmic dynein-mediated assembly of pericentrin and gamma tubulin onto centrosomes. Mol. Biol. Cell *11*, 2047–2056.

Zhou, Z.H., Dougherty, M., Jakana, J., He, J., Rixon, F.J., and Chiu, W. (2000). Seeing the herpesvirus capsid at 8.5 A. Science *288*, 877–880.

Mabit H., Nakano M.Y., Prank U., Saam B., **Döhner K.**, Sodeik B., Greber U.F.
Intact microtubules support adenovirus and herpes simplex virus infections.
Journal of Virology, 2002, 76: 9962-9971

This paper is the result of a cooperation with the group of Prof. Dr. Greber (University of Zürich, Zürich, Switzerland). During my Ph.D., I was involved in the experiments for Figs. 3A and 4B-D to validate the requirement of microtubules for HSV1 cell entry. Additionally, I supported Ute Prank in evaluating microscopic experiments addressing the cytotoxicity of the cytoskeleton inhibitors used (data not shown, but comparable with Fig. 1E). Additional experiments were performed by Ute Prank (Fig. 3B) and Beate Sodeik (Fig. 4A), respectively. The colleagues from Zürich performed all experiments with adenoviruses.

JOURNAL OF VIROLOGY, Oct. 2002, p. 9962–9971 Vol. 76, No. 19
0022-538X/02/$04.00+0 DOI: 10.1128/JVI.76.19.9962–9971.2002

Intact Microtubules Support Adenovirus and Herpes Simplex Virus Infections

Hélène Mabit,[1] Michel Y. Nakano,[1] Ute Prank,[2] Bianca Saam,[1] Katinka Döhner,[2] Beate Sodeik,[2] and Urs F. Greber[1]*

Zoologisches Institut, Universität Zürich, CH-8057 Zürich, Switzerland,[1] and Zentrum für Biochemie, Medizinische Hochschule Hannover, D-30623 Hannover, Germany[2]

Received 10 April 2002/Accepted 18 June 2002

Capsids and the enclosed DNA of adenoviruses, including the species C viruses adenovirus type 2 (Ad2) and Ad5, and herpesviruses, such as herpes simplex virus type 1 (HSV-1), are targeted to the nuclei of epithelial, endothelial, fibroblastic, and neuronal cells. Cytoplasmic transport of fluorophore-tagged Ad2 and immunologically detected HSV-1 capsids required intact microtubules and the microtubule-dependent minus-end-directed motor complex dynein-dynactin. A recent study with epithelial cells suggested that Ad5 was transported to the nucleus and expressed its genes independently of a microtubule network. To clarify the mechanisms by which Ad2 and, as an independent control, HSV-1 were targeted to the nucleus, we treated epithelial cells with nocodazole (NOC) to depolymerize microtubules and measured viral gene expression at different times and multiplicities of infections. Our results indicate that in NOC-treated cells, viral transgene expression was significantly reduced at up to 48 h postinfection (p.i.). A quantitative analysis of subcellular capsid localization indicated that NOC blocked the nuclear targeting of Ad2 and also HSV-1 by more than 90% at up to 7 h p.i. About 10% of the incoming Texas Red-coupled Ad2 (Ad2-TR) was enriched at the nucleus in microtubule-depleted cells at 5 h p.i. This result is consistent with earlier observations that Ad2-TR capsids move randomly in NOC-treated cells at less than 0.1 μm/s and over distances of less than 5 μm, characteristic of Brownian motion. We conclude that fluorophore-tagged Ad2 and HSV-1 particles are infectious and that microtubules play a prominent role in efficient nuclear targeting during entry and gene expression of species C Ads and HSV-1.

Many viruses, including adenoviruses (Ads) and herpesviruses, spread by intracellular transport within infected host cells, thus increasing the viral load in target organs and possibly causing severe disease (44). The 51 human Ad serotypes—classified into six species (A to F)—have distinct tropisms (19). For example, Ad type 2 (Ad2) and Ad5 (species C) and Ad3 (species B) are associated with upper-airway infections. Other serotypes are linked to epidemic keratoconjunctivitis (species D), pneumonia (species E), enteric infections (species A and F), or infections of hematopoietic cells (41). The *Herpesviridae* family consists of the alpha-, beta- and gammaherpesviruses. Like Ads, alphaherpesviruses, including herpes simplex virus type 1 (HSV-1), infect different cell types both in cultures and in their hosts. After infection of mucosal or damaged cutaneous epithelium, these neurotropic viruses establish latent infections, primarily in sensory ganglia, that, upon reactivation, lead to recurrent epidermal lesions (40, 55). The ability to infect a broad range of postmitotic cells has made both Ads and herpesviruses useful gene delivery vehicles (21) that are currently being evaluated in clinical trials (29, 39). For their application as therapeutic vectors and to identify new potential targets for antiviral therapy, it is crucial to understand how the genomes are targeted to the nucleus.

The entry mechanisms for Ads and herpesviruses have been well studied. Ads are internalized by receptor-mediated endocytosis that is dependent on F actin and leave the endosomal pathway at various sites (recently reviewed in reference 11). The species C Ads, including Ad2 and Ad5, exit from a slightly acidic compartment of pH 6 at about 10 min postentry (16, 42), whereas Ad7 (species B) has been reported to escape from acidic late endosomes and lysosomes (32). In contrast, HSV-1 delivers its capsids into the cytosol upon fusion of the viral envelope with the plasma membrane (45, 46). Both viruses then target their capsids to the cell nucleus, uncoat, and inject the enclosed linear double-stranded DNA genomes through the nuclear pores into the nucleoplasm for replication (14, 35, 53).

A number of electron microscopy studies have shown that cytoplasmic capsids of both species C Ads and alphaherpesviruses can associate with microtubules (MTs) (5, 10, 27, 28, 31, 37, 45, 47, 57). Moreover, time-lapse fluorescence microscopy experiments of fluorophore-tagged Ads have demonstrated that Ads move along linear tracks of MTs (25, 26, 49). The motility of incoming particles is bidirectional, toward and away from the nucleus, but the overall motilities are toward the minus ends of MTs and require the major minus-end-directed motor dynein and the cofactor dynactin. If MTs are depolymerized with nocodazole (NOC), then the long-range linear motilities cease, the remaining short-range transport has no directional control and, most importantly, the efficiency of Ad2 DNA delivery is strongly reduced, as indicated by fluorescence in situ hybridization assays (48, 49).

Similar results have been reported for alphaherpesviruses.

* Corresponding author. Mailing address: Zoologisches Institut der Universität Zürich, Winterthurerstr. 190, CH-8057 Zürich, Switzerland. Phone: 41 1 635 4841. Fax: 41 1 635 6822. E-mail: ufgreber@zool.unizh.ch.

MT-depolymerizing agents block HSV-1 infections in cultures and in animal models (17, 22, 45, 51, 52). Moreover, incoming HSV-1 capsids colocalize with dynein and dynactin, and transport to the nucleus is reduced by the dynein inhibitors erythro-9[3-(2-hydroxynonyl)]adenine and dynamitin (6a, 22, 45). Axonal herpesvirus transport occurs at rates of 0.5 to 3.5 μm/s, with peak velocities of up to 5 μm/s (1, 28, 37, 43); viral structures are transported bidirectionally along linear tracks with high processivity over distances of up to 20 μm, as demonstrated by video microscopy with green fluorescent protein (GFP)-tagged mutants (1, 43; A. Wolfstein et al., unpublished data).

In a recent article, it was proposed that Ad5 infections do not require MTs (8). We therefore decided to conduct a quantitative analysis of Ad5-mediated gene expression and Texas Red (TR)-coupled Ad2 (Ad2-TR) subcellular localization in cells depleted of MTs; as an independent control, we included HSV-1. Our results show that the large majority of Ad2-TR, Ad5, and HSV-1 particles utilize intact MTs to reach the nucleus in order to infect nonpolarized epithelial cells.

MATERIALS AND METHODS

Cells and reagents. Immortalized human adenocarcinoma-derived alveolar epithelial A549 cells (ATCC CCL-185) were maintained in Dulbecco's modified Eagle's medium (Gibco Invitrogen, Basel, Switzerland) containing 7% Clone III serum (HyClone; Socochim, Geneva, Switzerland) and 1% nonessential amino acids, 2 mM glutamine, 100 U of penicillin/ml, and 0.1 mg of streptomycin/ml (all from Gibco-BRL). PtK_2 cells (ATCC CCL-56) and BHK-21 cells (ATCC CCL-10) were grown in 10% and Vero cells (ATCC CCL-81) were grown in 7.5% fetal calf serum containing minimal essential medium, 2 mM glutamine, nonessential amino acids and, for Vero cells, 100 U of penicillin/ml and 100 μg of streptomycin/ml. All cell lines were cultured in a humidified 5% CO_2–air atmosphere. NOC (Sigma) and paclitaxel (Calbiochem-Novabiochem or Sigma) were dissolved as 1,000-fold stocks in dimethyl sulfoxide (DMSO) and used as indicated below. For the immunofluorescence experiments, we used preadsorbed rabbit polyclonal antibodies raised against DNA-containing capsids (anti-heavy chain [HC]) or empty capsids (anti-light chain [LC]) to detect incoming viral capsids (4, 45). MTs were labeled with a mouse monoclonal antibody against β-tubulin (N357; Amersham, Little Chalfont, United Kingdom) (2).

Ad infection and gene expression. Ad2 was purified and coupled to TR as described previously to yield Ad2-TR (33). This virus was as infectious as the nonlabeled parent virus, as determined by plaque assays with A549 cells. The Ad5 derivative AE18, lacking the E1 and E3 regions, expressed *lacZ* from the cytomegalovirus (CMV) major promoter (provided by E. Vigne, Institut G. Roussy, Villejuif, France) (54). Luc-Ad5, lacking E1 and E3, expressed luciferase from a CMV promoter inserted into the E1 region (kindly provided by S. Hemmi and D. Serena, University of Zürich). In brief, this virus was constructed from a pPoly plasmid backbone (3) and plasmid pTG-H5 DL324 (kindly supplied by S. Rusconi, University of Fribourg, Fribourg, Switzerland). Cells were seeded in 24-well dishes (Costar; Integra Biosciences) or on glass coverslips 1 to 2 days before the experiment. Prior to infection, 60 to 90% confluent cells were exposed to NOC in DMSO or just DMSO alone in Dulbecco's modified Eagle's medium for 1 h and then were infected with AE18 at 100 to 10,000 physical particles per cell at 37°C. At various times after the addition of the virus, cells were either analyzed for their viability or lysed, and lysates were assayed for β-galactosidase (β-Gal) activity and protein content. β-Gal activity was measured by a β-Gal enzyme assay (Promega Corporation). The cells in 1 well of a 24-well dish were washed with phosphate-buffered saline (PBS) at 7, 24, 32, or 48 h postinfection (p.i.) and lysed in 400 μl of reporter lysis buffer (Promega) for 15 min at room temperature under slowly rocking conditions. The lysates were centrifuged in a microcentrifuge at 4°C for 2 min, and 30 μl of the supernatants was mixed with the same volume of 2× enzyme reaction buffer (Promega) and incubated at 37°C for various times. The reactions were stopped by the addition of 100 μl of 1 M sodium carbonate. The absorbance was read at 420 nm with a spectrophotometer (MRX microplate reader; Dynatech Laboratories; BioLogics, Gainesville, Va). The background activity of noninfected A549 cells was subtracted from the measurements. The protein content of each lysate was measured with Micro BCA protein assay reagent (Pierce), and the results are expressed as enzymatic units per milligram of protein per minute. The luciferase activity of infected cells was determined with cell lysates at 7 h p.i. by using a commercial assay system (Promega). The cells in 1 well of a 24-well dish were washed with PBS and lysed in 400 μl of reporter lysis buffer. The centrifuged lysates (20 μl) were placed in an opaque 96-well plate for luciferase activity measurements with a Multilabel Counter (Wallac Victor^2 1420; Perkin-Elmer), which injected 50 μl of luciferase assay reagent into each well.

HSV-1 infection and gene expression. Wild-type HSV-1 strain F (ATCC VR-733) and mutant strain [KOS]tk12 were amplified and purified as described previously (45). Immediate-early viral gene expression was analyzed by using mutant [KOS]tk12, which lacks the viral thymidine kinase gene and encodes the enzyme β-Gal under the control of the immediate-early ICP4 promoter of HSV-1 (kindly provided by P. Spear, Northwestern University, Chicago, Ill.) (56). PtK_2 cells were cultured in 24-well plates at a density of 4×10^4 to 5×10^4 cells per well for 1 day. They were pretreated with NOC or paclitaxel in DMSO or just DMSO alone for 1 h, cooled to 4°C, and incubated with virus for 2 h as described elsewhere (6a, 45). Unbound virus was removed by repeated washing in PBS, and the cells were further incubated in culture medium at 37°C.

At different times, the cells were lysed with 0.5% Triton X-100 (TX-100) in PBS containing 1 mg of bovine serum albumin/ml and protease inhibitors at 37°C for 15 min. Lysates were then incubated with 3.5 mg of *o*-nitrophenyl-β-D-galactopyranoside/ml in 73 mM Na_2HPO_4–16 mM NaH_2PO_4–0.2 mM KH_2PO_4–0.4 mM KCl–17 mM NaCl. The enzymatic activity of β-Gal was measured after about 2 h at 420 nm by using a plate reader (Spectra Count microplate photometer; Packard Instrument Company, Meriden, Conn.). On a parallel plate, cells were fixed with 3% (wt/vol) paraformaldehyde (PFA) in PBS for 20 min, washed with water, and then stained with 0.25 mg of crystal violet/ml in 5% ethanol for 10 min to quantify the amount of cells present after different treatments. After several washes in water, the plates were dried, and the bound crystal violet was dissolved in 100% ethanol and quantified by measuring the optical density at 590 nm (17). Crystal violet staining gave a linear signal over cell concentrations ranging from at least 3×10^3 to 3×10^5 cells per well (data not shown).

Quantification of subcellular viral targeting. To analyze the subcellular distribution of incoming HSV-1 capsids, Vero or PtK_2 cells were infected in the presence of 0.5 mM cycloheximide. The cells were then (i) fixed with 100% methanol for 4 min at −20°C after a 10-s preextraction in 0.5% TX-100–80 mM PIPES-KOH (pH 6.8)–2 mM $MgSO_4$–10 μM paclitaxel to visualize MTs and capsids as described previously (45), (ii) fixed and permeabilized simultaneously with PHEMO-fix (3.7% [wt/vol] PFA, 0.05% [wt/vol] glutaraldehyde, and 0.5% TX-100 in PHEMO-buffer [see below]) for 10 min and washed with PHEMO-buffer (68 mM PIPES-KOH [pH 6.9], 15 mM EGTA, 3 mM $MgCl_2$, 10% DMSO) to label MTs, or (iii) fixed with 3% (wt/vol) PFA in PBS for 20 min and then permeabilized with 0.1% (vol/vol) TX-100 for exactly 5 min. The remaining PFA was inactivated by incubating the cells with 50 mM NH_4Cl–PBS for 10 min. Immunolabeling was performed as described elsewhere (6a, 45). The cells were examined either with a modified confocal microscope (model MRC600; Bio-Rad Laboratories, Hercules, Calif.) attached to an Axiovert microscope (Carl Zeiss, Inc., Thornwood, N.Y.) with separate filters for each fluorochrome or with a Leica SP1 microscope (×63 oil-immersion objective; numeric aperature, 1.32) with UV excitation at 351 and 364 nm and with fluorescein isothiocyanate (468 nm), TR (568 nm), and long-pass emission filters in sequential recording mode at a section thickness of 0.5 μm. Images were processed with Photoshop 5.0 (Adobe). The subcellular distributions of Ad2-TR and HSV-1 (immunolabeled with an anti-LC antibody) were determined by quantitative fluorescence microscopy of cells fixed with PHEMO-fix by the procedure described earlier (33).

Cell viability assay. Cell viability was assessed with a live/dead viability/cytotoxicity two-color fluorescence assay (L-3224; Molecular Probes). This assay measures intracellular esterase activity with the cell-permeable substrate Calcein-AM, which is converted by live cells to the fluorescent polyanion calcein (excitation, 495 nm; emission, 515 nm), which is retained in living cells by the intact plasma membrane. In addition, we used the non-cell-permeating DNA dye ethidium homodimer-1 (EthD-1) (excitation, 495 nm; emission, 635 nm), which is detected in cells with compromised membranes, i.e., dead cells. In this assay, live cells have a green fluorescent cytoplasm but no EthD-1 signal, whereas dead cells lack green fluorescence and are stained with EthD-1. The assays were performed by washing cells once with PBS and incubating them with Calcein-AM (0.8 μM for A549 cells and 0.2 μM for PtK_2 cells) and EthD-1 (0.8 μM for A549 cells and 0.1 μM for PtK_2 cells) in Hanks' medium (Gibco-BRL) at 37°C for 15 min. Cells were washed with Hanks' medium, and fluorescence was analyzed with a Leica inverted fluorescence microscope equipped with a ×63 oil-immersion objective (numeric aperture, 1.32), a band-pass excitation filter, and a double-pass emission filter as described earlier (49). Images were recorded with Meta-

Morph software (Universal Imaging Corporation) and batch processed with Photoshop 5.0.

RESULTS

Glotzer et al. (8) recently suggested that Ad5 infection of the epithelial cell line A549 occurred in the absence of MTs (8), contradicting earlier results (26, 49). A reexamination of the role of MTs in Ad infection was therefore warranted.

NOC is an inhibitor of Ad5 infection. We first analyzed adenovirus transgene expression in A549 cells containing intact or disrupted MTs. Cells were preincubated with different concentrations of the MT-depolymerizing agent NOC at 37°C for 60 min (20) and then were inoculated with β-Gal-expressing Ad5 (β-Gal–Ad5) at 10,000 physical particles per cell, equivalent to about 300 associated particles per cell (48). The particle-to-PFU ratio is estimated to be on the order of 20 to 100, corresponding to 3 to 15 bound infectious particles per cell (18). β-Gal activity was measured in cell lysates at 7 h p.i., the earliest time point that gave a reliable reading. The lowest concentration of NOC (0.2 μM) had no effect on β-Gal expression, whereas 2 μM NOC resulted in 40% inhibition and 20 μM NOC resulted in greater than 80% inhibition compared to the results obtained for untreated cells (Fig. 1A). The latter conditions are sufficient to completely depolymerize MTs in Vero cells (45) (Fig. 4A, panel d), HeLa cells (49), or A549 cells (Fig. 2A, panel e), whereas PtK_2 cells require 50 μM NOC (data not shown). A549 cells were therefore treated with 20 μM NOC, and β-Gal activity was measured at 7, 24, and 48 h after inoculation with 1,000 and 10,000 particles per cell. In both instances, there was a severe reduction of gene expression, with 85% inhibition at 7 h p.i. and 50 to 70% inhibition at 24 and 48 h p.i. (Fig. 1B). The effect of NOC was reversible, as indicated by washing the cells with drug-free medium at 180 min p.i. and incubating them for another 4 h in the absence of drug (Fig. 1C). When NOC was added at 3 h p.i., when a large fraction of the incoming DNA had been delivered to the nucleoplasm (49, 53), there was only marginal inhibition of viral gene expression. This result indicated that most of the infectious particles had reached the nucleus at 3 h p.i. In contrast, when NOC was present throughout the infection, β-Gal expression was reduced by 85% compared to that in control cells.

We next tested the effect of NOC on the gene expression of a different virus, Luc-Ad5. This strategy enabled us to reduce the viral load to 10 particles per cell and still measure transgene activity as early as 7 h p.i. Consistent with the β-Gal activity results, 20 μM NOC reduced luciferase activity by 50 to 70% at 10, 100, 1,000, or 10,000 particles per cell (Fig. 1D). Importantly, the assay was linear in this range. We next analyzed whether NOC affected the viability of the cells either in the presence or in the absence of β-Gal–Ad5. Cells were pretreated with NOC (20 μM) for 1 h, infected or not infected with Ad5, and then stained with the vital dyes Calcein-AM and EthD-1. Intact live cells excluded EthD-1 and cytosolic esterases hydrolyzed Calcein-AM, thus generating green fluorescent Calcein. All cells on the coverslip were EthD-1 negative and Calcein positive (Fig. 1E, panels a to f), unlike cells that had been treated with methanol (Fig. 1E, panels g to i). Importantly, there was no cell loss from the coverslips, as verified by differential interference contrast imaging (Fig. 1E, panels c, f, and i).

NOC blocks the nuclear accumulation of Ad2-TR. If NOC is an early inhibitor of Ad5 infection, then it could have an effect on genome trafficking. To visualize cytoplasmic particles, we used fluorescent Ad2-TR containing two to four TR molecules per hexon trimer, corresponding to 200 to 400 TR molecules per virion (13, 33). Importantly, this virus is as infectious as unlabeled virus and is not aggregated, as judged by electron microscopy of negatively stained particles and population analysis of viral fluorescence (33). A recent study showed that the DNA genome of purified Ad2 separates from the capsid at the nuclear pore complex (NPC) and that the remainder of the capsid tends to form aggregates or becomes undetectable (53). A549 cells were treated with different concentrations of NOC as described above, and Ad2-TR was bound to the cell surface at 4°C for 1 h to synchronize the infection at 37°C in the presence or in the absence of the drug. One set of cells was fixed at 75 min p.i. and stained for MTs. Clearly, increasing amounts of NOC progressively depolymerized MTs (Fig. 2A), whereas DMSO alone had no effect on the morphology of the MT network. By use of a fast Fourier transformation algorithm, viral fluorescence was quantitated in the cell periphery, the cytoplasmic area, and the nucleus, including a perinuclear region of 1.5 μm (33). While control cells had low peripheral and cytoplasmic but high nuclear fluorescence signals (less than 1 but more than 5 fluorescence units per unit area, respectively), 20 μM NOC-treated cells showed almost no nuclear accumulation of Ad2-TR (1.6 fluorescence units per unit area); instead, there was a significant increase in the peripheral and cytoplasmic fluorescence intensity ($P < 0.01$) (Fig. 2B).

We next carried out a time course experiment either in the absence or in the presence of 20 μM NOC. As expected, the nuclear and perinuclear fluorescence of control cells increased to greater than 5 fluorescence units per unit area at 75 min p.i. compared to 1 unit at 0 min p.i., while the peripheral and cytoplasmic Ad2-TR fluorescence decreased to less than 0.2 unit (Fig. 2C). At 150 min, however, the viral capsid load in the nuclear and perinuclear area decreased to less than two, indicative of viral disassembly, which peaks at between 150 and 180 min p.i. (14, 53). The strong decrease in nuclear Ad2-TR particles coincided with a robust increase in peripheral and cytoplasmic virus, suggesting that viral capsids or fragments were transported back to the periphery. Interestingly, the nuclear fluorescence increased again at 300 and 420 min p.i. ($P = 0.05$) and the peripheral fluorescence decreased. These results suggested a second transport wave of Ad2-TR toward the nucleus. This experiment confirms that in control cells, our measurements of fluorescent capsids are quantitative at least until 75 min p.i., the onset of capsid disassembly.

The subcellular virus distribution in NOC-treated cells was fundamentally different from that in control cells. At up to 150 min p.i., the viral capsid load in the nuclear and perinuclear region was no different from the charge at 0 min p.i.; i.e., there was no enrichment of Ad2-TR near the nucleus (Fig. 2D). The virus concentrations in the cytoplasm and the periphery were slightly reduced. Interestingly, we found a small but significant accumulation of Ad2-TR near the nucleus ($P < 0.01$) at 300 min p.i. Approximately 10% of the viral fluorescence appar-

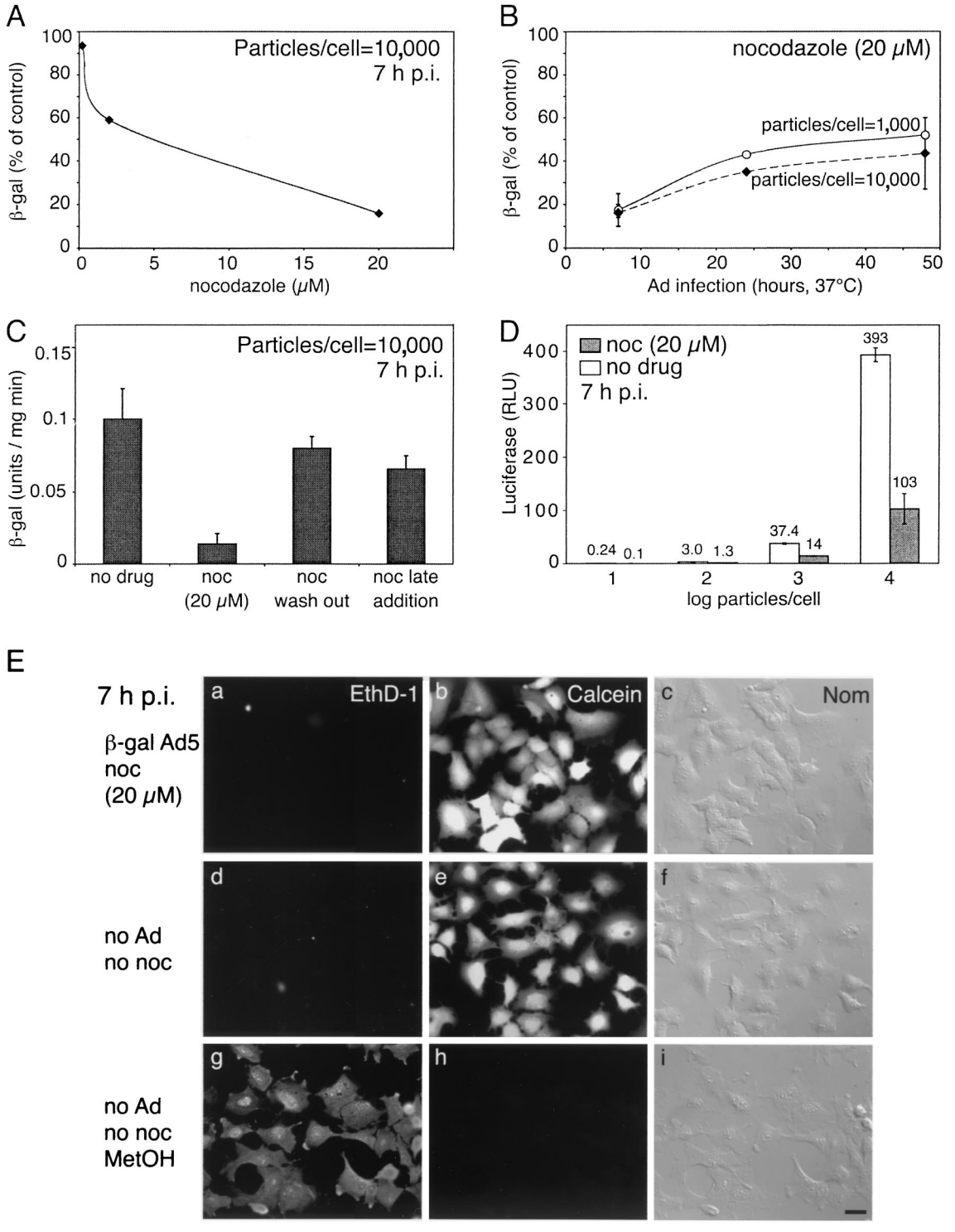

FIG. 1. Ad5-mediated gene expression requires intact MTs. (A to D) A549 cells were not treated or treated with the indicated concentrations of NOC for 1 h and then infected with β-Gal–Ad5 (A to C) or Luc-Ad5 (D) for the indicated times at 37°C. Gene expression was normalized to that of drug-free infected cells (A and B) or is reported as enzymatic units per milligram of protein per minute (C) or relative light units (D) at room temperature. The reversibility of the effects of NOC was tested by washing out the drug at 180 min, and the postentry effects of NOC were assessed by adding the drug at 180 min p.i. (C). Error bars indicate standard errors of the means. (E) Toxicity of NOC for β-Gal–Ad5-infected cells (a to c) and noninfected cells (d to f) at 7 h p.i. with ethidium bromide (a, d, and g) and calcein (b, e, and h) staining and with Nomarksi (Nom) differential interference contrast imaging (c, f, and i). Note that dead cells were EthD-1 positive and calcein negative; see, e.g., methanol (MetOH, 70% for 30 min)-treated cells (g to i). NOC-treated or infected cells were all alive. Bar, 40 μm.

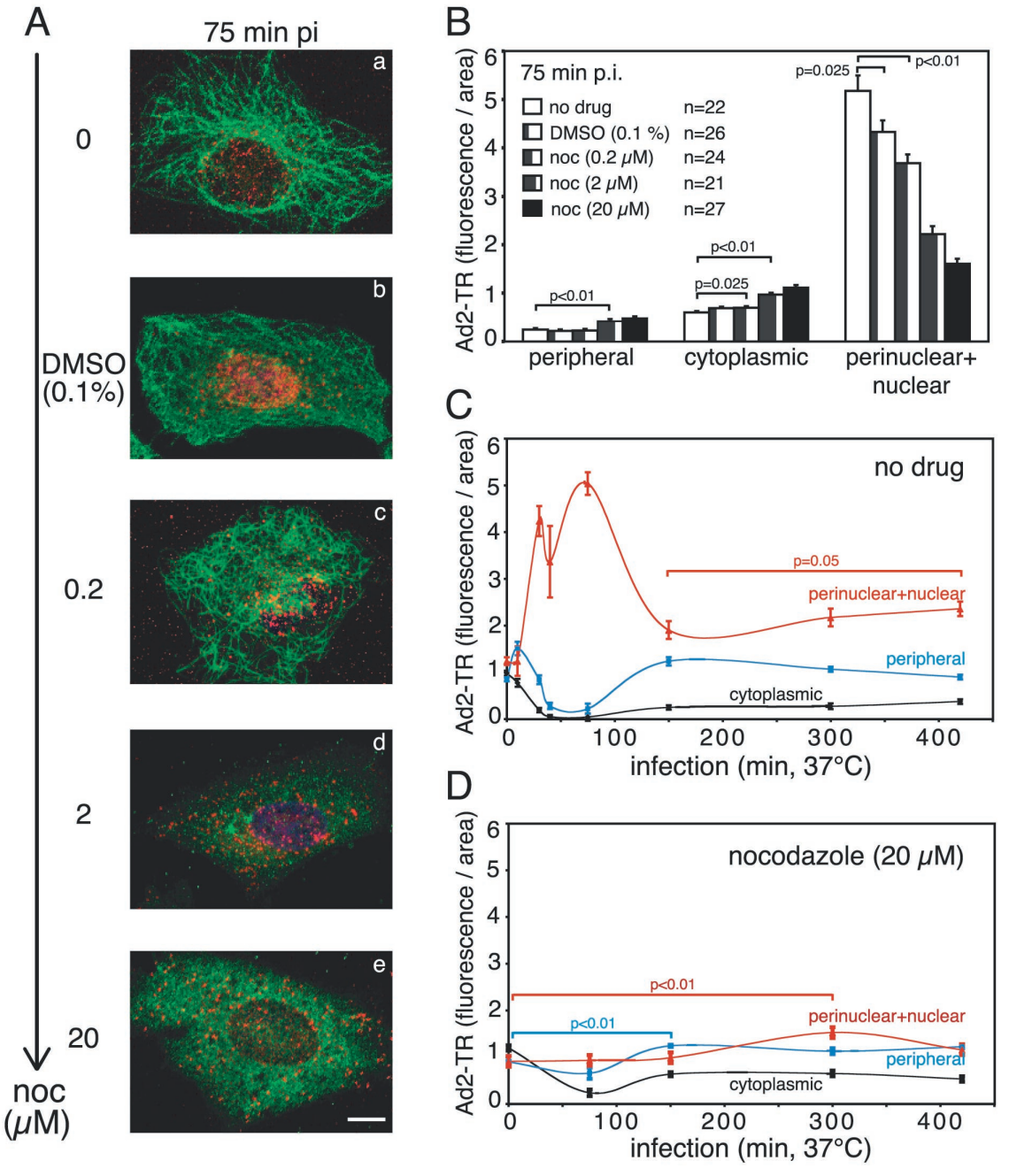

FIG. 2. NOC blocks nuclear targeting of Ad2-TR in A549 cells. Ad2-TR was cold bound to A549 cells not pretreated or pretreated with different concentrations of NOC. Cells were warmed for the indicated times at 37°C in the presence or in the absence of NOC and then fixed with PHEMO-fix. (A) Entire set of projected confocal laser scanning microscopy sections of representative cells depicting Ad2-TR (red), MTs (green), and the nucleus (4′,6′-diamidino-2-phenylindole; dark blue). Note the disappearance of the MTs with increasing concentrations of NOC and the lack of nuclear accumulation of Ad2-TR. Bar, 10 μm. (B) Quantification of the subcellular localization of Ad2-TR in the periphery, the cytoplasm, and the nuclear and perinuclear region of cells treated with different concentrations of NOC (n, number of cells analyzed). (C) Quantification of the subcellular localization of Ad2-TR in A549 control cells over time. Note that the nuclear transport of Ad2-TR peaks at 80 to 90 min p.i., with corresponding reductions in peripheral and cytoplasmic particles. (D) Quantification of the subcellular localization of Ad2-TR in the absence of MTs (NOC treatment). Note the lack of nuclear transport at times before 200 min p.i. and the slight increase in nuclear accumulation at 300 min p.i. Error bars indicate standard errors of the means.

ently reached the nucleus in the absence of MTs. At least some nuclear capsids must have been genome-containing particles, since we detected viral gene expression in the presence of NOC. The reduction in the nuclear capsid signal at 420 min p.i. might have been due to capsid disassembly. In summary, these results indicate that more than 90% of the incoming Ad2-TR did not reach the nucleus in the absence of MTs and that this transport block strongly reduced viral gene expression.

NOC blocks HSV-1-mediated gene expression. MTs are a major intracellular trafficking route of alphaherpesviruses. We therefore tested the effect of NOC on HSV-1 gene delivery using the expression of β-Gal activity controlled by the viral immediate-early promoter of ICP4. PtK_2 cells were pretreated with different concentrations of NOC, incubated with HSV-1 [KOS]tk12 in the cold, infected in the presence or in the absence of drug at 37°C for 4 h, and analyzed for β-Gal activity. The results clearly indicate that NOC is a dose-dependent inhibitor of HSV-1 infection (Fig. 3A). The maximal inhibition of approximately 90% was obtained with 25 μM NOC. This effect was due neither to cell loss, as indicated by cell quantification with crystal violet, nor to cell death, as measured by the live/dead assay (data not shown). We next analyzed the effect of 25 μM NOC on HSV-1 infection in a time course experiment at multiplicities of infection (MOIs) of 2 and 10 from 3 to 7 h p.i. Under all conditions, NOC inhibited viral gene expression in the range of 80 to 90% (Fig. 3B). However, the inhibition was not complete. At an MOI of 10, there was a modest increase in gene expression from 3 to 7 h p.i., indicating that a small fraction of infectious virus had reached the nucleus independently of MTs.

NOC inhibits nuclear targeting of incoming HSV-1. We next tested to what extent NOC affected MTs. Vero cells were preincubated with different concentrations of NOC for 1 h, incubated in the cold with HSV-1, and warmed in the presence or in the absence of drug for 2 h. The highest concentration of NOC (20 μM) completely depolymerized MTs and led to a random cytoplasmic localization of HSV-1 capsids (Fig. 4A, panel d). In the absence of drug, however, the MT network was intact and incoming HSV-1 localized predominantly to the nucleus (Fig. 4A, panel a). Intermediate concentrations of NOC (0.4 and 2 μM) had partial effects on MTs and HSV-1 nuclear targeting (Fig. 4A, panels b and c).

To assess the effect of NOC on the subcellular trafficking of HSV-1, we quantitated viral capsid fluorescence in the periphery, the cytoplasm, and the nuclear and perinuclear region by using the same method as that used for Ad2-TR. In the absence of drug, there was a strong enrichment of HSV-1 near the nucleus and a significant decrease in the peripheral and cytoplasmic viral load at 120 and 180 min p.i. ($P < 0.01$) (Fig. 4B). NOC, however, blocked the nuclear accumulation as well as the cytoplasmic reduction of HSV-1 at 120 and 180 min p.i., compared to the results obtained at 30 min p.i., but did not affect the reduction of virus in the periphery (Fig. 4C). These results suggested that viral trafficking through the cortex was independent of MTs, unlike further cytoplasmic transport, which largely required intact MTs. This conclusion was further supported by experiments with the MT-stabilizing drug paclitaxel (10 μM), which allowed a strong enrichment of HSV-1 near the nucleus, although this enrichment was slightly less pronounced than that in drug-free cells. Accordingly, paclitaxel had only minimal effects on the expression of β-Gal (average inhibition, 20 to 30%). Significantly, paclitaxel did not inhibit the transport of virus through the cell periphery (Fig. 4D). We conclude that HSV-1 capsid transport occurs on stabilized MTs, suggesting that it does not depend on MT treadmilling or dynamic instability.

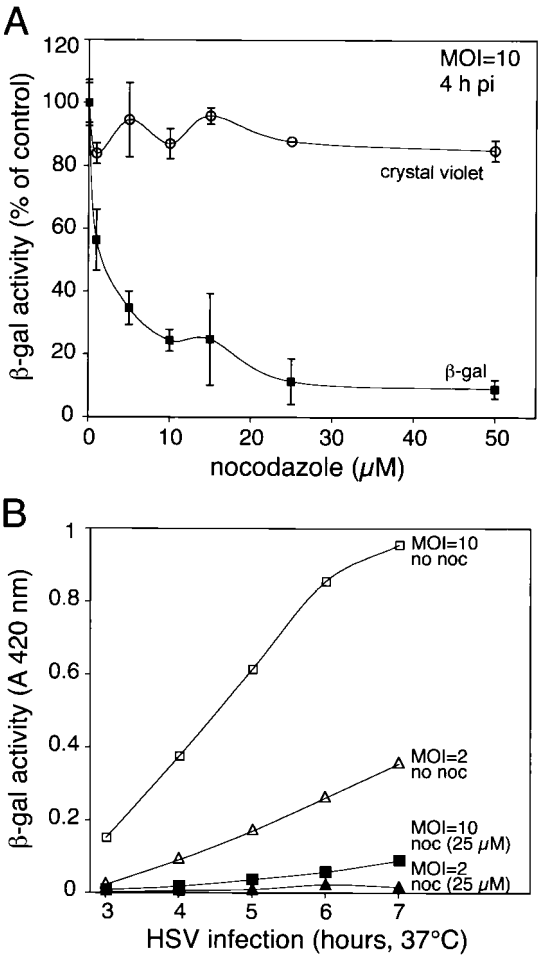

FIG. 3. Intact MTs are required for HSV-1 mediated gene expression. (A) PtK_2 cells were treated with DMSO (control) or NOC for 1 h at 37°C and then incubated with the β-Gal-expressing HSV-1 strain [KOS]tk12 at 4°C for 2 h (MOI, 10). The unbound viruses were removed, and the cells were shifted to 37°C in the presence or in the absence of NOC to initiate infection. Cells were lysed at 4 h p.i., and the amount of β-Gal was quantitated (squares). Cells on parallel dishes were quantified by using the binding of crystal violet (circles). The means and standard deviations for duplicate samples are shown. Note that with increasing NOC concentrations, the amount of immediate-early viral gene expression was inhibited. (B) Time course of HSV-1 gene expression. Cells were infected in the absence (filled symbols) or in the presence (open symbols) of MTs with HSV-1 [KOS]tk12 (MOI of 2 [triangles] or MOI of 10 [squares]), lysed at different times p.i., and analyzed for β-Gal expression (absorbance at 420 nm). At both MOIs and at all times tested, NOC clearly reduced immediate-early viral gene expression. The crystal violet assay showed no significant loss of cells under these conditions (<5%) (data not shown).

DISCUSSION

Using quantitative subcellular localization of incoming viral capsids and quantification of viral gene expression in the absence or in the presence of NOC, an MT-depolymerizing agent, we found that MTs play a crucial role in delivering Ad and HSV-1 genomes to the nuclei of epithelial cells. The NOC inhibition was reversible (45, 49; this study), NOC had no effect on cellular gene expression (data not shown), and only minor

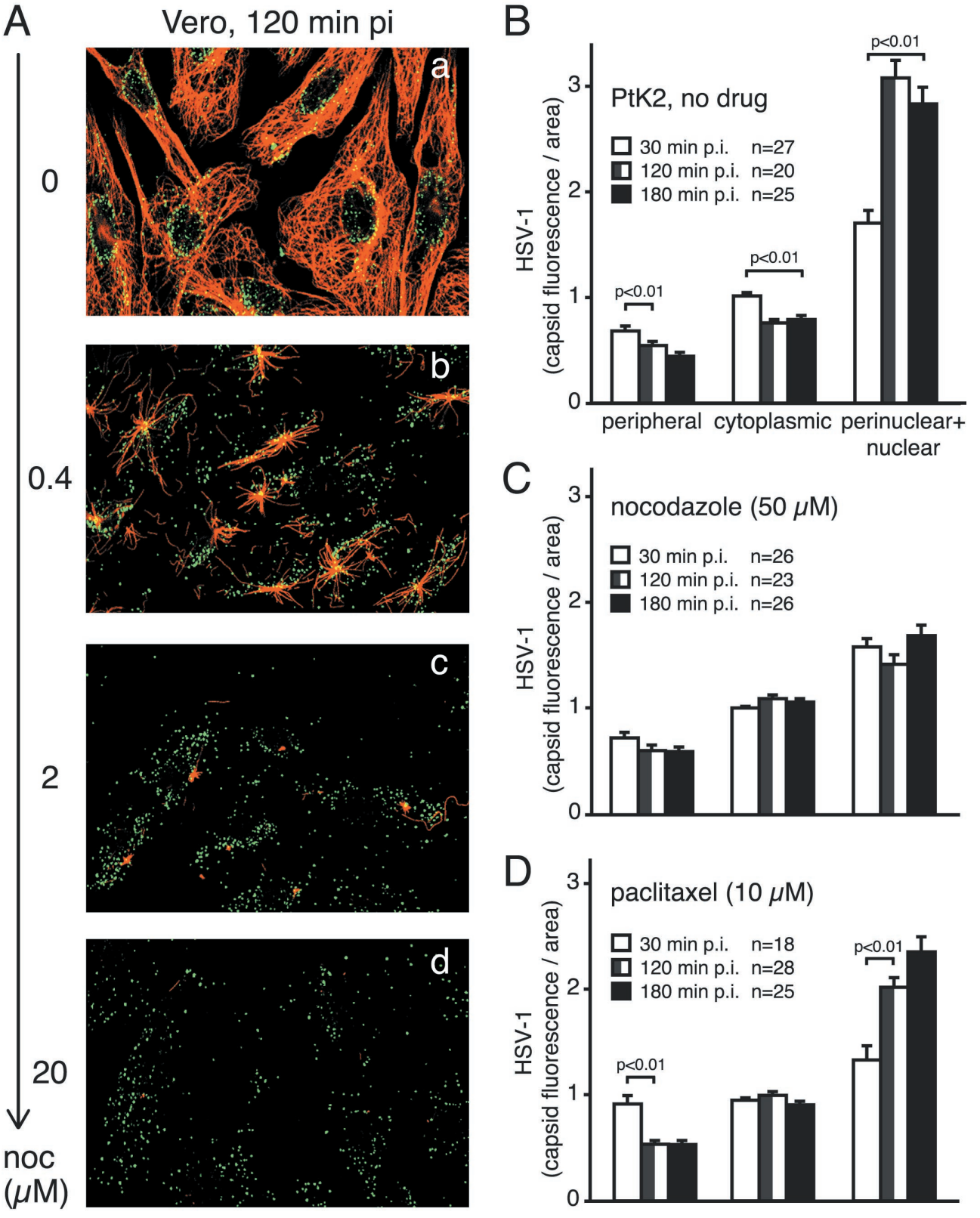

FIG. 4. NOC inhibits the nuclear targeting of HSV-1 in Vero and PtK_2 cells. (A) Vero cells were infected in the absence or in the presence of different concentrations of NOC with 50 PFU of HSV-1 per cell for 2 h and then fixed in methanol after preextraction. Samples were stained with anti-HC (green) and antitubulin (red) and analyzed by confocal laser scanning microscopy. Note the disappearance of the MTs with increasing concentrations of NOC and the lack of nuclear HSV-1 capsids. (B to D) Quantification of subcellular localization of HSV-1 in PtK_2 cells infected with 80 PFU per cell in the absence of drug (B), in the presence of 50 μM NOC (C), or in the presence of 10 μM paclitaxel (D). Cells were fixed at 30, 120, or 180 min p.i. and labeled with anti-LC. n, number of cells. Error bars indicate standard errors of the means. MTs in Vero cells were completely depolymerized at lower concentrations of NOC than were those in PtK_2 cells (data not shown).

effects on viral gene expression after particle transport to the nucleus had occurred (this study). We therefore concluded, as others have before, that NOC is not a general inhibitor of transcription or translation but acts predominantly on the MT network (20).

MTs are required for viral capsid transport. There are several explanations for why NOC treatment did not completely inhibit the delivery of viral DNA into the nucleus. Virions can enter from the plasma membrane proximal to the nuclear envelope. These particles are separated from the nucleus by only a few micrometers. Another possibility is that cytosolic virions use an MT-independent transport mechanism, such as an actin-based system (36, 38); that they are transported on short, randomly oriented MT filaments resistant to NOC; or that they exploit diffusion. All of these processes would stop when the capsid binds to the NPC, leading to particle enrichment at the nucleus. Clearly, Ad2-TR particles are able to explore a few micrometers of cytosolic space in the absence of MTs (8, 49); thus, particles entering from the plasma membrane proximal to the nucleus will most likely not require MTs to reach the NPC. This means that careful kinetic measurements are necessary to reveal the role of any cytoplasmic transport system.

We predict that cells that are particularly small will be infected in the absence of MTs if enough time is allowed. This scenario may, in fact, have obscured the role of MTs in Ad infection (5, 50). Our measurements here reveal that nuclear transport of both Ad2 and HSV-1 from distal areas to the nucleus is blocked in the absence of MTs. Since HSV-1 infection of polarized neuronal cells in a compartmentalized culture absolutely depends on MTs (22), the results obtained with HSV-1 confirm that the quantitative imaging procedures that we used for Ad2 and HSV-1 are reliable. The role of MTs in cytoplasmic particle trafficking is in agreement with the results of studies of endocytic and exocytic membrane traffic and axonal transport, where NOC was found to be a kinetic rather than an absolute inhibitor of membrane traffic (9, 24).

Capsid transport and viral gene expression required neither MT treadmilling nor the dynamic instability of MTs, since paclitaxel (at concentrations of 180 nM to 10 μM) had only slight effects on Ad2 and HSV-1 infections. Likewise, cells expressing MAP4, which stabilizes the MT network (34), transported Ad2 to the nucleus even faster than control cells (49); low concentrations of paclitaxel or NOC (5 nM), suppressing MT dynamics without depolymerizing MTs, have similar effects (6, 7). Thus, preferentially stabilized MTs effectively support viral transport to the nucleus. A further indication that Ad2 utilizes MTs for nuclear targeting came from experiments in which transport directionality was controlled. Ad2 was found to stimulate two distinct signaling pathways which both enhance the MT-dependent minus-end-directed transport of Ad2 capsids (48). In the absence of stimulation, viral motility was directed toward the cell periphery, dependent on intact MTs.

Live imaging of MT-dependent and independent Ad transport. Glotzer et al. (8) recently questioned the role of MTs in Ad5 infection. They traced incoming Ad5 that contained a GFP-tetracycline repressor fusion protein (GFP-TetR) bound to operator sequences in the Ad5 DNA genome but were not able to detect fast retrograde motions of GFP-TetR-tagged Ad5, unlike other reports with fluorophore-tagged Ad (26, 48, 49).

There are several not mutually exclusive possibilities for why Glotzer et al. (8) missed the fast minus-end-directed motility of Ad. The first possibility involves temperature. Glotzer et al. (8) used room temperature for their live experiments, whereas we always conducted our live experiments at 37°C with a temperature-controlled sample holder. The second possibility involves longer intervals between subsequent frames. While we recorded frame intervals of 1 to 2 s, Glotzer et al. (8) used frame intervals of 3 to 5 s. Longer intervals make it less likely that high-speed elementary motion steps will be detected. The third possibility involves imaging with PBS. For their tracing experiments, Glotzer et al. (8) used PBS lacking glucose and other nutrients, whereas we used growth medium without serum (and sometimes also without phenol red). Depending on the duration of the incubation, PBS may reduce the ATP levels in the cells. Interestingly, the vast majority of the particles (about 15 to 20 particles, corresponding to about 95%) in the study of Glotzer et al. (8) were apparently nonmotile during the 14-s period depicted in their Fig. 4A. This result is again in contrast to our imaging of 40 to 60% motile particles (7, 48, 49). The fourth possibility involves imaging at shorter wavelengths and longer exposure times. Glotzer et al. (8) used GFP-tagged Ad and thus had to use an excitation beam of about 500 nm. Their exposure times were between 1 and 1.5 s, whereas our exposure times were between 0.2 and 0.4 s, i.e., four or five times shorter and thus less phototoxic. The published images in the study of Glotzer et al. (8) demonstrate photobleaching effects after as few as five frames (their Fig. 4A). Phototoxicity is known to affect the viability of cells; thus, their results are difficult to compare with our data. We imaged the TR fluorophore with a 595-nm excitation and were able to record several hundred subsequent frames (48, 49). The fifth possibility involves statistical analysis. Due to the limited data set that Glotzer et al. (8) were able to collect, their statistical analysis was limited. They processed between 20 and 218 frames per assay, whereas we included several thousand frames per assay. Thus, our standard deviations of the mean are smaller and the differences between various conditions (e.g., plus or minus NOC) are highly significant for our measurements (one-sided *t* tests). The sixth possibility involves the subcellular area of particle tracing. Figure 4 in the study of Glotzer et al. (8) shows that 8 out of 11 traced particles were in a region proximal to the nucleus, i.e., separated by less than 10 μm from the nuclear envelope. The perinuclear region is known to be elevated compared to the flat periphery. Motility in this region can also occur along the *z* axis and thus toward and away from the detector; i.e., the observed velocities in the perinuclear region might have been underestimated. Many studies, including ours, have therefore traced organelles (23) and viruses (reviewed in reference 12) in the peripheral flat regions of the cytoplasm and have used cells that are extensively spread out (see, e.g., reference 30). The final possibility involves the nature of GFP-TetR-tagged Ad particles. Glotzer et al. (8) used GFP-TetR-tagged Ad5 in which GFP-TetR was bound to operator sequences in the genomic DNA. Using biochemical assays, they demonstrated that the tag cofractionated with a viral DNA binding protein at 30 min p.i., but the stability of this interaction later in infection was not characterized. It is also unclear

what fraction of the particles was recovered in their analysis at 30 min p.i., since the control fractionation sample at 0 min p.i. was missing. They then performed all their fluorescence motility experiments at times between 30 and 80 min p.i.; thus, it is unknown whether the tag was in fact still on the viral particle. That the tag could prematurely dissociate from the DNA was suggested by their observations that GFP-TetR was not found to be imported into the nucleus but that viral DNA was apparently imported. In addition, it is not known whether the tagged DNA was completely packaged into the virion. If packaging was incomplete, then it is possible that some of the DNA dissociated from the capsid prior to capsid arrival at the nucleus. The dissociated DNA might or might not have been tagged with GFP-TetR and thus might have appeared as fluorescent puncta. It is likely that these puncta would have had motilities different from those of our Ad2-TR.

Besides these important technical differences in the live fluorescence experiments, another major difference between the study of Glotzer et al. (8) and our study is the effect of NOC on the movement of particles to the nucleus. Glotzer et al. (8) found no effect of NOC on the movement of GFP-TetR-tagged Ad DNA. Given the limitations of their tracing experiments, this result is not surprising. Glotzer et al. (8) measured slow short-range transport in both control and NOC-treated cells, i.e., MT-independent transport. Their static analysis, however, showed that GFP-TetR-tagged particles were found at the microtubule organizing center at 30 to 40 min p.i. when MTs were present but not when they were absent. This finding fully agrees with our findings and further supports the notion that the live analyses of Glotzer et al. (8) had technical limitations obscuring the detection of fast motility steps.

It is important that the fluorescent dots that we detected with Ad2-TR correspond to single viral particles that have the same infectivity as their "parental" nonlabeled particles (33). Quantitative subcellular localization of capsids in static images indicated that in control cells, about 65% of the Ad2-TR accumulates over the nuclear and perinuclear region at 90 min p.i. (33). This finding is in good agreement with the Ad2-TR motilities in epithelial and fibroblastic cells (e.g., HeLa cells, rat kangaroo PtK_2 cells, African green monkey TC7 cells, or mouse embryo fibroblasts), which are biased toward the nucleus and have net population speeds on the order of several micrometers per minute (48, 49). Elementary motility events were between 0.2 and 0.4 μm/s and reached minus-end-directed peak velocities of up to 2.6 μm/s. Moreover, capsids were transported over short ranges as well as long distances, consistent with processive motor-driven motility. Overexpression of the p50 subunit of the dynactin complex or antidynein antibodies indicated that the minus-end-directed MT motor complex dynein-dynactin has a key function in transporting Ad2 as well as HSV-1 to the nucleus (6a, 26, 49). We conclude that MTs are instrumental for the trafficking of Ad2 and HSV-1 particles to the nucleus.

NOC inhibits Ad and HSV-1 infections. Consistent with a role of MTs in transporting infectious DNA to the nucleus, we found viral gene expression to be significantly inhibited in cells lacking MTs. These cells remained on the substratum and showed no signs of leakiness, i.e., cell death. With different viruses (Ad2, Ad5, and HSV-1), different cell lines (Vero, PtK_2, A549, and HeLa), different MT-depolymerizing agents (vinblastine [45] and NOC [this study]), different genes (ICP4, β-Gal, and luciferase [45; this study]), different promoters (HSV-1 ICP4 and CMV immediate early), and different MOIs (from 2 to 100 PFU/cell), viral gene expression was in all instances found to be inhibited by 50 to 90%.

Our results again contrast those of Glotzer et al. (8). These authors reported data suggesting that NOC had no effect on the expression of luciferase from transgenic Ad5 or on infection, as estimated by counting of immunostained cells expressing the immediate-early viral protein E1A. NOC also appeared to have no effect on GFP expression encoded by Ad5, as determined by counting of green fluorescent cells. While the percentage of fluorescent cells can be easily determined, the fluorescent signal may not be linear over a wide range of protein concentrations. Measuring an enzymatic activity, such as luciferase or β-Gal, however, allows for unambiguous quantification if the assay is performed within the linear range of the enzymatic activity. Glotzer et al. (8) reported that 1,000 particles per cell gave an average of about 10^2 luciferase light units at 4 h p.i., whereas 10 times as much virus (10,000 particles per cell) resulted in 5×10^4 light units. This value is 50-fold more than what would be expected if the measurements followed linear kinetics. Moreover, there was essentially no increase in the luciferase signal from 6 to 24 h p.i. with 10,000 particles per cell, suggesting that the assay had been saturated.

In summary, we conclude that intact MTs and their associated motors support the transport of infectious Ad and HSV-1 particles to the nucleus and thereby enhance the kinetics of infection. Based on earlier results (14, 15, 35, 45, 53), we argue that the Ad and HSV-1 genomes remain enclosed in capsids during their cytosolic passage to the nucleus. Only when these capsids arrive at the NPC will they be disassembled and their DNA released and imported into the nucleus for transcription and replication.

ACKNOWLEDGMENTS

Hélène Mabit and Michel Y. Nakano contributed equally to this work.

We thank S. Hemmi and D. Serena for generous gifts of Luc-Ad5, I. Vigne and P. Yeh for Ad5 derivative AE18, P. Spear for HSV-1 [KOS]tk12, R. Eisenberg and G. Cohen for antibodies against HSV-1 capsids, R. Stidwill and P. Groscurth for confocal laser scanning microscopy imaging, and D. Meder (Hannover, Germany) for assistance with the β-Gal assay.

This work was supported by the Swiss National Science Foundation and the Kanton Zürich (support given to U.F.G.), as well as by the German Research Council (DFG; grant SO403-1 to B.S.).

REFERENCES

1. **Bearer, E. L., X. O. Breakefield, D. Schuback, T. S. Reese, and J. H. LaVail.** 2000. Retrograde axonal transport of herpes simplex virus: evidence for a single mechanism and a role for tegument. Proc. Natl. Acad. Sci. USA **97:**8146–8150.
2. **Blose, S. H., D. I. Meltzer, and J. R. Feramisco.** 1984. 10-nm filaments are induced to collapse in living cells microinjected with monoclonal and polyclonal antibodies against tubulin. J. Cell Biol. **98:**847–858.
3. **Chartier, C., E. Degryse, M. Gantzer, A. Dieterle, A. Pavirani, and M. Mehtali.** 1996. Efficient generation of recombinant adenovirus vectors by homologous recombination in *Escherichia coli*. J. Virol. **70:**4805–4810.
4. **Cohen, G. H., M. Ponce de Leon, H. Diggelmann, W. C. Lawrence, S. K. Vernon, and R. J. Eisenberg.** 1980. Structural analysis of the capsid polypeptides of herpes simplex virus types 1 and 2. J. Virol. **34:**521–531.
5. **Dales, S., and Y. Chardonnet.** 1973. Early events in the interaction of adenoviruses with HeLa cells. IV. Association with microtubules and the nuclear pore complex during vectorial movement of the inoculum. Virology **56:**465–483.

6. **Derry, W. B., L. Wilson, and M. A. Jordan.** 1995. Substoichiometric binding of taxol suppresses microtubule dynamics. Biochemistry **34:**2203–2211.

6a. **Döhner, K., A. Wolfstein, J. Prank, C. Echeverri, D. Dujardin, R. Vallee, and B. Sodeik.** 2002. Function of dynein and dynactin in herpes simplex capsid transport. Mol. Biol. Cell **13:**2559–2573.

7. **Giannakakou, P., M. Y. Nakano, K. C. Nicolaou, A. O'Brate, J. Yu, M. V. Blagosklonny, U. F. Greber, and T. Fojo.** 2002. Enhanced microtubule-dependent trafficking and p53 nuclear accumulation by suppression of microtubule dynamics. Proc. Natl. Acad. Sci. USA **99**:10855–10860.

8. **Glotzer, J. B., A. I. Michou, A. Baker, M. Saltik, and M. Cotten.** 2001. Microtubule-independent motility and nuclear targeting of adenoviruses with fluorescently labeled genomes. J. Virol. **75:**2421–2434.

9. **Goldstein, L. S., and Z. Yang.** 2000. Microtubule-based transport systems in neurons: the roles of kinesins and dyneins. Annu. Rev. Neurosci. **23:**39–71.

10. **Granzow, H., F. Weiland, A. Jons, B. G. Klupp, A. Karger, and T. C. Mettenleiter.** 1997. Ultrastructural analysis of the replication cycle of pseudorabies virus in cell culture: a reassessment. J. Virol. **71:**2072–2082.

11. **Greber, U. F.** 2002. Signalling in viral entry. Cell Mol. Life Sci. **59:**608–626.

12. **Greber, U. F., and E. Carafoli.** 2002. Signalling takes control of nucleocytoplasmic transport. EMBO Rep. **3:**410–414.

13. **Greber, U. F., M. Y. Nakano, and M. Suomalainen.** 1998. Adenovirus entry into cells: a quantitative fluorescence microscopy approach. Methods Mol. Med. **21:**217–230.

14. **Greber, U. F., M. Suomalainen, R. P. Stidwill, K. Boucke, M. Ebersold, and A. Helenius.** 1997. The role of the nuclear pore complex in adenovirus DNA entry. EMBO J. **16:**5998–6007.

15. **Greber, U. F., P. Webster, J. Weber, and A. Helenius.** 1996. The role of the adenovirus protease in virus entry into cells. EMBO J. **15:**1766–1777.

16. **Greber, U. F., M. Willetts, P. Webster, and A. Helenius.** 1993. Stepwise dismantling of adenovirus 2 during entry into cells. Cell **75:**477–486.

17. **Hammonds, T. R., S. P. Denyer, D. E. Jackson, and W. L. Irving.** 1996. Studies to show that with podophyllotoxin the early replicative stages of herpes simplex virus type 1 depend upon functional cytoplasmic microtubules. J. Med. Microbiol. **45:**167–172.

18. **Horwitz, M. S.** 1990. Adenoviridae and their replication, p. 1679–1721. *In* B. N. Fields and D. M. Knipe (ed.), Virology, 2nd ed., vol. 1. Raven Press, New York, N.Y.

19. **Horwitz, M. S.** 1996. Adenoviruses, p. 2149–2171. *In* B. N. Fields, D. M. Knipe, and P. M. Howley (ed.), Fields virology, 3rd ed., vol. 1. Raven Press, Philadelphia, Pa.

20. **Jordan, M. A., and L. Wilson.** 1999. The use and action of drugs in analyzing mitosis. Methods Cell Biol. **61:**267–295.

21. **Kay, M. A., J. C. Glorioso, and L. Naldini.** 2001. Viral vectors for gene therapy: the art of turning infectious agents into vehicles of therapeutics. Nat. Med. **7:**33–40.

22. **Kristensson, K., E. Lycke, M. Roytta, B. Svennerholm, and A. Vahlne.** 1986. Neuritic transport of herpes simplex virus in rat sensory neurons in vitro. Effects of substances interacting with microtubular function and axonal flow [nocodazole, taxol and erythro-9-[3-(2-hydroxynonyl)]adenine]. J. Gen. Virol. **67:**2023–2028.

23. **Künzi, V., M. Glatzel, M. Y. Nakano, U. F. Greber, F. van Leuwen, and A. Aguzzi.** Unhampered prion neuroinvasion despite impaired fast axonal transport in transgenic mice overexpressing four-repeat tau. J. Neurosci., in press.

24. **Lane, J., and V. Allan.** 1998. Microtubule-based membrane movement. Biochim. Biophys. Acta **1376:**27–55.

25. **Leopold, P. L., B. Ferris, I. Grinberg, S. Worgall, N. R. Hackett, and R. G. Crystal.** 1998. Fluorescent virions—dynamic tracking of the pathway of adenoviral gene transfer vectors in living cells. Hum. Gene Ther. **9:**367–378.

26. **Leopold, P. L., G. Kreitzer, N. Miyazawa, S. Rempel, K. K. Pfister, E. Rodriguez-Boulan, and R. G. Crystal.** 2000. Dynein- and microtubule-mediated translocation of adenovirus serotype 5 occurs after endosomal lysis. Hum. Gene Ther. **11:**151–165.

27. **Luftig, R. B., and R. R. Weihing.** 1975. Adenovirus binds to rat brain microtubules in vitro. J. Virol. **16:**696–706.

28. **Lycke, E., K. Kristensson, B. Svennerholm, A. Vahlne, and R. Ziegler.** 1984. Uptake and transport of herpes simplex virus in neurites of rat dorsal root ganglia cells in culture. J. Gen. Virol. **65:**55–64.

29. **Markert, J. M., M. D. Medlock, S. D. Rabkin, G. Y. Gillespie, T. Todo, W. D. Hunter, C. A. Palmer, F. Feigenbaum, C. Tornatore, F. Tufaro, and R. L. Martuza.** 2000. Conditionally replicating herpes simplex virus mutant, G207 for the treatment of malignant glioma: results of a phase I trial. Gene Ther. **7:**867–874.

30. **Matteoni, R., and T. E. Kreis.** 1987. Translocation and clustering of endosomes and lysosomes depends on microtubules. J. Cell Biol. **105:**1253–1265.

31. **Miles, B. D., R. B. Luftig, J. A. Weatherbee, R. R. Weihing, and J. Weber.** 1980. Quantitation of the interaction between adenovirus types 2 and 5 and microtubules inside infected cells. Virology **105:**265–269.

32. **Miyazawa, N., R. G. Crystal, and P. L. Leopold.** 2001. Adenovirus serotype 7 retention in a late endosomal compartment prior to cytosol escape is modulated by fiber protein. J. Virol. **75:**1387–1400.

33. **Nakano, M. Y., and U. F. Greber.** 2000. Quantitative microscopy of fluorescent adenovirus entry. J. Struct. Biol. **129:**57–68.

34. **Nguyen, H. L., S. Chari, D. Gruber, C. M. Lue, S. J. Chapin, and J. C. Bulinski.** 1997. Overexpression of full- or partial-length Map4 stabilizes microtubules and alters cell growth. J. Cell Sci. **110:**281–294.

35. **Ojala, P. M., B. Sodeik, M. W. Ebersold, U. Kutay, and A. Helenius.** 2000. Herpes simplex virus type 1 entry into host cells: reconstitution of capsid binding and uncoating at the nuclear pore complex in vitro. Mol. Cell. Biol. **20:**4922–4931.

36. **Pantaloni, D., C. Le Clainche, and M. F. Carlier.** 2001. Mechanism of actin-based motility. Science **292:**1502–1506.

37. **Penfold, M. E., P. Armati, and A. L. Cunningham.** 1994. Axonal transport of herpes simplex virions to epidermal cells: evidence for a specialized mode of virus transport and assembly. Proc. Natl. Acad. Sci. USA **91:**6529–6533.

38. **Ploubidou, A., and M. Way.** 2001. Viral transport and the cytoskeleton. Curr. Opin. Cell Biol. **13:**97–105.

39. **Ries, S., and W. M. Korn.** 2002. ONYX-015: mechanisms of action and clinical potential of a replication-selective adenovirus. Br. J. Cancer **86:**5–11.

40. **Roizman, B., and D. M. Knipe.** 2001. Herpes simplex viruses and their replication, p. 1123–1183. *In* D. M. Knipe and P. M. Howley (ed.), Fundamental virology, 4th ed. Lippincott-Raven, Philadelphia, Pa.

41. **Segerman, A., Y. F. Mei, and G. Wadell.** 2000. Adenovirus types 11p and 35p show high binding efficiencies for committed hematopoietic cell lines and are infective to these cell lines. J. Virol. **74:**1457–1467.

42. **Seth, P., M. C. Willingham, and I. Pastan.** 1985. Adenovirus-dependent release of ^{51}Cr from KB cells at an acidic pH. J. Biol. Chem. **259:**14350–14353.

43. **Smith, G. A., S. P. Gross, and L. W. Enquist.** 2001. Herpesviruses use bidirectional fast-axonal transport to spread in sensory neurons. Proc. Natl. Acad. Sci. USA **98:**3466–3470.

44. **Sodeik, B.** 2000. Mechanisms of viral transport in the cytoplasm. Trends Microbiol. **8:**465–472.

45. **Sodeik, B., M. W. Ebersold, and A. Helenius.** 1997. Microtubule-mediated transport of incoming herpes simplex virus 1 capsids to the nucleus. J. Cell Biol. **136:**1007–1021.

46. **Spear, P. G., R. J. Eisenberg, and G. H. Cohen.** 2000. Three classes of cell surface receptors for alphaherpesvirus entry. Virology **275:**1–8.

47. **Stidwill, R. S., and U. F. Greber.** 2000. Intracellular virus trafficking reveals physiological characteristics of the cytoskeleton. News Physiol. Sci. **15:**67–71.

48. **Suomalainen, M., M. Y. Nakano, K. Boucke, S. Keller, and U. F. Greber.** 2001. Adenovirus-activated PKA and p38/MAPK pathways boost microtubule-mediated nuclear targeting of virus. EMBO J. **20:**1310–1319.

49. **Suomalainen, M., M. Y. Nakano, K. Boucke, S. Keller, R. P. Stidwill, and U. F. Greber.** 1999. Microtubule-dependent minus and plus end-directed motilities are competing processes for nuclear targeting of adenovirus. J. Cell Biol. **144:**657–672.

50. **Svensson, U., and R. Persson.** 1984. Entry of adenovirus 2 into HeLa cells. J. Virol. **51:**687–694.

51. **Topp, K. S., K. Bisla, N. D. Saks, and J. H. Lavail.** 1996. Centripetal transport of herpes simplex virus in human retinal pigment epithelial cells in vitro. Neuroscience **71:**1133–1144.

52. **Topp, K. S., L. B. Meade, and J. H. LaVail.** 1994. Microtubule polarity in the peripheral processes of trigeminal ganglion cells: relevance for the retrograde transport of herpes simplex virus. J. Neurosci. **14:**318–325.

53. **Trotman, L. C., N. Mosberger, M. Fornerod, R. P. Stidwill, and U. F. Greber.** 2001. Import of adenovirus DNA involves the nuclear pore complex receptor CAN/Nup214 and histone H1. Nat. Cell Biol. **3:**1092–1100.

54. **Vigne, E., I. Mahfouz, J. F. Dedieu, A. Brie, M. Perricaudet, and P. Yeh.** 1999. RGD inclusion in the hexon monomer provides adenovirus type 5-based vectors with a fiber knob-independent pathway for infection. J. Virol. **73:**5156–5161.

55. **Wagner, E. K., and D. C. Bloom.** 1997. Experimental investigation of herpes simplex virus latency. Clin. Microbiol. Rev. **10:**419–443.

56. **Warner, M. S., R. J. Geraghty, W. M. Martinez, R. I. Montgomery, J. C. Whitbeck, R. L. Xu, R. J. Eisenberg, G. H. Cohen, and P. G. Spear.** 1998. A cell surface protein with herpesvirus entry activity (Hveb) confers susceptibility to infection by mutants of herpes simplex virus type 1, herpes simplex virus type 2, and pseudorabies virus. Virology **246:**179–189.

57. **Weatherbee, J. A., R. B. Luftig, and R. R. Weihing.** 1977. Binding of adenovirus to microtubules. II. Depletion of high-molecular-weight microtubule-associated protein content reduces specificity of in vitro binding. J. Virol. **21:**732–742.

Wolfstein A., Nagel C.-H., Radtke K., **Döhner K.**, Allan V.J., Sodeik B.
The inner tegument promotes herpes simplex virus capsid motility along microtubules *in vitro*.
Traffic, 2006, 7: 227-237

I discussed and evaluated all data with the other authors, and was involved in writing the manuscript. During my Ph.D. time, I performed some *in vitro* binding assays for this study that were not used for the final figures of the paper. The binding experiments shown in the paper were performed by Kerstin Radtke and André Wolfstein. The results published in this manuscript are the basis of the Ph.D. thesis of my colleague André Wolfstein.

Wolfstein, A., Nagel, C.H., Radtke, K., Döhner, K., Allan, V.J. and Sodeik, B. (2006)
The inner tegument promotes herpes simplex virus capsid motility along microtubules *in vitro*
Traffic, 7: 227-237

Traffic
Volume 7 Page 227 - February 2006
doi:10.1111/j.1600-0854.2005.00379.x

Volume 7 Issue 2

The Inner Tegument Promotes Herpes Simplex Virus Capsid Motility Along Microtubules *in vitro*

André Wolfstein[1], Claus-Henning Nagel[1], Kerstin Radtke[1], Katinka Döhner[1], Victoria J. Allan[2] and Beate Sodeik[1,]*

After viral fusion, capsids of the neurotropic herpes simplex virus are transported along microtubules (MT) to the nuclear pores for viral genome uncoating, nuclear transcription and replication. After assembly and egress from the nucleus, cytosolic capsids are transported to host membranes for secondary envelopment or to the axon terminal for further viral spread. Using GFP-tagged capsids, Cy3-labelled MT and cytosol, we have reconstituted viral capsid transport *in vitro*. In the presence of ATP, capsids moved along MT up to 30 μm. Blocking the function of dynactin, a cofactor of dynein and kinesin-2, inhibited the transport. Removing outer tegument proteins from the capsids increased *in vitro* motility. In contrast, capsids isolated from infected nuclei that were devoid of inner as well as outer tegument proteins showed little interaction with dynein and its cofactor dynactin. Our data suggest that the inner tegument of alphaherpesviruses contains viral receptors for MT motors.

Döhner, K., Schmidt, S., Radtke, K., Sodeik, B.
The eclipse phase of herpes simplex virus type 1 infection: efficient dynein-mediated nuclear targeting in the absence of the small capsid protein VP26.
manuscript in preparation for Journal of Virology

In this manuscript, I characterized the virus mutants HSV1-ΔVP26 und HSV1-GFPVP26. All experiments for this paper were performed during my Ph.D. studies. I generated data for figures 3, 4, 6, 7 and 8. Figure 1 was prepared by Simone Schmidt and myself, and figure 2 by Kerstin Radtke and myself. Experiments for figure 5 were performed by Simone Schmidt. Ute Prank technically assisted me with experiments for figure 3. Beate Sodeik and I wrote the manuscript (to be submitted 02/12/05).

The eclipse phase of herpes simplex virus type 1 infection: efficient dynein-mediated nuclear targeting in the absence of the small capsid protein VP26

Katinka Döhner, Simone Schmidt, Kerstin Radtke & Beate Sodeik

Institute of Virology, Hannover Medical School, Germany

Corresponding author:
Beate Sodeik
Institut für Virologie, OE5230
Medizinische Hochschule Hannover
Carl-Neuberg-Str. 1
D-30623 Hannover
Germany
Phone: +49 - 511 - 532 2846
FAX: +49 - 511 - 532 8736
Email: Sodeik.Beate@MH-Hannover.de

Number of pages:	35
Number of characters:	72,894
Number of figures:	8
Running title:	MT transport in the absence of HSV1-VP26

Abstract.

Cytoplasmic dynein together with its cofactor dynactin transports incoming herpes simplex virus type 1 (HSV1) capsids along microtubules (MT) to the MT-organizing center (MTOC). From the MTOC, capsids move further to the nuclear pore where the viral genome is released into the nucleoplasm. The small capsid protein VP26 can interact with dynein light chains, and may recruit dynein to the capsid. Therefore, we analyzed nuclear targeting of incoming HSV1-ΔVP26 capsids devoid of VP26, and of HSV1-GFPVP26 capsids expressing GFPVP26 instead of VP26.

To compare the cell entry of different strains, we characterized the inocula by plaque titration, viral DNA content, protein composition, and particle composition. Preparations with a low particle to PFU ratio and efficient nuclear targeting were considered to be of higher quality than those containing many defective particles which were unable to induce plaque formation. When cells were infected with HSV1-wildtype, HSV1-ΔVP26 or HSV1-GFPVP26, viral capsids were transported along MT to the nucleus. Moreover, when dynein function was inhibited by overexpression of the dynactin subunit dynamitin, less capsids of HSV1-wildtype, -ΔVP26 and -GFPVP26 arrived at the nucleus. Thus, even in the absence of the potential viral dynein receptor VP26, HSV1 used MT and dynein for efficient nuclear targeting. These data suggest that besides VP26, HSV1 encodes other receptors for dynein or dynactin.

Abbreviations.

DHC, dynein heavy chain; DIC, dynein intermediate chain; HSV1, Herpes Simplex Virus Type 1; GFP, green fluorescent protein; mAb, monoclonal antibody; MOI, multiplicity of infection; MT, microtubule; MTOC, MT organizing center; pAb, polyclonal antibody; PFU, plaque forming units; VP26, viral protein 26; wt, wildtype.

Key words.

Herpes simplex virus, nuclear targeting, microtubules, dynein, VP26.

Introduction.

Virions, subviral particles and viral proteins are actively transported during cell entry, assembly and egress (15, 51, 58, 61). Early in infection many viruses use microtubules (MT) for efficient nuclear targeting, either for cytosolic transport of naked viral particles, or for transport inside vesicles (14), e.g. herpes simplex virus type 1 (HSV1) (62), human cytomegalovirus (46), human immunodeficiency virus (38), adenovirus (33, 65), parvoviruses (57, 64), simian virus 40 (49), influenza virus (32) or hepatitis B virus (23).

MT are polar cytoskeletal filaments assembled from α-/β-tubulin with a very dynamic plus- and a less dynamic minus-end. N-type kinesins carry cargo towards the MT plus-ends, and are involved in transport of viral particles to the plasma membrane during egress (28, 30, 52, 72). Cytoplasmic dynein in cooperation with its cofactor dynactin or C-type kinesins catalyze transport towards MT minus-ends (48, 56, 70). In many cell types, the MT minus-ends are clustered at the MTOC that is often in close proximity to the nucleus. Cytoplasmic dynein is required for nuclear targeting of human immunodeficiency virus reverse transcription complexes (38), and capsids of adenovirus (33, 65), canine parvovirus (64) and HSV1 (16).

The HSV1 virion consists of four structural components: a double-stranded DNA genome of 152 kbp, a capsid shell with a diameter of 125 nm, the tegument, and a membranous envelope (53). The major morphological units of the icosahedral capsid are (i) the UL6 master portal at one of the 12 vertices, (ii) 11 pentons at the remaining vertices made by 5 copies of the major capsid protein VP5, and (iii) 150 hexons at the capsid edges and surfaces, that contain 6 copies of each, VP5 and the small capsid protein VP26 (42, 53, 67, 76). Moreover, all herpesviruses are characterized by a protein layer named tegument that consists of about 20 different polypeptides, which is located between the envelope and the capsid. The

bulk of the tegument is not icosahedrally ordered, but a small portion in the vicinity of the vertices shows icosahedral symmetry (27, 78).

HSV1 infects many cell types by pH-independent fusion of the viral envelope with the plasma membrane, thereby inserting envelope proteins into the plasma membrane, and releasing the tegument and the DNA-containing capsid into the cytosol (25, 43-45, 62). In addition, some cell types are productively infected after entry by endocytosis, and fusion with the membrane of an early endosomal compartment (25, 41, 43-45). In epithelial and neuronal cells, the incoming capsids are transported along microtubules (MT) to the MTOC (31, 35, 62, 66). From the MTOC capsids proceed to nuclear pores, where the viral genomes are injected into the nucleoplasm for viral transcription and replication (2, 47, 62).

Incoming HSV1 capsids colocalize with dynein and its cofactor dynactin (16, 62). Moreover, blocking dynein function by overexpression of the dynactin subunit dynamitin inhibits capsid transport to the nucleus and immediate-early viral gene expression (16). Cytoplasmic dynein consists of two dynein heavy chains, two dynein intermediate chains, two dynein light intermediate chains and several dynein light chains (70). The small HSV1 capsid protein VP26 can interact *in vitro* with the 14 kDa dynein light chains of the Tctex family (17). MT mediated nuclear targeting is considered to be essential for HSV1 in cells such as neurons, where the presynaptic plasma membrane is located far away from the nucleus (31). However in epithelial cells, depolymerization of the MT network inhibits HSV1 infection significantly but not completely (35, 62). Thus, a structural viral protein that is not essential for virus replication such as VP26 (12) may be responsible for the recruitment of dynein or dynactin to incoming capsids.

To study the viral requirements for HSV1 capsid transport during cell entry, we analyzed the nuclear targeting of incoming HSV1-ΔVP26 deleted for VP26 (12), and also of HSV1-GFPVP26 that expresses a fusion protein of green fluorescent protein (GFP) and VP26

instead of VP26 (13). The GFPVP26 fusion protein does not interfere with virus replication in tissue culture, and is incorporated into virions during capsid assembly (13). When cells were infected with HSV1-ΔVP26 or HSV1-GFPVP26 preparations of high quality, cytosolic capsids distinguished from endocytosed virions by the lack of colocalization with viral membrane antigens accumulated at the nuclear envelope in a MT-dependent manner. Furthermore, interfering with dynein function by overexpression of the dynactin subunit dynamitin reduced nuclear targeting of both, HSV1-ΔVP26 and HSV1-GFPVP26. Thus, even in the absence of the potential viral dynein receptor VP26, HSV1 used MT and dynein/dynactin for efficient nuclear targeting. Therefore, besides VP26 other HSV1 proteins must be able to recruit dynein either directly or via its cofactor dynactin to the incoming capsids for MT transport.

Materials and Methods.

Cells and primary antibodies. BHK-21 cells (ATCC CCL-10) and PtK_2 cells (ATCC CCL-56) were grown in 10%, Vero cells (ATCC CCL-81) in 7.5% fetal calf serum (Invitrogen, Paisley, UK). All media contained Eagle´s MEM with 2 mM glutamine and non-essential amino acids (Cat.-No. 04-08510; Cytogen, Sinn, Germany). Several structural herpes virus proteins were detected by the anti-HSV1 rabbit polyclonal antibody (pAb) Remus V (47), the major capsid protein VP5 by the rabbit pAb NC-1 (8) or the mouse monoclonal antibodies (mAbs) LP12, 5C10 or 8F5 (50, 69), US11 by mouse mAb #28 (54), VP16 by rabbit pAb SW7 (73), VP13/14 by rabbit pAb R220 (74). The membrane proteins gB and gD were immunolabeled by rabbit pAb R68 or mouse mAb DL6, respectively (19, 20), the immediate early protein ICP0 by mouse mAb 11060 (21), and vimentin using the mouse mAb V9 (Boehringer, Mannheim, Germany). VP26 was visualized with a rabbit pAb generated against His_6-tagged VP26 (provided by A. Helenius, ETH, Schweiz). To monitor

incoming viral capsids we used pre-adsorbed (62) rabbit pAbs raised against DNA-containing (anti-HC) or empty capsids (anti-LC; (8).

Preparation of inocula. Concentrated stocks containing secreted, extracellular virions of HSV1-wt strain F (ATCC VR-733), HSV1-wt strain KOS (ATCC VR-1493), HSV1-ΔVP26 strain KOS expressing β-galactosidase instead of the small capsid protein VP26 (KΔ26Z; (12), or HSV1-GFPVP26 strain KOS in which VP26 had been replaced by GFPVP26 (K26GFP; (13) were essentially prepared as described (62) but using linear nycodenz (Axis-shield PoC, AS, Oslo, Norway) instead of sucrose gradients. Secreted extracellular viral particles were pelleted from the medium of cells infected with an MOI (multiplicity of infection) of 0.01 PFU per cell for two days for HSV1-wt or three days for HSV1-ΔVP26 and HSV1-GFPVP26. The resuspended sediment was layered on top of a 10 to 40 % (w/v) nycodenz gradient in MNT buffer (20 mM MES, 100 mM NaCl, 30 mM Tris, pH 7.4) and spun at 50,000 x g for 2 h at 4°C (55). The virus band in the middle of the gradient was harvested, snap frozen and stored in single-use aliquots at -80 °C.

We obtained the best virus preparations, as defined by low particle and low viral genome to PFU ratios, when we harvested at an early time point when nearly all cells were rounded, but only detached from the substrate after knocking them off, and when we used nycodenz instead of sucrose gradients. Due to its high osmotic strength, sucrose may induce shrinking of the enveloped viral particles upon entering the gradient, and abrupt swelling and even rupture upon diluting the virus-containing sucrose band in the inoculating medium.

In addition, we characterized the supernatants of infected cells stored at 4°C for 2 to 5 days without further concentration. Since we analyzed HSV1 mutants attenuated in the efficiency of assembly and egress compared to HSV1-wt (12, 13), virus was not harvested from cells infected at a very low MOI as described by Everett et al. (22), but from cells synchronously infected with an MOI of 3 PFU per cell. However, these supernatants

contained a higher proportion of particles deficient in efficient nuclear targeting than virus preparations purified on nycodenz gradients, and therefore the latter were used for all experiments described here except for Fig. 2A and Fig. 5. All virus preparations were plaque titrated on Vero cells (16, 62).

Real time detection PCR. Gradient purified virions were diluted 1,000-fold in DNase I reaction buffer (10 mM Tris-HCl, pH 7.5, 2.5 mM $MgCl_2$, 0.5 mM $CaCl_2$) to a final volume of 495 µl. To determine the amount of viral DNA protected in capsids and virions, the samples were incubated either without or with 5 units of protease-free DNase I (ABgene, Epsom, UK) for 30 min at 37°C, and then further for 10 min at 75°C to inactivate the DNase. 25 µg salmon sperm DNA (Invitrogen) was added as carrier subsequent to DNase I inactivation. After the DNA had been purified using the QIAamp DNA Blood Mini Kit (Qiagen, Hilden, Germany), a real time detection PCR was performed using the LightCycler® FastStart DNA Master HybProbe kit (Roche Diagnostics, Mannheim, Germany),

the forward sense primer 5′-CCACGAGACCGACATGGAGC-3′,

the reverse antisense primer 5′-GTGCTYGGTGTGCGACCCCTC-3′,

the fluorescein coupled donor probe 5′-TGTTGGCGACTGGCGACTTTG-3′-fluorescein and, the R640 coupled acceptor probe R640-5′-TACATGTCCCCGTTTTACGGCTACCGG-3′-phosphate which are all specific to the coding region of HSV1 gB (gene UL27), and the Roche LightCycler® 1.5. After one cycle of denaturation (95°C for 10 min), 55 cycles of amplification were performed (95°C for 10 s, 58°C for 15 s, 72°C for 15 s). During the 58°C phases, the acceptor fluorescence was measured at 640 nm, and from these data the DNA concentration of the probes was calculated using standards of known DNA concentration.

SDS PAGE and immunoblots. To analyze the protein composition, extracelluar virions were pelleted, in some cases further purified on nycodenz gradients, solubilized in sample buffer (50 mM Tris-HCl, pH 6.8, 1% [w/v] SDS, 1% (v/v) β-mercaptoethanol, 5% [v/v]

glycerol, 0.001% [w/v] bromphenolblue) and loaded onto SDS gels. Following SDS PAGE, proteins were either stained with 0.1% (w/v) Coomassie Brilliant Blue R-250 and 0.1% (w/v) Coomassie Brilliant Blue G-250 in 10% acetic acid and 50% methanol or transferred to nitrocellulose membranes. The membranes were washed with PBS containing 0.1% (v/v) Tween 20 (PBS-T). After blocking in 5% lowfat milk in PBS-T, the membranes were incubated with primary antibodies diluted in 5% lowfat milk in PBS-T, washed in PBS-T, incubated with the secondary alkaline phosphatase-conjugated goat anti-rabbit or anti-mouse IgG antibodies (Dianova, Hamburg, Germany) diluted in 5% lowfat milk in PBS-T. After washing with PBS-T, the membranes were transferred to TSM (100 mM Tris-HCl, pH 9.5, 100 mM NaCl, 5 mM $MgCl_2$) and stained with 0.2 mM nitroblue tetrazolium chloride and 0.8 mM 5-bromo-4-chloro-indoyl-3-phosphate in TSM.

To analyze HSV1 immediate early gene expression, confluent PtK_2 cells grown in 6-cm culture dishes were pre-incubated for 1 h at 37°C without or with 50 µM nocodazole to depolymerize the MT network. The cells were then pre-cooled in ice-cold RPMI with 25 mM HEPES and 0.1 % BSA (RPMI-BSA), and inoculated for 2 h on ice with 20 PFU per cell in RPMI-BSA without or with 50 µM nocodazole. Unbound virus was removed by washing with ice-cold RPMI-BSA, and the cells were further incubated at 37°C and 5% CO_2 in PtK_2-medium with or without nocodazole. After 2 to 7 h, the cells were washed with PBS, lysed in hot sample buffer, scraped and resuspended. Samples were incubated at 95°C, resuspended to shear DNA, stored at –20°C and analyzed by immunoblots as described above.

Negative staining and electron microscopy. Preparations of HSV1-wt (F), HSV1-ΔVP26 and HSV1-GFPVP26 were purified via nycodenz gradients and diluted to 8 x 10^6 PFU/5 µl with 25% nycodenz solution. After adsorption on carbon-coated copper grids and washing with PBS and water, the preparations were negatively stained using 2% uranyl acetate (Merck, Darmstadt, Germany). Samples were analyzed with an EM 10 electron microscope (Carl Zeiss AG, Jena, Germany) at 80 kV.

Transfection. For transient transfections we used the plasmids pEGFP-C1 (BD Biosciences, Mountain View, CA, USA) expressing enhanced green fluorescent protein (GFP) and pDynamitin-EGFP expressing dynamitin-GFP under the control of the cytomegalovirus immediate-early promoter (16). PtK_2 or Vero cells were seeded in 24-well plates at a density of 3 x 10^4 cells/well for 19 h, and then transfected with 0.3 µg/well DNA and 0.75 µl/well Gene Juice reagent (Merck Biosciences, Schwalbach, Germany) according to the manufacturer's protocol. 30 h post transfection, the cells were infected with HSV1.

Immunofluorescence microscopy. PtK_2 or Vero cells grown on coverslips in 24-well dishes were synchronously infected with HSV1 in the absence or presence of 50 µM nocodazole. To prevent synthesis of progeny virus, 0.5 mM cycloheximide (Sigma-Aldrich) was added. The cells were fixed with 3% paraformaldehyde, permeabilized with 0.1% Triton-X-100 and labeled with antibodies as described previously (16, 62). Nuclei were stained by 1 µg/ml Hoechst 33258 (Sigma-Aldrich, Taufkirchen, Germany). The specimens were analyzed with a Nikon Eclipse E800 microscope (Nikon Instruments, Kanagawa, Japan) equipped with the appropriate fluorescence microscopy filter sets. The cell margins and nuclei were visualized by phase contrast, and images were taken with a digital interline charge coupled device camera (Micromax-5MHz-782Y; Princeton Instruments Inc. USA) controlled by the IPLab 3.2 software. Images were further processed using the programs Metmorph 5.0.5 (Univeral Imaging Corporation, West Chester, USA) and Adobe Photoshop 6.0.

Results

Viral inocula differ in the particle to PFU ratio. To be able to compare HSV1-wildtype (wt) with the mutants HSV1-ΔVP26 and HSV1-GFPVP26 in cell entry experiments, we characterized the particle composition of the inocula. Different viral particles can be released from HSV1 infected cells into the culture medium either by secretion or by cell lysis (Fig. 1): (i) vesicles containing viral membrane proteins but neither tegument nor capsid proteins, (ii) so called L-particles which consist of tegument surrounded by an envelope with viral membrane proteins (63), (iii) enveloped and tegumented capsids which lack the viral DNA, (iv) non-infectious and (v) infectious virions. Such particles can be detected by several methods. Antibodies raised against viral membrane proteins detect all particles, anti-tegument antibodies all particles except vesicles with viral membrane but without tegument proteins, and anti-capsid antibodies recognize only the capsid containing particles. Using a viral genome specific PCR, the number of particles containing viral genomes can be quantified, whereas only infectious virions will form plaques. Compared to HSV1-wt, the mutants HSV1-ΔVP26 and HSV1-GFPVP26 are assembled less efficiently (11-13). Virus preparations of the mutants might therefore contain a higher number of defective particles that can be impaired in any stage of the viral life cycle including cell entry, and the relative amounts of the different particle types might differ between wildtype and mutant preparations.

First of all, we confirmed the specificity of the generated anti-VP26 antibodies, and the identity of the viral mutants. Immunoblotting using VP5 as a loading control (Fig. 2A, right) showed no anti-VP26 reactive bands for HSV1-ΔVP26, whereas in HSV1-wt and HSV1-GFPVP26 samples VP26-positive bands were detected at the expected molecular weights of VP26 and GFPVP26, respectively (Fig. 2A, left).

To compare the efficiency of cell entry and nuclear targeting, and to identify inocula with the lowest possible amount of defective particles, several virus preparations of HSV1-wt strains F and KOS, HSV1-ΔVP26 and HSV1-GFPVP26 were compared regarding the titer of infectious particles (PFU), viral DNA content, protein composition, number of viral particles, and nuclear targeting. To reduce the amount of possible cellular contaminants, we did not use virions from infected cells. Instead, we always harvested released virions from the medium of infected cells, and purified them on linear nycodenz gradients (except for Fig. 2A and Fig. 5).

Different preparations of the same strain or the same mutant varied in their viral DNA to PFU ratio (Table 1). Our best HSV1-wt and HSV1-GFPVP26 virus preparations had a viral DNA to PFU ratio of 2 to 3, whereas the best HSV1-ΔVP26 preparation had a viral DNA to PFU ratio of about 5. The preparations were further analyzed by Coomassie stained SDS gels and immunoblots. Preparations characterized by a low viral genome to PFU ratio (Fig. 2B, lanes 1-4) had also lower amounts of viral proteins than preparations with a high viral genome to PFU ratio (lanes 5-7) when equal quantities of PFU were loaded (lanes 1-5 and 7; in lane 6 only ~25% of PFU were loaded compared to all other lanes). The overall protein composition of all three strains, and the relative ratios of glycoproteins, tegument and capsid proteins were similar suggesting that neither deletion nor GFP-tagging of VP26 altered the ratios of the different particles present in the medium of infected cells significantly (fig. 2B and 2C). Electron microscopy (Fig. 2D-G) demonstrated that in comparison to virus preparations with a low viral genome to PFU ratio, preparations with a high viral genome to PFU ratio contained much more particles per volume. Thus, a low viral genome to PFU ratio correlated with a low particle to PFU ratio.

HSV1 preparations with a low particle to PFU ratio showed efficient nuclear targeting. Next, we used immunofluorescence microscopy to analyze the nuclear targeting efficiency of different virus preparations. In all experiments analyzing the subcellular localization of incoming HSV1 particles (Fig. 3-4 and 6-8), cycloheximide was added to prevent the synthesis of progeny virus. PtK_2 cells were infected for 3 h with an MOI of 50 PFU/cell with HSV1-wt (F), HSV1-wt (KOS), HSV1-ΔVP26 or HSV1-GFPVP26, and double-labeled with antibodies against capsids (anti-HC; in red in Fig. 3) and the HSV1 membrane protein gD (DL6; green in Fig. 3). Capsids derived from HSV1-wt characterized by low viral genome to PFU ratio reached the nuclear envelope with high efficiency (a: strain F, c: strain KOS). In contrast, capsids of an HSV1-wt preparation with a high viral genome to PFU ratio also accumulated at the nucleus, but relatively more particles remained in the cell periphery (Fig. 3b). Therefore, virus preparations with a low genome/PFU ratio were assumed to be of high quality, whereas preparations with a high genome/PFU ratio were supposed to be of lower quality. Similar results were obtained for the capsids derived from the mutants (Fig. 3e-h). However, if compared to HSV1-wt of high quality (Fig. 3a and c), after 3 h of infection with our best HSV1-ΔVP26 preparation (Fig. 3e) relatively more capsids remained in the cell periphery. At 3 h p.i. the gD signal of virus preparations of lower quality (Fig. 3b) was higher than the gD signal of high quality virus preparations (Fig. 3a, c, g).

We concluded that for meaningful entry experiments, high quality preparations of wt and mutant viruses had to be used. The quality of virus preparations was assessed by evaluating the results from plaque assays, PCR, protein gels, immunoblots and microscopic experiments. If we had compared a HSV1-ΔVP26 mutant preparation of lower quality characterized by a high viral DNA/PFU ratio (Fig. 3f) with an HSV1-wt preparation of high quality (Fig. 3a and c), we would have erroneously concluded that VP26 was required for efficient nuclear

targeting. However, the best HSV1-ΔVP26 preparations showed efficient nuclear targeting (Fig. 3e), although less pronounced than HSV1-wt (Fig. 3a) and HSV1-GFPVP26 (Fig. 3g).

HSV1-ΔVP26 and HSV1-GFPVP26 do not develop mature VP5 hexon epitopes. When we analyzed the subcellular localization of incoming HSV1, we noticed that in contrast to HSV1-wt strains F and KOS, the capsids of HSV1-ΔVP26 and HSV1-GFPVP26 were not labeled with the monoclonal antibodies 5C10 (Fig. 4) and 8F5 (not shown). 5C10 and 8F5 recognize different VP5 epitopes that are displayed on mature hexons but not on pentons (69). In contrast, the monoclonal antibody LP12 (50) and the polyclonal antibody NC-1 (8), both directed against VP5, as well as the polyclonal antibodies anti-HC and anti-LC against DNA-containing and empty capsids, respectively (8), labeled capsids of the four tested HSV1 strains with similar efficiencies (not shown; for anti-HC c.f. Figs. 3, 6, 7, 8). These data suggest that the formation of the VP5 epitopes 5C10 and 8F5 epitopes, which are specific to mature hexons, required VP26 during virus assembly, and did neither form in the absence of VP26, nor in the presence of GFPVP26.

HSV1-ΔVP26 and HSV1-GFPVP26 require MT for viral gene expression. Efficient expression of HSV1 immediate-early genes from wt strains requires MT (35, 36, 62). To test whether this was also true for HSV1-GFPVP26 and HSV1-ΔVP26, PtK_2 cells were infected at an MOI of 20 PFU/cell in the presence or absence of 50 μM nocodazole, which reversibly depolymerizes MT (29). The immediate early HSV1 protein ICP0 was detected as early as 2 h post infection, and increased until 7 h post infection, the latest time point analyzed (not shown). The ICP0 expression of HSV1-wt was higher than ICP0 expression of HSV1-ΔVP26 and HSV1-GFPVP26 (Fig. 5). However, in all HSV1 strains tested, viral gene expression at 7 h p.i. was strongly reduced when cells were infected in the presence of nocodazole (Fig. 5).

Thus, HSV1-ΔVP26 and HSV1-GFPVP26 required MT for efficient immediate-early gene expression.

MT mediate the nuclear targeting of HSV1-ΔVP26. Reduced expression of ICP0 in the absence of MT (Fig. 5) could either be due to impaired capsid transport, or due to reduced nuclear targeting of the HSV1 transcription factor VP16 which is provided by the incoming tegument (5, 16, 62). Therefore, the subcellular localization of incoming HSV1-wt, HSV1-ΔVP26 and HSV1-GFPVP26 was determined using antibodies to capsids and to gD, an HSV1 envelope protein. Unless epitopes are degraded during infection, anti-capsid and anti-gD antibodies label virions bound to the cell surface or inside endosomes, while cytosolic capsids are only recognized by capsid antibodies and lack viral membrane epitopes.

In PtK_2 cells infected with HSV1-wt (Fig. 6, a and d), the majority of capsids (a, red in d; arrowheads) was already separated from gD (green in d) as early as 30 min p.i.. Few capsids still colocalized with gD (arrows in d). At 3 h p.i., capsids (b, red in e) accumulated around the nucleus as described before (16, 35, 62). Particles at the nuclear envelope did not colocalize with gD (green in e) suggesting that they were not virions in endocytic compartments but cytosolic capsids as has been shown before by electron microscopy (62). However, the gD signal was severely reduced at 3 h p.i. (e) when compared to 30 min p.i. (d). A reduction of glycoprotein signal during infection was also observed with gB, and both signals were already decreased at 2 h p.i. (not shown). This suggested that viral glycoproteins of the inoculum were degraded or at least denatured early in infection. In contrast, the intensity of the capsid signal increased between 0 min and 2 h p.i. (not shown, but compare a and b of Fig. 6; (62), indicating that the accessibility of capsid epitopes might increase during this period. When MT were depolymerized, nuclear targeting was reduced (c, red in f).

Similar results were obtained when infecting with HSV1-ΔVP26 (Fig. 6g-l). At 30 min

p.i., the capsid (g, red in j) and gD (green in j) signals were distributed over the entire cytoplasm. Many capsids had already separated from the gD signal (arrowheads in j), while other capsid signals still colocalized with gD (arrows in j). Compared to infection with HSV1-wt (d), the fraction of capsid signals that colocalized with gD at 30 min p.i. was higher after infection with HSV1-ΔVP26 (j). In the presence of MT, most HSV1-ΔVP26 capsids accumulated at the nuclear envelope at 3 h p.i. (h, red in k). However, compared to wt-HSV1, there were relatively more viral particles distributed over the entire cytoplasm (see also Fig. 3). Capsids at the nucleus or in the perinuclear area (arrowheads) did not colocalize with gD (green in k), suggesting that they had lost their envelope, whereas several viral particles in the cell periphery contained both, capsid as well as gD antigens (arrows in k). The latter either represented virions bound to the plasma membrane, or internalized into endosomes. When MT were depolymerized, HSV1-ΔVP26 particles were randomly distributed over the entire cytoplasm at 3 h p.i. (i, red in l), but in contrast to early time points, the majority of the capsids (arrowheads) did no longer colocalize with gD (green in l). Therefore, as HSV1-wt, HSV1-ΔVP26 also required MT for efficient nuclear targeting.

MT mediate the nuclear targeting of HSV1-GFPVP26. Next, we analyzed the subcellular localization of incoming HSV1-GFPVP26 particles (Fig. 7a-f). In PtK_2 cells infected for 30 min, the capsids (red in d) were distributed over the entire cytoplasm and in most cases colocalized with GFP (a, green in d; arrowheads), but not with the gD signal (blue in d). There was also a partial colocalization of capsid and gD signals (arrows in d) and of GFP and gD signals (asterisks in d). At 3 h p.i., capsids accumulated at the nuclear envelope (red in e). Compared to HSV1-wt, there was a slightly higher proportion of viral particles that remained in the cell periphery (compare Fig. 3c and 3g). Particles at the nucleus labeled with anti-capsid antibody (red in e) did not colocalize with gD (blue in e), suggesting that particles

at the nuclear rim had lost their envelope and represented cytosolic capsids. Nuclear targeting of HSV1-GFPVP26 was clearly reduced in the absence of MT (c and f). Like HSV1-wt, HSV1-GFPVP26 required MT for nuclear targeting and immediate-early viral gene expression. Thus, attaching GFP to VP26 did not interfere with efficient nuclear targeting of incoming capsids.

HSV1-ΔVP26 and HSV1-GFPVP26 nuclear targeting in Vero cells. Since HSV1 productively infects some cells after entry by endocytosis (25, 41, 43-45), and since the entry mechanism into PtK_2 cells is so far unclear, it was possible that viral particles were transported to the PtK_2 nucleus inside endosomes, and that this cytoplasmic transport of endosomes was therefore not affected by deleting a capsid protein. In contrast, Vero cells are known to be productively infected by fusion of the viral envelope and the plasma membrane (44, 45, 62). We therefore infected Vero cells with HSV1-wt, HSV1-ΔVP26 and HSV1-GFPVP26. In Vero cells, HSV1-ΔVP26 and HSV-GFPVP26 also reached the nuclear envelope in a MT-dependent manner (Fig. 7g-l). Thus, VP26 is not essential for MT transport during cell entry, and HSV1 must contain additional receptors for minus-end directed MT motors in the tegument or on the capsid.

Dynamitin overexpression reduces nuclear targeting of HSV1-ΔVP26 and HSV1-GFPVP26. Dynein and its cofactor dynactin catalyze MT-mediated nuclear targeting of HSV1-wt (16, 62). To test whether they were also required for nuclear targeting of HSV1-ΔVP26 and HSV1-GFPVP26, we overexpressed the dynactin subunit dynamitin (Fig. 8) which blocks dynein mediated transport (4, 18).

In both, PtK_2 (a-c) and Vero cells (g-i) overexpressing dynamitin-GFP (nuclei marked by ***N***) less HSV1-wt (a and d), HSV1-ΔVP26 (b and e) and HSV1-GFPVP26 (c and f) capsids

reached the nucleus compared to untransfected cells (nuclei marked by **N**). More viral particles were still distributed over the entire cytoplasm (arrowheads) or located in the cell periphery (arrows) at 3 h p.i.. In contrast, overexpression of GFP (d-f; j-l; nuclei of transfected cells marked by ***N***) had no effect on nuclear targeting of capsids. Thus, in PtK_2 and Vero cells, HSV1-ΔVP26, HSV1-GFPVP26 and HSV1-wt used MT and dynein/dynactin for transport to the nucleus.

Discussion

Incoming cytosolic HSV1 capsids utilize dynein and dynactin for efficient MT mediated transport from the cell periphery to the nucleus (16, 62). Although the small capsid protein VP26 has been shown to interact with dynein light chains of the Tctex family (17), an HSV1 strain deleted for VP26 (HSV1-ΔVP26) and an HSV1 strain in which VP26 had been replaced by GFPVP26 (HSV1-GFPVP26) also required MT and dynein for efficient nuclear targeting. Thus, other HSV1 structural proteins besides VP26 could provide a viral receptor for cytoplasmic dynein or its cofactor dynactin.

High quality virus preparations are required to study virus cell entry. The characterization of several HSV1-wt and mutant virus preparations by plaque titration, PCR, biochemical and microscopic approaches revealed that different preparations of the same strain varied significantly with regard to their particle to PFU ratio. Virus preparations with a higher viral genome to PFU ratio contained more viral protein and more viral particles, and were less efficiently targeted to the nucleus. Therefore, these virus preparations were considered to be of lower quality than preparations with a lower DNA to PFU ratio.

According to this definition, the best HSV1-ΔVP26 preparations were of lower quality than the best wild type preparations. This was most likely due to a less efficient assembly of

the mutants (11, 12). Based on the analysis of an HSV1-ΔVP26 preparation of lower quality, we would have concluded that VP26 was required for efficient MT transport. Therefore, it was crucial to carefully characterize the inocula and to identify high quality virus preparations, especially when the entry of the HSV1 mutants was analyzed. HSV1-ΔVP26 incoming capsids of good preparations were efficiently transported to the nucleus, although less completely than capsids of HSV1-wt or HSV1-GFPVP26.

The formation of some hexon-specific VP5 epitopes requires VP26. VP26 is localized on VP5 hexons but not on VP5 pentons even if present in 8-fold molar excess (3, 68, 79, 80). In contrast to HSV1-wt strains F and KOS, viral particles of HSV1-ΔVP26 and HSV1-GFPVP26 did not display 8F5 and 5C10 epitopes, while other anti-VP5 antibodies such as the mAb LP12 (50), anti-NC-1 (8), anti-HC, and anti-LC (8) recognized HSV1-wt, HSV1-ΔVP26 and HSV1-GFPVP26 with similar affinity.

The mAbs 5C10 and 8F5 recognize specifically mature VP5 in hexons (7, 24, 37, 69). Their epitope formation requires ATP (9), as does the assembly of VP26 onto the hexons of angularized capsids (6). Our data indicated that VP26 binding was not a consequence of 8F5/5C10 epitope formation, but that their formation required VP26 during virus assembly. This suggests that VP26 might induce conformational changes in VP5 which lead to epitope formation. 5C10 or 8F5 epitopes neither formed in the absence of VP26, nor in the presence of GFPVP26.

HSV1-ΔVP26 and HSV1-GFPVP26 capsids require MT for efficient nuclear targeting. VP26 interacts with the 14 kDa dynein light chains Tctex-1 and rp3 in yeast two hybrid and GST-pulldown assays (17), and this interaction could contribute to the dynein

mediated MT transport of incoming HSV1 capsids. Thus, we tested the roles of MT and dynein during the entry of HSV1-ΔVP26 and HSV1-GFPVP26.

After infection with HSV1-ΔVP26 or HSV1-GFPVP26, efficient expression of the immediate-early HSV1 gene ICP0 required MT. Moreover, HSV1-ΔVP26 and HSV1-GFPVP26 capsids accumulated at the nuclear envelope of PtK_2 cells in a MT-dependent manner. However, compared to infection with HSV1-wt, the nuclear targeting of HSV1-ΔVP26 was slightly less efficient, but this was most likely due to the higher amount of defective particles present in the mutant virus preparation. HSV1-ΔVP26 and HSV1-GFPVP26 particles at the nuclear envelope did not colocalize with the viral membrane protein gD suggesting that these particles were free cytosolic capsids.

Since the gD signal decreased during infection, we could not completely rule out that capsid signals not colocalizing with gD represented virions inside endosomes whose gD had been degraded or denatured. However, during infection with HSV1-wt, particles at the nuclear envelope were shown to be cytosolic capsids by electron microscopy (47, 62). Therefore, most probably these gD-free HSV1-ΔVP26 and HSV1-GFPVP26 particles around the nucleus also represented free cytosolic capsids.

HSV1 can productively infect some cell types after entry by endocytosis (25, 41, 43-45). In contrast, Vero cells are shown to be productively infected after fusion at the plasma membrane (44, 45, 62). 30 min p.i., the capsid signal of HSV1-ΔVP26 colocalized more frequently with gD than that of HSV1-wt. This might reflect that, compared to wt-HSV1, the HSV1-ΔVP26 virus preparations contained more defective particles that might have bound to the plasma membrane, but did not enter cells, or that were taken up by endocytosis. However, HSV1-ΔVP26 and HSV1-GFPVP26 also accumulated at the nuclear envelope of Vero cells in a MT-dependent manner. Even after endocytic uptake, capsids are released from endosomes as early as 30 min p.i. (45). At this time point, the capsid signal was still

distributed over the entire cytoplasm, suggesting that after an early release from endosomes, cytosolic capsids rather than endocytosed virions were transported to the nucleus. Taken together these data suggest that cytosolic capsids of HSV1-ΔVP26 and HSV1-GFPVP26 were transported along MT to the nucleus.

HSV1-ΔVP26 and HSV1-GFPVP26 require dynein/dynactin for efficient nuclear targeting. HSV1-ΔVP26 lacking the potential dynein receptor VP26 (17) also utilized MT for efficient nuclear targeting, and as a consequence viral immediate-early gene expression. In addition to dynein and its cofactor dynactin, some C-type kinesins are involved in minus-end directed MT transport during interphase (48), and could theoretically have transported HSV1 to the nucleus in the absence of VP26. Therefore, we overexpressed the dynactin subunit dynamitin to test whether dynein and its cofactor dynactin were involved in nuclear targeting of HSV1-ΔVP26 and HSV1-GFPVP26. Overexpression of dynamitin disrupts the dynactin complex and reduces dynein and kinesin-2 mediated transport processes (10, 56).

In PtK_2 and Vero cells, nuclear targeting of HSV1-ΔVP26 and HSV1-GFPVP26 was reduced by dynamitin overexpression. Kinesin-2, the second target of dynamitin overexpression, is a plus-end directed MT motor (28), and therefore unlikely to catalyze minus-end directed transport of HSV1. To our knowledge, an effect of dynamitin overexpression on minus-end directed kinesins has not been reported. Furthermore, anti-dynamitin antibodies do not reduce binding of early endosomes to MT, which is mediated by kinesin-1 and the minus-end directed kinesin KIFC2. Rather, they reduce binding of late endosomes to MT which is mediated by dynein and kinesin-2 (1). This suggests that interfering with dynactin function does not disturb the interaction between minus-end directed kinesins, their cargo and MT. Although we cannot formerly exclude that minus-end directed kinesins contributed to nuclear targeting of HSV1, it seems more likely that dynein in

cooperation with its cofactor dynactin catalyzed the transport of HSV1-ΔVP26 and HSV1-GFPVP26 to the nucleus.

In summary, our data indicate that cytosolic capsids of HSV1-ΔVP26 and HSV1-GFPVP26 as HSV1-wt use cytoplasmic dynein and dynactin for MT transport to the nucleus. Therefore, HSV1-GFPVP26 provides an excellent model to study MT-mediated transport in living cells. Our data concur with results from Desai et al. (1998) who showed that in the mouse ocular model transport to trigeminal ganglia is not reduced in the absence of VP26. This is consistent with our data suggesting that VP26 has no important function in minus-end directed transport during cell entry. Instead, the potential interaction between VP26 and the dynein light chains might play a role during HSV1 assembly, when cytosolic capsids are transported to the site of secondary budding (39, 40).

However in an *in vitro* binding assay, capsids of HSV1-ΔVP26 and HSV1-GFPVP26 bound dynein and dynactin as efficiently as capsids of HSV1-wt (77). Furthermore, compared to capsids which contained VP26 but no tegument or capsids with complete tegument, capsids whose outer tegument had been partially removed bound dynein and dynactin most efficiently. Moreover, the latter showed the strongest motility along MT *in vitro* (77). Such capsids contained the inner tegument proteins VP1-3 and UL37 as well as VP16, which might connect inner and outer tegument (71, 77). These data suggested that VP26 was not sufficient and that inner tegument proteins and/or VP16 were required for motor recruitment and MT motility. Moreover, excessive tegument coating rather reduced transport. Supposedly, removal of outer tegument proteins either renders a hidden motor receptor accessible or dislodges a viral transport inhibitor (77).

These hypotheses are supported by *in vivo* studies demonstrating that most of the HSV1 tegument and VP11/12, VP13/14, VP16 and VP22 of pseudorabies virus, the porcine alphaherpesvirus, detach from the incoming capsid upon fusion and stay at the plasma

membrane, whereas the inner tegument proteins VP1-3, UL37 and US3 remain attached to the capsids (26, 34, 62, 75). In neurons, GFP-tagged pseudorabies virus particles undergo bidirectional transport during entry and egress, with retrograde transport predominating during entry and anterograde transport during egress (59, 60). The direction of net transport during entry and egress of alphaherpesviruses may be controlled by varying the tegument composition, by the tegument-associated kinases US3 and UL13, or by regulating the activity of MT motors during the different stages of the viral life cycle (34, 60).

Altogether the *in vivo* and *in vitro* experiments suggest that besides VP26, HSV1 must encode at least one additional receptor for dynein or dynactin and that HSV1 inner tegument proteins are likely candidates.

Acknowledgement. At the MHH (Hannover Medical School), Jessica Janus, Claus-Henning Nagel, Dieter Petzhold and Sabine Hübner are acknowledged for assistance in immunofluorescence experiments, plaque assays, and real time detection PCR. We thank K. Theusner, M. Messerle, R. Bauerfeind, C.-H. Nagel and A. Wolfstein for many helpful discussions and critical readings of the manuscript. We are grateful to P.G. Spear (Feinberg School of Medicine of Northwestern University, Chicago, USA) for HSV1-wt strain KOS and to P. Desai (Johns Hopkins University School of Medicine, Baltimore, Maryland, USA) for HSV1-ΔVP26 and HSV1-GFPVP26. We thank G.H. Cohen & R.J. Eisenberg (University of Pennsylvania, School of Medicine, Philadelphia, USA), W.W. Newcomb & J. Brown (University of Virginia Health System, Charlottesville, USA), A.C. Minson (University of Cambridge, Cambridge, United Kingdom) R.D. Everett (MRC Virology Unit, Institute of Virology, Glasgow, Scotland, United Kingdom), and A. Helenius (Institute of Biochemistry, Swiss Federal Institute of Technology, Zürich, Switzerland) for the generous gift of antibodies. Our research is supported by the German Research Council (*Deutsche*

Forschungsgemeinschaft So403/1; So403/2). S.S. received a MHH fellowship of the State of Lower Saxony, Germany and K. R. a fellowship by the Center of Infection Biology at the MHH.

Tables.

Table 1. Characterization of various HSV1 inocula.

Virus	genomes/ml (x 10^9)	PFU/ml (x 10^9)	viral DNA/PFU	nuclear targeting
HSV1-wt strain F	12.4 (5.0)	4.4	2.8 (1.2)	+++
	42.3 (33.5)	2.8	15.1 (12.0)	-
HSV1-wt strain KOS	15.8 (8.3)	7.0	2.3 (1.1)	+++
HSV1-ΔVP26	15.9 (6.7)	3.0	5.3 (2.3)	++
	4.2 (1.5)	0.45	9.4 (3.4)	+
HSV1-GFPVP26	4.2 (1.8)	1.6	2.6 (1.1)	+++
	12.8 (10.2)	3.1	4.1 (3.3)	+

Various preparations of HSV1-wt, HSV1-ΔVP26 or HSV1-GFPVP26 were plaque titrated on Vero cells (PFU/ml; in quadruplets), and the amount of viral DNA was determined by quantitative real time detection PCR (genome/ml; in duplicates) either without or after DNase I treatment (data in brackets), followed by DNase I inactivation. The best HSV1-ΔVP26 preparations had a higher viral DNA/PFU ratio than the best HSV1-wt and HSV1-GFPVP26 stocks. In all cases, preparations with low viral DNA/PFU ratios were more efficient in nuclear capsid targeting than those of a high viral DNA/PFU ratio. All virus preps contained viral DNA that was not encapsidated, since DNase I treatment reduced the amount of genomes detected by PCR.

Figure legends

Figure 1: HSV1 viral particles potentially present in an inoculum. The inoculum may consist of vesicles with viral membrane proteins, vesicles with viral membrane and tegument proteins (L-particles), enveloped particles with tegument and capsid, but without viral DNA, non-infectious and infectious virions. Antibodies raised against viral membrane proteins detect all depicted particles, and anti-tegument antibodies recognize all particles except vesicles with viral membrane but without tegument proteins. Capsid antibodies detect the capsid containing particles. DNA-containing particles are identified by PCR, whereas only infectious virions are perceived by plaque assays.

Figure 2: HSV1 preparations of the same strain or the same mutant vary in the particle to PFU and the genome to PFU ratios. A: Viral particles harvested from the medium of cells infected with HSV1-wt strain F (1), HSV-GFPVP26 (2), or HSV1-ΔVP26 (3) were subjected to linear 8-16% SDS-PAGE, blotted, and probed with antibodies against VP26 (left) or VP5 (right). HSV1-wt (1) and HSV1-GFPVP26 (2), but not HSV1-ΔVP26 (3) contained anti-VP26 positive bands at the respective molecular weights of VP26 (12 kDa) and GFPVP26 (39 kDa) (left). Anti-VP5 (NC-1) was used as a loading control (right).

B and C. Gradient purified virus preparations of HSV1-wt strain F (lanes 1, 5), HSV1-wt strain KOS (lane 2), HSV1-GFPVP26 (lanes 2, 6), or HSV1-ΔVP26 (lanes 3, 7) were subjected to SDS-PAGE, and the gels were either stained with Coomassie (B), or blotted and probed with antibodies to VP26, VP5, US11, gB, VP16, VP13/14, and Remus V, an antibody that recognizes several capsid, tegument and glycoproteins of HSV1 (C). HSV1-wt strain F, HSV1-wt strain KOS, HSV1-ΔVP26 or HSV1-ΔVP26 had a very similar overall protein composition (B and C). When 1.3 x 10^8 PFU per lane were loaded, virus preparations with a

low viral DNA/PFU ratio (lanes 1 to 4) contained less protein than preparations with a higher DNA/PFU ratio (lanes 5 to 7). Gradient purified virus was subjected to linear 7.5 to 18% SDS PAGE at a concentration of 1.3 x 10^8 PFU/lane (lanes 1 to 5, 7) or 0.4 x 10^8 PFU/lane (lane 6). Note that only 25% of the PFU of HSV1-ΔVP26 with a high viral DNA/PFU ratio (lane 6) had been loaded onto the gel resulting in a protein concentration similar to the 100% loaded for HSV1-wt strain F (lane 1).

D to G. An HSV1-wt (F) preparation with a low viral genome to PFU ratio (2.8; D) contained less particles than a preparation of the same virus with a high viral genome to PFU ratio (15.1; E). Both preparations contained unenveloped capsids (arrowhead) as well as enveloped virus (arrow). HSV1-ΔVP26 (F) and HSV1-GFPVP26 (G) preparations with viral genome to PFU ratios of 2.6 and 4.1, respectively contained similar amounts of particles. 8x10^6 PFU/sample gradient purified virus preparations of HSV1-wt strain F (D and E), HSV1-ΔVP26 (F) and HSV1-GFPVP26 (G) were analyzed by electron microscopy after negative staining.

Figure 3: Incoming capsids derived from high quality preparations were efficiently transported to the nucleus. After infection with virus preparations with a low DNA/PFU ratio (a, c, e, g), a larger proportion of viral particles labeled with anti-HC (red) reached the nucleus within 3 h p.i. than after infection with a preparation with a higher DNA/PFU ratio (b, f, h). HSV1-wt preparations of high quality (a, c) showed the most efficient nuclear targeting, followed by HSV1-GFPVP26 preparations with a low DNA/PFU ratio (g). Nuclear targeting of HSV1-ΔVP26 preparations with a medium DNA/PFU ratio (e) was somewhat lower when compared to HSV1-wt (a, c) or HSV1-GFPVP26 (g) stocks with a low DNA/PFU ratio. Cells infected with virus preparations of high quality (a, c, g) showed little labeling for the viral membrane protein gD (green) compared to cells infected with virus

preparations with high DNA/PFU ratios at 3 h p.i. (b, f, h). PtK_2 cells were infected with HSV1-wt, HSV1-ΔVP26 or HSV-GFPVP26 preparations at an MOI of 50 PFU/cell in the presence of cycloheximide. The cells were fixed, permeabilized and labeled with anti-HC (red) and anti-gD (green). The nuclei (N) and cell margins were indicated by dashed or continuous white lines, respectively.

Figure 4: No mature VP5 epitopes on HSV1-ΔVP26 or HSV1-GFPVP26 capsids. The mAb 5C10 detected incoming nuclear HSV1-wt (a), but not HSV1-ΔVP26 (b) or HSV1-GFPVP26 (c) capsids. In contrast, cells infected in parallel and labeled with the capsid antibody anti-HC (see Figs. 3, 6, 7, or 8) had a strong punctuate signal at the nuclear envelope. PtK_2 cells were infected for 4 h in the presence of cycloheximide at an MOI of 50 PFU/cell with HSV1-wt strain F (a) HSV1-ΔVP26 (b) or HSV1-GFPVP26 (c) or mock-infected (d), fixed, permeabilized and labeled with the mAb 5C10 (a-d). Nuclei were stained with Hoechst 33258 (e-h). The Hoechst images were individually processed due to differences in the labeling intensity.

Figure 5: HSV1-wt, HSV1-GFPVP26 and HSV1-ΔVP26 required MT for efficient immediate-early viral gene expression. For all three viruses, there was less ICP0 expressed when the cells had been infected in the presence of nocodazole which depolymerizes MT. PtK_2 cells were infected for 7 h at an MOI of 20 PFU/cell in the absence or presence of 50 μM nocodazole. Cell lysates were loaded onto 5.5 to 18 % SDS gels, blotted, and probed with anti-ICP0, an immediate-early HSV1 protein (upper panel), and anti-vimentin antibody as a loading control (lower panel). Note that the molecular weight of ICP0 was higher in the KOS strains HSV1-GFPVP26 and HSV1-ΔVP26 than in the HSV1-wt strain F.

Figure 6: Subcellular localization of HSV1 capsid and membrane proteins during the early phase of infection. (a-f) 30 min after infection with HSV1-wt strain KOS, capsids (a, red in d) and gD (green in d) were distributed over the entire cytoplasm. Already this early, most capsids were devoid of gD (arrowheads in d), only few capsid signals still colocalized with gD (arrows; yellow in d). At 3 h p.i., most HSV1-wt capsids accumulated at the nuclear envelope (b, red in e), where they did not colocalize with gD (green in e). The gD signal was reduced after 3 h compared to 30 min p.i. in the presence (green in e) and absence of MT (green in f). When MT had been depolymerized (c and f), most capsids remained distributed over the entire cytoplasm even 3 h after infection (c, red in f).

(g-l) 30 min after infection with HSV1-ΔVP26, the capsid signal was distributed over the entire cytoplasm (g, red in j), and often had already separated from gD (arrowheads in j). Some capsid signals (arrows in j) still colocalized with gD (green in j). At 3 h post infection, the majority of HSV1-ΔVP26 capsids accumulated at the nuclear envelope (h, red in k), where they did not colocalize with gD (green in k). The gD in the cell periphery was often clustered and colocalized with the peripheral capsid signal (yellow in k; arrows). In the absence of MT, the capsid signal remained distributed over the entire cytoplasm at 3 h p.i. (i, red in l), but in most cases no longer colocalized with gD (green in l). In the cell periphery, there was some co-localization of capsid with gD (yellow in l; arrows).

PtK_2 cells were infected in the presence of cycloheximide with HSV1-wt strain KOS (a-f) or HSV1-ΔVP26 (g-l) at an MOI of about 50 PFU/cell for 30 min (a, d, g, j) or 3 h in the absence (b, e, h, k) or presence of 50 μM nocodazole (c, f, i, l). Cells were fixed, permeabilized and labelled with anti-capsid (a-c and g-i; red in d-f and j-l; anti-HC) and anti-gD antibodies (green in d-f and j-l; DL6). The nuclei (N) and cell margins were indicated with dashed or continuous lines, respectively (d-f and j-l). To visualize the degree of colocalization, the pixel shift between the red and green channel was not corrected in the

overlays (d-f, j-l).

Figure 7: Efficient nuclear targeting of HSV1-GFFPVP26 capsids required MT. PtK_2 cells (a-f). The GFP signal was distributed over the entire cytoplasm (a, green in d) and often colocalized with the capsid signal (red in d; arrowheads) at 30 min p.i. with HSV1-GFPVP26. In contrast, the gD signal (blue in d) was mostly separated from the capsid/GFP signal and rarely colocalized with capsid (arrows) or GFP (asterisks) signals. At 3 h post infection, GFP particles had accumulated at the nucleus (b, green in e). Not all of the particles labeled with anti-capsid antibodies (red in e) also displayed GFP fluorescence (b, green in e). Neither the nuclear anti-capsid nor the GFP signal colocalized with gD (blue in e). The gD signal was strongly diminished 3 h p.i. (e). In the absence of MT, HSV1-GFPVP26 particles were randomly distributed over the entire cytoplasm even after 3 h of infection (c and f). The cells were infected in the presence of cycloheximide at an MOI of about 50 PFU/cell for 30 min (a and d) or 3 h in the absence (b and e) or presence of 50 µM nocodazole (c and f). Cells were fixed, permeabilized and labeled with anti-capsid (d-f in red; anti-HC) and anti-gD antibodies (d-f in blue; DL6). GFP (a-c and d-f in green) was detected by its intrinsic fluorescence. The nuclei (N) and cell margins were indicated with dashed or continuous lines, respectively (d-f). The pixel shifts between the red, green and blue channels were not corrected (d-f).

Vero cells (g-l). At 3 h p.i., many HSV1-wt (g), HSV1-ΔVP26 (h) and HSV1-GFPVP26 (i) capsids accumulated around the nucleus of Vero cells. When MT had been depolymerized during infection, HSV1-wt (j), HSV1-ΔVP26 (k) and HSV1-GFPVP26 (l) capsids remained randomly distributed over the entire cytoplasm. Vero cells were infected in the presence of cycloheximide for 3 h with wt-HSV1 strain KOS (a, d), HSV1-ΔVP26 (b, e) or HSV1-GFPVP26 (i, l) at an MOI of 50 PFU/cell in the absence (a-c) or presence of 50 µM nocodazole (d-f). Cells were fixed, permeabilized and labeled with anti-capsid antibody (anti-HC). The nuclei (N) and cell margins were marked with dashed and continuous lines,

respectively. Arrowheads indicate capsids which colocalize with GFP, arrows point to capsid signals which colocalize gD, and asterisks show GFP signals which colocalize with gD (d-f).

Detailed Figure 7, for reviewer's information, corresponds to Fig. 7, a-f:

Efficient nuclear targeting of HSV1-GFFPVP26 capsids required MT. After 30 min infection with HSV1-GFPVP26, the GFP signal was distributed over the entire cytoplasm (a, green in d) and often colocalized with the capsid signal (a', red in d; arrowheads). In contrast, most of the gD signal (a'', blue in d) was separated from the GFP/capsid signal. Only few gD signals colocalized with capsid (arrows) or GFP (asterisks) signals. At 3 h p.i., capsids had accumulated at the nucleus (b', red in e). Not all of the particles labeled with anti-capsid antibodies also displayed GFP fluorescence (b, green in e). Neither the nuclear anti-capsid, nor the GFP signal colocalized with gD (b'', blue in e). The gD signal was strongly diminished 3 h post infection (b'', blue in e). In the absence of MT, the HSV1-GFPVP26 particles were randomly distributed over the entire cytoplasm even after 3 h of infection (c, c' and f). PtK_2 cells were infected in the presence of cycloheximide with HSV1-GFPVP26 at a MOI of 50 PFU/cell for 30 min (a, a', a'', d) or 3 h in the absence (b, b', b'', e) or presence of 50 μM nocodazole (c, c', c'', f). Cells were fixed, permeabilized and labeled with anti-capsid (a'-c'; anti-HC) and anti-gD (a''-c''). GFP (a-c) was detected by its intrinsic fluorescence. The nuclei (N) and cell margins were marked with dashed or continuous lines, respectively (d-f). The pixel shifts between the red, green and blue channels were not corrected (d-f). Arrowheads indicate capsids which colocalize with GFP, arrows capsid signals which colocalize gD, and asterisks GFP signals which colocalize with gD (d-f).

Figure 8: Dynamitin reduced nuclear targeting in the presence and absence of VP26. In PtK_2 cells (a-f) or Vero cells (g-l) overexpressing dynamitin-GFP (a-c; g-l), less HSV1-wt (a, g), HSV1-ΔVP26 (b, h) and HSV1-GFPVP26 (c, i) capsids reached the nucleus than in

untransfected cells. The overexpression of GFP (d-f; j-l) had no effect on nuclear targeting of HSV1-wt (d, j), HSV1-ΔVP26 (e, k) or HSV1-GFPVP26 (f, l) capsids. The cells were transfected with dynamitin-GFP (a-c; g-i) or GFP (d-f; j-l) for 30 h and then infected with HSV1-wt strain KOS (a, d, g, j), HSV1-ΔVP26 (b, e, h, k) or HSV1-GFPVP26 (c, f, i, l) for 3 h in the presence of cycloheximide at an MOI of 50 PFU/cell. Cells were fixed and labeled with an anti-capsid antibody (anti-HC). Dynamitin-GFP and GFP were detected by their intrinsic fluorescence (not shown). Overexpressing cells were marked by an ***N*** in italics, untransfected cells by a normal **N**. The nuclei and cell margins were indicated with dashed and continuous white lines, respectively. Arrows point to capsids in the cell periphery, arrowheads to capsids distributed in the cytoplasm.

Additional information to Figure 8 for reviewer's information: PtK_2 and Vero cells overexpressing dynamitin-GFP or GFP. PtK_2 cells (a-f) or Vero cells (g-l) overexpressing dynamitin-GFP (a-c; g-i) or GFP (d-f; j-l) were detected by their intrinsic fluorescence. In Figure 8 overexpressing cells were marked by an ***N*** in italics, while untransfected cells are indicated by a normal **N**.

References

1. Bananis, E., S. Nath, K. Gordon, P. Satir, R. J. Stockert, J. W. Murray, and A. W. Wolkoff. 2004. Microtubule-dependent movement of late endocytic vesicles in vitro: requirements for Dynein and Kinesin. Mol Biol Cell 15:3688-97.
2. Batterson, W., D. Furlong, and B. Roizman. 1983. Molecular genetics of herpes simplex virus. VIII. further characterization of a temperature-sensitive mutant defective in release of viral DNA and in other stages of the viral reproductive cycle. J Virol 45:397-407.
3. Booy, F. P., B. L. Trus, W. W. Newcomb, J. C. Brown, J. F. Conway, and A. C. Steven. 1994. Finding a needle in a haystack: detection of a small protein (the 12-kDa VP26) in a large complex (the 200-MDa capsid of herpes simplex virus). Proc Natl Acad Sci U S A 91:5652-6.
4. Burkhardt, J. K., C. J. Echeverri, T. Nilsson, and R. B. Vallee. 1997. Overexpression of the dynamitin (p50) subunit of the dynactin complex disrupts dynein-dependent maintenance of membrane organelle distribution. J Cell Biol 139:469-84.
5. Campbell, M. E., J. W. Palfreyman, and C. M. Preston. 1984. Identification of herpes simplex virus DNA sequences which encode a trans-acting polypeptide responsible for stimulation of immediate early transcription. J Mol Biol 180:1-19.
6. Chi, J. H., and D. W. Wilson. 2000. ATP-Dependent localization of the herpes simplex virus capsid protein VP26 to sites of procapsid maturation. J Virol 74:1468-76.
7. Church, G. A., and D. W. Wilson. 1997. Study of herpes simplex virus maturation during a synchronous wave of assembly. J Virol 71:3603-12.
8. Cohen, G. H., M. Ponce de Leon, H. Diggelmann, W. C. Lawrence, S. K. Vernon, and R. J. Eisenberg. 1980. Structural analysis of the capsid polypeptides of herpes simplex virus types 1 and 2. J Virol 34:521-31.
9. Dasgupta, A., and D. W. Wilson. 1999. ATP depletion blocks herpes simplex virus DNA packaging and capsid maturation. J Virol 73:2006-15.
10. Deacon, S. W., A. S. Serpinskaya, P. S. Vaughan, M. Lopez Fanarraga, I. Vernos, K. T. Vaughan, and V. I. Gelfand. 2003. Dynactin is required for bidirectional organelle transport. J Cell Biol 160:297-301.
11. Desai, P., J. C. Akpa, and S. Person. 2003. Residues of VP26 of herpes simplex virus type 1 that are required for its interaction with capsids. J Virol 77:391-404.
12. Desai, P., N. A. DeLuca, and S. Person. 1998. Herpes simplex virus type 1 VP26 is not essential for replication in cell culture but influences production of infectious virus in the nervous system of infected mice. Virology 247:115-24.
13. Desai, P., and S. Person. 1998. Incorporation of the green fluorescent protein into the herpes simplex virus type 1 capsid. J Virol 72:7563-8.
14. Döhner, K., C. H. Nagel, and B. Sodeik. 2005. Viral stop-and-go along microtubules: taking a ride with dynein and kinesins. Trends Microbiol 13:320-7.
15. Döhner, K., and B. Sodeik. 2004. The role of the cytoskeleton during viral Infection. Curr Top Microbiol Immunol 285:67-108.
16. Döhner, K., A. Wolfstein, U. Prank, C. Echeverri, D. Dujardin, R. Vallee, and B. Sodeik. 2002. Function of dynein and dynactin in herpes simplex virus capsid transport. Mol Biol Cell 13:2795-809.
17. Douglas, M. W., R. J. Diefenbach, F. L. Homa, M. Miranda-Saksena, F. J. Rixon, V. Vittone, K. Byth, and A. L. Cunningham. 2004. Herpes simplex virus type 1 capsid protein VP26 interacts with dynein light chains RP3 and Tctex1 and plays a role in retrograde cellular transport. J Biol Chem 279:28522-30.
18. Echeverri, C. J., B. M. Paschal, K. T. Vaughan, and R. B. Vallee. 1996. Molecular characterization of the 50-kD subunit of dynactin reveals function for the complex in chromosome alignment and spindle organization during mitosis. J Cell Biol 132:617-33.
19. Eisenberg, R. J., D. Long, M. Ponce de Leon, J. T. Matthews, P. G. Spear, M. G. Gibson, L. A. Lasky, P. Berman, E. Golub, and G. H. Cohen. 1985. Localization of epitopes of herpes simplex virus type 1 glycoprotein D. J Virol 53:634-44.
20. Eisenberg, R. J., M. Ponce de Leon, H. M. Friedman, L. F. Fries, M. M. Frank, J. C. Hastings, and G. H. Cohen. 1987. Complement component C3b binds directly to purified glycoprotein C of herpes simplex virus types 1 and 2. Microb Pathog 3:423-35.
21. Everett, R. D., A. Orr, and M. Elliott. 1991. High level expression and purification of herpes simplex virus type 1 immediate early polypeptide Vmw110. Nucleic Acids Res 19:6155-61.
22. Everett, R. D., G. Sourvinos, C. Leiper, J. B. Clements, and A. Orr. 2004. Formation of nuclear foci of the herpes simplex virus type 1 regulatory protein ICP4 at early times of infection: localization,

dynamics, recruitment of ICP27, and evidence for the de novo induction of ND10-like complexes. J Virol 78:1903-17.
23. Funk, A., M. Mhamdi, L. Lin, H. Will, and H. Sirma. 2004. Itinerary of hepatitis B viruses: delineation of restriction points critical for infectious entry. J Virol 78:8289-300.
24. Gao, M., L. Matusick-Kumar, W. Hurlburt, S. F. DiTusa, W. W. Newcomb, J. C. Brown, P. J. McCann, 3rd, I. Deckman, and R. J. Colonno. 1994. The protease of herpes simplex virus type 1 is essential for functional capsid formation and viral growth. J Virol 68:3702-12.
25. Gianni, T., G. Campadelli-Fiume, and L. Menotti. 2004. Entry of herpes simplex virus mediated by chimeric forms of nectin1 retargeted to endosomes or to lipid rafts occurs through acidic endosomes. J Virol 78:12268-76.
26. Granzow, H., B. G. Klupp, and T. C. Mettenleiter. 2005. Entry of pseudorabies virus: an immunogold-labeling study. J Virol 79:3200-5.
27. Grünewald, K., P. Desai, D. C. Winkler, J. B. Heymann, D. M. Belnap, W. Baumeister, and A. C. Steven. 2003. Three-dimensional structure of herpes simplex virus from cryo-electron tomography. Science 302:1396-8.
28. Hirokawa, N., and R. Takemura. 2005. Molecular motors and mechanisms of directional transport in neurons. Nat Rev Neurosci 6:201-14.
29. Jordan, M. A., and L. Wilson. 1999. The use and action of drugs in analyzing mitosis. Methods Cell Biol 61:267-95.
30. Jouvenet, N., P. Monaghan, M. Way, and T. Wileman. 2004. Transport of African swine fever virus from assembly sites to the plasma membrane is dependent on microtubules and conventional kinesin. J Virol 78:7990-8001.
31. Kristensson, K., E. Lycke, M. Roytta, B. Svennerholm, and A. Vahlne. 1986. Neuritic transport of herpes simplex virus in rat sensory neurons in vitro. Effects of substances interacting with microtubular function and axonal flow [nocodazole, taxol and erythro-9-3-(2-hydroxynonyl)adenine]. J Gen Virol 67:2023-8.
32. Lakadamyali, M., M. J. Rust, H. P. Babcock, and X. Zhuang. 2003. Visualizing infection of individual influenza viruses. Proc Natl Acad Sci U S A 100:9280-5.
33. Leopold, P. L., G. Kreitzer, N. Miyazawa, S. Rempel, K. K. Pfister, E. Rodriguez-Boulan, and R. G. Crystal. 2000. Dynein- and microtubule-mediated translocation of adenovirus serotype 5 occurs after endosomal lysis. Hum Gene Ther 11:151-65.
34. Luxton, G. W., S. Haverlock, K. E. Coller, S. E. Antinone, A. Pincetic, and G. A. Smith. 2005. Targeting of herpesvirus capsid transport in axons is coupled to association with specific sets of tegument proteins. Proc Natl Acad Sci U S A 102:5832-7.
35. Mabit, H., M. Y. Nakano, U. Prank, B. Saam, K. Döhner, B. Sodeik, and U. F. Greber. 2002. Intact microtubules support adenovirus and herpes simplex virus infections. J Virol 76:9962-71.
36. Marozin, S., U. Prank, and B. Sodeik. 2004. Herpes simplex virus type 1 infection of polarized epithelial cells requires microtubules and access to receptors present at cell-cell contact sites. J Gen Virol 85:775-86.
37. Matusick-Kumar, L., W. Hurlburt, S. P. Weinheimer, W. W. Newcomb, J. C. Brown, and M. Gao. 1994. Phenotype of the herpes simplex virus type 1 protease substrate ICP35 mutant virus. J Virol 68:5384-94.
38. McDonald, D., M. A. Vodicka, G. Lucero, T. M. Svitkina, G. G. Borisy, M. Emerman, and T. J. Hope. 2002. Visualization of the intracellular behavior of HIV in living cells. J Cell Biol 159:441-52.
39. Mettenleiter, T. C. 2004. Budding events in herpesvirus morphogenesis. Virus Res 106:167-80.
40. Mettenleiter, T. C. 2002. Herpesvirus assembly and egress. J Virol 76:1537-47.
41. Milne, R. S., A. V. Nicola, J. C. Whitbeck, R. J. Eisenberg, and G. H. Cohen. 2005. Glycoprotein D receptor-dependent, low-pH-independent endocytic entry of herpes simplex virus type 1. J Virol 79:6655-63.
42. Newcomb, W. W., R. M. Juhas, D. R. Thomsen, F. L. Homa, A. D. Burch, S. K. Weller, and J. C. Brown. 2001. The UL6 gene product forms the portal for entry of DNA into the herpes simplex virus capsid. J Virol 75:10923-32.
43. Nicola, A. V., J. Hou, E. O. Major, and S. E. Straus. 2005. Herpes simplex virus type 1 enters human epidermal keratinocytes, but not neurons, via a pH-dependent endocytic pathway. J Virol 79:7609-16.
44. Nicola, A. V., A. M. McEvoy, and S. E. Straus. 2003. Roles for endocytosis and low pH in herpes simplex virus entry into HeLa and Chinese hamster ovary cells. J Virol 77:5324-32.
45. Nicola, A. V., and S. E. Straus. 2004. Cellular and viral requirements for rapid endocytic entry of herpes simplex virus. J Virol 78:7508-17.
46. Ogawa-Goto, K., K. Tanaka, W. Gibson, E. Moriishi, Y. Miura, T. Kurata, S. Irie, and T. Sata. 2003. Microtubule network facilitates nuclear targeting of human cytomegalovirus capsid. J Virol 77:8541-7.
47. Ojala, P. M., B. Sodeik, M. W. Ebersold, U. Kutay, and A. Helenius. 2000. Herpes simplex virus type 1

entry into host cells: reconstitution of capsid binding and uncoating at the nuclear pore complex in vitro. Mol Cell Biol 20:4922-31.
48. Ovechkina, Y., and L. Wordeman. 2003. Unconventional motoring: an overview of the Kin C and Kin I kinesins. Traffic 4:367-75.
49. Pelkmans, L., J. Kartenbeck, and A. Helenius. 2001. Caveolar endocytosis of simian virus 40 reveals a new two-step vesicular-transport pathway to the ER. Nat Cell Biol 3:473-83.
50. Phelan, A., J. Dunlop, A. H. Patel, N. D. Stow, and J. B. Clements. 1997. Nuclear sites of herpes simplex virus type 1 DNA replication and transcription colocalize at early times postinfection and are largely distinct from RNA processing factors. J Virol 71:1124-32.
51. Ploubidou, A., and M. Way. 2001. Viral transport and the cytoskeleton. Curr Opin Cell Biol 13:97-105.
52. Rietdorf, J., A. Ploubidou, I. Reckmann, A. Holmstrom, F. Frischknecht, M. Zettl, T. Zimmermann, and M. Way. 2001. Kinesin-dependent movement on microtubules precedes actin-based motility of vaccinia virus. Nat Cell Biol 3:992-1000.
53. Roizman, B., and D. M. Knipe. 2001. Herpes simplex viruses and their replication, p. 2399-2459. *In* B. N. Fields, D. M. Knipe, P. M. Howley, and e. al. (ed.), Fundamental Virology, 4th edition. Lippincott-Raven Publishers, Philadelphia.
54. Roller, R. J., and B. Roizman. 1992. The herpes simplex virus 1 RNA binding protein US11 is a virion component and associates with ribosomal 60S subunits. J Virol 66:3624-32.
55. Sathananthan, B., E. Rodahl, T. Flatmark, N. Langeland, and L. Haarr. 1997. Purification of herpes simplex virus type 1 by density gradient centrifugation and estimation of the sedimentation coefficient of the virion. Apmis 105:238-46.
56. Schroer, T. A. 2004. Dynactin. Annu Rev Cell Dev Biol 20:759-79.
57. Seisenberger, G., M. U. Ried, T. Endress, H. Buning, M. Hallek, and C. Brauchle. 2001. Real-time single-molecule imaging of the infection pathway of an adeno- associated virus. Science 294:1929-32.
58. Smith, G. A., and L. W. Enquist. 2002. BREAK INS AND BREAK OUTS: Viral Interactions with the Cytoskeleton of Mammalian Cells. Annu Rev Cell Dev Biol 18:135-61.
59. Smith, G. A., S. P. Gross, and L. W. Enquist. 2001. Herpesviruses use bidirectional fast-axonal transport to spread in sensory neurons. Proc Natl Acad Sci U S A 98:3466-70.
60. Smith, G. A., L. Pomeranz, S. P. Gross, and L. W. Enquist. 2004. Local modulation of plus-end transport targets herpesvirus entry and egress in sensory axons. Proc Natl Acad Sci U S A.
61. Sodeik, B. 2000. Mechanisms of viral transport in the cytoplasm. Trends Microbiol 8:465-72.
62. Sodeik, B., M. W. Ebersold, and A. Helenius. 1997. Microtubule-mediated transport of incoming herpes simplex virus 1 capsids to the nucleus. J Cell Biol 136:1007-21.
63. Subak-Sharpe, J. H., and D. J. Dargan. 1998. HSV molecular biology: general aspects of herpes simplex virus molecular biology. Virus Genes 16:239-51.
64. Suikkanen, S., T. Aaltonen, M. Nevalainen, O. Valilehto, L. Lindholm, M. Vuento, and M. Vihinen-Ranta. 2003. Exploitation of microtubule cytoskeleton and dynein during parvoviral traffic toward the nucleus. J Virol 77:10270-9.
65. Suomalainen, M., M. Y. Nakano, S. Keller, K. Boucke, R. P. Stidwill, and U. F. Greber. 1999. Microtubule-dependent plus- and minus end-directed motilities are competing processes for nuclear targeting of adenovirus. J Cell Biol 144:657-72.
66. Topp, K. S., K. Bisla, N. D. Saks, and J. H. Lavail. 1996. Centripetal transport of herpes simplex virus in human retinal pigment epithelial cells in vitro. Neuroscience 71:1133-44.
67. Trus, B. L., N. Cheng, W. W. Newcomb, F. L. Homa, J. C. Brown, and A. C. Steven. 2004. Structure and polymorphism of the UL6 portal protein of herpes simplex virus type 1. J Virol 78:12668-71.
68. Trus, B. L., F. L. Homa, F. P. Booy, W. W. Newcomb, D. R. Thomsen, N. Cheng, J. C. Brown, and A. C. Steven. 1995. Herpes simplex virus capsids assembled in insect cells infected with recombinant baculoviruses: structural authenticity and localization of VP26. J Virol 69:7362-6.
69. Trus, B. L., W. W. Newcomb, F. P. Booy, J. C. Brown, and A. C. Steven. 1992. Distinct monoclonal antibodies separately label the hexons or the pentons of herpes simplex virus capsid. Proc Natl Acad Sci U S A 89:11508-12.
70. Vallee, R. B., J. C. Williams, D. Varma, and L. E. Barnhart. 2004. Dynein: An ancient motor protein involved in multiple modes of transport. J Neurobiol 58:189-200.
71. Vittone, V., E. Diefenbach, D. Triffett, M. W. Douglas, A. L. Cunningham, and R. J. Diefenbach. 2005. Determination of interactions between tegument proteins of herpes simplex virus type 1. J Virol 79:9566-71.
72. Ward, B. M., and B. Moss. 2004. Vaccinia Virus A36R Membrane Protein Provides a Direct Link between Intracellular Enveloped Virions and the Microtubule Motor Kinesin. J Virol 78:2486-93.
73. Weinheimer, S. P., B. A. Boyd, S. K. Durham, J. L. Resnick, and D. R. O'Boyle, 2nd. 1992. Deletion of the VP16 open reading frame of herpes simplex virus type 1. J Virol 66:258-69.
74. Whittaker, G. R., M. P. Riggio, I. W. Halliburton, R. A. Killington, G. P. Allen, and D. M. Meredith.

1991. Antigenic and protein sequence homology between VP13/14, a herpes simplex virus type 1 tegument protein, and gp10, a glycoprotein of equine herpesvirus 1 and 4. J Virol 65:2320-6.
75. Willard, M. 2002. Rapid Directional Translocations in Virus Replication. J Virol 76:5220-5232.
76. Wingfield, P. T., S. J. Stahl, D. R. Thomsen, F. L. Homa, F. P. Booy, B. L. Trus, and A. C. Steven. 1997. Hexon-only binding of VP26 reflects differences between the hexon and penton conformations of VP5, the major capsid protein of herpes simplex virus. J Virol 71:8955-61.
77. Wolfstein, A., C. H. Nagel, K. Radtke, K. Döhner, V. J. Allan, and B. Sodeik. *Traffic*, in press. The inner tegument promotes herpes simplex virus capsid motility along microtubules in vitro.
78. Zhou, Z. H., D. H. Chen, J. Jakana, F. J. Rixon, and W. Chiu. 1999. Visualization of tegument-capsid interactions and DNA in intact herpes simplex virus type 1 virions. J Virol 73:3210-8.
79. Zhou, Z. H., J. He, J. Jakana, J. D. Tatman, F. J. Rixon, and W. Chiu. 1995. Assembly of VP26 in herpes simplex virus-1 inferred from structures of wild-type and recombinant capsids. Nat Struct Biol 2:1026-30.
80. Zhou, Z. H., B. V. Prasad, J. Jakana, F. J. Rixon, and W. Chiu. 1994. Protein subunit structures in the herpes simplex virus A-capsid determined from 400 kV spot-scan electron cryomicroscopy. J Mol Biol 242:456-69.

assay	vesicle with viral membrane proteins	L-particle	enveloped and tegumented capsid without viral DNA	non-infectious virion	infectious virion
	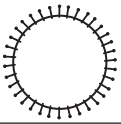	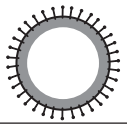	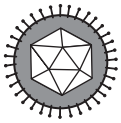	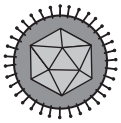	
viral membrane proteins	+	+	+	+	+
tegument proteins	-	+	+	+	+
capsid proteins	-	-	+	+	+
PCR	-	-	-	+	+
plaque assay	-	-	-	-	+

Döhner et al. (2005); Figure 1
HSV1 viral particles potentially present in an inoculum.

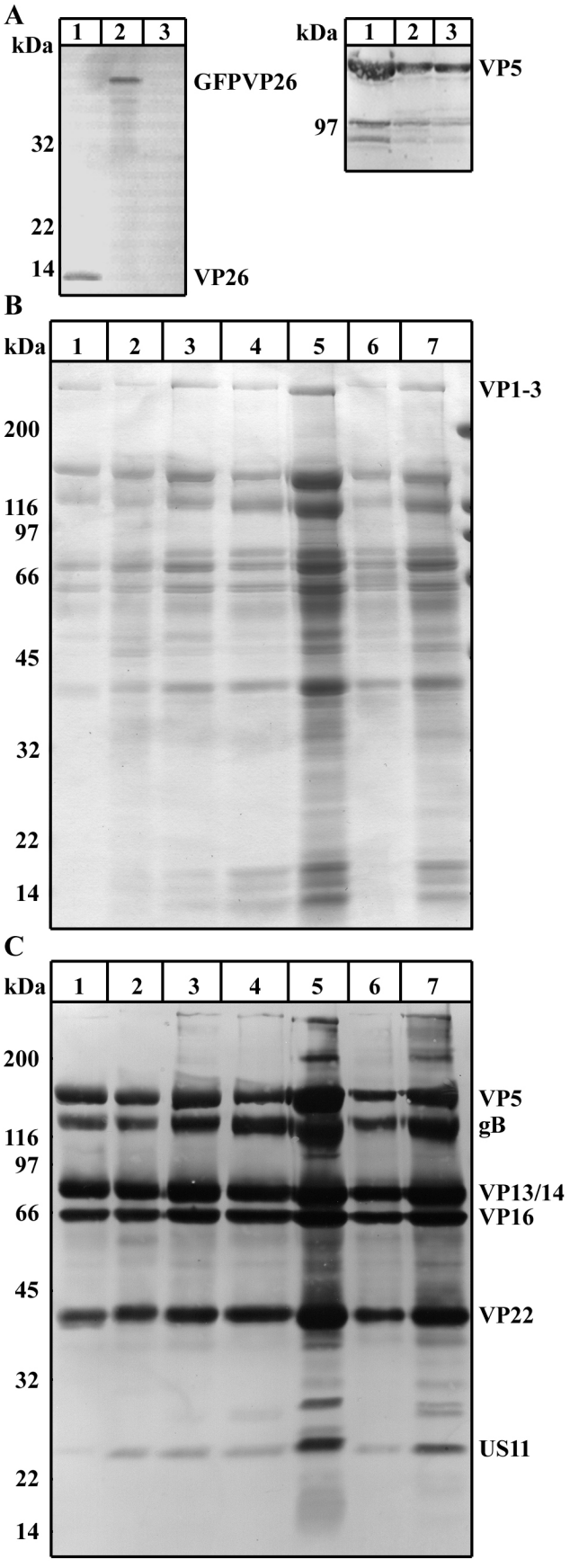

Döhner et al. (2005); Figure 2
Protein composition of HSV1-wt, HSV1-ΔVP26 and HSV1-GFPVP26 inocula.

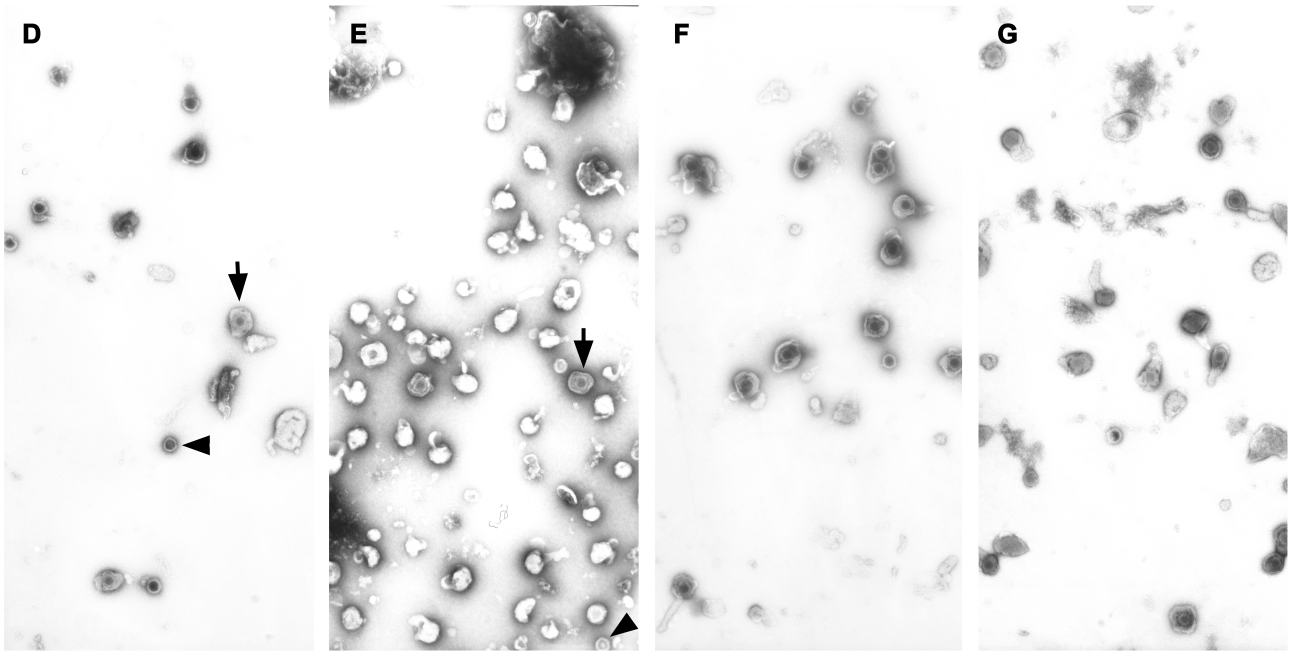

Döhner et al. (2005); Figure 2D-2G
Composition of HSV1-wt with low (D) and high (E) viral genome to PFU ratios, HSV1-ΔVP26 (F) and HSV1-GFPVP26 (G) preparations. All inocula have the same PFU, yet particle numbers differ.

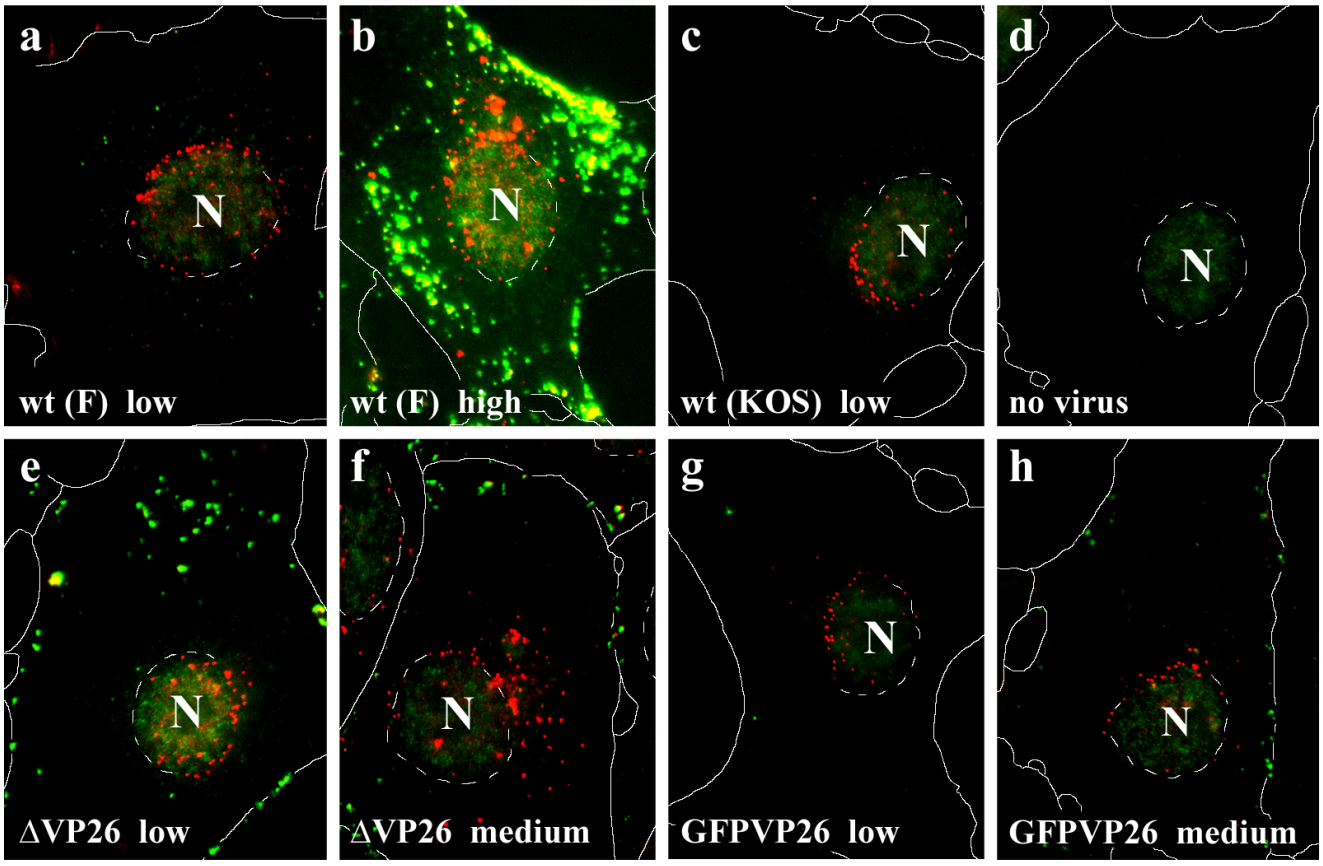

Döhner et al. (2005); Figure 3
Incoming capsids from virus preparations with a low viral DNA/PFU ratio were transported more efficiently to the nucleus than those with a higher DNA/PFU ratio.

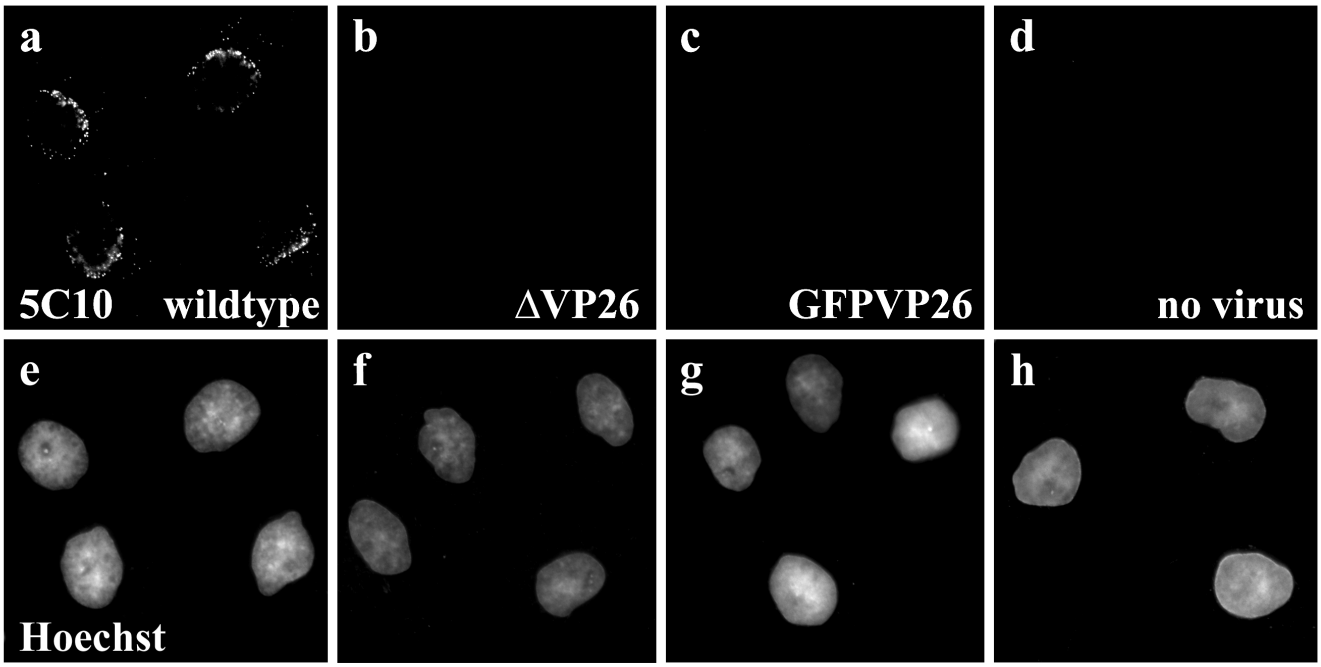

Döhner et al. (2005); Figure 4
No mature VP5 epitopes on HSV1-ΔVP26 or HSV1-GFPVP26 capsids.

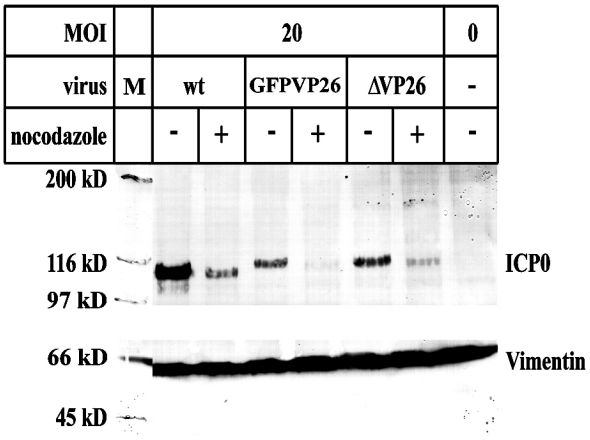

Döhner et al. (2005); Figure 5
HSV1-wt, HSV1-ΔVP26 and HSV1-GFPVP26 required MT for efficient immediate-early viral gene expression.

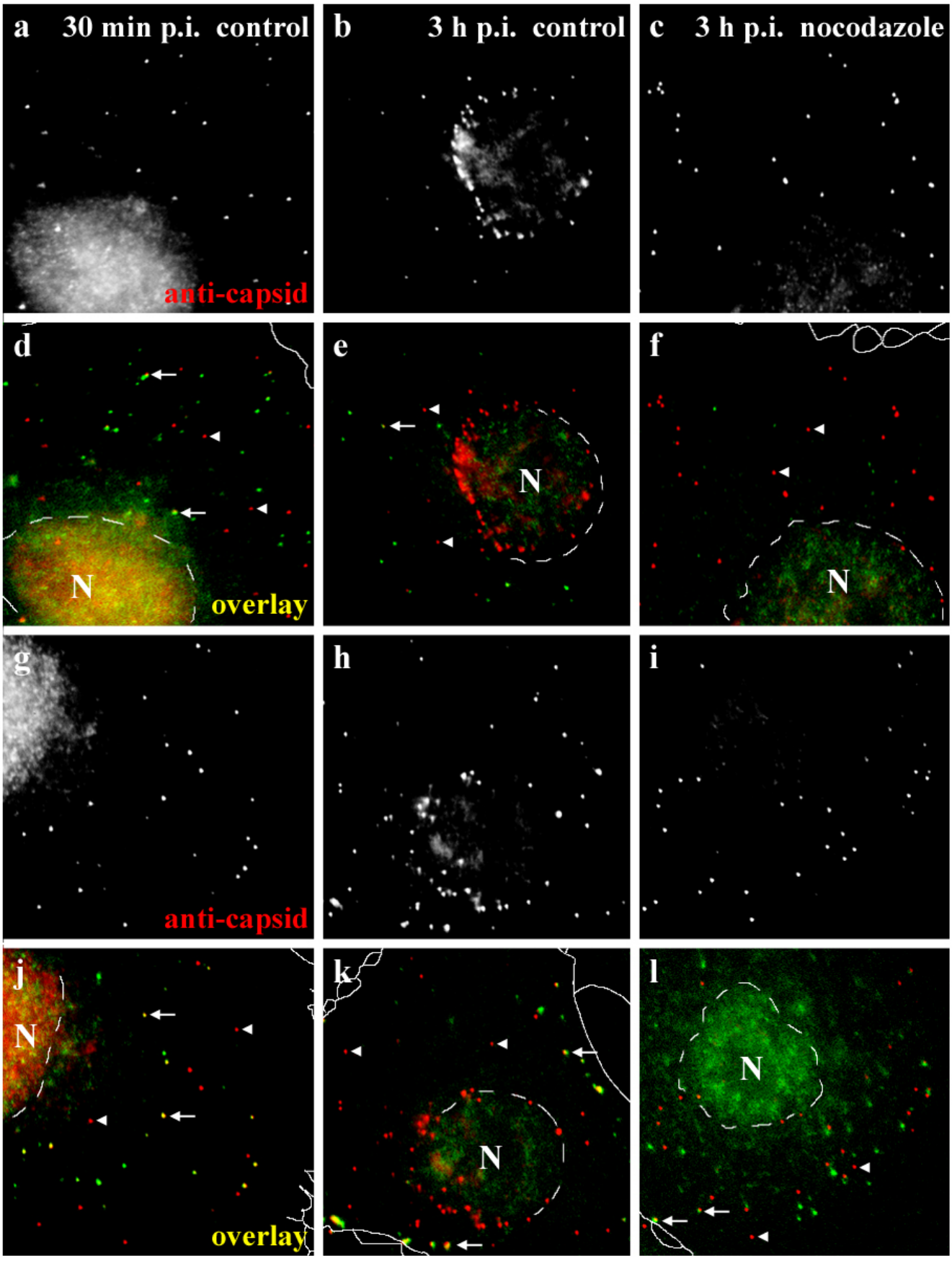

Döhner et al. (2005); Figure 6
Subcellular localization of capsids and viral membrane proteins during the early phase of HSV1-wt (a-f) and HSV1-ΔVP26 (g-l) infection.

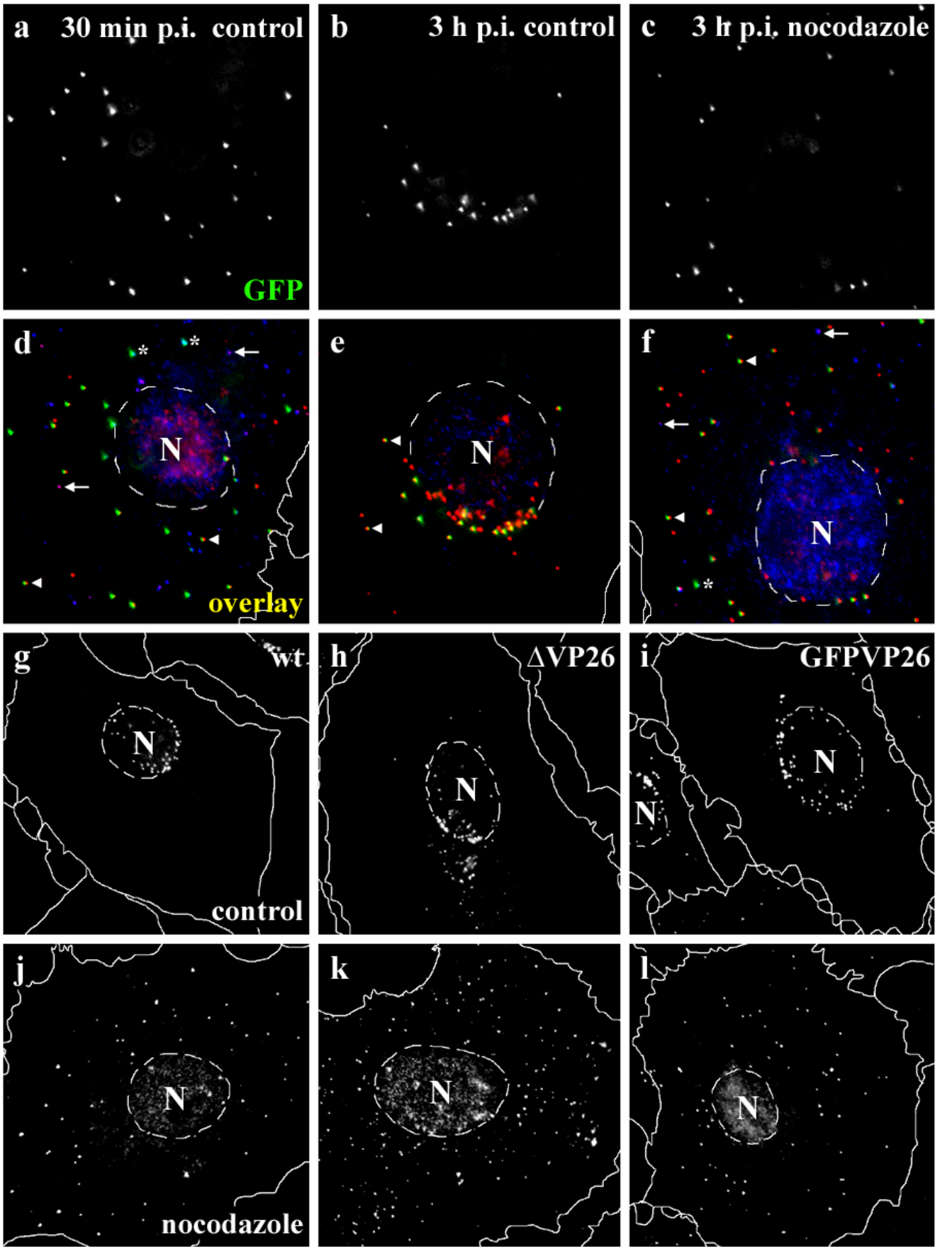

Döhner et al. (2005); Figure 7
Efficient nuclear targeting of HSV1-GFPVP26 required MT (a-f).
MT mediated efficient nuclear targeting of HSV1-wt, HSV1-ΔVP26, and HSV1-GFPVP26 in Vero cells (g-l).

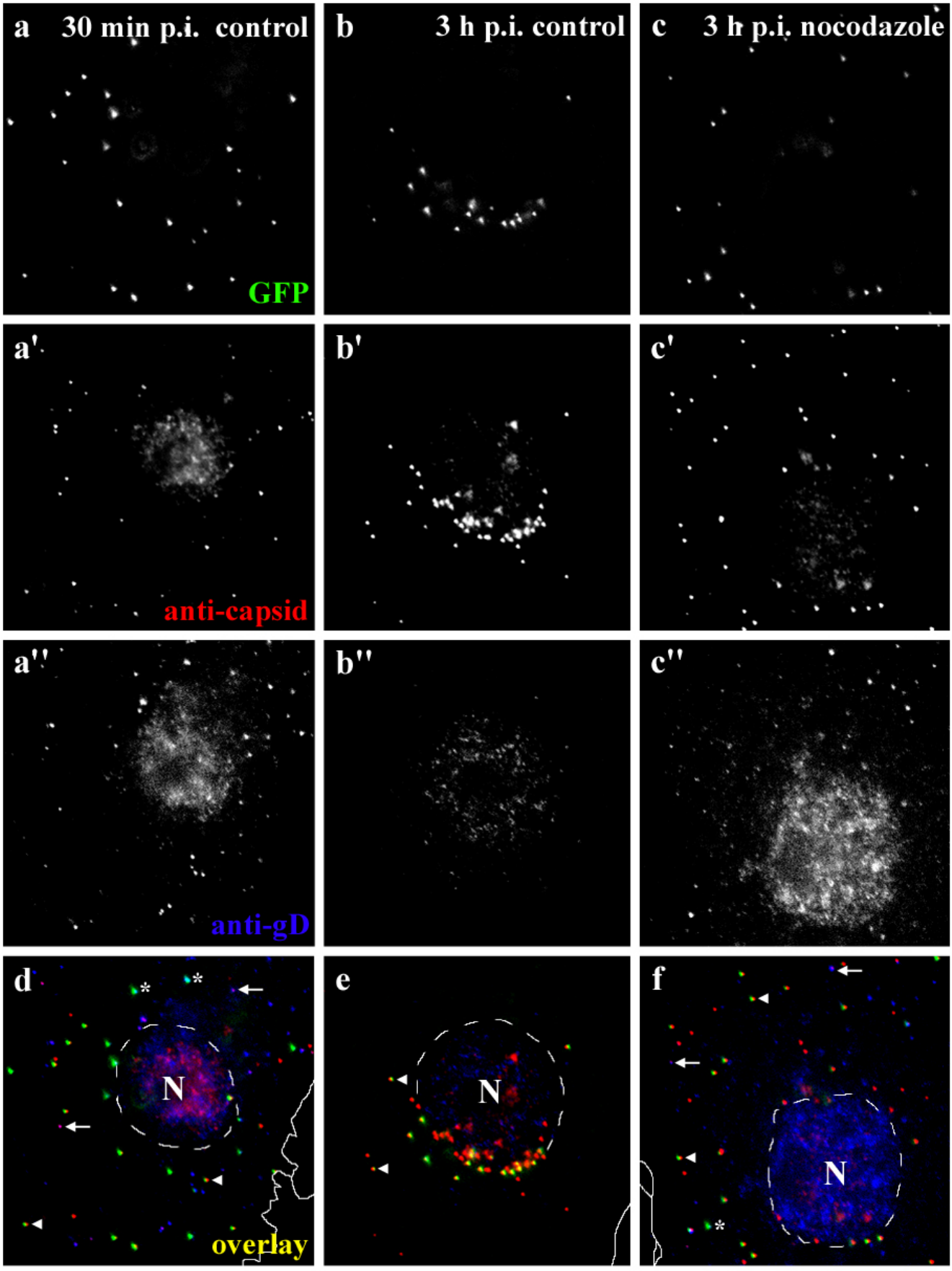

Döhner et al. (2005)
Detailed Figure 7 for reviewer's information: corresponds to Figure 7, a-f
Efficient nuclear targeting of HSV1-GFPVP26 capsids required MT.

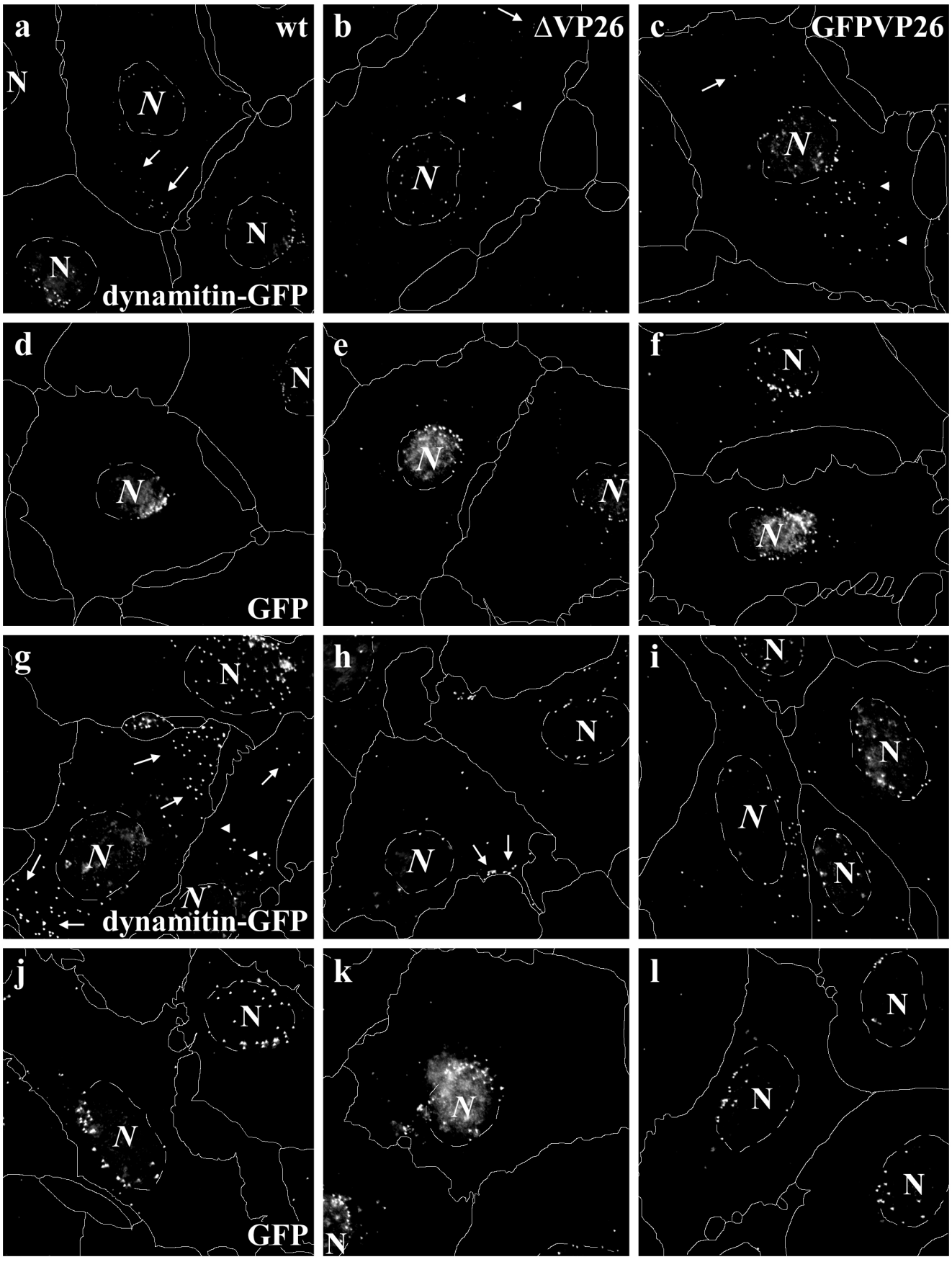

Döhner et al. (2005); Figure 8
Dynamitin overexpression reduced nuclear targeting in the presence and absence of VP26 in PtK_2 (a-f) and Vero cells (g-l).

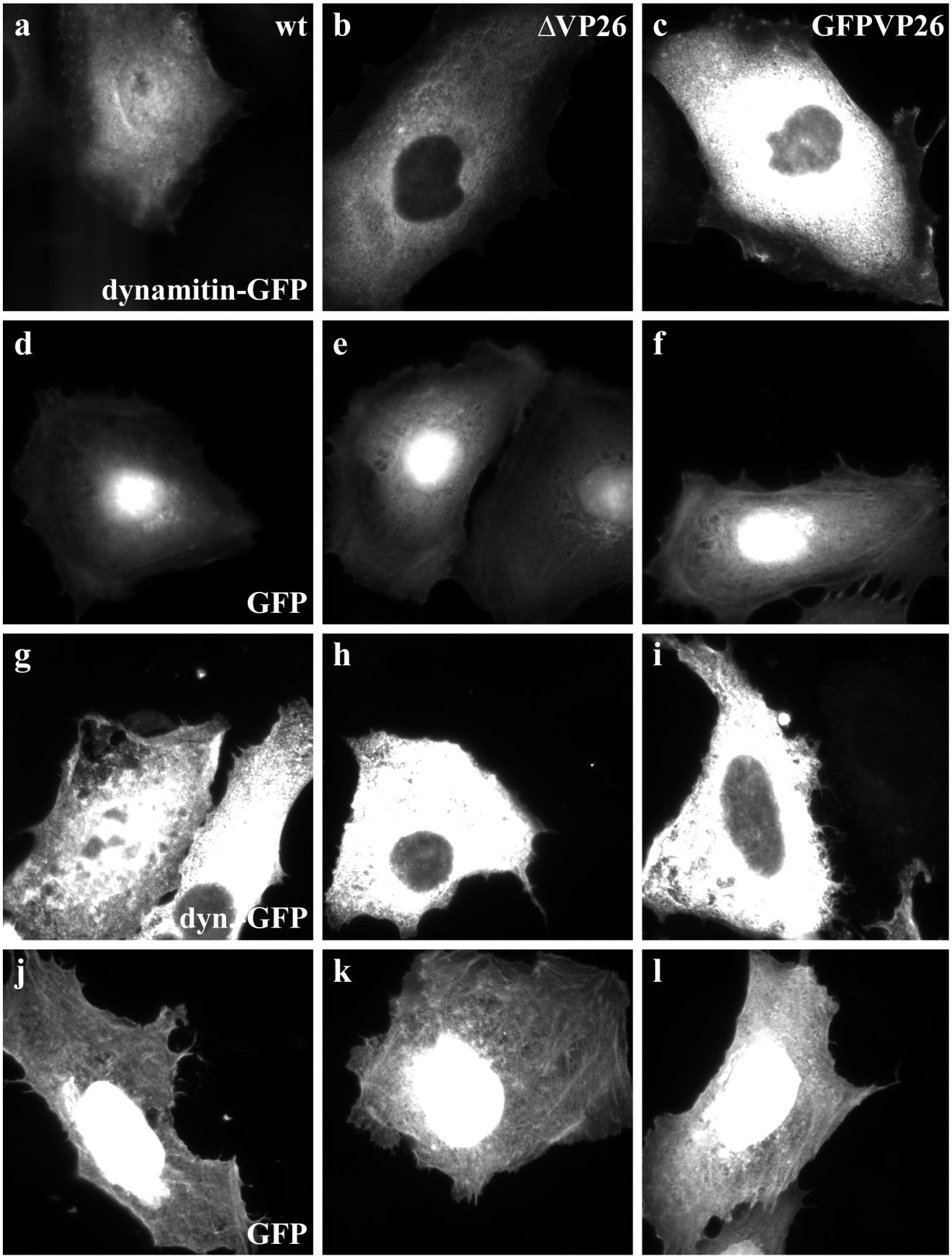

Döhner et al. (2005); additional information to Figure 8 for reviewer's information (c.f. Figure 8)

GFP fluorescence of dynamitin-GFP (a-c; g-i) or GFP (d-f; j-l) expressing PtK_2 (a-f) or Vero cells (g-l) infected with HSV1-wt (left), HSV1-ΔVP26 (middle) or HSV1-GFPVP26 (right).

Döhner & Sodeik (2004)
The Role of the Cytoskeleton During ViraI Infection
in Membrane Trafficking in Viral Replication, Editor: Mark Marsh
Current Topics in Microbiology and Immunology; Volume 285, p. 67-108

The Role of the Cytoskeleton During Viral Infection

Katinka Döhner and B. Sodeik*

Department of Virology, OE 5230, Hannover Medical School, Hannover
Carl-Neuberg-Str. 1, 30625 Hannover, Germany

*Corresponding author, email: Sodeik.Beate@mh-hannover.de

Abstract Upon infection, virions or subviral nucleoprotein complexes are transported from the cell surface to the site of viral transcription and replication. During viral egress, particles containing viral proteins and nucleic acids again move from the site of their synthesis to that of virus assembly and further to the plasma membrane. Because free diffusion of molecules larger than 500 kDa is restricted in the cytoplasm, viruses as well as cellular organelles employ active, energy-consuming enzymes for directed transport. This is particularly evident in the case of neurotropic viruses that travel long distances in the axon during retrograde or anterograde transport. Viruses use two strategies for intracellular transport: Viral components either hijack the cytoplasmic membrane traffic or they interact directly with the cytoskeletal transport machinery. In this review we describe how viruses—particularly members of the *Herpesviridae*, *Adenoviridae*, *Parvoviridae*, *Poxviridae*, and *Baculoviridae*—make use of the microtubule and the actin cytoskeleton. Analysing the underlying principles of viral cytosolic transport will be helpful in the design of viral vectors to be used in research as well as human gene therapy, and in the identification of new antiviral target molecules.

1 Introduction

As obligate intracellular parasites, viruses use and manipulate the cell's machinery for membrane trafficking, transcription, splicing, nuclear pore transport and protein synthesis. In fact, these cellular processes were elucidated to a large extent by studying viral systems. Here, we discuss the molecular interactions of viruses with the host cytoskeleton and the mechanisms of viral cytoplasmic transport.

Any viral life cycle can be divided into the following phases: (1) adsorption to the cell, (2) penetration of the plasma or endosome membrane, (3) genome uncoating and release from a viral nucleoprotein complex or capsid, (4) early viral protein synthesis, (5) genome replication, (6) late viral protein synthesis, (7) virus assembly/maturation and finally (8) viral release or egress. We define phases (1)–(3), up to the stage at which the viral genome has been unpacked for transcription and replication, collectively as "viral cell entry".

Virions, subviral particles or nucleoprotein complexes are transported during cell entry from the cell surface to the site of viral transcription and replication, as well as from the site of synthesis to that of virus assembly and back to the plasma membrane for virus egress (for recent reviews see Cudmore et al. 1997; Sodeik 2000; Ploubidou and Way 2001; Smith and Enquist 2002). Because free diffusion of molecules larger than 500 kDa is restricted in the cytoplasm compared to dilute solutions, viruses as well as cellular organelles and chromosomes depend on active

Table 1. Viruses that use the cytoskeleton

Virus family Examples	Genome	Morphology Diameter	Cytosolic structure	Mode of entry	Site of replication
Rhabdoviridae Rabies virus Mokola virus	ss (−) RNA ~12 kb	Envelope 75×180 nm^2	Internal ribo-nucleoprotein core	Endocytosis Fusion with endosomal membrane	Cytosol
Picornaviridae Poliovirus	ss (+) RNA ~ 8 kb	No envelope 30 nm	Genome	Fusion pore at plasma or endosomal membrane	Cytosol, on small vesicles
Herpesviridae HSV1 PRV	dsDNA 120–230 kb	Envelope 150–200 nm	Icosahedral capsid	Fusion at plasma membrane	Nucleus
Retroviridae HIV-1	ss (+) RNA dimer 2×7–13 kb	Envelope 80–130 nm	Internal nucleocapsid, reverse transcription complex	Fusion at plasma membrane, endocytosis possible	Cytosolic reverse transcription, nuclear transcription
Adenoviridae Ad2, Ad5	dsDNA 36–38 kb	No envelope 70–100 nm	Icosahedral capsid	Endocytosis, lysis	Nucleus
Parvoviridae CPV AAV	ssDNA (+) or (−) 5 kb	No envelope 18–26 nm	Icosahedral capsid ???	Endocytosis, fusion pore?	Nucleus
Poxviridae Vaccinia virus	dsDNA 130–300 kb	Envelope 2 infectious forms: IMV 200×300 nm^2	Complex cores, IMV, IEV	Unclear, different for IMV or EEV	Perinuclear viral factories
Baculoviridae AcMNPV	dsDNA 90–160 kb	Envelope 30–60×300 nm^2	Rod-shaped nucleocapsid	Endocytosis, membrane fusion	Nucleus

ds, double stranded; ss, single stranded

mechanisms for directed transport (Luby-Phelps 2000). This is particularly evident in the case of neurotropic viruses that travel long distances in the axon during retrograde or anterograde transport (Smith and Enquist 2002). For example, it would take a herpes virus capsid 231 years to diffuse 10 mm in the axonal cytoplasm (Sodeik 2000).

Viruses use two alternative strategies for intracellular transport. One is to hijack cytoplasmic membrane traffic. During cell entry many viruses pass through the endocytic pathway to the cell centre (see the chapter by Sieczkarski and Whittaker, this volume). After budding, virions travel inside vesicles derived from the endoplasmic reticulum and the Golgi apparatus to the plasma membrane for viral egress (see the chapter by Maggioni and Braakman, this volume). Alternatively, viral components interact directly with the cytoskeletal transport machinery. It is helpful to distinguish between cytoplasmic and cytosolic transport. The first is a general term referring to both transport inside a membrane and cytosolic transport. The latter involves direct interactions between cytosolic viral components and the cytoskeleton (Sodeik 2000).

We begin with an overview of the organisation and function of the cytoskeleton and then discuss selected viruses whose cytoplasmic transport is either well characterised in molecular terms, such as herpesvirus and adenovirus, or mechanistically unique, as for vaccinia virus and baculovirus (Table 1).

2 The Cytoskeleton

The host cytoskeleton forms a three-dimensional network which is regulated by many accessory proteins and defines the cell's shape as well as its internal organisation. It mediates physical robustness, cell–cell contact, cell crawling, cell division, organelle or RNA transport during interphase and chromosome movement during mitosis or meiosis. Cytoskeletal filaments are assembled by non-covalent binding from protein subunits: Monomeric actin polymerises into microfilaments with a diameter of 5–6 nm, dimeric tubulin assembles hollow tubes of 25 nm and proteins such as keratin or vimentin form 10-nm intermediate filaments.

2.1 Intermediate Filaments

The intermediate filament proteins show a characteristic tripartite domain organization. N- and C-terminal globular head and tail domains of varying size and sequence flank a centrally located rod domain which mediates lateral interactions during assembly (Coulombe et al. 2001). The rope-like intermediate filaments span the entire cytosol and provide mechanical strength against shear forces.

Intermediate filaments do not seem to play any role in intracellular transport because they have no polarity and no motor proteins have been identified which use them as tracks.

During the late phase of many viral infections, intermediate filaments are rearranged or disassembled by viral proteases (Chen et al. 1993; Ferreira et al. 1994; Luftig and Lupo 1994; Brunet et al. 2000). If the intermediate filaments are disassembled, microinjected beads can diffuse more freely (Luby-Phelps 2000). One could assume that the same holds true for viral particles, and that viral modification of the intermediate filaments facilitates egress.

The formation of aggresomes also leads to the reorganisation of intermediate filaments into a perinuclear cage in a cellular attempt to sequester misfolded and unassembled protein subunits (Garcia-Mata et al. 1999; Kopito 2000). African Swine Fever virus might actually exploit this pathway in order to concentrate viral structural proteins for assembly in a viral factory (Heath et al. 2001).

2.2 Actin Filaments

The most abundant protein of many cells, actin, exists in monomeric form as globular actin or G-actin and in filamentous form called F-actin or microfilaments. Polymerisation proceeds by the reversible endwise addition of actin subunits that stimulates hydrolysis of bound ATP. Each filament is polarised, and its ends have distinct biochemical properties. The fast-growing end is called the barbed or plus-end, and the slow-growing end the pointed or minus-end (Welch and Mullins 2002). In cells, polymerisation occurs primarily at the plus-end and must be tightly regulated, because the turnover of actin subunits in vivo is 100–200 times faster than with pure actin (Zigmond 1993).

Actin filaments are flexible structures which are organised into a variety of linear bundles and arrays, two-dimensional networks or three-

dimensional gels. Numerous G- and F-actin binding proteins regulate the monomer pool, the formation of filaments and higher-order networks as well as filament depolymerisation for monomer recycling. For example, binding of the Arp2/3 complex to the lateral side of actin filaments leads to a dendritic pattern of actin filament nucleation (Welch and Mullins 2002).

Besides actin filaments dispersed throughout the entire cell, all cells contain a cortical network of actin filaments, generally oriented with their plus-ends facing towards the plasma membrane. This actin cortex is the key player in various cell motility processes which are based on filament assembly and the action of myosins (Welch and Mullins 2002; Kieke and Titus 2003).

However, the actin cortex beneath the plasma membrane can also be an obstacle for virus entry or budding (Marsh and Bron 1997). This may be the reason why many viruses enter cells via endosomes which easily traverse the actin cortex (see the chapter by Sieczkarski and Whittaker, this volume). Certain viruses might even fuse with either the plasma membrane or an endosome depending on the cell type they are infecting (Miller and Hutt-Fletcher 1992; Nicola et al. 2003).

The cortical actin might also be a barrier for virus assembly at the plasma membrane. The cortical actin might be locally depolymerised, or the force of actin polymerisation could be used to drive the budding process (Cudmore et al. 1997; Garoff et al. 1998). Recent evidence suggests that a shell of cortical actin also surrounds many membrane organelles. Thus viruses could pick up actin and actin-binding proteins during budding as has been shown for human immunodeficiency virus (HIV) (Ott et al. 1996; Liu et al. 1999; Wilk et al. 1999).

Regulated binding to cytosolic actin filaments can control the subcellular localisation of a protein; an example is the nucleoprotein of influenza virus (Digard et al. 1999). Despite many reports on nuclear actin only recent evidence supports a role of nuclear actin in chromatin remodelling, splicing, nuclear import and export (reviewed in Rando et al. 2000; Pederson and Aebi 2002). Many viruses use actin during replication, but with the exception of nucleocapsid assembly of some baculoviruses (Kasman and Volkman 2000) and the export of unspliced genomic HIV-1 RNAs (Kimura et al. 2000; Hofmann et al. 2001), these activities all occur within the cytoplasm.

2.3 Microtubules

Microtubules (MTs) are long, hollow cylinders assembled from heterodimers of α- and β-tubulin and MT-associated proteins (MAPs). The head-to-tail association of tubulin into 13 protofilaments leads to the formation of MTs, which are further stabilised by lateral interactions between adjacent protofilaments. MTs are, like actin filaments, polar structures with a dynamic fast-growing plus-end and a less dynamic minus-end (Desai and Mitchison 1997; Downing 2000). The overall subcellular MT organisation is highly polarised. MT dynamics vary considerably between different regions of a cell, during the cell cycle and throughout differentiation. Thus MT turnover is tightly controlled in space and over time.

The plus-ends of MTs are the primary sites of MT growth and shortening, resulting in a phenomenon called dynamic instability (Mitchison and Kirschner 1984). After subunit addition at the end, the GTP bound to β-tubulin is slowly hydrolysed. The consecutive loss of this GTP-tubulin cap leads to catastrophic MT depolymerisation. GTP-tubulin is more likely to be added to a GTP-tubulin cap than to a MT rapidly depolymerising. Plus-end binding proteins such as CLIP-170, EB1 or APC stabilise a region of about 1 μm at the plus-end of MTs and thus enable them to interact with the plasma membrane, organelles or the kinetochores of chromosomes. This search-and-capture mechanism prevents depolymerisation, and the MT stabilisation can even reorient the MTOC and thus the entire MT network (Howard and Hyman 2003).

In most animal cells, minus-ends are attached to a MT-organising centre (MTOC) called a centrosome and typically located close to the cell nucleus whereas the plus-ends are pointing towards the cell periphery and plasma membrane. However, several cell types contain a substantial number of non-centrosomal MTs (Keating and Borisy 1999). Even at steady state—when a population of MTs has reached constant mass—individual MTs may be polymerising or depolymerising, and such dynamics modulate intracellular transport (Keating and Borisy 1999; Giannakakou et al. 2002). Polarised epithelial cells are characterised by an apical and a basal MT web and longitudinally arranged MTs which point with their minus-ends to the apical and with their plus-ends to the basal membrane (Topp et al. 1996). Neuronal MTs in axons are also longitudinally arranged with their minus-ends pointing to the soma and their plus-ends to the axon terminal, whereas most dendrites have MTs of mixed polarity (Goldstein and Yang 2000; Hirokawa and Takemura 2003).

Many MAPs such as tau contain a basic domain which interacts with MTs via the acidic C-terminal domains of tubulin which are exposed on the MT surface (Downing 2000). Also, viral proteins with a basic domain such as many RNA- or DNA-binding proteins have the potential to interact with the MT surface (Elliott and O'Hare 1997; Ploubidou et al. 2000; Mallardo et al. 2001).

MTs are involved in long-distance transport as highlighted by the transport requirements through neuronal dendrites and axons. Moreover, the reversible association to MTs and motors regulates the subcellular localisation of important signalling proteins and transcription factors (Ziegelbauer et al. 2001; Giannakakou et al. 2002; Schnapp 2003).

3 Molecular Motors

Many proteins interact with tubulin and actin to regulate their structural organisation. A subset of those, the motor proteins, use conformational changes powered by ATP hydrolysis to transport cargo along the filaments. If motors are fixed on a surface such as a membrane, they move the filaments relative to that surface. If instead the filament is fixed, motors transport cargo along that filament.

Myosins mediate translocation along actin filaments, whereas dynein and kinesins move on MTs. It has been suggested that in animal cells long-range transport occurs along MTs and short-range transport along actin filaments (reviewed in Brown 1999; Verhey 2003). A viral particle could be transported either by directly recruiting a motor or by attaching to a cargo of a given motor. Moreover, polymerising actin filaments can push around different cargo such as endocytic vesicles, intracellular bacteria or vaccinia virus (Frischknecht and Way 2001).

3.1 Myosins

All myosins share a common N-terminal motor domain of about 500 amino acids that binds to actin filaments (www.mrc-lmb.cam.ac.uk/myosin/myosin.html). A flexible neck region connects the motor domain to a tail region of variable size which determines the specific function of each myosin and the specificity of cargo binding. Myosins have been grouped into 18 classes according to homologous sequences in the tail domain (Kieke and Titus 2003).

Most myosins walk towards the plus-ends of actin filaments, with the exception of myosin VI and possibly myosin IXb, which are minus-end-directed motors (Kieke and Titus 2003). The myosin IIs are often called 'conventional' myosins and include the best-studied example of skeletal muscle myosin. Cytoplasmic myosin II consists of two heavy chains and two pairs of light chains. Myosin II generates contractile forces during cytokinesis, maintains cortical tension and is crucial for cell motility. Myosin I, V and VI are involved in membrane traffic; moreover, myosin I plays a role in cell motility and signal transduction (Kieke and Titus 2003).

3.2 Kinesins

Kinesins transport membranes, cytoskeletal filaments, viral particles, mRNAs and proteins along MTs and are engaged in organising the mitotic spindle as well as chromosome translocation (Hirokawa and Takemura 2003). The defining criterion for a kinesin is a MT-binding motor domain of 320 amino acids, which is folded into a core with an overall structure similar to myosins and G proteins (Schliwa and Woehlke 2003; www.proweb.org/kinesin//index.html). The motor domain is linked to structural and regulatory domains, which attach to other cofactors, adaptor proteins or interaction modules (Karcher et al. 2002; Schnapp 2003). The kinesins are sorted into three groups according to the position of the motor domain at the N-terminus, an internal position, or the C-terminus, hence the names Kin-N, Kin-I and Kin-C kinesins, and based on homology into 14 classes (Hirokawa and Takemura 2003).

N-type kinesins, which include conventional kinesin (kinesin-1, KIF5), move towards MT plus-ends. Kinesin-1 is a heterodimer of two heavy chains (KHC) that each contain a motor domain, an α-helical stalk responsible for dimerization and a C-terminal tail domain that binds two light chains (KLC). The KLCs can dock onto adaptors or cargo receptors and link kinesin to the cargo (Hirokawa and Takemura 2003). Kinesin-1 transports various cargos such as axonal vesicles, mitochondria, lysosomes, endocytic vesicles, tubulin oligomers, intermediate filament proteins or mRNA complexes (Hirokawa and Takemura 2003). Kinesin-1 is also responsible for the transport of vaccinia virus (VV) to the plasma membrane (Rietdorf et al. 2001).

The respective cargos of the N-type kinesins KIF1A and KIF1B are synaptic vesicles and mitochondria (Nangaku et al. 1994; Okada et al. 1995). The N-type heterotrimeric kinesin with the KIF3 heavy chains

mediates axonal transport of fodrin-containing vesicles, and in epithelial cells KIF3 interacts with APC, a MT plus-end binding protein (Takeda et al. 2000; Jimbo et al. 2002). Kin-C kinesins move towards the MT minus-ends (Hirokawa and Takemura 2003). Most C-type kinesins act during mitosis, but some are implicated in membrane transport in neuronal dendrites and polarised epithelial cells (Hanlon et al. 1997; Saito et al. 1997; Noda et al. 2001; Xu et al. 2002). Kin-I kinesins most likely do not work as motors but destabilise MTs (Desai et al. 1999; Hunter et al. 2003).

3.3 Cytoplasmic Dynein

Axonemal and cytoplasmic dyneins transport cargo towards MTs minus-ends. Axonemal dyneins provide the driving force for the beating movement of cilia and flagella (King 2003). Cytoplasmic dynein plays an essential role during mitosis and is responsible for the perinuclear localisation of several organelles around the MTOC as well as retrograde organelle transport in axons (Karki and Holzbaur 1999). Cytoplasmic dynein is also required for the transport of non-membranous cargo such as NuMA, aggresomes, viral capsids, neurofilaments and pericentrin particles (Merdes and Cleveland 1997; Garcia-Mata et al. 1999; Suomalainen et al. 1999; Shah et al. 2000; Sharp et al. 2000; Young et al. 2000; Döhner et al. 2002). It is even involved in the transport of mRNAs and proteins regulating transcription (Galigniana et al. 2001; Giannakakou et al. 2002; Tekotte and Davis 2002).

Cytoplasmic dynein is a 20 S protein complex in the shape of a Y and consists of two dynein heavy chains (DHCs; 530 kDa), two intermediate chains (DICs; 70–80 kDa), four light intermediate chains (DLICs; 50–60 kDa), and three families of light chains (DLCs, 7–14 kDa, see below; Karki and Holzbaur 1999; King 2003). DHCs are members of the AAA family of ATPases and mediate MT binding, ATP hydrolysis and force generation (King 2000). The DICs belong to the WD-repeat protein family and are located at the base of the dynein motor. DLICs, DICs and DLCs have been implicated in motor regulation and cargo binding (King 2003). The subunits differ in their subcellular localisation and tissue expression, suggesting that cytoplasmic dynein exists in many distinct isoforms with unique subunit composition (Nurminsky et al. 1998; Tai et al. 2001).

For most, if not all, minus-end-directed transport processes cytoplasmic dynein requires a cofactor called dynactin (Karki and Holzbaur

1999). Dynactin is another large 20 S protein complex consisting of 11 different subunits (Holleran et al. 1998; Eckley et al. 1999). The $p150^{Glued}$ subunit of dynactin binds directly to the DICs. Interestingly, dynactin was recently reported to also play a role in melanosome transport catalysed by heterotrimeric kinesin (Deacon et al. 2003).

3.3.1 Binding Partners of Dynein Light Chains

Many DLC binding partners have been identified in yeast two-hybrid screens, sometimes supported by GST-pull down or co-immunoprecipitation assays after transient overexpression of the proteins. However, it has often been difficult to confirm these interactions with endogenous proteins under physiological conditions, and to prove that they lead to the recruitment of a motor. Based on sequence homology, DLCs have been grouped into the LC7/Roadblock, LC8/PIN and Tctex families (King 2003).

Members of the LC7 family bind to DICs and play a role in intracellular transport and mitosis in *Drosophila* (Bowman et al. 1999; Susalka et al. 2002). A mammalian member, mLC7, interacts with transforming growth factor-β (Tang et al. 2002).

DLCs of the LC8/PIN family bind to neuronal nitric oxide synthase and are therefore also called PIN for 'protein inhibitor of nitric oxide synthase' (Jaffrey and Snyder 1996). Further interaction partners are IκBα, Bim of the Bcl-2 family, postsynaptic density-95/guanylate kinase domain-associated protein, nuclear respiratory factor, the erect wing gene product in *Drosophila*, swallow protein, DIC and, interestingly, the 3′-UTR of parathyroid hormone RNA (King 2003). LC8/PIN is also a subunit of the actin motor myosin V (Espindola et al. 2000). The interaction often involves a conserved K/R-XTQT or G-I/V-QVD sequence motif in the DLC binding partner (Lo et al. 2001; Rodriguez-Crespo et al. 2001; Martinez-Moreno et al. 2003).

LC8/PIN also interacts with the phosphoprotein of rabies and Mokola virus (Raux et al. 2000; Jacob et al. 2000). Rabies virus spreads via neurons and travels long distances from the site of entry to the neuronal cell body. Axonal transport of rabies virus requires intact MTs, but it is unclear whether vesicles containing virions or cytosolic capsids are transported (Ceccaldi et al. 1989; Tsiang et al. 1991). Rabies viruses deleted for the LC8 binding motif no longer incorporate LC8, but pathogenesis is only impaired in already attenuated strains, and only in very young mice (Mebatsion 2001; Poisson et al. 2001). LC8/PIN also binds to p54 of

African swine fever virus, whose infection is inhibited if dynein is blocked (Alonso et al. 2001; Heath et al. 2001). Yeast two-hybrid screens revealed an interaction between HIV integrase and DYN2, a putative LC8-like yeast dynein light chain of 92 amino acids (Richard de Soultrait et al. 2002). Several additional potential viral interaction partners for LC8/PIN such as HSV1 helicase, adenovirus protease, vaccinia virus (VV) polymerase and, surprisingly, the extracellular domain of respiratory syncytial virus attachment protein have been identified by screening libraries of overlapping dodecapeptides in ligand blots (Martinez-Moreno et al. 2003).

DLCs of the Tctex class bind to Doc2, $p59^{fyn}$ kinase, rhodopsin, FIP1, Trk receptors, DIC, the cytosolic tail of CD5 and CD155, often via the binding motif K/R-K/R-XX-K/R (King 2003). CD155 is the receptor for poliovirus that invades the CNS by haematogenous or neural spread (Mueller et al. 2002). After binding to the receptor the poliovirus genome is released into the cytosol through a membrane pore. It is unclear whether pore formation occurs already at the plasma membrane or after delivery to an endosome (Hogle 2002). If axonal transport occurs inside an endocytic membrane, the binding of CD155 to Tctex-1 and thus possibly dynein could mediate retrograde transport of virus-containing vesicles to the cell body of the motor neuron (Mueller et al. 2002).

4
Experimental Approaches

4.1
The Tool Kit

There are several reversible pharmacological drugs that target cytoskeletal proteins. The response of different cell types to these drugs varies greatly, and therefore each inhibitor is tested initially with different concentrations and incubation times (Jordan and Wilson 1999).

Cytochalasin and latrunculin depolymerise actin filaments, whereas jasplakinolide promotes actin polymerisation (Cooper 1987; Bubb et al. 1994; Ayscough 1998). Colchicine, colcemide, vincristine, vinblastine and nocodazole (podophyllotoxin) depolymerise MTs, whereas taxol (paclitaxel) stabilises the MT network (Jordan and Wilson 1999). Because all these are not competitive inhibitors but interfere with the dynamic equilibrium between subunits and filaments, the cells need to be treated for quite some time, until an effect on the steady-state distribu-

tion of the cytoskeleton is manifested (Cooper 1987; Jordan and Wilson 1999).

Butanedione monoxime (BDM) inhibits ATP hydrolysis of myosin II, V, VI and possibly I (Herrmann et al. 1992; Cramer and Mitchison 1995). However, higher concentrations may also target other ATPases (Schlichter et al. 1992; Mojon et al. 1993; Phillips and Altschuld 1996). KT5926, wortmannin and ML-7 block the activity of myosin light chain kinase, and thus the only known downstream target, the non-muscle myosin II (Nakanishi et al. 1990; Nakanishi et al. 1992; Ruchhoeft and Harris 1997). Adociasulfate blocks kinesins (Sakowicz et al. 1998), and dyneins are inhibited by erythro-9-[3-(2-hydroxynonyl)]adenine that also affects adenosine deaminase and cGMP-stimulated phosphodiesterase (Penningroth 1986; Mery et al. 1995).

Microinjecting function-blocking antibodies, adding anti-sense or small interfering RNAs or overexpressing a dominant-negative protein can inhibit many motors. For example, excess dynamitin blocks dynactin and overexpression of the cargo-binding domain of KLC inhibits conventional kinesin (Echeverri et al. 1996; Burkhardt et al. 1997; Valetti et al. 1999; Rietdorf et al. 2001).

Testing many inhibitors aiming at alternative targets by different molecular mechanisms provides a guide for analysing the role of the cytoskeleton in virus infection. To determine which viral proteins are involved in cytoplasmic transport, viral mutants with defined genotypes have been generated.

4.2 Video Microscopy

Intracellular movement of host and viral particles is best analysed by video or digital time-lapse microscopy (Lippincott-Schwartz et al. 2000; Zhang et al. 2002). This technique adds another dimension to the analysis of fixed cells, because not only the steady-state distribution of viral components but also the dynamics of their transport is analysed. Because of their small size and limited contrast, viral particles with the exception of vaccinia virus need to be tagged with a fluorescent molecule for tracking in live cells.

Direct chemical coupling to small fluorescent dyes was used to analyse cytoplasmic transport of non-enveloped viruses (Georgi et al. 1990; Leopold et al. 1998; Suomalainen et al. 1999). Because many viruses undergo substantial disassembly steps during entry (Greber et al. 1993),

one needs to identify the protein to which the dye has been attached and, if possible, analyse trafficking of differently tagged viral structures.

To analyse the infection of enveloped viruses, the fluorescent tag must be linked to a structure which after membrane fusion remains associated with the genome during its cytosolic passage. Green fluorescent protein (GFP)-tagged capsid or core proteins have been used to track pseudorabies virus and HIV (Smith et al. 2001; McDonald et al. 2002). Because all viral particles can be taken up by endocytosis, even if that is not their physiological entry port (see the chapter by Sieczkarski and Whittaker, this volume), experiments using fluorescently labelled virions require care to distinguish cytosolic particles from those in endosomes (Suomalainen et al. 1999; McDonald et al. 2002; Sodeik 2002). Likewise, when analysing viral egress, one needs to distinguish GFP-tagged virions from GFP-fusion protein in the biosynthetic pathway or in the cytosol (Rietdorf et al. 2001). The recent improvements in the design of fluorescent proteins allow dual-colour imaging of different viral particles in live cells (Zhang et al. 2002).

Attaching multiple fluorescent molecules to a virus or subviral particle could alter virus assembly and subsequently virus entry. Fluorescent dyes are usually quite hydrophobic, and GFP is a protein of 27 kDa resulting in a rather large mutation of any viral protein. Therefore, it is crucial to test with several assays that a GFP-tagged virus behaves similarly to the unlabelled virus. Among the physiological cargo of dynein are aggregated protein complexes that are packed into aggresomes at the MTOC (Garcia-Mata et al. 1999; Kopito 2000). Thus the cells might send many non-functional viral proteins along MTs to the MTOC for refolding or final degradation (Sodeik 2002).

Many of these issues can now be overcome by single-molecule imaging techniques (Seisenberger et al. 2001). However, they require specialised equipment to visualise the emission with a low signal-to-noise ratio. Most results so far have been obtained with a high ratio of dye to particle. With the use of fluorescent proteins with improved excitation and emission spectra and digital cameras with increasing sensitivity, movies of viral cytoplasmic transport at physiological conditions can now be recorded.

4.3
Virological Assays, Cytoskeletal Cooperation, and Viral Modifications

Besides suitable tools to analyse the cytoskeleton, many experiments have been developed to study individual phases of a viral life cycle. In

addition to blocking cytoplasmic transport, the inhibitors used could also influence viral infection in other ways.

For example, because a cell's membrane traffic relies heavily on actin and MT transport, important host factors, such as viral receptors, could mis-localise, thus resulting in a reduced or increased virus binding, internalisation or other changes in the viral life cycle (Döhner et al. 2002). If the readout for cytoplasmic transport during virus entry is nuclear viral gene expression, a potential role of nuclear actin or myosin in viral transcription should be considered (Pederson and Aebi 2002). The host cytoskeleton can also directly influence viral transcription as shown for paramyxoviruses or reverse transcription and viral budding as in the case of HIV (Sasaki et al. 1995; Bukrinskaya et al. 1998; Gupta et al. 1998).

Moreover, the three types of cytoskeletal filaments are interdependent entities which operate together in cells (Fuchs and Yang 1999; Goode et al. 2000). The last years have shown a close interaction between MT plus-ends and the actin cortex, and several proteins provide physical links between different filament types (Coulombe et al. 2000; Allan and Näthke 2001; Leung et al. 2002). Thus a prolonged incubation with any of the inhibitors could lead to pleiotropic effects. For example, targeting MTs with depolymerising drugs or with antibodies to stable MTs also results in the collapse of intermediate filaments to a perinuclear region (Gurland and Gundersen 1995).

Many cells contract, and in the extreme case completely round up, if actin filaments are disassembled, because their substrate adhesion via focal contacts is weakened (Ayscough 1998). This reduces the transport distances, for example from the plasma membrane to the nucleus, and cargo could reach a particular binding site such as the nuclear pore in the absence of the appropriate filament system by diffusion rather than by active transport as under physiological conditions. Moreover, although cytoskeletal filaments provide tracks for cytoplasmic viral transport, they also restrict the space that is open for translocation (Luby-Phelps 2000). Thus depolymerising cytoskeletal filaments removes both transport trails and steric barriers.

For these reasons, it is sometimes difficult to determine the precise functional role of the cytoskeleton during virus infection. In addition, late in infection the cytoskeletal filaments are often rearranged, complicating the analysis of their role during assembly and egress (Avitabile et al. 1995; Brunet et al. 2000; Dreschers et al. 2001). However, by taking these caveats and limitations into consideration, we have learnt an amazing amount about the molecular cross-talk between viruses and the host cytoskeleton.

5
Neurotropic Herpesvirus and Cytoplasmic Transport

5.1
Microtubule Transport During Entry

Neurotropic viruses are dependent on efficient transport because they travel long distances during pathogenesis. Prominent examples are the alphaherpesviruses such as human herpes simplex virus (HSV). After initial replication in exposed mucosal epithelia, progeny virions enter local nerve endings of peripheral neurons and the capsid without the envelope is retrogradely transported to the nucleus located in a peripheral nerve ganglion. Here, HSV1 establishes a latent infection that on stress can be reactivated to a lytic infection of the neuron. Newly synthesised virus is then released from the nerve endings and re-infects the peripheral epithelial tissue (Roizman and Knipe 2001; Smith and Enquist 2002). MTs are required in epithelial and neuronal cells as well as during entry and egress (Kristensson et al. 1986; Topp et al. 1994, 1996; Avitabile et al. 1995; Sodeik et al. 1997; Miranda-Saksena et al. 2000; Kotsakis et al. 2001; Mabit et al. 2002).

The fusion of the HSV1 envelope with the plasma membrane releases into the cytosol a capsid and about 20 different proteins of the tegument, a protein layer encasing the capsid. The capsid, associated with a subset of tegument proteins, is transported along MTs to the MTOC, localised in the cell centre, and further to the nucleus (Kristensson et al. 1986; Lycke et al. 1988; Sodeik et al. 1997; Mabit et al. 2002). The docking of the capsid at the nuclear pore induces the translocation of the viral genome into the nucleoplasm (Ojala et al. 2000), where viral replication, transcription and later during infection capsid assembly take place (Fig. 1A).

Incoming HSV1 capsids co-localise with cytoplasmic dynein and dynactin in epithelial cells (Sodeik et al. 1997; Döhner et al. 2002). Electron micrographs of detergent-extracted, infected cells reveal structures resembling the Y-shaped cytoplasmic dynein at the capsid vertices (Sodeik et al. 1997), where the tegument has a more ordered structure and the tegument protein VP1-3 might be located (Zhou et al. 1999). Moreover, inhibiting dynein function by the overexpression of dynamitin reduces transport of HSV1 capsids to the nucleus and early viral gene expression without having any effect on virus binding or internalisation (Döhner et al. 2002). Whether and how capsids move further from the MTOC to the nuclear pore complex is unclear (Sodeik 2002).

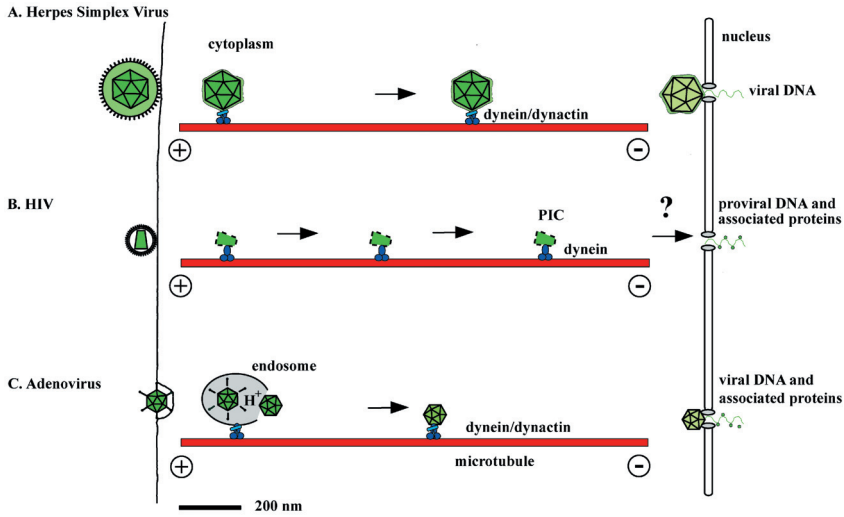

Fig. 1A–C. Cytosolic transport during virus entry. **A** After fusion of the envelope of herpes simplex virus type 1 (HSV1) with the plasma membrane, the capsid (*dark green*) and the tegument proteins (*green*) are released into the cytosol. The capsid with a subset of tegument proteins associated binds to microtubules (*red*) and is transported by dynein and dynactin (*blue*) to the MT-organising centre where the MT minus-ends are located. After capsid (*light green*) binding to the nuclear pore complex, the viral DNA is injected into the nucleoplasm. **B** Human immunodeficiency virus type-1 (HIV-1) enters cells by fusion with the plasma membrane. During passage through the cytosol, the viral RNA genome is reverse transcribed into DNA in a structure called reverse transcription complex or preintegration complex *(PIC*; *green*). This structure co-localises with microtubules (*red*) and requires dynein (*blue*) for its transport to the nucleus. The proviral DNA is imported into the nucleus and integrated into a host chromosome. **C** Adenovirus of the subgroup C is internalised by receptor-mediated endocytosis and induces lysis of the endosome (*grey*) to access the cytosol. The cytosolic capsid (*green*) binds to microtubules (*red*) and is transported by dynein and dynactin (*blue*) to the cell centre. During entry, the capsids are stepwise disassembled (indicated by the different shades of *green*). At the nuclear pores, the viral DNA and associated proteins are released from the capsid (*light green*) and imported into the nucleoplasm

In vivo analysis of the entry into epithelial cells by time-lapse digital fluorescence microscopy showed that GFP-tagged capsids moved along MTs towards *and* away from the nucleus with maximal speeds of 1.1 µm/s (Döhner, Büttner, Wolfstein, Schmidt and Sodeik, in preparation). Incoming pseudorabies virus, another alphaherpesvirus, moves at rates averaging 1.3 µm/s. The transport is saltatory and bi-directional,

but in neuronal processes with a retrograde bias towards the cell body (Smith and Enquist 2002).

Alphaherpesvirus capsids must possess a viral receptor either for dynein or for dynactin, which allows them to engage the host MT system for efficient transport from the plasma membrane to the host nucleus, a particularly long distance after infection of neurons via a synapse. In unpolarised epithelial cells capsids show minus- and plus-ended directed transport during entry, whereas in cultured neurons the retrograde transport towards the nucleus predominates.

5.2 Microtubule Transport During Egress

Herpesvirus capsids assemble in the nucleus and after genome packaging acquire a primary envelope by budding at the inner nuclear membrane. The traditional view was that from then on the virus particle remained within the secretory pathway and was released from infected cells by fusion of a vesicle containing the enveloped virion with the plasma membrane (reviewed in Roizman and Knipe 2001; Mettenleiter 2002). In this scenario, all tegument proteins were added to the capsids already in the nucleus, and cytoplasmic transport was mediated by the interaction of membrane vesicles, possibly modified by the addition of viral proteins, with the host cytoskeleton.

Several studies in the last decade suggested that many if not all herpesviruses use an alternative pathway. Accordingly, transiently enveloped viral particles leave the periplasmic space by fusion with the outer nuclear envelope or the membrane of the endoplasmic reticulum which is continuous with the nuclear envelope (Roizman and Knipe 2001; Mettenleiter 2002). By this procedure, capsids traverse the nuclear envelope and reach the cytosol. The naked cytosolic capsids can recruit tegument proteins and engage the host cytoskeleton to travel to the site of secondary envelopment. Newly synthesised HSV1 particles tagged with GFP-VP11/12 move along MTs over distances of up to 49 μm with average velocities of 2 μm/s (Willard 2002).

In unpolarised epithelial cells, secondary envelopment most likely occurs at the *trans*-Golgi network (TGN) or an endosome (Skepper et al. 2001; Mettenleiter 2002). In non-infected cultured cells, these organelles are clustered around the MTOC in close proximity to the nucleus. Thus, at least early during assembly, again dynein possibly assisted by dynactin could transport the capsids to the desired location. However, later during infection, the MTs are marginalised in bundles to the periphery

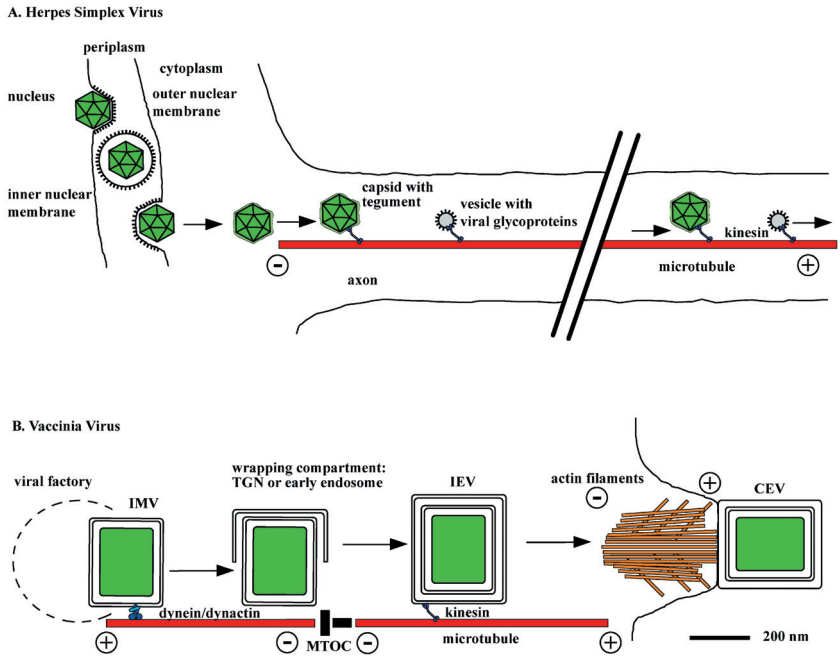

Fig. 2A, B. Cytosolic transport during virus egress. **A** After nuclear HSV1 capsid assembly and genome packaging, the capsid (*dark green*) acquires a primary envelope by budding at the inner nuclear membrane. This primary envelope is lost by subsequent fusion with the outer nuclear membrane, and the capsid is released into the cytosol. Most if not all tegument proteins (*light green*) are acquired in the cytosol or during the second envelopment. In neurons, capsids with associated tegument and membrane vesicles (*grey*) containing viral envelope proteins are transported along microtubules (*red*) to the presynapse. Axonal transport is mediated by conventional kinesin (*dark blue*). Presumably, secondary envelopment occurs in the nerve endings. **B** The intracellular mature form (IMV) of vaccinia virus containing the core (*green*) is assembled in viral factories located in the cytoplasm. The IMV is transported to the MTOC region along MTs by dynein (*blue*) and dynactin (light blue). At the MTOC, the IMV is enwrapped by a membrane cisterna derived from the *trans*-Golgi network or an early endosome, resulting in the formation of the intracellular enveloped virus (IEV). The IEV requires MTs and conventional kinesin (*dark blue*) for its transport to the plasma membrane. Shortly before or after fusion of the outer IEV membrane with the plasma membrane, polymerisation of actin filaments (*orange*) is induced. The cell-associated virus (CEV) is pushed on top of a long microvillus into the medium or a neighbouring cell

of the cytoplasm, and there is no longer an obvious MTOC (Avitabile et al. 1995; Elliott and O'Hare 1998, 1999; Kotsakis et al. 2001). The reorganisation of the MT network most likely also changes the steady-state distribution of the membrane organelles. The localisation of MT plus- or minus-ends has not been determined late in infection, and therefore it is difficult to predict which MT motors would then catalyse capsid transport to the organelle of secondary envelopment.

In a typical neuronal axon, the MT plus-ends are uniformly oriented towards the synapses and the minus-ends to the cell body (Goldstein and Yang 2000). There are no reasons to believe that this organisation is changed during a herpesvirus infection. Progeny virus spreads via the axons, and the traditional model predicted that axonal transport of fully assembled virions occurs inside vesicles. However almost 10 years ago Cunningham and collaborators demonstrated that in human primary sensory neurons HSV1 naked capsids were closely associated with axonal MTs (Penfold et al. 1994). This study suggested that in neurons the secondary envelopment might take place in the presynapse (Fig. 2A).

Immune labelling showed that the glycoproteins are transported in vesicles, separately and with different kinetics from the capsids (Holland et al. 1999; Miranda-Saksena et al. 2000; Ohara et al. 2000). In pseudorabies virus, the type II integral membrane protein US9 is required for targeting of all tested viral membrane proteins to the axon, but not for axonal transport of capsids and some tegument proteins (Tomishima and Enquist 2001). Immunoelectron microscopy showed that progeny axonal cytosolic capsids co-localise with conventional kinesin (Diefenbach et al. 2002). As during virus entry, GFP-tagged pseudorabies virus is transported in both directions in axons late in infection. But during egress the anterograde transport predominates. Average plus-end-directed velocities are 2 μm/s and minus-end directed velocities 1.3 μm/s (Smith et al. 2001).

Thus, during axonal transport, progeny capsids recruit a plus-end MT motor, most likely conventional kinesin. In epithelial cells a minus-end-directed MT motor could ensure, at least early during assembly, transport to the organelle of secondary envelopment.

5.3 Biochemical Analysis of Viral Capsid Transport

Several assays have been developed to characterise the host factors as well as the viral receptors involved in MT transport. GFP-labelled capsids were isolated after detergent extraction of purified virions (Bearer

et al. 2000; Wolfstein, Nagel, Döhner, Allan and Sodeik, in preparation). Bearer et al. (2000) injected such capsids into the giant axon of the squid *Loligo paelei*, a classic system to analyse fast MT-mediated transport. HSV1 capsids labelled with co-packaged VP16-GFP that had been expressed from a complementing cell line moved in a continuous fashion in retrograde direction with average velocities of 2.2 μm/s. This unidirectional, non-saltatory movement is different to the motility of GFP-tagged herpes particles after infection of vertebrate cells (Smith et al. 2001; Willard 2002; Döhner, Büttner, Wolfstein, Schmidt and Sodeik, in preparation).

Wolfstein et al. (in preparation) reconstituted capsid motility in vitro with Cy3-labeled MTs, VP26GFP-tagged capsids, an ATP-regenerating system and a cytosolic protein fraction. In vitro transport was also saltatory, with long continuous runs of more than 10 μm in one direction, and the capsids often changed MTs. In this assay capsid transport along MTs depended on their tegument composition. It could be inhibited by the addition of recombinant dynamitin, suggesting that the motility was catalysed by dynein or heterotrimeric kinesin (Wolfstein, Nagel, Döhner, Allan and Sodeik, in preparation). Such biochemical assays can now be used to characterise the molecular interactions between viral and host factors.

5.4 Interaction of Herpesvirus with Cytoskeletal Proteins

VP22, one of the major tegument proteins of HSV1, and GFP-VP22 colocalise with MTs after transfection, whereas in infected cells VP22 does not show a prominent enrichment on MTs (Elliott and O'Hare 1997, 1999; Kotsakis et al. 2001). The transient restructuring of the MT network during virus infection coincides with the translocation of VP22 from the cytoplasm to the nucleus (Kotsakis et al. 2001). Transient expression of VP22 or infection with HSV1 leads to a stabilisation and hyperacetylation of MTs (Elliott and O'Hare 1998, 1999). A basic VP22 fragment contains the MT binding domain (Martin et al. 2002).

In addition, VP22 interacts with non-muscle myosin II, and the myosin inhibitor BDM reduces virus yields (van Leeuwen et al. 2002). Because VP22 is released into the cytosol on HSV1 fusion with the plasma membrane, this interaction could also facilitate the penetration of the actin cortex by the incoming viral capsid.

The first herpesvirus protein reported to interact with the DIC subunit of cytoplasmic dynein in GST pull down assays was the UL34 of

HSV1, with a predicted type II integral membrane topology (Ye et al. 2000; Reynolds et al. 2002). UL34 of HSV and pseudorabies virus is targeted to the inner nuclear membrane, where during budding it is incorporated into the primary envelope of periplasmic virions (Klupp et al. 2000; Reynolds et al. 2002). In contrast to the inner nuclear membrane, cytoplasmic membranes and extracellular virions do not contain UL34; thus it cannot be involved in viral cytoplasmic transport.

The heavy chain of conventional kinesin interacts with the HSV1 tegument protein US11. Moreover, US11 and the major capsid protein VP5 were reported to be transported with similar kinetics into the axons of dissociated rat neurons (Diefenbach et al. 2002).

6 Retrovirus Entry and Budding

HIV, the most prominent representative of retroviruses, enters cells primarily by membrane fusion at the plasma membrane (Greene and Peterlin 2002), although some strains can also infect cells via endocytic uptake (Fackler and Peterlin 2000). During passage through the cytosol, the viral RNA genome is reverse transcribed into DNA in a structure named the reverse transcription complex (RTC) or pre-integration complex (PIC). PIC is targeted to the nuclear pore complex and imported into the nucleus, and the HIV genome is integrated into a chromosome (Greene and Peterlin 2002; see the chapter by Byland and Marsh, this volume, and Fig. 1B).

Cytochalasin prevents the co-clustering of the HIV receptors CD4 and CXCR4 on gp120 binding and thus somehow inhibits efficient HIV fusion with the plasma membrane (Iyengar et al. 1998). On cell fractionation RTCs are localised in a cytoskeletal fraction, and reverse transcription requires intact actin filaments (Bukrinskaya et al. 1998).

Intracellular trafficking of HIV can be visualised with a GFP-Vpr fusion protein which is packaged into virions (McDonald et al. 2002). By live cell imaging GFP-Vpr-labelled subviral particles co-localise with MTs, move in curvilinear paths in the cytoplasm and accumulate around the MTOC as early as 2 h after infection. HIV transport is completely blocked in the presence of both nocodazole and latrunculin, but not by either one alone. The incoming PIC of human foamy virus, another retrovirus, also accumulates around the MTOC by a MT depending transport (Saib et al. 1997).

When dynein is inhibited by a microinjected antibody, the relative transport of RTCs to the nucleus is reduced (McDonald et al. 2002). Interestingly, in this situation the RTCs accumulate in the cell periphery, similar to what has been described for HSV capsids after overexpression of dynamitin (Döhner et al. 2002). Moreover, yeast two-hybrid assays showed an interaction of HIV integrase with the yeast homologue of dynein LC8 (Richard de Soultrait et al. 2002).

Most likely, HIV subviral particles that are assembled in the cytoplasm also use active transport to reach the plasma membrane, where retrovirus budding often takes place (Greene and Peterlin 2002). Both MTs and the binding motive for the host factor hnRNP A2 present in genomic HIV RNA are involved in trafficking of RNA granules (Mouland et al. 2001). The human T cell leukaemia virus, a retrovirus distantly related to HIV, requires a cell-cell junction and MTs for efficient transmission. T cell adhesion induces a rapid reorganisation of the MT network towards the junction that becomes a kind of virological synapse for budding (Igakura et al. 2003).

Filamentous actin and myosin seem to play important roles during HIV budding at the plasma membrane (Sasaki et al. 1995). The interaction of the HIV negative effector Nef with Vav, the host guanine nucleotide exchange factor of Cdc42 and Rac—two small GTPases regulating the actin cytoskeleton—could modify the actin cortex before virus budding (Fackler et al. 1999). Nef is also packaged into virions (10–100 molecules/particle) and has an important role in viral entry early after virus fusion but before the completion of reverse transcription (Schaeffer et al. 2001; Forshey and Aiken 2003). It is tempting to speculate that Nef, possibly in concert with other proteins of the RTC, could again remodel the actin cortex to facilitate access to the MT plus-ends for further transport.

The kinesin motor KIF4A is abundantly expressed in neurons and transports vesicles containing the cell adhesion protein L1 (Peretti et al. 2000). Yeast two-hybrid assays and chromatography showed that Gag polyproteins and matrix protein of murine leukaemia virus, HIV and SIV bind to KIF4 (Kim et al. 1998; Tang et al. 1999). Such an interaction could mediate a plus-end-directed transport of the RTC during entry, as well as the transport of RNA granules to the plasma membrane for assembly.

7
Adenovirus Entry and Microtubules

The cell entry of adenovirus is characterised by the stepwise disassembly of incoming virions (Greber et al. 1993; Fig. 1C). Adenoviruses are internalised by receptor-mediated endocytosis and induce the lysis of endosomal membranes to gain access to the cytosol (Shenk 2001). Ad2 and Ad5 virions of the subgroup C attach to MTs in vitro and in vivo (Luftig and Weihing 1975; Miles et al. 1980). If cells have been treated with vincristine to induce MT paracrystals, the virions display projections emanating from the vertices that are shorter and thicker than the fibre, and thus might represent bound host factors (Dales and Chardonnet 1973). The capsids use dynein for transport along MTs towards the MTOC because depolymerising the MT network, overexpressing dynamitin and microinjection of function-blocking dynein antibodies all inhibit Ad2 and Ad5 infection (Suomalainen et al. 1999; Leopold et al. 2000; Mabit et al. 2002).

As with herpesvirus, it is unclear whether and how viral capsids which have reached the MTOC are forwarded to the nuclear pores. Dynamic MTs are not required for nuclear targeting of incoming Ad particles. In fact, suppressing MT dynamics enhances the nuclear targeting efficiency of Ad2 (Giannakakou et al. 2002; Mabit et al. 2002). At the nuclear pores the viral DNA is injected into the nucleoplasm (Greber et al. 1993; Trotman et al. 2001), where viral replication, transcription and capsid assembly take place.

Analysing Ad2 particles that were visualised by the covalent attachment of fluorescent dyes, Suomalainen et al. (1999) described two types of motilities. Several transport events last for several seconds with an average velocity of 0.3–0.5 μm/s, depending on the cell type, and peak velocities of up to 2.6 μm/s which are directed exclusively towards the MTOC. Other particles rapidly alter direction towards or away from the nucleus with speeds of up to 0.5 μm/s. As with many other viruses, the incoming Ad2 particles induce a complex signalling cascade, which in this case activates protein kinase A and p38/MAPK pathways to boost minus-end-directed MT capsid transport (Suomalainen et al. 2001). In contrast to Ad2, Leopold et al. (1998, 2000) showed that labelled Ad5 particles rarely switch directions but also move along curvilinear tracks with an average speed of 2.2 μm/s. In the absence of a MT network, both groups detected only short-range random movements (Suomalainen et al. 1999; Leopold et al. 2000).

Glotzer et al. (2001) labelled Ad5 particles by co-packaging a GFP-labelled protein that bound to specific sequences engineered into the viral genome. Such particles moved both towards and away from the nucleus and, surprisingly, with comparable peak velocities of 1 μm/s and average velocities of 0.32 μm/s or 0.26 μm/s, irrespective of the presence or absence of MTs. Moreover, viral gene expression is not reduced if MTs have been depolymerised before infection (Glotzer et al. 2001). To explain these conflicting results on cytosolic adenovirus capsid transport, the parallel analysis of differently labelled particles with an identical experimental set-up and time resolution will be necessary (for a discussion, see Mabit et al. 2002).

The adenoviral protein Ad E3-14.7K, an inhibitor of TNFα-induced cell death, interacts with a small GTPase called FIP1, which in turn interacts with TCTEL1, a human homologue of the DLC Tctex-1 (Lukashok et al. 2000). Because Ad E3-14.7K is not a structural protein, it cannot have a role in cytosolic transport of Ad particles. However, many cellular proteins require MT-mediated transport to reach their final destination (Giannakakou et al. 2000), and the interaction of Ad E3-14.7K with a FIP1-TCTEL1 complex could aid in its cytosolic trafficking.

Altogether these studies suggest that adenovirus capsids possess a viral receptor either for dynein or for dynactin, which allows them to use MTs for efficient transport to the host nucleus after exit from the endosome. The disruption of the intermediate filament network facilitates viral egress (Chen et al. 1993), and progeny adenoviruses are released by cell lysis.

8
Parvovirus Entry and Microtubules

Parvoviruses enter cells by receptor-mediated endocytosis and seem to cross endosomal membranes at different stages of the endocytic pathway. Canine parvovirus (CPV) is detected in clathrin-coated vesicles, recycling endosomes, late endosomes and finally lysosomes, and CPV-containing vesicles are often associated with MTs. The transport from early to late endosomes as well as that of CPV-containing vesicles to the perinuclear area requires intact MTs and cytoplasmic dynein (Aniento et al. 1993; Suikkanen et al. 2002). Injected anti-capsid antibodies block CPV infection, suggesting that capsids enter the cytosol during infection. Moreover, nocodazole and a microinjected anti-dynein antibody block the nuclear accumulation of the injected capsids, suggesting that cyto-

solic CPV are transported by dynein along MTs to the nucleus (Suikkanen et al. 2003).

Adeno-associated virus (AAV) particles also move in a nocodazole- and cytochalasin B-sensitive manner to the nucleus. However, it remains to be determined whether virions are transported inside vesicles or freely in the cytosol (Sanlioglu et al. 2000). Real-time imaging of viral particles labelled with a single fluorescent molecule shows diffusion of free virions, diffusion of virus within endosomes and directed MT-dependent motion with velocities of 1.8–3.7 μm/s (Seisenberger et al. 2001).

9
Poxviruses—Multiple Cargos for Microtubules and Actin Tails

9.1
Cytosolic Vaccinia Virus Cores

The most complicated virus in terms of entry and assembly is vaccinia virus (VV), a poxvirus. One of its unique features is the formation of two infectious viral particles. Assembly commences in viral factories leading to the formation of the intracellular mature virus (IMV; Sodeik et al. 1993), a large enveloped brick-shaped particle. Relative to the IMV, the extracellular enveloped virus (EEV) has one additional membrane, the so-called envelope (Smith et al. 2002; Sodeik and Krijnse-Locker 2002).

Because both forms lead to infection, they must differ in how the DNA genome is uncoated and released into the cytosol where viral replication takes place. There are conflicting reports on whether both EEV and IMV, or only IMV, require actin filaments for entry and whether both or only IMV enter directly at the plasma membrane rather than by endocytosis (Payne and Norrby 1978; Doms et al. 1990; Vanderplasschen et al. 1998). In a recent study, the cells responded only to IMV but not EEV with the formation of long cell surface protrusions which were induced by a signalling cascade involving the actin-binding protein ezrin and the small GTPase Rac (Krijnse Locker et al. 2000). Accordingly, the IMV but not the EEV requires actin dynamics and filopodia for entry at the plasma membrane.

Although VV entry is still poorly understood, at the end of this process cores lacking any membrane are delivered into the cytosol. Early VV mRNAs are first transcribed inside these cores and then accumulate

in large granular structures which recruit ribosomes for translation and are some distance away from the cores (Mallardo et al. 2001). Both the cores and the early mRNAs are associated with MTs, and nocodazole reduces mRNA synthesis (Mallardo et al. 2001). The in vitro binding of isolated cores to MTs requires the DNA- and RNA-binding protein L4R and the core protein A10L, which both co-localise with stabilised MTs in infected cells (Ploubidou et al. 2000; Mallardo et al. 2001).

Next, the incoming genome is uncoated, released from the core and amplified in specialised replication sites that are surrounded by membranes of the endoplasmic reticulum (Tolonen et al. 2001). After synthesis of the structural proteins from the late mRNAs, IMVs are formed within cytoplasmic viral factories from non-infectious precursors called crescents and immature virions (Fig. 2B).

9.2 Particle Transport During Virus Egress

Overexpression of dynamitin, or the deletion of the IMV protein A27L, inhibits the minus-end-directed MT transport of IMV particles from the viral factories to the MTOC (Ploubidou et al. 2000; Sanderson et al. 2000; Fig. 2B). At the MTOC, the IMV is wrapped in a membrane cisterna derived from the -TGN or an early endosome and intracellular enveloped virus (IEV) with two additional membranes relative to the IMV is formed (Smith et al. 2002). If cells are infected in the presence of nocodazole, no IEVs are made and there is a threefold reduction in the amount of IMVs synthesized (Ploubidou et al. 2000).

IEVs move to the plasma membrane in a saltatory and directional manner with an average speed of 1–2 μm/s along MTs and even switch from one MT to another (Geada et al. 2001; Hollinshead et al. 2001; Rietdorf et al. 2001; Ward and Moss 2001). IEVs co-localise with kinesin-1, and the overexpression of the cargo-binding domain of KLC inhibits their transport (Rietdorf et al. 2001). Besides kinesin, the integral membrane protein A36R and the peripheral membrane protein F12L are necessary for IEV transport to the plasma membrane (Rietdorf et al. 2001; van Eijl et al. 2002).

Shortly before or after the fusion of the outer membrane of IEV with the plasma membrane, the polymerisation of actin filaments is induced (Hollinshead et al. 2001). The cell-associated virus (CEV) that remains attached to the plasma membrane for quite some time is pushed on top of a long microvillus into the medium or a neighbouring cell at a speed of 2.8 μm/s (Cudmore et al. 1995). This process facilitates VV spread in

a cell monolayer and in the tissue. The IEV protein A36R, which has an unusual long cytosolic tail and no obvious mammalian homologues, is the vaccinia actin tail nucleator. Tyr phosphorylation of A36R by a member of the Src-kinase family leads to the recruitment of the adaptor proteins Nck and Grb2, the WASP-interacting protein (WIP) as well as N-WASP (Wiskott-Aldrich syndrome protein). WASP activates the Arp2/3 complex and thus motility based on actin polymerisation (Frischknecht et al. 1999; Moreau et al. 2000; Scaplehorn et al. 2002). Another interesting rearrangement of the host actin cytoskeleton is the induction of cell migration that depends on early VV gene expression and the formation of cellular projections up to 160 μm in length that requires late VV gene expression (Sanderson et al. 1998).

Considering how many different types of large VV particles have to be shuffled around during entry and assembly, it is probably not surprising that there is considerable cross-talk between VV proteins and both cytosolic transport systems, MTs and microfilaments.

10
Actin Remodelling During Baculovirus Infection

Baculoviruses such as *Autographa californica M* nuclear polyhedrosis virus (AcMNPV) catalyse several distinct rearrangements of the actin cytoskeleton during different stages of the viral infection.

After virus uptake by endocytosis and acid-induced endosomal escape, the incoming cytosolic capsids induce prominent transient actin cables which often have a single capsid at one end and seem to be involved in capsid transport to the nucleus (Charlton and Volkman 1993; van Loo et al. 2001). Isolated AcMNPV capsids can nucleate actin polymerisation in vitro, and competition data with cytochalasin suggest that these capsids bind to the minus-end of the filaments (Lanier and Volkman 1998). Two AcMNPV proteins, p39 and p78/83, can bind to actin directly (Lanier and Volkman 1998). Moreover, p78/83 contains regions of homology to WASP which bind monomeric actin and the Arp2/3 complex which nucleates assembly of new actin filaments (Machesky et al. 2001). This suggests that p78/83 could function as a viral WASP homolog in inducing actin filament assembly.

Interestingly, in contrast to other viruses, depolymerising the MTs with nocodazole speeds up the onset of baculovirus gene expression, at least in transduction experiments using mammalian cells, whereas infection in the presence of cytochalasin reduces the infection efficiency (van

Loo et al. 2001). The myosin inhibitor BDM inhibits capsid transport to the nucleus, suggesting that a myosin could also be involved in capsid transport (Lanier and Volkman 1998).

The expression of the early viral protein Arif-1 (actin rearrangement-inducing factor 1) is responsible for second modification of the actin cytoskeleton, the appearance of actin aggregates localised at the plasma membrane (Roncarati and Knebel-Mörsdorf 1997). The amino acid sequence of Arif-1 predicts a N-terminal signal peptide and three transmembrane regions of about 20 amino acids each, and, moreover, Arif-1 seems to be phosphorylated at tyrosine residues (Dreschers et al. 2001). Arif-1 is not required for infection of cultured cells but might play a role during pathogenesis in insects.

The later phases of baculovirus infection are characterized by the appearance of F-actin inside the nucleus in a ring close to the nuclear membrane which is essential for nucleocapsid morphogenesis (Ohkawa and Volkman 1999). Six gene products of AcMNPV are required for the recruitment of G-actin to the nucleus (Ohkawa et al. 2002).

11 Perspectives

There is probably not a single virus for which the cytoskeleton does not play important roles during entry, replication, assembly or egress. With the emerging technologies in digital time-lapse microscopy, the further characterisation of viral transport will improve our understanding of the underlying host mechanisms.

Deciphering the molecular interactions between viruses and the cytoskeleton could provide important new targets for the development of antiviral therapy. Although the cytoskeletal filaments and associated motors play major roles in the cellular metabolism, viruses might interact with these structures via unique sites different from the cellular interaction partners. Other potential targets might be specific host proteins which viruses use to hook onto the cytoplasmic transport machinery.

In our quest to develop efficient vectors for therapeutic gene expression, it has become apparent that the transport of naked DNA to the nucleus, where transcription usually takes place, is a major barrier for the transfection of non-dividing cells, and hence for the application of human non-viral gene therapy vectors in vivo. However, several viruses have found effective solutions to this problem, namely successful negotiation with the host cytoskeleton to ensure efficient cytoplasmic trans-

portation to the nuclear pores of the nuclear envelope. The future design of viral vectors will include these specific nuclear targeting mechanisms while deleting any factors responsible for cell toxicity and the induction of the immune response.

Acknowledgements We thank Rudi Bauerfeind (Cell Biology, MHH) and Elena Korenbaum (Biophysical Chemistry, MHH) for many helpful suggestions on the manuscript and Oliver Fackler (Virology, University of Heidelberg) for insightful discussions on HIV cell entry.

References

Allan, V, Näthke, IS (2001) Catch and pull a microtubule: getting a grasp on the cortex. Nat Cell Biol 3: E226–8

Alonso, C, Miskin, J, Hernaez, B, Fernandez-Zapatero, P, Soto, L, Canto, C, Rodriguez-Crespo, I, Dixon, L, Escribano, JM (2001) African swine fever virus protein p54 interacts with the microtubular motor complex through direct binding to light-chain dynein. J Virol 75:9819–27

Aniento, F, Emans, N, Griffiths, G, Gruenberg, J (1993) Cytoplasmic dynein-dependent vesicular transport from early to late endosomes. J Cell Biol 123:1373–87

Avitabile, E, Di Gaeta, S, Torrisi, MR, Ward, PL, Roizman, B, Campadelli-Fiume, G (1995) Redistribution of microtubules and Golgi apparatus in herpes simplex virus-infected cells and their role in viral exocytosis. J Virol 69:7472–82

Ayscough, K (1998) Use of latrunculin-A, an actin monomer-binding drug. Methods Enzymol 298:18–25

Bearer, EL, Breakefield, XO, Schuback, D, Reese, TS, LaVail, JH (2000) Retrograde axonal transport of herpes simplex virus: evidence for a single mechanism and a role for tegument. Proc Natl Acad Sci U S A 97:8146–50

Bowman, AB, Patel-King, RS, Benashski, SE, McCaffery, JM, Goldstein, LS, King, SM (1999) *Drosophila* roadblock and *Chlamydomonas* LC7: a conserved family of dynein-associated proteins involved in axonal transport, flagellar motility, and mitosis. J Cell Biol 146:165–80

Brown, SS (1999) Cooperation between microtubule- and actin-based motor proteins. Annu Rev Cell Dev Biol 15:63–80

Brunet, JP, Jourdan, N, Cotte-Laffitte, J, Linxe, C, Geniteau-Legendre, M, Servin, A, Quero, AM (2000) Rotavirus infection induces cytoskeleton disorganization in human intestinal epithelial cells: implication of an increase in intracellular calcium concentration. J Virol 74:10801–6

Bubb, MR, Senderowicz, AM, Sausville, EA, Duncan, KL, Korn, ED (1994) Jasplakinolide, a cytotoxic natural product, induces actin polymerization and competitively inhibits the binding of phalloidin to F-actin. J Biol Chem 269:14869–71

Bukrinskaya, A, Brichacek, B, Mann, A, Stevenson, M (1998) Establishment of a functional human immunodeficiency virus type 1 (HIV-1) reverse transcription complex involves the cytoskeleton. J Exp Med 188:2113–25

Burkhardt, JK, Echeverri, CJ, Nilsson, T, Vallee, RB (1997) Overexpression of the dynamitin (p50) subunit of the dynactin complex disrupts dynein-dependent maintenance of membrane organelle distribution. J Cell Biol 139:469–84

Ceccaldi, PE, Gillet, JP, Tsiang, H (1989) Inhibition of the transport of rabies virus in the central nervous system. J Neuropathol Exp Neurol 48:620–30

Charlton, CA, Volkman, LE (1993) Penetration of *Autographa californica* nuclear polyhedrosis virus nucleocapsids into IPLB Sf 21 cells induces actin cable formation. Virology 197:245–54

Chen, PH, Ornelles, DA, Shenk, T (1993) The adenovirus L3 23-kilodalton proteinase cleaves the amino-terminal head domain from cytokeratin 18 and disrupts the cytokeratin network of HeLa cells. J Virol 67:3507–14

Cooper, JA (1987) Effects of cytochalasin and phalloidin on actin. J Cell Biol 105:1473–8

Coulombe, PA, Bousquet, O, Ma, L, Yamada, S, Wirtz, D (2000) The 'ins' and 'outs' of intermediate filament organization. Trends Cell Biol 10:420–8

Coulombe, PA, Ma, L, Yamada, S, Wawersik, M (2001) Intermediate filaments at a glance. J Cell Sci 114:4345–7

Cramer, LP, Mitchison, TJ (1995) Myosin is involved in postmitotic cell spreading. J Cell Biol 131:179–89

Cudmore, S, Cossart, P, Griffiths, G, Way, M (1995) Actin-based motility of vaccinia virus. Nature 378:636–8

Cudmore, S, Reckmann, I, Way, M (1997) Viral manipulations of the actin cytoskeleton. Trends Microbiol 5:142–8

Dales, S, Chardonnet, Y (1973) Early events in the interaction of adenoviruses with HeLa cells. IV. Association with microtubules and the nuclear pore complex during vectorial movement of the inoculum. Virology 56:465–83

Deacon, SW, Serpinskaya, AS, Vaughan, PS, Fanarraga, ML, Vernos, I, Vaughan, KT, Gelfand, VI (2003) Dynactin is required for bidirectional organelle transport. J Cell Biol 160:297–301

Desai, A, Mitchison, TJ (1997) Microtubule polymerization dynamics. Annu Rev Cell Dev Biol 13:83–117

Desai, A, Verma, S, Mitchison, TJ, Walczak, CE (1999) Kin I kinesins are microtubule-destabilizing enzymes. Cell 96:69–78

Diefenbach, RJ, Miranda-Saksena, M, Diefenbach, E, Holland, DJ, Boadle, RA, Armati, PJ, Cunningham, AL (2002) Herpes simplex virus tegument protein US11 interacts with conventional kinesin heavy chain. J Virol 76:3282–3291

Digard, P, Elton, D, Bishop, K, Medcalf, E, Weeds, A, Pope, B (1999) Modulation of nuclear localization of the influenza virus nucleoprotein through interaction with actin filaments. J Virol 73:2222–31

Döhner, K, Wolfstein, A, Prank, U, Echeverri, C, Dujardin, D, Vallee, R, Sodeik, B (2002) Function of dynein and dynactin in herpes simplex virus capsid transport. Mol Biol Cell 13:2795–809

Doms, RW, Blumenthal, R, Moss, B (1990) Fusion of intra- and extracellular forms of vaccinia virus with the cell membrane. J Virol 64:4884–92

Downing, KH (2000) Structural basis for the interaction of tubulin with proteins and drugs that affect microtubule dynamics. Annu Rev Cell Dev Biol 16:89–111

Dreschers, S, Roncarati, R, Knebel-Mörsdorf, D (2001) Actin rearrangement-inducing factor of baculoviruses is tyrosine phosphorylated and colocalizes to F-actin at the plasma membrane. J Virol 75:3771–8

Echeverri, CJ, Paschal, BM, Vaughan, KT, Vallee, RB (1996) Molecular characterization of the 50-kD subunit of dynactin reveals function for the complex in chromosome alignment and spindle organization during mitosis. J Cell Biol 132:617–33

Eckley, DM, Gill, SR, Melkonian, KA, Bingham, JB, Goodson, HV, Heuser, JE, Schroer, TA (1999) Analysis of dynactin subcomplexes reveals a novel actin-related protein associated with the arp1 minifilament pointed end. J Cell Biol 147:307–20

Elliott, G, O'Hare, P (1997) Intercellular trafficking and protein delivery by a herpesvirus structural protein. Cell 88:223–33

Elliott, G, O'Hare, P (1998) Herpes simplex virus type 1 tegument protein VP22 induces the stabilization and hyperacetylation of microtubules. J Virol 72:6448–55

Elliott, G, O'Hare, P (1999) Live-cell analysis of a green fluorescent protein-tagged herpes simplex virus infection. J Virol 73:4110–9

Espindola, FS, Suter, DM, Partata, LB, Cao, T, Wolenski, JS, Cheney, RE, King, SM, Mooseker, MS (2000) The light chain composition of chicken brain myosin-Va: calmodulin, myosin-II essential light chains, and 8-kDa dynein light chain/PIN. Cell Motil Cytoskeleton 47:269–81

Fackler, OT, Luo, W, Geyer, M, Alberts, AS, Peterlin, BM (1999) Activation of Vav by Nef induces cytoskeletal rearrangements and downstream effector functions. Mol Cell 3:729–39

Fackler, OT, Peterlin, BM (2000) Endocytic entry of HIV-1. Curr Biol 10:1005–8

Ferreira, LR, Moussatche, N, Moura Neto, V (1994) Rearrangement of intermediate filament network of BHK-21 cells infected with vaccinia virus. Arch Virol 138:273–85

Forshey, BM, Aiken, C (2003) Disassembly of human immunodeficiency virus type 1 cores in vitro reveals association of Nef with the subviral ribonucleoprotein complex. J Virol 77:4409–14

Frischknecht, F, Moreau, V, Rottger, S, Gonfloni, S, Reckmann, I, Superti-Furga, G, Way, M (1999) Actin-based motility of vaccinia virus mimics receptor tyrosine kinase signalling. Nature 401:926–9

Frischknecht, F, Way, M (2001) Surfing pathogens and the lessons learned for actin polymerization. Trends Cell Biol 11:30–38

Fuchs, E, Yang, Y (1999) Crossroads on cytoskeletal highways. Cell 98:547–50

Galigniana, MD, Radanyi, C, Renoir, JM, Housley, PR, Pratt, WB (2001) Evidence that the peptidylprolyl isomerase domain of the hsp90-binding immunophilin FKBP52 is involved in both dynein interaction and glucocorticoid receptor movement to the nucleus. J Biol Chem 276:14884–9

Garcia-Mata, R, Bebok, Z, Sorscher, EJ, Sztul, ES (1999) Characterization and dynamics of aggresome formation by a cytosolic GFP-chimera. J Cell Biol 146:1239–54

Garoff, H, Hewson, R, Opstelten, DJ (1998) Virus maturation by budding. Microbiol Mol Biol Rev 62:1171–90

Geada, MM, Galindo, I, Lorenzo, MM, Perdiguero, B, Blasco, R (2001) Movements of vaccinia virus intracellular enveloped virions with GFP tagged to the F13L envelope protein. J Gen Virol 82:2747–60

Georgi, A, Mottola-Hartshorn, C, Warner, A, Fields, B, Chen, LB (1990) Detection of individual fluorescently labeled reovirions in living cells. Proc Natl Acad Sci U S A 87:6579–83

Giannakakou, P, Nakano, M, Nicolaou, KC, O'Brate, A, Yu, J, Blagosklonny, MV, Greber, UF, Fojo, T (2002) Enhanced microtubule-dependent trafficking and p53 nuclear accumulation by suppression of microtubule dynamics. Proc Natl Acad Sci U S A 99:10855–60

Giannakakou, P, Sackett, DL, Ward, Y, Webster, KR, Blagosklonny, MV, Fojo, T (2000) p53 is associated with cellular microtubules and is transported to the nucleus by dynein. Nat Cell Biol 2:709–17

Glotzer, JB, Michou, AI, Baker, A, Saltik, M, Cotten, M (2001) Microtubule-independent motility and nuclear targeting of adenoviruses with fluorescently labeled genomes. J Virol 75:2421–34

Goldstein, LS, Yang, Z (2000) Microtubule-based transport systems in neurons: the roles of kinesins and dyneins. Annu Rev Neurosci 23:39–71

Goode, BL, Drubin, DG, Barnes, G (2000) Functional cooperation between the microtubule and actin cytoskeletons. Curr Opin Cell Biol 12:63–71

Greber, UF, Willetts, M, Webster, P, Helenius, A (1993) Stepwise dismantling of adenovirus 2 during entry into cells. Cell 75:477–86

Greene, WC, Peterlin, BM (2002) Charting HIV's remarkable voyage through the cell: Basic science as a passport to future therapy. Nat Med 8:673–80

Gupta, S, De, BP, Drazba, JA, Banerjee, AK (1998) Involvement of actin microfilaments in the replication of human parainfluenza virus type 3. J Virol 72:2655–62

Gurland, G, Gundersen, GG (1995) Stable, detyrosinated microtubules function to localize vimentin intermediate filaments in fibroblasts. J Cell Biol 131:1275–90

Hanlon, DW, Yang, Z, Goldstein, LS (1997) Characterization of KIFC2, a neuronal kinesin superfamily member in mouse. Neuron 18:439–51

Heath, CM, Windsor, M, Wileman, T (2001) Aggresomes resemble sites specialized for virus assembly. J Cell Biol 153:449–55

Herrmann, C, Wray, J, Travers, F, Barman, T (1992) Effect of 2,3-butanedione monoxime on myosin and myofibrillar ATPases. An example of an uncompetitive inhibitor. Biochemistry 31:12227–32

Hirokawa, N, Takemura, R. (2003). Kinesin superfamily proteins. *In* Molecular Motors (M. Schliwa, ed.), pp. 79–109. Wiley-VCH Verlag, Weinheim

Hofmann, W, Reichart, B, Ewald, A, Muller, E, Schmitt, I, Stauber, RH, Lottspeich, F, Jockusch, BM, Scheer, U, Hauber, J, Dabauvalle, MC (2001) Cofactor requirements for nuclear export of Rev response element (RRE)- and constitutive transport element (CTE)-containing retroviral RNAs. An unexpected role for actin. J Cell Biol 152:895–910

Hogle, JM (2002) Poliovirus cell entry: common structural themes in viral cell entry pathways. Annu Rev Microbiol 56:677–702

Holland, DJ, Miranda-Saksena, M, Boadle, RA, Armati, P, Cunningham, AL (1999) Anterograde transport of herpes simplex virus proteins in axons of peripheral human fetal neurons: an immunoelectron microscopy study. J Virol 73:8503–11

Holleran, EA, Karki, S, Holzbaur, EL (1998) The role of the dynactin complex in intracellular motility. Int Rev Cytol 182:69–109

Hollinshead, M, Rodger, G, Van Eijl, H, Law, M, Hollinshead, R, Vaux, DJ, Smith, GL (2001) Vaccinia virus utilizes microtubules for movement to the cell surface. J Cell Biol 154:389–402

Howard, J, Hyman, AA (2003) Dynamics and mechanics of the microtubule plus end. Nature 422:753–8

Hunter, AW, Caplow, M, Coy, DL, Hancock, WO, Diez, S, Wordeman, L, Howard, J (2003) The kinesin-related protein MCAK is a microtubule depolymerase that forms an ATP-hydrolyzing complex at microtubule ends. Mol Cell 11:445–57

Igakura, T, Stinchcombe, JC, Goon, PK, Taylor, GP, Weber, JN, Griffiths, GM, Tanaka, Y, Osame, M, Bangham, CR (2003) Spread of HTLV-I between lymphocytes by virus-induced polarization of the cytoskeleton. Science 299:1713–6

Iyengar, S, Hildreth, JE, Schwartz, DH (1998) Actin-dependent receptor colocalization required for human immunodeficiency virus entry into host cells. J Virol 72:5251–5

Jacob, Y, Badrane, H, Ceccaldi, PE, Tordo, N (2000) Cytoplasmic dynein LC8 interacts with lyssavirus phosphoprotein. J Virol 74:10217–22

Jaffrey, SR, Snyder, SH (1996) PIN: an associated protein inhibitor of neuronal nitric oxide synthase. Science 274:774–7

Jimbo, T, Kawasaki, Y, Koyama, R, Sato, R, Takada, S, Haraguchi, K, Akiyama, T (2002) Identification of a link between the tumour suppressor APC and the kinesin superfamily. Nat Cell Biol 4:323–7

Jordan, MA, Wilson, L (1999) The use and action of drugs in analyzing mitosis. Methods Cell Biol 61:267–95

Karcher, RL, Deacon, SW, Gelfand, VI (2002) Motor-cargo interactions: the key to transport specificity. Trends Cell Biol 12:21–7

Karki, S, Holzbaur, EL (1999) Cytoplasmic dynein and dynactin in cell division and intracellular transport. Curr Opin Cell Biol 11:45–53

Kasman, LM, Volkman, LE (2000) Filamentous actin is required for lepidopteran nucleopolyhedrovirus progeny production. J Gen Virol 81:1881–8

Keating, TJ, Borisy, GG (1999) Centrosomal and non-centrosomal microtubules. Biol Cell 91:321–9

Kieke, MC, Titus, MA. (2003). The myosin superfamily: An overview. *In* Molecular Motors (M. Schliwa, ed.), pp. 3–44. Wiley-VCH Verlag, Weinheim

Kim, W, Tang, Y, Okada, Y, Torrey, TA, Chattopadhyay, SK, Pfleiderer, M, Falkner, FG, Dorner, F, Choi, W, Hirokawa, N, Morse, HC, 3rd (1998) Binding of murine leukemia virus Gag polyproteins to KIF4, a microtubule-based motor protein. J Virol 72:6898–901

Kimura, T, Hashimoto, I, Yamamoto, A, Nishikawa, M, Fujisawa, JI (2000) Rev-dependent association of the intron-containing HIV-1 gag mRNA with the nuclear actin bundles and the inhibition of its nucleocytoplasmic transport by latrunculin-B. Genes Cells 5:289–307

King, SM (2000) AAA domains and organization of the dynein motor unit. J Cell Sci 113:2521–6

King, SM. (2003). Dynein motors: Structure, mechanochemistry and regulation. *In* Molecular Motors (M. Schliwa, ed.), pp. 45–78. Wiley-VCH Verlag, Weinheim

Klupp, BG, Granzow, H, Mettenleiter, TC (2000) Primary envelopment of pseudorabies virus at the nuclear membrane requires the UL34 gene product. J Virol 74:10063–73

Kopito, RR (2000) Aggresomes, inclusion bodies and protein aggregation. Trends Cell Biol 10:524–30

Kotsakis, A, Pomeranz, LE, Blouin, A, Blaho, JA (2001) Microtubule reorganization during herpes simplex virus type 1 infection facilitates the nuclear localization of VP22, a major virion tegument protein. J Virol 75:8697–711

Krijnse Locker, J, Kuehn, A, Schleich, S, Rutter, G, Hohenberg, H, Wepf, R, Griffiths, G (2000) Entry of the two infectious forms of vaccinia virus at the plasma membrane is signaling-dependent for the IMV but not the EEV. Mol Biol Cell 11:2497–511

Kristensson, K, Lycke, E, Roytta, M, Svennerholm, B, Vahlne, A (1986) Neuritic transport of herpes simplex virus in rat sensory neurons in vitro. Effects of substances interacting with microtubular function and axonal flow [nocodazole, taxol and erythro-9-3-(2-hydroxynonyl)adenine]. J Gen Virol 67:2023–8

Lanier, LM, Volkman, LE (1998) Actin binding and nucleation by *Autographa californica M* nucleopolyhedrovirus. Virology 243:167–77

Leopold, PL, Ferris, B, Grinberg, I, Worgall, S, Hackett, NR, Crystal, RG (1998) Fluorescent virions: dynamic tracking of the pathway of adenoviral gene transfer vectors in living cells. Hum Gene Ther 9:367–78

Leopold, PL, Kreitzer, G, Miyazawa, N, Rempel, S, Pfister, KK, Rodriguez-Boulan, E, Crystal, RG (2000) Dynein- and microtubule-mediated translocation of adenovirus serotype 5 occurs after endosomal lysis. Hum Gene Ther 11:151–65

Leung, CL, Green, KJ, Liem, RK (2002) Plakins: a family of versatile cytolinker proteins. Trends Cell Biol 12:37–45

Lippincott-Schwartz, J, Roberts, TH, Hirschberg, K (2000) Secretory protein trafficking and organelle dynamics in living cells. Annu Rev Cell Dev Biol 16:557–89

Liu, B, Dai, R, Tian, CJ, Dawson, L, Gorelick, R, Yu, XF (1999) Interaction of the human immunodeficiency virus type 1 nucleocapsid with actin. J Virol 73:2901–8

Lo, KW, Naisbitt, S, Fan, JS, Sheng, M, Zhang, M (2001) The 8-kDa dynein light chain binds to its targets via a conserved (K/R)XTQT motif. J Biol Chem 276:14059–66

Luby-Phelps, K (2000) Cytoarchitecture and physical properties of cytoplasm: volume, viscosity, diffusion, intracellular surface area. Int Rev Cytol 192:189–221

Luftig, RB, Lupo, LD (1994) Viral interactions with the host-cell cytoskeleton: the role of retroviral proteases. Trends Microbiol 2:178–82

Luftig, RB, Weihing, RR (1975) Adenovirus binds to rat brain microtubules in vitro. J Virol 16:696–706

Lukashok, SA, Tarassishin, L, Li, Y, Horwitz, MS (2000) An adenovirus inhibitor of tumor necrosis factor alpha-induced apoptosis complexes with dynein and a small GTPase. J Virol 74:4705–9

Lycke, E, Hamark, B, Johansson, M, Krotochwil, A, Lycke, J, Svennerholm, B (1988) Herpes simplex virus infection of the human sensory neuron. An electron microscopy study. Arch Virol 101:87–104

Mabit, H, Nakano, MY, Prank, U, Saam, B, Döhner, K, Sodeik, B, Greber, UF (2002) Intact microtubules support adenovirus and herpes simplex virus infections. J Virol 76:9962–71

Machesky, LM, Insall, RH, Volkman, LE (2001) WASP homology sequences in baculoviruses. Trends Cell Biol 11:286–7

Mallardo, M, Schleich, S, Krijnse Locker, J (2001) Microtubule-dependent organization of vaccinia virus core-derived early mRNAs into distinct cytoplasmic structures. Mol Biol Cell 12:3875–91

Marsh, M, Bron, R (1997) SFV infection in CHO cells: cell-type specific restrictions to productive virus entry at the cell surface. J Cell Sci 110:95–103

Martin, A, O'Hare, P, McLauchlan, J, Elliott, G (2002) Herpes simplex virus tegument protein VP22 contains overlapping domains for cytoplasmic localization, microtubule interaction, and chromatin binding. J Virol 76:4961–70

Martinez-Moreno, M, Navarro-Lerida, I, Roncal, F, Albar, JP, Alonso, C, Gavilanes, F, Rodriguez-Crespo, I (2003) Recognition of novel viral sequences that associate with the dynein light chain LC8 identified through a pepscan technique. FEBS Lett 544:262–267

McDonald, D, Vodicka, MA, Lucero, G, Svitkina, TM, Borisy, GG, Emerman, M, Hope, TJ (2002) Visualization of the intracellular behavior of HIV in living cells. J Cell Biol 159:441–52

Mebatsion, T (2001) Extensive attenuation of rabies virus by simultaneously modifying the dynein light chain binding site in the P protein and replacing Arg333 in the G protein. J Virol 75:11496–502

Merdes, A, Cleveland, DW (1997) Pathways of spindle pole formation: different mechanisms; conserved components. J Cell Biol 138:953–6

Mery, PF, Pavoine, C, Pecker, F, Fischmeister, R (1995) Erythro-9-(2-hydroxy-3-nonyl)adenine inhibits cyclic GMP-stimulated phosphodiesterase in isolated cardiac myocytes. Mol Pharmacol 48:121–30

Mettenleiter, TC (2002) Herpesvirus assembly and egress. J Virol 76:1537–47

Miles, BD, Luftig, RB, Weatherbee, JA, Weihing, RR, Weber, J (1980) Quantitation of the interaction between adenovirus types 2 and 5 and microtubules inside infected cells. Virology 105:265–9

Miller, N, Hutt-Fletcher, LM (1992) Epstein-Barr virus enters B cells and epithelial cells by different routes. J Virol 66:3409–14

Miranda-Saksena, M, Armati, P, Boadle, RA, Holland, DJ, Cunningham, AL (2000) Anterograde transport of herpes simplex virus type 1 in cultured, dissociated human and rat dorsal root ganglion neurons. J Virol 74:1827–39

Mitchison, T, Kirschner, M (1984) Dynamic instability of microtubule growth. Nature 312:237–42

Mojon, D, Zhang, W, Oetliker, H (1993) Inhibition by 2,3-butanedione-monoxime of mitochondrial ADP-dependent respiration and muscle contraction. Biochem Mol Biol Int 31:501–7

Moreau, V, Frischknecht, F, Reckmann, I, Vincentelli, R, Rabut, G, Stewart, D, Way, M (2000) A complex of N-WASP and WIP integrates signalling cascades that lead to actin polymerization. Nat Cell Biol 2:441–8

Mouland, AJ, Xu, H, Cui, H, Krueger, W, Munro, TP, Prasol, M, Mercier, J, Rekosh, D, Smith, R, Barbarese, E, Cohen, EA, Carson, JH (2001) RNA trafficking signals in human immunodeficiency virus type 1. Mol Cell Biol 21:2133–43

Mueller, S, Cao, X, Welker, R, Wimmer, E (2002) Interaction of the poliovirus receptor CD155 with the dynein light chain Tctex-1 and its implication for poliovirus pathogenesis. J Biol Chem 277:7897–904

Nakanishi, S, Kakita, S, Takahashi, I, Kawahara, K, Tsukuda, E, Sano, T, Yamada, K, Yoshida, M, Kase, H, Matsuda, Y, et al. (1992) Wortmannin, a microbial product inhibitor of myosin light chain kinase. J Biol Chem 267:2157–63

Nakanishi, S, Yamada, K, Iwahashi, K, Kuroda, K, Kase, H (1990) KT5926, a potent and selective inhibitor of myosin light chain kinase. Mol Pharmacol 37:482–8

Nangaku, M, Sato-Yoshitake, R, Okada, Y, Noda, Y, Takemura, R, Yamazaki, H, Hirokawa, N (1994) KIF1B, a novel microtubule plus end-directed monomeric motor protein for transport of mitochondria. Cell 79:1209–20

Nicola, AV, McEvoy, AM, Straus, SE (2003) Roles for endocytosis and low pH in herpes simplex virus entry into HeLa and Chinese hamster ovary cells. J Virol 77:5324–32

Noda, Y, Okada, Y, Saito, N, Setou, M, Xu, Y, Zhang, Z, Hirokawa, N (2001) KIFC3, a microtubule minus end-directed motor for the apical transport of annexin XIIIb-associated Triton-insoluble membranes. J Cell Biol 155:77–88

Nurminsky, DI, Nurminskaya, MV, Benevolenskaya, EV, Shevelyov, YY, Hartl, DL, Gvozdev, VA (1998) Cytoplasmic dynein intermediate-chain isoforms with different targeting properties created by tissue-specific alternative splicing. Mol Cell Biol 18:6816–25

Ohara, PT, Chin, MS, LaVail, JH (2000) The spread of herpes simplex virus type 1 from trigeminal neurons to the murine cornea: an immunoelectron microscopy study. J Virol 74:4776–86

Ohkawa, T, Rowe, AR, Volkman, LE (2002) Identification of six *Autographa californica* multicapsid nucleopolyhedrovirus early genes that mediate nuclear localization of G-actin. J Virol 76:12281–9

Ohkawa, T, Volkman, LE (1999) Nuclear F-actin is required for AcMNPV nucleocapsid morphogenesis. Virology 264:1-4

Ojala, PM, Sodeik, B, Ebersold, MW, Kutay, U, Helenius, A (2000) Herpes simplex virus type 1 entry into host cells: reconstitution of capsid binding and uncoating at the nuclear pore complex in vitro. Mol Cell Biol 20:4922–31

Okada, Y, Yamazaki, H, Sekine-Aizawa, Y, Hirokawa, N (1995) The neuron-specific kinesin superfamily protein KIF1A is a unique monomeric motor for anterograde axonal transport of synaptic vesicle precursors. Cell 81:769–80

Ott, DE, Coren, LV, Kane, BP, Busch, LK, Johnson, DG, Sowder, RC, 2nd, Chertova, EN, Arthur, LO, Henderson, LE (1996) Cytoskeletal proteins inside human immunodeficiency virus type 1 virions. J Virol 70:7734–43

Payne, LG, Norrby, E (1978) Adsorption and penetration of enveloped and naked vaccinia virus particles. J Virol 27:19–27

Pederson, T, Aebi, U (2002) Actin in the nucleus: what form and what for? J Struct Biol 140:3-9

Penfold, ME, Armati, P, Cunningham, AL (1994) Axonal transport of herpes simplex virions to epidermal cells: evidence for a specialized mode of virus transport and assembly. Proc Natl Acad Sci U S A 91:6529–33

Penningroth, SM (1986) Erythro-9-[3-(2-hydroxynonyl)]adenine and vanadate as probes for microtubule-based cytoskeletal mechanochemistry. Methods Enzymol 134:477–87

Peretti, D, Peris, L, Rosso, S, Quiroga, S, Caceres, A (2000) Evidence for the involvement of KIF4 in the anterograde transport of L1-containing vesicles. J Cell Biol 149:141–52

Phillips, RM, Altschuld, RA (1996) 2,3-Butanedione 2-monoxime (BDM) induces calcium release from canine cardiac sarcoplasmic reticulum. Biochem Biophys Res Commun 229:154–7

Ploubidou, A, Moreau, V, Ashman, K, Reckmann, I, Gonzalez, C, Way, M (2000) Vaccinia virus infection disrupts microtubule organization and centrosome function. EMBO J 19:3932–44

Ploubidou, A, Way, M (2001) Viral transport and the cytoskeleton. Curr Opin Cell Biol 13:97–105

Poisson, N, Real, E, Gaudin, Y, Vaney, MC, King, S, Jacob, Y, Tordo, N, Blondel, D (2001) Molecular basis for the interaction between rabies virus phosphoprotein P and the dynein light chain LC8: dissociation of dynein-binding properties and transcriptional functionality of P. J Gen Virol 82:2691–6

Rando, OJ, Zhao, K, Crabtree, GR (2000) Searching for a function for nuclear actin. Trends Cell Biol 10:92–7

Raux, H, Flamand, A, Blondel, D (2000) Interaction of the rabies virus P protein with the LC8 dynein light chain. J Virol 74:10212–6

Reynolds, AE, Wills, EG, Roller, RJ, Ryckman, BJ, Baines, JD (2002) Ultrastructural localization of the herpes simplex virus type 1 UL31, UL34, and US3 proteins suggests specific roles in primary envelopment and egress of nucleocapsids. J Virol 76:8939–52

Richard de Soultrait, V, Caumont, A, Durrens, P, Calmels, C, Parissi, V, Recordon, P, Bon, E, Desjobert, C, Tarrago-Litvak, L, Fournier, M (2002) HIV-1 integrase interacts with yeast microtubule-associated proteins. Biochim Biophys Acta 1575:40–8

Rietdorf, J, Ploubidou, A, Reckmann, I, Holmstrom, A, Frischknecht, F, Zettl, M, Zimmermann, T, Way, M (2001) Kinesin-dependent movement on microtubules precedes actin-based motility of vaccinia virus. Nat Cell Biol 3:992–1000

Rodriguez-Crespo, I, Yelamos, B, Roncal, F, Albar, JP, Ortiz de Montellano, PR, Gavilanes, F (2001) Identification of novel cellular proteins that bind to the LC8 dynein light chain using a pepscan technique. FEBS Lett 503:135–41

Roizman, B, Knipe, DM. (2001). Herpes simplex viruses and their replication. *In* Fundamental Virology (D. M. Knipe and P. M. Howley, eds.), pp. 1123–1183. Lippincott Williams & Wilkins, Philadelphia

Roncarati, R, Knebel-Mörsdorf, D (1997) Identification of the early actin-rearrangement-inducing factor gene, arif-1, from *Autographa californica* multicapsid nuclear polyhedrosis virus. J Virol 71:7933–41

Ruchhoeft, ML, Harris, WA (1997) Myosin functions in *Xenopus* retinal ganglion cell growth cone motility in vivo. J Neurobiol 32:567–78

Saib, A, Puvion-Dutilleul, F, Schmid, M, Peries, J, de The, H (1997) Nuclear targeting of incoming human foamy virus Gag proteins involves a centriolar step. J Virol 71:1155–61

Saito, N, Okada, Y, Noda, Y, Kinoshita, Y, Kondo, S, Hirokawa, N (1997) KIFC2 is a novel neuron-specific C-terminal type kinesin superfamily motor for dendritic transport of multivesicular body-like organelles. Neuron 18:425–38

Sakowicz, R, Berdelis, MS, Ray, K, Blackburn, CL, Hopmann, C, Faulkner, DJ, Goldstein, LS (1998) A marine natural product inhibitor of kinesin motors. Science 280:292–5

Sanderson, CM, Hollinshead, M, Smith, GL (2000) The vaccinia virus A27L protein is needed for the microtubule-dependent transport of intracellular mature virus particles. J Gen Virol 81 Pt 1:47–58

Sanderson, CM, Way, M, Smith, GL (1998) Virus-induced cell motility. J Virol 72:1235–43

Sanlioglu, S, Benson, PK, Yang, J, Atkinson, EM, Reynolds, T, Engelhardt, JF (2000) Endocytosis and nuclear trafficking of adeno-associated virus type 2 are controlled by rac1 and phosphatidylinositol-3 kinase activation. J Virol 74:9184–96

Sasaki, H, Nakamura, M, Ohno, T, Matsuda, Y, Yuda, Y, Nonomura, Y (1995) Myosin-actin interaction plays an important role in human immunodeficiency virus type 1 release from host cells. Proc Natl Acad Sci U S A 92:2026–30

Scaplehorn, N, Holmstrom, A, Moreau, V, Frischknecht, F, Reckmann, I, Way, M (2002) Grb2 and Nck act cooperatively to promote actin-based motility of vaccinia virus. Curr Biol 12:740–5

Schaeffer, E, Geleziunas, R, Greene, WC (2001) Human immunodeficiency virus type 1 Nef functions at the level of virus entry by enhancing cytoplasmic delivery of virions. J Virol 75:2993–3000

Schlichter, LC, Pahapill, PA, Chung, I (1992) Dual action of 2,3-butanedione monoxime (BDM) on K^+ current in human T lymphocytes. J Pharmacol Exp Ther 261:438–46

Schliwa, M, Woehlke, G (2003) Molecular motors. Nature 422:759–65

Schnapp, BJ (2003) Trafficking of signaling modules by kinesin motors. J Cell Sci 116:2125–35

Seisenberger, G, Ried, MU, Endress, T, Buning, H, Hallek, M, Brauchle, C (2001) Real-time single-molecule imaging of the infection pathway of an adeno-associated virus. Science 294:1929–32

Shah, JV, Flanagan, LA, Janmey, PA, Leterrier, JF (2000) Bidirectional translocation of neurofilaments along microtubules mediated in part by dynein/dynactin. Mol Biol Cell 11:3495–508

Sharp, DJ, Rogers, GC, Scholey, JM (2000) Cytoplasmic dynein is required for poleward chromosome movement during mitosis in *Drosophila* embryos. Nat Cell Biol 2:922–30

Shenk, T. (2001). Adenoviridae: The viruses and their replication. *In* Fundamental Virology (D. M. Knipe and P. M. Howley, eds.), pp. 1053–1088. Lippincott Williams & Wilkins, Philadelphia

Skepper, JN, Whiteley, A, Browne, H, Minson, A (2001) Herpes simplex virus nucleocapsids mature to progeny virions by an envelopment→deenvelopment→reen-\to*reenvelopmentpathway*.*JVirol*75 : 5697 − −702

Smith, GA, Enquist, LW (2002) Break ins and break outs: Viral interactions with the cytoskeleton of mammalian cells. Annu Rev Cell Dev Biol 18:135–61

Smith, GA, Gross, SP, Enquist, LW (2001) Herpesviruses use bidirectional fast-axonal transport to spread in sensory neurons. Proc Natl Acad Sci U S A 98:3466–70

Smith, GL, Vanderplasschen, A, Law, M (2002) The formation and function of extracellular enveloped vaccinia virus. J Gen Virol 83:2915–31

Sodeik, B (2000) Mechanisms of viral transport in the cytoplasm. Trends Microbiol 8:465–72

Sodeik, B (2002) Unchain my heart, baby let me go—the entry and intracellular transport of HIV. J Cell Biol 159:393–5

Sodeik, B, Doms, RW, Ericsson, M, Hiller, G, Machamer, CE, van 't Hof, W, van Meer, G, Moss, B, Griffiths, G (1993) Assembly of vaccinia virus: role of the intermediate compartment between the endoplasmic reticulum and the Golgi stacks. J Cell Biol 121:521–41

Sodeik, B, Ebersold, MW, Helenius, A (1997) Microtubule-mediated transport of incoming herpes simplex virus 1 capsids to the nucleus. J Cell Biol 136:1007–21

Sodeik, B, Krijnse-Locker, J (2002) Assembly of vaccinia virus revisited: de novo membrane synthesis or acquisition from the host? Trends Microbiol 10:15–24

Suikkanen, S, Aaltonen, T, Nevalainen, M, Välilehto, O, Lindholm, L, Vuento, M, Vihinen-Ranta, M (2003) Exploitation of microtubule cytoskeleton and dynein during parvoviral traffic towards the nucleus. J Virol 77:10270–9

Suikkanen, S, Saajarvi, K, Hirsimaki, J, Valilehto, O, Reunanen, H, Vihinen-Ranta, M, Vuento, M (2002) Role of recycling endosomes and lysosomes in dynein-dependent entry of canine parvovirus. J Virol 76:4401–11

Suomalainen, M, Nakano, MY, Boucke, K, Keller, S, Greber, UF (2001) Adenovirus-activated PKA and p38/MAPK pathways boost microtubule-mediated nuclear targeting of virus. EMBO J 20:1310–9

Suomalainen, M, Nakano, MY, Keller, S, Boucke, K, Stidwill, RP, Greber, UF (1999) Microtubule-dependent plus- and minus end-directed motilities are competing processes for nuclear targeting of adenovirus. J Cell Biol 144:657–72

Susalka, SJ, Nikulina, K, Salata, MW, Vaughan, PS, King, SM, Vaughan, KT, Pfister, KK (2002) The roadblock light chain binds a novel region of the cytoplasmic dynein intermediate chain. J Biol Chem 277:32939–46

Tai, AW, Chuang, JZ, Sung, CH (2001) Cytoplasmic dynein regulation by subunit heterogeneity and its role in apical transport. J Cell Biol 153:1499–510

Takeda, S, Yamazaki, H, Seog, DH, Kanai, Y, Terada, S, Hirokawa, N (2000) Kinesin superfamily protein 3 (KIF3) motor transports fodrin-associating vesicles important for neurite building. J Cell Biol 148:1255–65

Tang, Q, Staub, CM, Gao, G, Jin, Q, Wang, Z, Ding, W, Aurigemma, RE, Mulder, KM (2002) A novel transforming growth factor-beta receptor-interacting protein that is also a light chain of the motor protein dynein. Mol Biol Cell 13:4484–96

Tang, Y, Winkler, U, Freed, EO, Torrey, TA, Kim, W, Li, H, Goff, SP, Morse, HC, 3rd (1999) Cellular motor protein KIF-4 associates with retroviral Gag. J Virol 73: 10508–13

Tekotte, H, Davis, I (2002) Intracellular mRNA localization: motors move messages. Trends Genet 18:636–42

Tolonen, N, Doglio, L, Schleich, S, Krijnse Locker, J (2001) Vaccinia virus DNA replication occurs in endoplasmic reticulum-enclosed cytoplasmic mini-nuclei. Mol Biol Cell 12:2031–46

Tomishima, MJ, Enquist, LW (2001) A conserved α-herpesvirus protein necessary for axonal localization of viral membrane proteins. J Cell Biol 154:741–752

Topp, KS, Bisla, K, Saks, ND, Lavail, JH (1996) Centripetal transport of herpes simplex virus in human retinal pigment epithelial cells in vitro. Neuroscience 71:1133–44

Topp, KS, Meade, LB, LaVail, JH (1994) Microtubule polarity in the peripheral processes of trigeminal ganglion cells: relevance for the retrograde transport of herpes simplex virus. J Neurosci 14:318–25

Trotman, LC, Mosberger, N, Fornerod, M, Stidwill, RP, Greber, UF (2001) Import of adenovirus DNA involves the nuclear pore complex receptor CAN/Nup214 and histone H1. Nat Cell Biol 3:1092–100

Tsiang, H, Ceccaldi, PE, Lycke, E (1991) Rabies virus infection and transport in human sensory dorsal root ganglia neurons. J Gen Virol 72:1191–4

Valetti, C, Wetzel, DM, Schrader, M, Hasbani, MJ, Gill, SR, Kreis, TE, Schroer, TA (1999) Role of dynactin in endocytic traffic: effects of dynamitin overexpression and colocalization with CLIP-170. Mol Biol Cell 10:4107–20

van Eijl, H, Hollinshead, M, Rodger, G, Zhang, WH, Smith, GL (2002) The vaccinia virus F12L protein is associated with intracellular enveloped virus particles and is required for their egress to the cell surface. J Gen Virol 83:195–207

van Leeuwen, H, Elliott, G, O'Hare, P (2002) Evidence of a role for nonmuscle myosin II in herpes simplex virus type 1 egress. J Virol 76:3471–81

van Loo, ND, Fortunati, E, Ehlert, E, Rabelink, M, Grosveld, F, Scholte, BJ (2001) Baculovirus infection of nondividing mammalian cells: mechanisms of entry and nuclear transport of capsids. J Virol 75:961–70

Vanderplasschen, A, Hollinshead, M, Smith, GL (1998) Intracellular and extracellular vaccinia virions enter cells by different mechanisms. J Gen Virol 79:877–87

Verhey, KJ. (2003). Motors and membrane trafficking. *In* Molecular Motors (M. Schliwa, ed.), pp. 377–409. Wiley-VCH Verlag, Weinheim

Ward, BM, Moss, B (2001) Vaccinia virus intracellular movement is associated with microtubules and independent of actin tails. J Virol 75:11651–63

Welch, MD, Mullins, RD (2002) Cellular control of actin nucleation. Annu Rev Cell Dev Biol 18:247–88

Wilk, T, Gowen, B, Fuller, SD (1999) Actin associates with the nucleocapsid domain of the human immunodeficiency virus Gag polyprotein. J Virol 73:1931–40

Willard, M (2002) Rapid directional translocations in virus replication. J Virol 76:5220–5232

Xu, Y, Takeda, S, Nakata, T, Noda, Y, Tanaka, Y, Hirokawa, N (2002) Role of KIFC3 motor protein in Golgi positioning and integration. J Cell Biol 158:293–303

Ye, GJ, Vaughan, KT, Vallee, RB, Roizman, B (2000) The herpes simplex virus 1 U(L)34 protein interacts with a cytoplasmic dynein intermediate chain and targets nuclear membrane. J Virol 74:1355–63

Young, A, Dictenberg, JB, Purohit, A, Tuft, R, Doxsey, SJ (2000) Cytoplasmic dynein-mediated assembly of pericentrin and gamma tubulin onto centrosomes. Mol Biol Cell 11:2047–56

Zhang, J, Campbell, RE, Ting, AY, Tsien, RY (2002) Creating new fluorescent probes for cell biology. Nat Rev Mol Cell Biol 3:906–18

Zhou, ZH, Chen, DH, Jakana, J, Rixon, FJ, Chiu, W (1999) Visualization of tegument-capsid interactions and DNA in intact herpes simplex virus type 1 virions. J Virol 73:3210–8

Ziegelbauer, J, Shan, B, Yager, D, Larabell, C, Hoffmann, B, Tjian, R (2001) Transcription factor MIZ-1 is regulated via microtubule association. Mol Cell 8:339–49

Zigmond, SH (1993) Recent quantitative studies of actin filament turnover during cell locomotion. Cell Motil Cytoskeleton 25:309–16

Review TRENDS in Microbiology Vol.13 No.7 July 2005

Viral stop-and-go along microtubules: taking a ride with dynein and kinesins

Katinka Döhner, Claus-Henning Nagel and Beate Sodeik

Institute of Virology, Hannover Medical School, D-30623 Hannover, Germany

Incoming viral particles move from the cell surface to sites of viral transcription and replication. By contrast, during assembly and egress, subviral nucleoprotein complexes and virions travel back to the plasma membrane. Because diffusion of large molecules is severely restricted in the cytoplasm, viruses use ATP-hydrolyzing molecular motors of the host for propelling along the microtubules, which are the intracellular highways. Recent studies have revealed that, besides travelling inside endocytic or exocytic vesicles, viral proteins interact directly with dynein or kinesin motors. Understanding the molecular mechanisms of cytoplasmic viral transport will aid in the construction of viral vectors for human gene therapy and the search for new antiviral targets.

Intracellular trafficking

Viruses are obligate intracellular parasites and therefore depend on the cellular machinery for membrane trafficking, nuclear import and export, and gene expression. In fact, the molecular mechanisms of these processes have been elucidated to a large extent by studying viral systems. Although diffusion is efficient for translocation over very short distances, it does not provide a means for directed long-distance transport. Moreover, the free diffusion of molecules larger than 500 kDa is restricted in the cytoplasm if compared with diluted buffers, this being a result of molecular crowding by organelles, the cytoskeleton and high protein concentrations [1]. It has been calculated that a herpes simplex virus (HSV) capsid would need 231 years for a diffusional translocation of 1 cm in axonal cytoplasm [2]. Thus, for intracellular transport, viruses again use host machinery [2–5].

The cellular and viral solution to master intracellular trafficking is an organized network of three cytosolic filaments – actin filaments, intermediate filaments and microtubules (MTs) – which are regulated by many kinases and phosphatases, in addition to tubulin- or actin-binding proteins (Box 1). Moreover, these filaments operate together, and several proteins provide direct links between them [5,6]. The highways for long distance transport are polar MTs (Box 1) with distinct minus- and plus-ends; their ATP-hydrolyzing motors are dyneins (Box 2) and kinesins (Box 3). Because a particular motor moves only in one direction, the cell-specific organization

Box 1. Microtubules (MTs) are part of the host cytoskeleton

MTs are long, hollow cylinders assembled from equally oriented heterodimers of α- and β-tubulin and MT-associated proteins [79]. This head-to-tail association gives MTs an intrinsic structural polarity with distinct ends: the 'minus'-end depolymerizes if not stabilized by other proteins, and it polymerizes three times slower than the opposite 'plus'-end. MTs grow primarily at the plus-end, but can also depolymerize from the plus-end, a phenomenon called dynamic instability that leads to alternating phases of growth and shrinkage. This dynamic instability anables temporal and spatial flexibility in MT organization. Tubulin dimers are arranged in 13 protofilaments that are nucleated by the MT-organizing centre (MTOC). MTs can detach from an MTOC, and the resulting non-centrosomal MTs either depolymerize or are stabilized by minus-end protein complexes [77]. Plus-end-binding proteins stabilize the plus-end, and enable interaction with the actin cortex, organelles or kinetochores. This search-and-capture mechanism together with MT-associated proteins can stabilize an existing MT network [80]. Different cell types contain different MT arrays that reach the entire cytosol [78] (see Figure 1 in main text).

Box 2. Cytoplasmic dynein and its cofactor dynactin

Most minus-end-directed microtubule (MT) transport is catalyzed by cytoplasmic dynein, a 20 S protein complex consisting of two dynein heavy chains (DHCs; 520 kDa), two dynein intermediate chains (DICs; 74 kDa), several dynein light intermediate chains (DLICs; 53–57 kDa) and a series of dynein light chains (DLCs) from the LC8, Tctex/rp3 and LC7/roadblock families [7]. The C terminus of DHC comprises both the globular head that hydrolyses ATP and a stalk that terminates in a MT-binding domain. The N terminus mediates DHC dimerization and binding to DLIC and to DIC, which also binds to DLCs. DIC, DLIC and DLC are implicated in cargo binding and regulation of motor activity. There are two DHC, two DIC, two DLIC, two LC7 and three LC8 genes, and further diversity is generated by different isoforms of DIC and DLIC. Dynein holoenzymes with different subunit composition can recognize diverse cargos.

Cytoplasmic dynein is assisted by another large protein complex of 20 S called dynactin, which enhances the processivity of dynein-mediated transport, and is involved in cargo binding [8]. Dynactin consists of a filament of the actin-related protein 1 (Arp1) and a flexible sidearm projecting from this filament (see Figure 2 in main text). The Arp1 filament is capped at its plus-end by the actin-capping protein CapZ, and at its minus-end by a heterotetrameric complex of Arp11, p62, p25 and p27. The projecting side arm consists of two copies of $p150^{Glued}$, four molecules of dynamitin and the homodimer p24/p22. The latter two form a shoulder-like structure that connects the $p150^{Glued}$ sidearm to the Arp1 filament. If dynamitin is present in large excess, the 20 S dynactin complex separates in two non-functional subcomplexes.

Corresponding author: Sodeik, B. (Sodeik.Beate@MH-Hannover.de).
Available online 9 June 2005

 0966-842X/$ - see front matter doi:10.1016/j.tim.2005.05.010

Box 3. The many members of the kinesin family

Kinesins are members of a superfamily containing 45 human proteins [9] (http://www.proweb.org/kinesin/MotorSeqTable.html; see Figure 2 in main text). They contain a microtubule (MT)-binding motor domain of 320 amino acids that is folded similarly to myosins and G proteins.

'Conventional kinesin' has two heavy chains (KHCs; kinesin-1; 120 kDa) and two light chains (KLCs; 64 kDa). KHCs are composed of a N-terminal motor domain, followed by a coiled-coil region that mediates dimerization. The N terminus of KLC interacts with the C terminus of KHC, and a tetratricopeptide motif (TPR) in the C terminus of KLC and the KHC tail mediate cargo binding. Three KHC and three KLC genes create different motors. Kinesin-1 can interact with cytoplasmic dynein through KLC and dynein intermediate chain [67].

Two members of the kinesin-2 family and the kinesin-associated protein (KAP) form a 'heterotrimeric kinesin', which mediates axonal and intraflagellar transport. The $p150^{Glued}$ subunit of dynactin interacts with KAP3 [66]. Members of the kinesin-3 family are monomeric in solution, but dimerize on membranes, and thus become processive. They have a pleckstrin-homology domain that facilitates membrane attachment and transport vesicles to the nerve terminals of motor neurons and mitochondria. Kinesin-4 is a homodimer involved in vesicle transport and mitosis. Kinesin-14 proteins carry their motor domain at the C terminus, and catalyse minus-end-directed transport.

of the MT determines the destination a specific motor can reach (Figure 1). Cytoplasmic dyneins [7,8] and C-type kinesins [9] power transport to MT minus-ends, whereas the N-type kinesins propel cargo to plus-ends [9].

Cells require MTs for long-term normal physiology, and viruses are obligate cellular parasites that completely depend on the physiology of the host cell [7–9]. Thus, it is no surprise that most, if not all, viral life cycles require MTs for efficient replication. Moreover, there is a growing list of reports showing that MT motors also catalyze the intracellular transport of many viral structures. To accomplish this, viruses use two alternative strategies: (1) hijacking of cytoplasmic membrane traffic, namely endocytosis for cell entry and exocytosis for egress, or (2) direct interaction of viral components with MT motors [2]. The latter is the focus of this review.

The membrane vesicles occupied by viruses might 'know' which motor to recruit, or cytosolic domains of viral membrane proteins could modify motor recruitment of the vesicle. Recent studies have revealed several potential direct interactions between viral components and MT motors (Table 1). Although the cell often uses

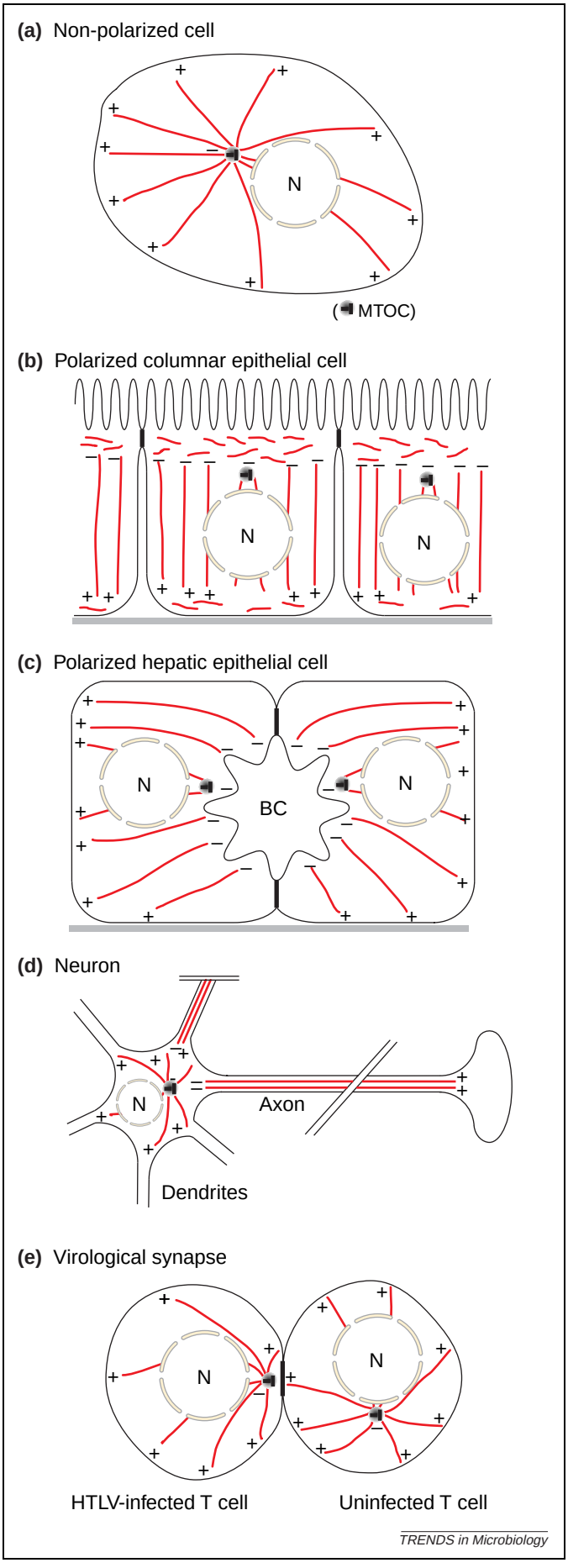

Figure 1. Organization of microtubules (MTs) in different cell types. **(a)** MTs (red) of unpolarized fibroblasts or epithelial cells radiate from the MT-organizing centre (MTOC) to the cell periphery, where their plus-ends (+) are located. The MTOC nucleates MT minus-ends (−) and is often close to the nucleus (N) [77]. **(b)** In polarized columnar epithelial cells, MTs form an apico-basal array with their plus-ends near the basal surface and the minus-ends pointing to the apical membrane. Moreover, there is an apical and a basal MT web composed of short filaments. Only few MTs are associated with the MTOC under the cell apex [77]. **(c)** In polarized hepatic epithelial cells, MT minus-ends point towards the bile canaliculi (BC; apical domain), whereas plus-ends face the basolateral membrane. Only few MTs are associated with the MTOC [78]. **(d)** In the soma of neurons, MTs are radially arranged with their minus-ends attached to the MTOC. Axons and dendrites contain noncentrosomal MTs. Axons have MTs of uniform polarity, with their plus-ends pointing towards the synapse. In the proximal region of dendrites, the polarity of MTs is mixed, whereas in the distal end, the polarity is the same as in the axon [9]. **(e)** During formation of a virological synapse (e.g. between an human T-cell leukaemia virus (HTLV)-infected T cell and an uninfected T cell), the MTOC of the infected cell is polarized towards the side of cell–cell contact [37].

Table 1. Motor subunits interacting with viral proteins[a]

Motor	Subunit	Viral interaction partner	Methods	Refs
Dynein	DIC-1a	HSV-1 nuclear protein UL34	GST-pulldown	[54]
	LC8	HSV-1 capsid protein VP5	Pepscan[b]	[81]
		HSV-1 helicase UL9	Pepscan	[81]
		HIV-1 integrase	Yeast two-hybrid	[82]
		Foamy virus Gag protein	Coimmunoprecipitation	[45]
		Ad protease	Pepscan	[81]
		VV polymerase	Pepscan	[81]
		ASFV p54	Yeast two-hybrid, Pepscan, coimmunoprecipitation, affinity chromatography, colocalization	[48,83]
		Rabies virus phosphoprotein	Yeast two-hybrid, Pepscan, coimmunoprecipitation	[83–85]
		Mokola virus phosphoprotein	Coimmunoprecipitation, colocalization, Pepscan, yeast two-hybrid	[83,86]
		Human papillomavirus E4 protein	Pepscan	[81]
		HRSV; extracellular domain of attachment glycoprotein	Pepscan	[81]
		Human coxsackievirus capsid protein	Pepscan	[81]
		Baculovirus ORF AMV179	Pepscan	[81]
		Yam mosaic potyvirus polyprotein	Pepscan	[81]
	Tctex-1, rp3	HSV-1 capsid protein VP26	Yeast two-hybrid, GST-pulldown	[52]
	TCTEL1	Ad 2; E3–14.7K through FIP-1	Yeast two-hybrid, GST-pulldown, coimmunoprecipitation	[87]
	Tctex-1	Poliovirus through poliovirus receptor CD155	Yeast two-hybrid, GST-pulldown, coimmunoprecipitation	[88,89]
Kinesin-1	KHC	HSV-1 US11	Affinity chromatography, GST-pulldown	[35]
	PAT1, subunit of a kinesin?	HSV-1 US11	Yeast two-hybrid, GST-pulldown, colocalization after transfection	[58]
	KLC	VV A36R	Yeast two-hybrid, GST-pulldown	[57]
Kinesin-3	KIF1A	HSV-2 UL56	Yeast two-hybrid, GST-pulldown, colocalization	[61]
Kinesin-4		Retroviral Gag	Yeast two-hybrid, GST-pulldown, coimmunoprecipitation	[62,90]

[a]Abbreviations: Ad, adenovirus; ASFV, African swine fever virus; FIP-1, 14.7K-interacting protein; GST, glutathione-S-transferase; HIV, human immunodeficiency virus; HRSV, human respiratory syncytial virus; HSV, herpes simplex virus; KHC, kinesin heavy chain; KIF, kinesin superfamily protein; KLC, kinesin light chain; ORF, open reading frame; PAT1, protein interacting with amyloid precursor protein tail 1; VV, vaccinia virus.
[b]Binding to synthetic dodecapeptides covalently bound to cellulose membrane.

adaptors to link a cargo with a specific motor [7–10], all viral examples described so far showed either transport inside vesicles or a direct interaction of a viral protein and a motor subunit. The recent advances in live cell imaging revealed that many cellular and viral cargos move along MTs in both directions, suggesting the recruitment of multiple motors and a careful regulation of motor activity [11,12]. This raises the questions as to how net transport is achieved, and which potential benefits such seemingly ATP-wasting phenomena might provide.

Analysing viral transport along microtubules

A broad spectrum of cell biology and virology tools is available to study the role of MT motors during viral infection [4,5,8]. Fluorophores or fluorescent proteins can be attached directly to a viral structure. Although such a tag might alter assembly or subsequent virus entry, quantitative virological, cell biological and genetic assays provide excellent controls to ascertain that a given fusion protein has taken the place and function of its wild-type counterpart [4,5]. The fluorescent signals might represent aggregated viral proteins, vesicles containing viral proteins, subviral intermediates in the assembly or disassembly pathway, cytosolic viral particles attached to vesicles, viruses inside vesicles, or extracellular virus. Simultaneous tagging of multiple viral and cellular components can distinguish between these possibilities [13–15].

Using fluorescent tags, viral particles were shown to move along MTs at a speed of $\sim$0.2–4 $\mu m\ sec^{-1}$, similar to speeds of cellular cargoes [13,15–25]. These are faster transport rates than are achieved by random walk [2]. Single molecule measurements showed that, under load, cytoplasmic dynein and kinesin-1 make steps of 8 nm [26,27]. For a processive motor that runs with 2 $\mu m\ sec^{-1}$, this calculates to $\sim$250 steps sec^{-1}. A human 100 m run roughly requires 50 steps and as little as 10 s, which corresponds to 5 steps sec^{-1}. Fluorescently tagged viral particles also enable the reconstruction of motility with defined components *in vitro* [8,18]. Such experiments facilitate the distinction of virus transport inside vesicles from direct interactions of MT motors.

Microtubule function during viral infection

Many viruses require MTs during cell entry for efficient nuclear targeting (Figure 1), either for cytosolic transport of naked viral particles or for transport inside vesicles. Examples are herpes simplex virus (HSV) [28], human cytomegalovirus [29], human immunodeficiency virus (HIV) [22], adenovirus (Ad) [16], parvoviruses [20,30], simian virus 40 (SV40) [19], influenza virus [24] or hepatitis B virus [31]. Even incoming cores of vaccinia virus (VV), which replicates in cytoplasmic viral factories, are transported along MTs [14]. MTs and the RNA-binding VV protein L4R are required for efficient transcription and translation of early VV mRNAs [32]. Nuclear targeting has been demonstrated *in vivo* with green fluorescent protein (GFP)-VP26-tagged pseudorabies virus (PRV) in neurons [15], GFP-Vpr-tagged HIV [22], fluorescent dyes directly coupled to Ad, SV40 and adeno-associated virus

[16,17,20] or intercalated in the membrane of influenza virus [24]. However, transgene expression of baculovirus in mammalian cells is increased if MTs are depolymerized [33]. Incoming baculovirus capsids induce prominent actin cables that are possibly involved in transport to the nucleus and, in this situation, the MTs might be obstacles rather than highways.

During assembly and egress, viruses also need MTs for trafficking inside exocytic vesicles or for cytosolic transport of capsids and nucleoprotein particles to the budding compartment. Whereas virus yields are reduced if MTs are depolymerized during assembly, the radial MT organization (Figure 1) of undifferentiated epithelial cells is lost late in HSV infection: MTs are marginalized in bundles to the cell periphery, and a microtubule-organizing centre (MTOC) is no longer recognizable [34]. Nevertheless, herpesvirus particles tagged with GFP-VP11/12 or GFP-VP26 translocate along MTs over distances of up to 49 μm [21,23]. If budding occurred at endosomes or the Golgi apparatus, which are mostly clustered around the MTOC, capsids should move to MT minus-ends; by contrast, in neurons, viral structures use plus-end-directed transport to axon terminals [4,5,15,35].

For budding, subviral HIV particles assembled in the cytosol are transported to the plasma membrane. Both MTs and the binding motif for the host RNA-binding protein hnRNP A2 present in genomic HIV RNA are involved in the trafficking of viral RNA granules [36]. Budding and transmission of the human T-cell leukaemia virus occurs at a virological synapse formed after adhesion between an infected cell and an uninfected T cell. In the infected cell, the MTOC rapidly moves towards the adhesion site, resulting in many MT plus-ends pointing towards the cell junction [37].

After assembly, the intracellular mature virus (IMV) of VV is transported from the viral factories to the MTOC [38,39], where it is wrapped by a membrane cisterna to form the intracellular enveloped virus (IEV; Figure 2). During its saltatory and directional transport to the cell periphery, the IEV occasionally switches MT [13]. The IEV outer membrane fuses with the plasma membrane. While still attached to the plasma membrane, the resulting cell-associated extracellular virus induces a cytosolic actin tail that can push it into a neighbouring cell [40]. Despite all this transport, the ability of the MTOC to nucleate MTs is destroyed during assembly of VV and African swine fever virus (ASFV) [38,41].

Viral interactions with dynein

By microinjecting function-blocking anti-dynein antibodies or overexpressing dynamitin (Box 2), the role of dynein was established for the efficient nuclear targeting of HSV, Ad or canine parvovirus (CPV) capsids [16,17,30,42], HIV reverse transcription complexes [22] and influenza virus [24]. Moreover, incoming HSV capsids colocalize with dynein and its cofactor dynactin [28,42], and Ad [43] in addition to CPV [30] capsids can interact with dynein and MT *in vitro*.

Dynein transports endosomes containing virions or cytosolic incoming viral particles to the MTOC, which in many cells is located close to their final destination, the nucleus (Figure 1). It is unclear whether and how viral particles move from the MTOC further to the nucleus [44]. Although viral capsids initially accumulate at the nuclear site facing the MTOC, they later distribute over the entire nuclear surface, suggesting additional transport mechanisms [28,42,45]. Recent analysis on retrograde transport in injured axons shows that dynein can interact with the nuclear import receptor importin-α and recruit a nuclear import cargo that is bound to importin-β [46]. In this axonuclear communication, minus-end-directed MT transport is coupled to nuclear import. Several viral proteins and even viral capsids bind to host importins [47]. Besides providing a mechanism to recruit dynein, importins could facilitate transport from the MTOC to the nucleus. Alternatively, viral particles might use plus-end-directed MT motors to proceed.

During virus assembly and egress, dynein can transport subviral particles to a budding organelle located close to the MTOC. ASFV infection is inhibited by MT depolymerization and dynamitin overexpression [48,49]. Dynein catalyses the transport of the IMV form of VV from the virus factory to the MTOC, where the wrapping in a membrane cisterna results in the formation of IEVs [38,39]. Moreover, dynein conveys newly synthesized Gag to the MTOC in Mason–Pfizer monkey virus infection [50]. The Env complex, which is localized in the pericentriolar recycling compartment, then triggers further transport to the plasma membrane.

These examples raise the question as to which viral proteins interact with which subunit of dynein or dynactin (Box 2). Dynactin is a multifunctional adaptor that helps MT motors to interact with many cellular cargos [8]. However, so far, only dynein subunits, mainly the dynein light chain (DLC), have been identified as potential direct interaction partners of viral proteins (Table 1). A human foamy virus vector lacking the LC8 binding motif in its Gag is less infectious, suggesting that Gag and dynein could mediate the MTOC localization during virus entry [45]. In many instances, the putative cargo-binding region on the different DLCs overlaps with their dynein intermediate chain (DIC)-binding region. Thus, this region could only be responsible for cargo recruitment if one subunit of the DLC dimer interacts through DIC with the dynein motor, and the other subunit of the DLC dimer interacts with the putative cargo [7,51]. This scenario would leave one DLC-binding site on the DIC dimer unoccupied. Moreover, LC8 is also present in other protein complexes, and binding to LC8 might have functions independent of dynein [7].

The small capsid protein VP26 of HSV-1 can interact with the DLCs Tctex-1 and rp3 [52]. Whereas microinjected capsids with VP26, but not capsids without VP26, accumulate at the nucleus [53], a VP26 deletion mutant delivers viral genomes as efficient as wild type to the neuronal nuclei in the trigeminal ganglia [53]. The HSV-1 primary envelope protein UL34 can interact with DIC [54]. Nevertheless, UL34 is unlikely to have a role in HSV cytoplasmic transport because it is absent from cytoplasmic membranes and cytoplasmic, in addition to extracellular, virions [55].

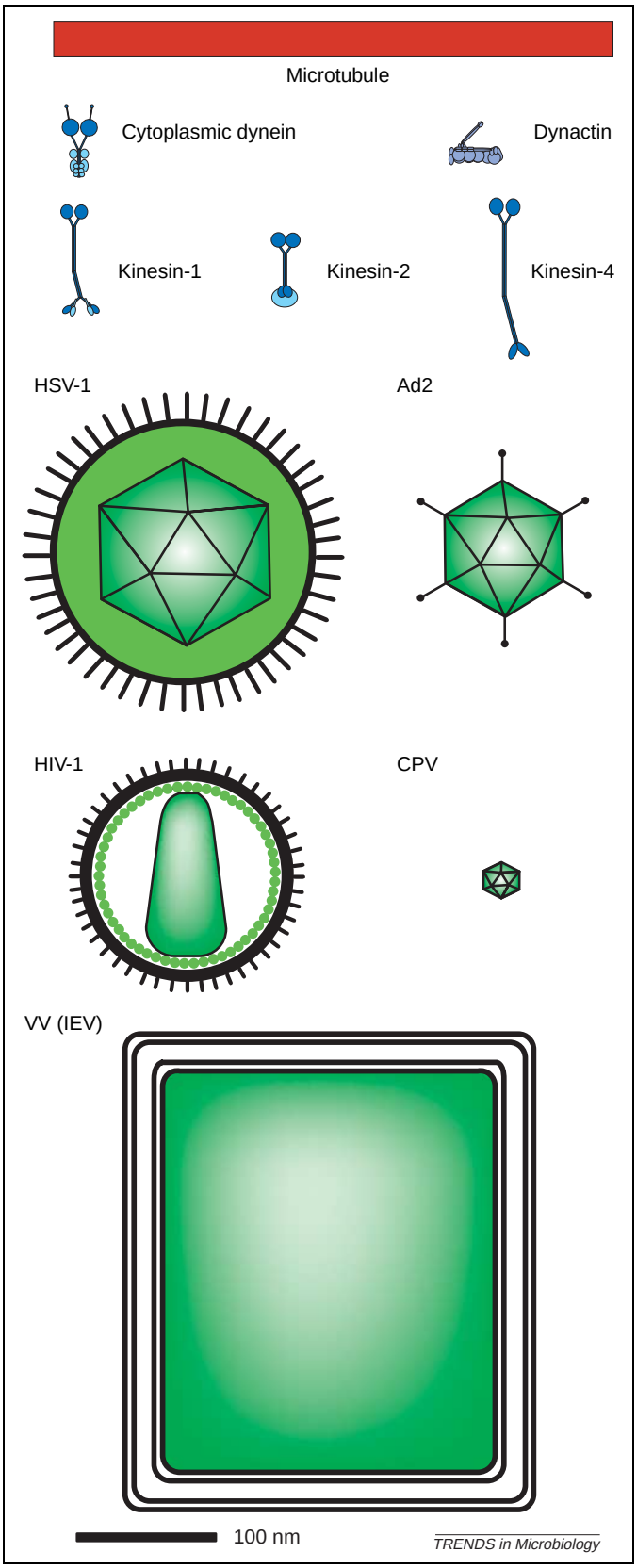

Figure 2. The morphology of viral cargos and microtubule (MT) motors. MTs (red) are hollow cylinders with a diameter of 25 nm. Cytoplasmic dynein heavy chains (DHC; dark blue) comprise the globular heads with a diameter of 12 nm and a 9 nm stalk that terminates in a MT-binding domain. The N-terminal DHC stem binds dynein light intermediate chains (DLCs) and dynein intermediate chains (DICs; light blue; [7]). Dynactin consists of a 10 nm×40 nm rod made mainly of Arp1, and a flexible sidearm of $p150^{Glued}$ projecting with a length of 25–50 nm from this filament [8]. Dynein and other motors are thought to bind to dynactin along or near the base of this arm. Each globular head of $p150^{Glued}$ has a MT-binding site, whereas the Arp1 filament has been implicated in cargo binding. Kinesin-1 (~80 nm length) has a rod-like structure with two heads with a diameter of 10 nm, a stalk, and a fan-like end. Kinesin-1 is a heterotetramer of two kinesin heavy chains (KHCs; dark blue) and two kinesin light chains (KLCs; light blue). Kinesin-2 (~54 nm length) is a heterotrimer of two KIF3 chains (dark blue) that form globular heads with a diameter of 10 nm, and one kinesin-associated protein (KAP; light blue). Kinesin-4 (~116 nm) is a dimer of two KIF4 chains with two globular heads of 12 nm diameter, a central α-helical coiled-coil stalk and a globular tail [9]. Herpes simplex virus (HSV) has a diameter of ~225 nm. It contains an icosahedral capsid (dark green) of 125 nm diameter enclosing the DNA genome, a tegument with ~20 proteins (light green) and an envelope that anchors the viral spikes (black). Adenoviruses (Ad) have a diameter of 70–100 nm. They consist of an icosahedral capsid (green) that encloses the genome and DNA-associated proteins. 12 fibres project from the vertices of the capsid and terminate in knobs (black). Human immunodeficiency virus type 1 (HIV-1) has a diameter of 145 nm. The two single-stranded RNA genomes and associated proteins are surrounded by a cone-shaped capsid (dark green). The matrix (light green) is localized underneath the envelope that contains viral glycoproteins (black). Canine parvovirus is an icosahedral capsid (green) with a diameter of 26 nm. The intracellular mature virus (IMV) of vaccinia virus (VV) is roughly brick shaped and measures ~300–310×240–250×110–140 nm. The intracellular enveloped virus (IEV) shown here contains two additional membranes. For comparison, all structures were drawn approximately to scale.

Viral interactions with kinesins

The kinesin family has a large variety of kinesin motor subunits [9] (Box 3). Thus, viruses can choose from many different plus-end-directed MT motors (Table 1).

The IEV of VV and ASFV particles that are transported from the trans-Golgi network to the cell surface colocalize with kinesin-1, and the overexpression of the cargo-binding domain of the KLC reduces the number of particles in the cell periphery [13,56]. VV mutants lacking the IEV protein A36R are arrested in the perinuclear region, and KLC binds directly to the cytosolic tail of A36R [13,57]. At the plasma membrane, the tyrosine kinase Src phosphorylates A36R, and thus mediates the transition from kinesin-1 transport to actin-tail formation [40].

Axonal HSV progeny capsids also colocalize with kinesin-1, and the predicted cargo-binding domain of kinesin heavy chain (KHC) recruits the major capsid protein VP5 and the tegument proteins VP16, VP22 and US11 from an infected cell lysate [35]. With VP16 and VP22 also binding to US11, the latter is considered the direct binding partner of KHC. This is also because recombinant US11, in contrast to VP16, binds to KHC, and because VP5 is not very accessible on the capsid surface after tegumentation. Recombinant US11 neither binds kinesin light chain (KLC) nor competes for its binding site on the KHC tail [35]. US11 also interacts with PAT1 in a region that has sequence similarity to the cargo-binding domain in KLC of kinesin-1 [58]. PAT1 is a nucleocytoplasmic host protein that binds to the cytosolic tail of amyloid precursor protein (APP) and to MTs in a nucleotide-dependent manner, but it is unclear whether it functions as a motor subunit [59]. The promiscuous C-terminal basic region of US11 binds to KHC and PAT1, but also to mRNAs, double-stranded RNA, rRNA, the antiviral protein kinase R (PKR) and PACT (PKR-activating protein), and proteins involved in cell growth arrest [35,58,60].

Secretory vesicles containing viral membrane proteins or even complete virions must also recruit plus-end-directed motors for transport to the plasma membrane. An example for this might be the binding of the C terminus

of HSV-UL56 to the kinesin-3 family member KIF1A [61]. Moreover, the matrix protein present in the cytosolic Gag polyprotein of many retroviruses binds to kinesin-4 [62], and this interaction might convey subviral particles to the plasma membrane for virus budding.

Bidirectional transport along microtubules

The great surprise from live cell imaging is that viruses like cellular organelles often stop and restart runs, switch between different MTs, and even change directions on a single MT resulting in saltatory movements and pauses for long periods with no apparent translocation. Many cargoes show plus-end- and minus-end-directed MT transport: mitochondria, intermediate filaments, ribonucleoprotein complexes, endosomes, phagosomes, lipid droplets and secretory vesicles [11,12,63,64]. This list is likely to grow because the ability to record bidirectional transport increases with improved temporal and spatial resolution [11,12]. Individual particles cannot be tracked unambiguously and short changes in direction might be missed if there are undocumented periods between consecutive frames.

Bidirectional transport has also been observed for PRV [15,21], HSV [23,42], Ad [16,65], HIV-1 [22] and influenza virus [24]. Whereas the latter is an endocytic voyager, the others probably represent direct interactions between viral structures and MT motors. Inhibition of dynein leads to more plus-end-directed transport of HSV, Ad and HIV to the cell periphery [16,22,42]. Dynamitin overexpression reduces the extent and frequency of minus-end-directed Ad transport, whereas plus-end-directed motion is detected more often [16].

Bidirectional MT transport can be used (1) to set up a homogenous or polarized distribution of a given cargo that could then be anchored to its subcellular destination, (2) to adjust quickly the net transport in response to an internal or external signal, (3) to step back to circumvent obstacles on the MT track, (4) to explore different regions of the cell, or (5) for error correction [12]. To achieve these goals, different motors on different cargos must be carefully regulated: dynein might be inactive on one cargo, and at the same time active on another [11,12,63]. This implies that viruses must 'know' how to activate MT motors to ensure net transport to their desired destination. Activation of protein kinase A and p38 mitogen-activated protein kinase (MAPK) during Ad entry stimulates the frequency and velocity of minus-end-directed motility [65]. On the basis of the experimental systems studied so far, three models have been developed to describe the potential regulation of bidirectional MT transport [11,12,63].

The first is a model of 'exclusive motor presence'. If there would be only a unique binding site on a particular cargo, binding of a plus-end- or a minus-end-directed motor could alternate but not occur simultaneously. To change direction, a bound motor would have to detach and another motor be recruited.

According to the second, 'tug-of-war', model, net transport is achieved when one type of motor is more active or makes larger steps than the other present on this cargo. In this scenario, interference for example with dynein activity would improve plus-end-directed transport. However, treatments designed to block dynein also abolish plus-end transport in some systems.

These results lead to the third model of 'coordinated regulation', in which motors with opposite polarity attach to a cargo, and their activities are coordinated by a common upstream mechanism. For example, PRV tagged with GFP-VP26 moves in both directions in axons, and coordinated regulation seems to be responsible for the dominance of the plus-end-directed transport late in infection [15,21].

The coordination of opposite-polarity motors could be mediated by dynactin, other adaptor proteins, or specific motor regulation by kinases or phosphatases [63]. The dynactin subunit $p150^{Glued}$ interacts with both DIC of dynein and kinesin-associated protein (KAP) of kinesin-2, overexpression of dynamitin can inhibit dynein and kinesin-2 transport, and dynein and kinesin-1 can physically interact with each other through DIC and KLC [66,67]. Moreover, dynein and kinesin-1 compete for an overlapping MT-binding site [68], and motor domains bound to MT might therefore prevent binding of other motors.

Live microscopy of defined viral particles analysed at high spatial and temporal resolution will reveal how and why so many cargoes including viruses use bidirectional transport (Box 4).

Microtubules in antiviral host responses?

Dynein also transports large protein aggregates to the MTOC where they are packaged into aggresomes [69]. Such aggresomes either recruit chaperones for refolding, proteasomes to clear this 'garbage' from the cytosol or are eliminated by autophagy that terminates in lysosomal degradation [70,71]. Could a cell treat an incoming viral particle as a large protein aggregate that should be degraded [44]? In this scenario, bidirectional MT transport might increase the chance of a viral particle to avoid degradation, and to get further from the MTOC to the nucleus. Moreover, it will be interesting to determine how dynein is recognizing a protein aggregate as garbage destined for degradation.

In a healthy cell, dynein LC8 has been proposed to inactivate Bim, a pro-apoptotic Bcl-2 member protein, but upon specific signals, LC8-Bim can bind to its receptor Bcl-2 on cellular membranes, and apoptosis is induced [72].

Box 4. Future questions

- Do viral and cellular microtubule (MT) motor receptors have homologous domains?
- Do viral and cellular MT motor receptors bind to the same motor subunits?
- Do viral cargos bind to multiple MT motors simultaneously or sequentially?
- How is net transport to MT minus- or plus-ends regulated during viral entry or egress?
- What viral or cellular signals trigger changes in transport direction?
- Do viruses use and regulate MT motors in the same way in different cell types (e.g. viral infection of epithelial cells versus infection of neurons)?
- Do viruses interfere with apoptosis and stress responses through dynein light chain?

Apoptosis is initiated by a defined proteolytic cascade and ultimately results in cell death. During apoptosis, most minus-end-directed MT transport is also inhibited because DIC and the dynactin subunit $p150^{Glued}$ are cleaved by caspases [73]. Many viruses induce apoptosis; however, they also encode proteins that block apoptosis [74]. Several viral proteins interact with LC8 (Table 1), and might therefore modulate Bim activity. The LC8-binding protein p54 of ASFV induces apoptosis after transient transfection, as does the infection with ASFV, possibly by p54 binding to LC8 and thus releasing Bim [48,75]. LC8 also interacts with IκB, which forms a heterodimer with NF-κB, which is involved in stress responses during virus infection and regulates the expression of many anti-apoptotic proteins [7,76].

Concluding remarks and future perspectives

MTs have important roles for most if not all viruses during entry, assembly or egress. Dynein is the motor for transport to the MTOC during virus entry and assembly. The interaction of viral proteins with kinesins emerges as a common feature during assembly and egress, and might also catalyse transport from the MTOC to the nucleus during entry. Many viral particles show bidirectional motility, but nevertheless achieve net transport to the minus- or plus-ends of MTs in different phases of their life cycle. With the emerging technologies in digital time-lapse microscopy, further analysis will dissect the underlying virus–host interactions. A major challenge will be to elucidate how viruses adjust the regulation of motor activity to fulfil their transport needs (Box 4).

This knowledge will aid in the development of viral vectors to express therapeutic proteins because viruses have perfected the art of protecting genetic material and transporting it to and within specific cells. Moreover, the viral binding sites on MT motors might provide new targets for the development of antiviral therapy. Although the host also depends on the motors, viruses might interact with them through unique sites. Finally, viral particles provide excellent tools to elucidate the regulation of bidirectional MT transport in animals, cells and *in vitro*.

Acknowledgements

Our research is supported by the *Deutsche Forschungsgemeinschaft* (DFG; So403/1; So403/2). C.-H.N. holds a PhD fellowship from the DFG-Graduate School on Mucosal host pathogen interactions (DFG-GK 745). We thank Kerstin Radtke (Virology, Hanover Medical School) for constructive comments on the manuscript and apologize to the many scientists and viruses whose interesting stories we could not mention owing to space limitations.

References

1 Luby-Phelps, K. (2000) Cytoarchitecture and physical properties of cytoplasm: volume, viscosity, diffusion, intracellular surface area. *Int. Rev. Cytol.* 192, 189–221
2 Sodeik, B. (2000) Mechanisms of viral transport in the cytoplasm. *Trends Microbiol.* 8, 465–472
3 Ploubidou, A. and Way, M. (2001) Viral transport and the cytoskeleton. *Curr. Opin. Cell Biol.* 13, 97–105
4 Smith, G.A. and Enquist, L.W. (2002) Break ins and break outs: viral interactions with the cytoskeleton of mammalian cells. *Annu. Rev. Cell Dev. Biol.* 18, 135–161
5 Döhner, K. and Sodeik, B. (2005) The role of the cytoskeleton during viral Infection. *Curr. Top. Microbiol. Immunol.* 285, 67–108
6 Kodama, A. *et al*. (2004) Coordinating cytoskeletal tracks to polarize cellular movements. *J. Cell Biol.* 167, 203–207
7 Vallee, R.B. *et al*. (2004) Dynein: an ancient motor protein involved in multiple modes of transport. *J. Neurobiol.* 58, 189–200
8 Schroer, T.A. (2004) Dynactin. *Annu. Rev. Cell Dev. Biol.* 20, 759–779
9 Hirokawa, N. and Takemura, R. (2005) Molecular motors and mechanisms of directional transport in neurons. *Nat. Rev. Neurosci.* 6, 201–214
10 Karcher, R.L. *et al*. (2002) Motor–cargo interactions: the key to transport specificity. *Trends Cell Biol.* 12, 21–27
11 Mallik, R. and Gross, S.P. (2004) Molecular motors: strategies to get along. *Curr. Biol.* 14, R971–R982
12 Welte, M.A. (2004) Bidirectional transport along microtubules. *Curr. Biol.* 14, R525–R537
13 Rietdorf, J. *et al*. (2001) Kinesin-dependent movement on microtubules precedes actin-based motility of vaccinia virus. *Nat. Cell Biol.* 3, 992–1000
14 Carter, G.C. *et al*. (2003) Vaccinia virus cores are transported on microtubules. *J. Gen. Virol.* 84, 2443–2458
15 Smith, G.A. *et al*. (2004) Local modulation of plus-end transport targets herpesvirus entry and egress in sensory axons. *Proc. Natl. Acad. Sci. U. S. A.* 101, 16034–16039
16 Suomalainen, M. *et al*. (1999) Microtubule-dependent plus- and minus end-directed motilities are competing processes for nuclear targeting of adenovirus. *J. Cell Biol.* 144, 657–672
17 Leopold, P.L. *et al*. (2000) Dynein- and microtubule-mediated translocation of adenovirus serotype 5 occurs after endosomal lysis. *Hum. Gene Ther.* 11, 151–165
18 Bearer, E.L. *et al*. (2000) Retrograde axonal transport of herpes simplex virus: evidence for a single mechanism and a role for tegument. *Proc. Natl. Acad. Sci. U. S. A.* 97, 8146–8150
19 Pelkmans, L. *et al*. (2001) Caveolar endocytosis of simian virus 40 reveals a new two-step vesicular-transport pathway to the ER. *Nat. Cell Biol.* 3, 473–483
20 Seisenberger, G. *et al*. (2001) Real-time single-molecule imaging of the infection pathway of an adeno-associated virus. *Science* 294, 1929–1932
21 Smith, G.A. *et al*. (2001) Herpesviruses use bidirectional fast-axonal transport to spread in sensory neurons. *Proc. Natl. Acad. Sci. U. S. A.* 98, 3466–3470
22 McDonald, D. *et al*. (2002) Visualization of the intracellular behavior of HIV in living cells. *J. Cell Biol.* 159, 441–452
23 Willard, M. (2002) Rapid directional translocations in virus replication. *J. Virol.* 76, 5220–5232
24 Lakadamyali, M. *et al*. (2003) Visualizing infection of individual influenza viruses. *Proc. Natl. Acad. Sci. U. S. A.* 100, 9280–9285
25 Sampaio, K.L. *et al*. (2005) Human cytomegalovirus labeled with green fluorescent protein for live analysis of intracellular particle movements. *J. Virol.* 79, 2754–2767
26 Mallik, R. *et al*. (2004) Cytoplasmic dynein functions as a gear in response to load. *Nature* 427, 649–652
27 Schnitzer, M.J. and Block, S.M. (1997) Kinesin hydrolyses one ATP per 8-nm step. *Nature* 388, 386–390
28 Sodeik, B. *et al*. (1997) Microtubule-mediated transport of incoming herpes simplex virus 1 capsids to the nucleus. *J. Cell Biol.* 136, 1007–1021
29 Ogawa-Goto, K. *et al*. (2003) Microtubule network facilitates nuclear targeting of human cytomegalovirus capsid. *J. Virol.* 77, 8541–8547
30 Suikkanen, S. *et al*. (2003) Exploitation of microtubule cytoskeleton and dynein during parvoviral traffic toward the nucleus. *J. Virol.* 77, 10270–10279
31 Funk, A. *et al*. (2004) Itinerary of hepatitis B viruses: delineation of restriction points critical for infectious entry. *J. Virol.* 78, 8289–8300
32 Mallardo, M. *et al*. (2001) Microtubule-dependent organization of vaccinia virus core-derived early mRNAs into distinct cytoplasmic structures. *Mol. Biol. Cell* 12, 3875–3891
33 van Loo, N.D. *et al*. (2001) Baculovirus infection of nondividing mammalian cells: mechanisms of entry and nuclear transport of capsids. *J. Virol.* 75, 961–970
34 Kotsakis, A. *et al*. (2001) Microtubule reorganization during herpes simplex virus type 1 infection facilitates the nuclear localization of VP22, a major virion tegument protein. *J. Virol.* 75, 8697–8711

35 Diefenbach, R.J. *et al*. (2002) Herpes simplex virus tegument protein US11 interacts with conventional kinesin heavy chain. *J. Virol.* 76, 3282–3291

36 Mouland, A.J. *et al*. (2001) RNA trafficking signals in human immunodeficiency virus type 1. *Mol. Cell. Biol.* 21, 2133–2143

37 Igakura, T. *et al*. (2003) Spread of HTLV-I between lymphocytes by virus-induced polarization of the cytoskeleton. *Science* 299, 1713–1716

38 Ploubidou, A. *et al*. (2000) Vaccinia virus infection disrupts microtubule organization and centrosome function. *EMBO J.* 19, 3932–3944

39 Sanderson, C.M. *et al*. (2000) The vaccinia virus A27L protein is needed for the microtubule-dependent transport of intracellular mature virus particles. *J. Gen. Virol.* 81, 47–58

40 Newsome, T.P. *et al*. (2004) SRC mediates a switch from microtubule- to actin-based motility of vaccinia virus. *Science* 306, 124–129

41 Jouvenet, N. and Wileman, T. (2005) African swine fever virus infection disrupts centrosome assembly and function. *J. Gen. Virol.* 86, 589–594

42 Döhner, K. *et al*. (2002) Function of dynein and dynactin in herpes simplex virus capsid transport. *Mol. Biol. Cell* 13, 2795–2809

43 Kelkar, S.A. *et al*. (2004) Cytoplasmic dynein mediates adenovirus binding to microtubules. *J. Virol.* 78, 10122–10132

44 Sodeik, B. (2002) Unchain my heart, baby let me go – the entry and intracellular transport of HIV. *J. Cell Biol.* 159, 393–395

45 Petit, C. *et al*. (2003) Targeting of incoming retroviral Gag to the centrosome involves a direct interaction with the dynein light chain 8. *J. Cell Sci.* 116, 3433–3442

46 Hanz, S. *et al*. (2003) Axoplasmic importins enable retrograde injury signaling in lesioned nerve. *Neuron* 40, 1095–1104

47 Greber, U.F. and Fornerod, M. (2005) Nuclear import in viral infections. *Curr. Top. Microbiol. Immunol.* 285, 109–138

48 Alonso, C. *et al*. (2001) African swine fever virus protein p54 interacts with the microtubular motor complex through direct binding to light-chain dynein. *J. Virol.* 75, 9819–9827

49 Heath, C.M. *et al*. (2001) Aggresomes resemble sites specialized for virus assembly. *J. Cell Biol.* 153, 449–455

50 Sfakianos, J.N. and Hunter, E. (2003) M-PMV capsid transport is mediated by Env/Gag interactions at the pericentriolar recycling endosome. *Traffic* 4, 671–680

51 Wu, H. *et al*. (2005) Solution structure of the Tctex1 dimer reveals a mechanism for dynein–cargo interactions. *Structure (Camb)* 13, 213–223

52 Douglas, M.W. *et al*. (2004) Herpes simplex virus type 1 capsid protein VP26 interacts with dynein light chains RP3 and Tctex1 and plays a role in retrograde cellular transport. *J. Biol. Chem.* 279, 28522–28530

53 Desai, P. *et al*. (1998) Herpes simplex virus type 1 VP26 is not essential for replication in cell culture but influences production of infectious virus in the nervous system of infected mice. *Virology* 247, 115–124

54 Ye, G.J. *et al*. (2000) The herpes simplex virus 1 U(L)34 protein interacts with a cytoplasmic dynein intermediate chain and targets nuclear membrane. *J. Virol.* 74, 1355–1363

55 Reynolds, A.E. *et al*. (2002) Ultrastructural localization of the herpes simplex virus type 1 UL31, UL34, and US3 proteins suggests specific roles in primary envelopment and egress of nucleocapsids. *J. Virol.* 76, 8939–8952

56 Jouvenet, N. *et al*. (2004) Transport of African swine fever virus from assembly sites to the plasma membrane is dependent on microtubules and conventional kinesin. *J. Virol.* 78, 7990–8001

57 Ward, B.M. and Moss, B. (2004) Vaccinia virus A36R membrane protein provides a direct link between intracellular enveloped virions and the microtubule motor kinesin. *J. Virol.* 78, 2486–2493

58 Benboudjema, L. *et al*. (2003) Association of the herpes simplex virus type 1 Us11 gene product with the cellular kinesin light-chain-related protein PAT1 results in the redistribution of both polypeptides. *J. Virol.* 77, 9192–9203

59 Zheng, P. *et al*. (1998) PAT1, a microtubule-interacting protein, recognizes the basolateral sorting signal of amyloid precursor protein. *Proc. Natl. Acad. Sci. U. S. A.* 95, 14745–14750

60 Mohr, I. (2004) Neutralizing innate host defenses to control viral translation in HSV-1 infected cells. *Int. Rev. Immunol.* 23, 199–220

61 Koshizuka, T. *et al*. (2005) Herpes simplex virus type 2 membrane protein UL56 associates with the kinesin motor protein KIF1A. *J. Gen. Virol.* 86, 527–533

62 Tang, Y. *et al*. (1999) Cellular motor protein KIF-4 associates with retroviral Gag. *J. Virol.* 73, 10508–10513

63 Haimo, L.T. (2003) Regulation of molecular motors. In *Molecular Motors* (Schliwa, M., ed.), pp. 411–432, Wiley-VCH

64 Verhey, K.J. (2003) Motors and membrane trafficking. In *Molecular Motors* (Schliwa, M., ed.), pp. 377–409, Wiley-VCH

65 Suomalainen, M. *et al*. (2001) Adenovirus-activated PKA and p38/MAPK pathways boost microtubule-mediated nuclear targeting of virus. *EMBO J.* 20, 1310–1319

66 Deacon, S.W. *et al*. (2003) Dynactin is required for bidirectional organelle transport. *J. Cell Biol.* 160, 297–301

67 Ligon, L.A. *et al*. (2004) A direct interaction between cytoplasmic dynein and kinesin I may coordinate motor activity. *J. Biol. Chem.* 279, 19201–19208

68 Mizuno, N. *et al*. (2004) Dynein and kinesin share an overlapping microtubule-binding site. *EMBO J.* 23, 2459–2467

69 Garcia-Mata, R. *et al*. (2002) Hassles with taking out the garbage: aggravating aggresomes. *Traffic* 3, 388–396

70 Kopito, R.R. (2000) Aggresomes, inclusion bodies and protein aggregation. *Trends Cell Biol.* 10, 524–530

71 Kirkegaard, K. *et al*. (2004) Cellular autophagy: surrender, avoidance and subversion by microorganisms. *Nat. Rev. Microbiol.* 2, 301–314

72 Marsden, V.S. and Strasser, A. (2003) Control of apoptosis in the immune system: Bcl-2, BH3-only proteins and more. *Annu. Rev. Immunol.* 21, 71–105

73 Lane, J.D. *et al*. (2001) Apoptotic cleavage of cytoplasmic dynein intermediate chain and p150(Glued) stops dynein-dependent membrane motility. *J. Cell Biol.* 153, 1415–1426

74 Hay, S. and Kannourakis, G. (2002) A time to kill: viral manipulation of the cell death program. *J. Gen. Virol.* 83, 1547–1564

75 Hernaez, B. *et al*. (2004) The African swine fever virus dynein-binding protein p54 induces infected cell apoptosis. *FEBS Lett.* 569, 224–228

76 Santoro, M.G. *et al*. (2003) NF-kappaB and virus infection: who controls whom. *EMBO J.* 22, 2552–2560

77 Dammermann, A. *et al*. (2003) The minus end in sight. *Curr. Biol.* 13, R614–R624

78 Müsch, A. (2004) Microtubule organization and function in epithelial cells. *Traffic* 5, 1–9

79 Nogales, E. (2000) Structural insights into microtubule function. *Annu. Rev. Biochem.* 69, 277–302

80 Howard, J. and Hyman, A.A. (2003) Dynamics and mechanics of the microtubule plus end. *Nature* 422, 753–758

81 Martinez-Moreno, M. *et al*. (2003) Recognition of novel viral sequences that associate with the dynein light chain LC8 identified through a pepscan technique. *FEBS Lett.* 544, 262–267

82 de Soultrait, V.R. *et al*. (2002) HIV-1 integrase interacts with yeast microtubule-associated proteins. *Biochim. Biophys. Acta* 1575, 40–48

83 Rodriguez-Crespo, I. *et al*. (2001) Identification of novel cellular proteins that bind to the LC8 dynein light chain using a pepscan technique. *FEBS Lett.* 503, 135–141

84 Raux, H. *et al*. (2000) Interaction of the rabies virus P protein with the LC8 dynein light chain. *J. Virol.* 74, 10212–10216

85 Poisson, N. *et al*. (2001) Molecular basis for the interaction between rabies virus phosphoprotein P and the dynein light chain LC8: dissociation of dynein-binding properties and transcriptional functionality of P. *J. Gen. Virol.* 82, 2691–2696

86 Jacob, Y. *et al*. (2000) Cytoplasmic dynein LC8 interacts with lyssavirus phosphoprotein. *J. Virol.* 74, 10217–10222

87 Lukashok, S.A. *et al*. (2000) An adenovirus inhibitor of tumor necrosis factor alpha-induced apoptosis complexes with dynein and a small GTPase. *J. Virol.* 74, 4705–4709

88 Mueller, S. *et al*. (2002) Interaction of the poliovirus receptor CD155 with the dynein light chain Tctex-1 and its implication for poliovirus pathogenesis. *J. Biol. Chem.* 277, 7897–7904

89 Ohka, S. *et al*. (2004) Receptor (CD155)-dependent endocytosis of poliovirus and retrograde axonal transport of the endosome. *J. Virol.* 78, 7186–7198

90 Kim, W. *et al*. (1998) Binding of murine leukemia virus Gag polyproteins to KIF4, a microtubule-based motor protein. *J. Virol.* 72, 6898–6901

Radtke, K., Döhner, K. & Sodeik, B. (2006)
Viral interactions with the cytoskeleton: a hitchhiker's guide to the cell
Cellular Microbiology, 8: 387-400

Cellular Microbiology
Volume 8 Page 387 - March 2006
doi:10.1111/j.1462-5822.2005.00679.x

Volume 8 Issue 3

Microreview

Viral interactions with the cytoskeleton: a hitchhiker's guide to the cell

*Kerstin Radtke[1], Katinka Döhner[1] and Beate Sodeik[1]**

Summary

The actin and microtubule cytoskeleton play important roles in the life cycle of every virus. During attachment, internalization, endocytosis, nuclear targeting, transcription, replication, transport of progeny subviral particles, assembly, exocytosis, or cell-to-cell spread, viruses make use of different cellular cues and signals to enlist the cytoskeleton for their mission. Viruses induce rearrangements of cytoskeletal filaments so that they can utilize them as tracks or shove them aside when they represent barriers. Viral particles recruit molecular motors in order to hitchhike rides to different subcellular sites which provide the proper molecular environment for uncoating, replicating and packaging viral genomes. Interactions between subviral components and cytoskeletal tracks also help to orchestrate virus assembly, release and efficient cell-to-cell spread. There is probably not a single virus that does not use cytoskeletal and motor functions in its life cycle. Being well informed intracellular passengers, viruses provide us with unique tools to decipher how a particular cargo recruits one or several motors, how these are activated or tuned down depending on transport needs, and how cargoes switch from actin tracks to microtubules to nuclear pores and back.